

# FRONTIERS IN LIFE SCIENCES AND RELATED TECHNOLOGIES



AGRICULTURAL SCIENCES BIOLOGY BIOCHEMISTRY  
BIOINFORMATICS BIOTECHNOLOGY BIOCONTROL  
BIOMECHANICS BIOCOMPUTERS BIOENGINEERING  
BIOELECTRONICS BIOPHYSICS BIOMATERIALS  
BIOMEDICAL SCIENCES BIOMONITORING BIOPOLYMERS  
CELL BIOLOGY CONSERVATION BIOLOGY CRYOBIOLOGY  
ECOLOGY ENVIRONMENTAL SCIENCES FOOD SCIENCES  
GENETICS GENOMICS IMMUNOTHERAPY MARINE SCIENCES  
MEDICAL SCIENCES MICROBIOLOGY MOLECULAR BIOLOGY  
METABOLOMICS NANOTECHNOLOGY NEUROSCIENCES  
PHYSIOLOGY PHARMACOGENOMICS PHARMACOLOGY  
POPULATION DYNAMICS PROTEOMICS REMEDIATION  
SYNTHETIC BIOLOGY SYSTEMATICS TOXICOLOGY

APRIL, 2025, VOLUME 6, ISSUE 1

## Contents

### Research Articles

- **Monosodium glutamate induces *tsc1* gene expression in fission yeast**

Merve Yilmazer, Damla Kale

Pages: 1-8

- **Microbiological changes of kefir traditionally produced from different milks according to storage time**

Hilal Dogan Guney, Ozlem Ozer Altundag, Meryem Colak

Pages: 9-14

- **The effect of nutritional education on nutritional knowledge level and diet quality in volleyball players living in a disadvantaged area**

Sevim Aytekin, Bilge Meral Koc

Pages: 15-20

- **Possible effect of E-SELECTIN (Ser128Arg), L-SELECTIN (Pro213Ser), P-SELECTIN (Thr715Pro) gene polymorphisms for COVID-19 disease severity**

Nebiye Nihan Bozkurt, Figen Guzelgul, Nejmiye Akkus, Kubra Sahin, Sadegul Savkin, Tuncay Yigit

Pages: 21-27

- **The effect of paclitaxel on cachexia-related gene *AZGP1* expression during adipocyte differentiation**

Ozlem Agirel, Ceyda Okudu

Pages: 28-34

- **Analysis of potential fire and explosion incidents in an LNG terminal in a port area using the FRAM method**

Ahmet Gokcan, Hacer Handan Demir, Rabia Akdogan, Fahri Oluk, Goksel Demir

Pages: 35-44

- **Assessing the performance of multivariate data analysis for predicting solar radiation using alternative meteorological variables**

Mustafa Ozbuldu, Yunus Emre Sekerli

Pages: 45-52

### Review Articles

- **Exploring the antioxidant and protective effects of usnic acid: Opportunities and challenges**

Tubanur Aslan Engin

Pages: 53-59

- **Telomerase reverse transcriptase promoter mutations in non-small cell lung cancer: Biology and clinical significance**

Onur Dulger

Pages: 60-64

- **The effects of mesenchymal stem cells on asthma**

Kemal Yuce

Pages: 65-71

**Issue Editorial Board**

**Prof. Dr. Ilhan DOGAN**

**Institution: Sakarya University of Applied Sciences**

**Doç. Dr. Bestenur YALCIN**

**Institution: Bahcesehir University**

**Prof. Dr. Memet Vezir KAHRAMAN**

**Institution: Marmara University**

**Doç. Dr. Onur INAM**

**Institution: Gazi University**

**Editor**

**Prof. Dr. Ibrahim Ilker OZYIGIT**

**Co-Editors**

**Asst. Prof. Dr. Ibrahim Ertugrul YALCIN**

**Assoc. Prof. Dr. Aysegul YILDIZ**

**Layout Editor**

**Asli HOCAOGLU OZYIGIT**



Research article

## Monosodium glutamate induces *tsc1* gene expression in fission yeast

Merve Yilmazer<sup>\*1</sup> , Damla Kale<sup>1</sup> 

<sup>1</sup> Istanbul University, Faculty of Science, Department of Molecular Biology and Genetics, 34134, Istanbul, Türkiye

### Abstract

Tuberous sclerosis complex (TSC) is a disease of cellular migration and proliferation that produces hamartomas (benign tumors or malignant cancers affecting the brain and skin) and also involves the eyes, lungs, kidneys, and heart in patterns that can vary throughout life. TSC is an autosomal dominantly inherited disease. Alterations in the TSC1 and TSC2 proteins that form the TSC complex are among the factors that cause the emergence of this disease. TSC1 and TSC2 proteins are the suppressors on the mTOR signaling pathway. The health risks of monosodium glutamate, the most commonly used food additive today, are still a controversial issue. However, there are studies revealing that monosodium glutamate has a negative effect on cell proliferation. In the present study, parental and *tsc1Δ* mutant fission yeast cells were used and the effects of monosodium glutamate on *tsc1* gene expression, cell proliferation, and apoptosis were investigated. It was observed that 8 mg/mL monosodium glutamate caused an increase in the expression of the *tsc1* gene. It was concluded that monosodium glutamate may disrupt cell homeostasis and affect cell division and apoptosis processes via the mTOR pathway, depending on the increase in the expression of the *tsc1* gene.

**Keywords:** Apoptosis; cell growth; fission yeast; monosodium glutamate; tuberous sclerosis complex

### 1. Introduction

A rare autosomal dominantly inherited disease, Tuberous Sclerosis, also known as Tuberous Sclerosis Complex (TSC), is characterized by the development of hamartomatous tumors in various organs such as the brain, heart, skin, eye, kidney, lung, and liver (Curatolo et al., 2022). The main clinical findings of this disease are epileptic seizure, neurodevelopmental delay, kidney tumors, skin tumors, and tumors in the heart and brain. It has been reported that epilepsy is the most common symptom of TSC (Nabbout et al., 2019). TSC occurs due to abnormal cellular differentiation, proliferation, and cell migration processes (Holmes et al., 2007; Kilic, 2021). *TSC1* and *TSC2* genes encode hamartin and tuberin proteins respectively and play a role in the emergence of tuberous sclerosis complex. The *TSC1* and *TSC2* genes are responsible for the regulation of the rapamycin (mTOR) pathway, and the hamartin-tuberin complex represses the mTOR pathway, which controls cell growth and proliferation. Hamartin protein also functions as a tumor

suppressor (Slegtenhorst et al., 1997). By interacting with other proteins, Hamartin regulates many cellular activities such as cell division, growth, autophagy, apoptosis, and angiogenesis, which are necessary for the proper functioning of cellular processes (Adhikari et al., 2010; Mallela and Kumar, 2021). Loss-of-function mutations of the *TSC1* and *TSC2* genes cause hyperactivation of the mTOR pathway, which leads to cellular and molecular consequences such as oxidative stress, network imbalance, and inflammation (Curatolo et al., 2024).

Signals such as hypoxia, nutrient availability and growth factors initiate the mTOR pathway and enable the activation of many processes such as transcription and translation control, cell cycle progression, and nutrient uptake (Fingar and Blenis, 2004; Vadysirisack and Ellisen, 2012; Fonseca et al., 2014). In eukaryotic cells, numerous cellular activities such as cell cycle differentiation, progression, and metabolism in response to changing environmental conditions are mediated by protein phosphorylation, and these processes are evolutionarily conserved. Two different multiprotein complexes, TORC1 and

\* Corresponding author.

E-mail address: [merve.yilmazer@istanbul.edu.tr](mailto:merve.yilmazer@istanbul.edu.tr) (M. Yilmazer).

<https://doi.org/10.51753/flsrt.1570290> Author contributions

Received 19 October 2024; Accepted 15 January 2025

Available online 30 April 2025

2718-062X © 2025 This is an open access article published by Dergipark under the [CC BY](https://creativecommons.org/licenses/by/4.0/) license.

TORC2, are involved in the mTOR pathway. mTORC1 activity is extremely sensitive to changes in cell growth conditions. The TSC1-TSC2 complex transduces signals from various cellular pathways to regulate mTORC1 activity appropriately. Thus, this complex plays a role as a sensor and regulator of growth conditions (Huang and Mannig, 2008; Nakashima and Tamanoi, 2010).

Numerous researches have been conducted using various animal models, including zebrafish, mice, rats, and non-human primates, in order to examine the disease's natural occurrence, evaluate the effectiveness of potential treatments, and look into the molecular mechanisms underlying TSC (Moavero et al., 2022; Aronica et al., 2023). Although significant progress has been made in understanding the molecular mechanisms in these models, there are also studies using human induced pluripotent stem cells (iPSCs) to investigate the effects of *TSC1* and *TSC2* mutations on human neurodevelopment (Niu et al., 2024). *Schizosaccharomyces pombe*, fission yeast, is frequently used as a model organism for eukaryotic cell studies (Zhao and Lieberman, 1995; Vyas et al., 2021) and is an important model, especially in cell cycle studies (Lee and Nurse, 1988; Hoffman et al., 2015). *S. pombe* has many orthologous genes conserved in vertebrates and the proteins that are the products of these genes (Hoffman et al., 2015). The *TSC1* gene encoding the TSC1 protein in Tuberous Sclerosis Complex (TSC) in human and the *tsc1* gene in *S. pombe* are orthologous genes (Wood et al., 2012). In eukaryotes, the TSC/Rheb/TORC1/S6K/S6 signaling pathway has a crucial role in the regulation of protein synthesis and growth and this pathway is conserved from human to yeast. Rheb, a small G-protein involved in the TORC1 pathway, is found a functional homologous in fission yeast. As in mammals, the TSC1-TSC2 complex and Rhl1 are precursors of the TORC1 pathway in fission yeast (Nakashima and Tamanoi, 2010).

Monosodium glutamate (MSG) is one of the amino acids found abundantly in nature. It is found in food as a flavor enhancer and is used as a food additive (E621) (Kazmi et al., 2017). In addition to ready-to-eat products, fertilizers used for organic agricultural products also contain MSG (Singh et al., 2011; Awang et al., 2020). Clinical trials on human and animal subjects have also revealed several potential health hazards of MSG. Muscular, gastrointestinal, circulatory, neurological, and cardiac disorders are some common samples (Kazmi et al., 2017). It has been shown that MSG can cause genotoxic effects in rats and lead to increased oxidative stress (Farombi and Onyema, 2006). Glutamate is an important stimulant neurotransmitter in the central nervous system, but excess use can lead to excitotoxicity (Kazmi et al., 2017). Excessive activation of the glutamate pathway and excessive influx of calcium ions into neurons are suggested as the biochemical mechanisms behind epileptic seizures. Furthermore, the overactivation of neurons has also been associated with other diseases such as Multiple Sclerosis (MS), Parkinson's, Huntington's, and Alzheimer's Disease. MSG, the most commonly used food additive, increases the level of free

glutamate in the brain, putting people at risk of developing these diseases (Singh and Panda, 2024). Studies to understand the possible hepatotoxic, neurotoxic, and genotoxic effects of MSG are limited. Further studies are needed to investigate the molecular and metabolic mechanisms associated with MSG.

This study aimed to investigate the molecular effect of monosodium glutamate on hamartin, which is located in the TSC complex and plays a role in cell growth, in fission yeast. In monosodium glutamate-treated cells (parental and *tsc1Δ* mutant strains), cell division and apoptosis were examined at the molecular level. Additionally, alterations caused by MSG in the expression level of the *tsc1* gene were investigated.

## 2. Materials and methods

### 2.1. Yeast strain and culture conditions

*S. pombe* parental ED666 (*h+/ade6-M210, ura4-D18, leu1-32*) and mutant *tsc1Δ* (*h+/ade6-M210, ura4-D18, leu1-32, SPAC22F3.13::KanMX4*) were obtained from Bioneer Corporation (version 5.0). Deletion of the *tsc1* gene in the *tsc1Δ* strain was confirmed by qPCR. *S. pombe* strains were grown in rich media (YEL; glucose 1%, yeast extract 0.5%) at 30°C. YEL contains the determined amount of MSG in the experimental group.

### 2.2. Determination of monosodium glutamate concentration and spot assay

To determine the extent of the resistance, serial 10-fold dilutions of the parental and *tsc1Δ* mutant strains which grow in liquid-rich media without MSG or containing an increasing concentration of MSG (0.1-10 mg mL<sup>-1</sup>) were spotted onto YEA plates (YEL with 2% agar). The plates were incubated for 3 days at 30°C. MSG concentrations were determined by comparing them with their untreated control of strains.

### 2.3. Growth of the cells

A standard growth curve analysis protocol was followed to determine the growth of the parental and *tsc1Δ* mutant strain in YEL media without or with monosodium glutamate (8 mg mL<sup>-1</sup>). The increase in cell growth was measured in a spectrophotometer (EON, Biotek Instruments Inc.) every 2 hours for 40 hours at 600 nm wavelength optical density. Time-dependent graphs of cell growth was obtained according to the standard curve (Petersen and Russell, 2016).

### 2.4. Gene expression analysis

Firstly, total RNA isolation was performed from parental and *tsc1Δ* mutant cells grown without MSG and containing 8 mg of MSG in rich-media by using "PureLink® RNA Mini Kit (Ambion® by Life Technologies)" according to the manufacturer's instructions. Some modifications were made to

**Table 1**  
Primer sequences used in the study.

Gene	Forward Primer	Reverse Primer
<i>act1</i>	TGCTCAATCTTCCTCCCTTG	CAAAGCTGAGGGTTGGAAAA
<i>tsc1</i>	GTGATGAGCAAGAAAGAG	CTTAGCCTCGTAAACAAC
<i>tor1</i>	GAAGCGTGTCTCAAATAAG	ACTACACCATCCTACATAAC
<i>atg14</i>	TCACCCTAGTTTACTCTCAACA	CGGCAATGTCCATAAAAACTC

use kit and the cells were mechanically homogenized in PBS by using glass beads. Then, isolated RNAs were converted to cDNA by “Applied Biosystems™ High-Capacity cDNA Reverse Transcription Kit”. Expressions of *tsc1* (hamartin), *tor1* (TORC2 serine/threonine protein kinase Tor1), *act1* (actin) and *atg14* (autophagy associated protein Atg14) genes were analyzed by using the “Thermo Scientific Applied Biosystems PowerUp SYBR™ Green PCR Master Mix”. *Act1* gene was used as the reference gene. The primers were designed in the “IDT Primer Quest Tool” program (Table 1). “Roche Light Cycler 480” was used for real-time PCR.

## 2.5. Imaging of apoptosis with fluorescence microscopy

Dual staining with ethidium bromide and acridine orange was used to examine apoptosis under a fluorescence microscope. The AO/EtBr dual staining experiment was carried out using Agus and colleagues’ (2018) modified protocol (Agus et al., 2018). After washing the cells with PBS, 5  $\mu\text{L}$  of AO/EtBr solution (60  $\mu\text{g mL}^{-1}$  AO and 100  $\mu\text{g mL}^{-1}$  EtBr dissolved in PBS) was added. Following a 5-minute incubation period at room temperature, the cells were cleaned with PBS and viewed using an Olympus BX53 fluorescent microscope. All cells were seen as green with AO at  $\lambda_{\text{ex}}=500$  nm and  $\lambda_{\text{em}}=530$  nm, whereas apoptotic cells were seen as orange-red with EtBr at  $\lambda_{\text{ex}}=510$  nm and  $\lambda_{\text{em}}=595$  nm. Cell counting was performed using the “Image J” program.

## 2.6. Statistical analysis

The qPCR analysis results were evaluated according to the

“Pfaffl” method (Pfaffl 2001). Statistical analyses were performed in GraphPad Prism 9 Software with Two-way ANOVA. The graph of apoptosis analysis was obtained by the GraphPad Prism 9 Software according to the results from “Image J” program.

## 3. Results

### 3.1. Spot assay and MSG concentration

Cells were cultured in the rich media containing different concentrations of MSG (0,1-10  $\text{mg mL}^{-1}$ ) for 24 hours. Serial 10-fold dilutions of cells cultured in rich media (YEA) without MSG or increasing concentration of MSG were spotted onto YEA plates. Based on the growth results, 8  $\text{mg mL}^{-1}$  concentrations of MSG were selected for the study (Fig. 1).

### 3.2. MSG reduced cell growth

Cells of parental and *tsc1* $\Delta$  mutant strain cultured in YEA media without or with monosodium glutamate (8  $\text{mg mL}^{-1}$ ) were followed for 40 hours to detect their time-dependent growth. According to the results of the time-dependent growth curve (Fig. 2), MSG caused a decrease and slowdown in cell proliferation.

### 3.3. Gene expression analysis

The expressions of *atg14*, *tor1*, and *tsc1* genes in parental and *tsc1* $\Delta$  mutant cells were comparatively analyzed. When 8  $\text{mg/mL}$  MSG was treated to parental cells, a 1.2-fold decrease in the expression of the *atg14* gene was observed, while a 4.3-fold,

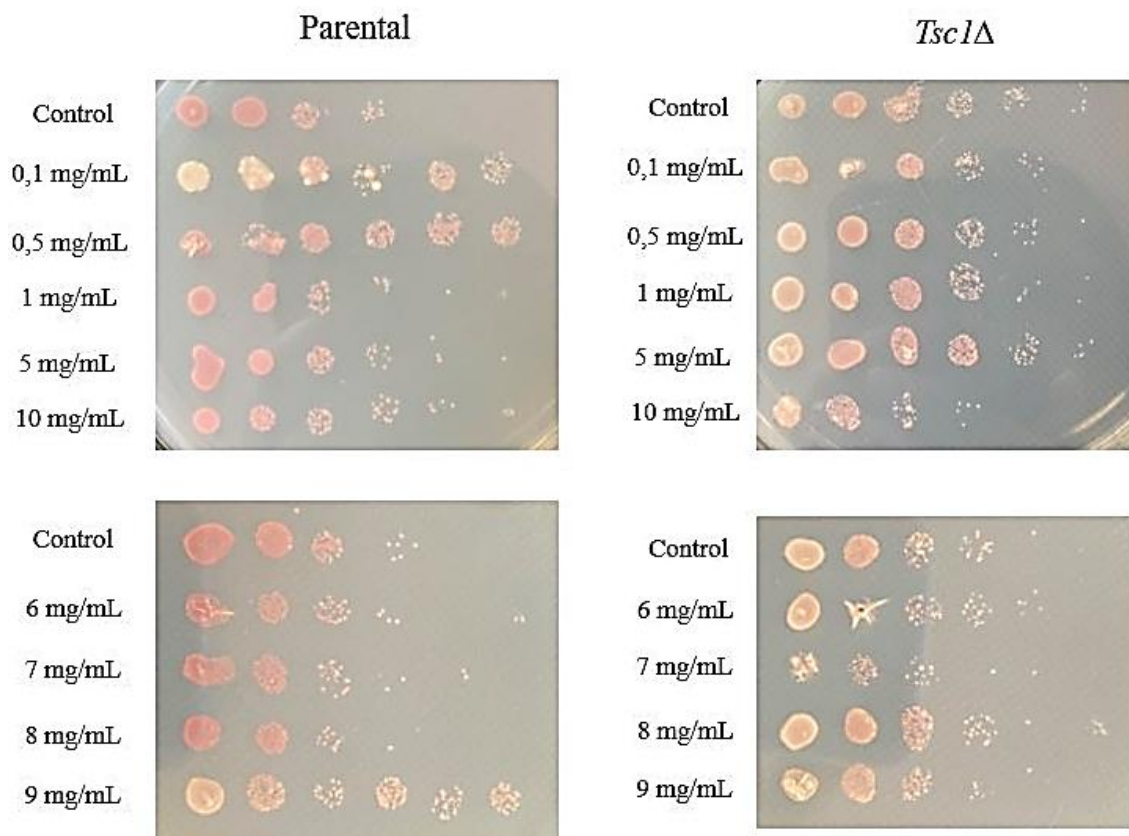
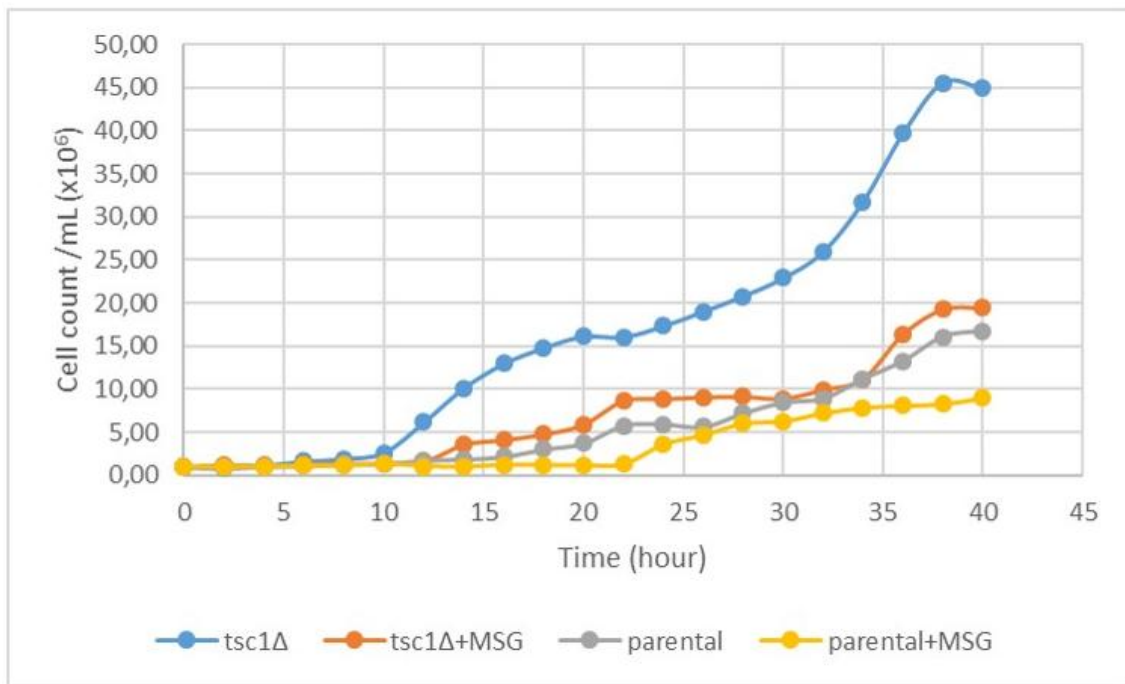


**Fig. 1.** Spot analyses in the rich media of parental and *tsc1* $\Delta$  mutant cells grown in a rich media containing MSG-free and different concentrations of MSG for 24 hours.



Cells	0 h	40 h
<i>tsc1Δ</i>	1 x 10 <sup>6</sup> cell/mL	44,87 x 10 <sup>6</sup> cell/mL
<i>tsc1Δ</i> +MSG		19,45 x 10 <sup>6</sup> cell/mL
parental		16,74 x 10 <sup>6</sup> cell/mL
parental+MSG		9 x 10 <sup>6</sup> cell/mL

**Fig. 2.** Time-dependent growth of the parental and *tsc1Δ* mutant strain in YEL media without or with 8mg/mL monosodium glutamate for 40 hours.

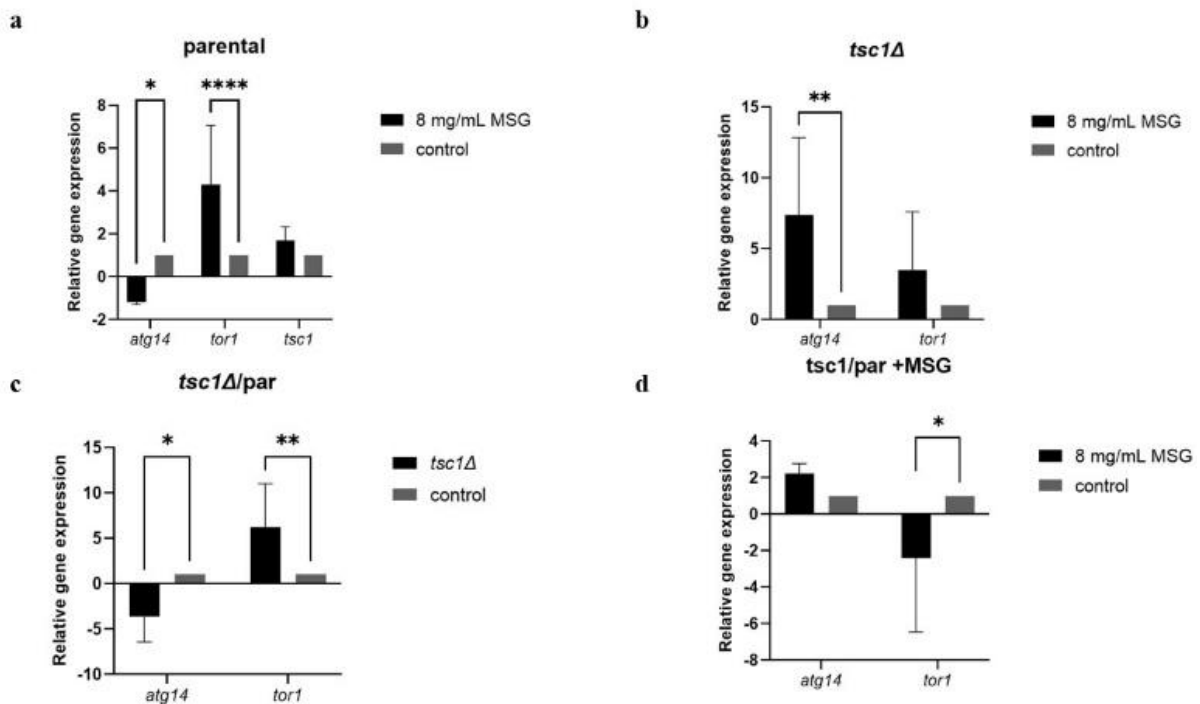


**Fig. 3.** Relative expression analysis of the *atg14*, *tor1*, and *tsc1* genes in parental and *tsc1Δ* mutant strains treated MSG or not. (a. in parental cells grown in media with or without MSG, b. in *tsc1Δ* mutant cells grown in media with or without MSG, c. *tsc1Δ* mutant cells versus parental cells grown in media without MSG, d. *tsc1Δ* mutant cells versus parental cells grown in media with MSG) Data were analysed using two-way ANOVA (\*P= 0.0128, 0.0166, 0.0219; \*\*P=0.0096, 0.0074; \*\*\*\*P<0.0001). The data presented were derived from three independent experiments.

and 1.7-fold increase in the expression of *tor1*, and *tsc1* genes was observed, respectively (Fig. 3a).

After treatment of 8 mg/mL MSG to *tsc1Δ* mutant cells, the expression levels of *atg14* and *tor1* genes increased 7.4 and 3.5 times, respectively (Fig. 3b).

In the absence of MSG, when the gene expression level of *tsc1Δ* cells was compared with the parental cells, the expression of the *atg14* gene was reduced by 3.6-fold, while the expression level of the *tor1* gene increased 6.2-fold. (Fig. 3c).

When MSG treated *tsc1Δ* mutant cells were compared with MSG treated parental cells at the gene expression level, a 2.2-fold increase in the expression of the *atg14* gene was observed. Additionally, the expression of the *tor1* gene decreased 2.4-fold (Fig. 3d). The expression of the *tsc1* gene was also examined in *tsc1Δ* cells for confirmation, and gene expression did not occur as expected.

### 3.4. Apoptosis under the fluorescence microscope

Apoptosis was detected by ethidium bromide/acridine orange dual staining. After cells were stained with AO/EtBr, they were captured under the fluorescence microscope. While all cells were observed in green, apoptotic cells were in orange due

to the uptake of EtBr. The experiment was repeated 3 times and many photos were taken. The examples of pictures for each experimental group are included in Fig. 4. The percentage of apoptosis was calculated by rating the number of red cells to the number of green cells. Cell counting was performed by the "Image J" program and 16 different (8 for AO +8 for EtBr) images for each cell type (total of 64 images) were screened. Only one of these images for each group was given as an example in Figure 5. It was found that apoptosis rates were 23.28%, 29.54%, 10.86%, and 15.24% in parental, MSG-treated parental, *tsc1Δ*, and MSG-treated *tsc1Δ* cells, respectively (Fig. 5).

## 4. Discussion

Tuberous sclerosis complex (TSC) is a multisystemic genetic disorder that results in benign tumors in various organs as a result of excessive activation of the mTOR pathway. The TSC protein complex consists of *TSC1/2* gene products, which are crucial for the PI3K/AKT/mTOR (PAM) signaling pathway. Mutations in the *TSC1* and *TSC2* genes are the primary cause of TSC, an autosomal dominant disorder. (Islam, 2021; Fu et al., 2024).

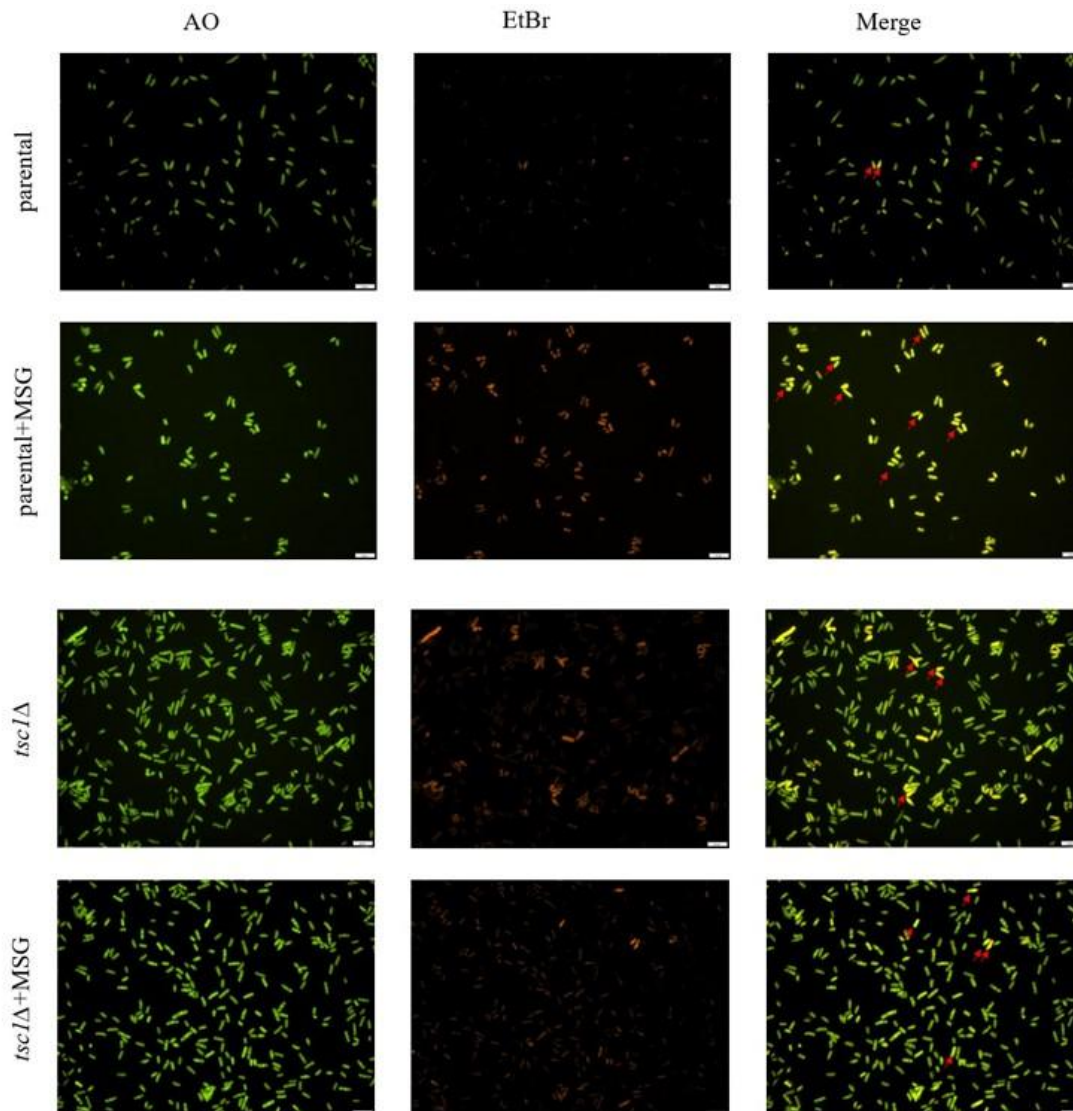


**Fig. 4.** After cells were stained with AO/EtBr to evaluate apoptosis, they were captured under the fluorescence microscope. (Red arrows indicate examples of apoptotic cells).

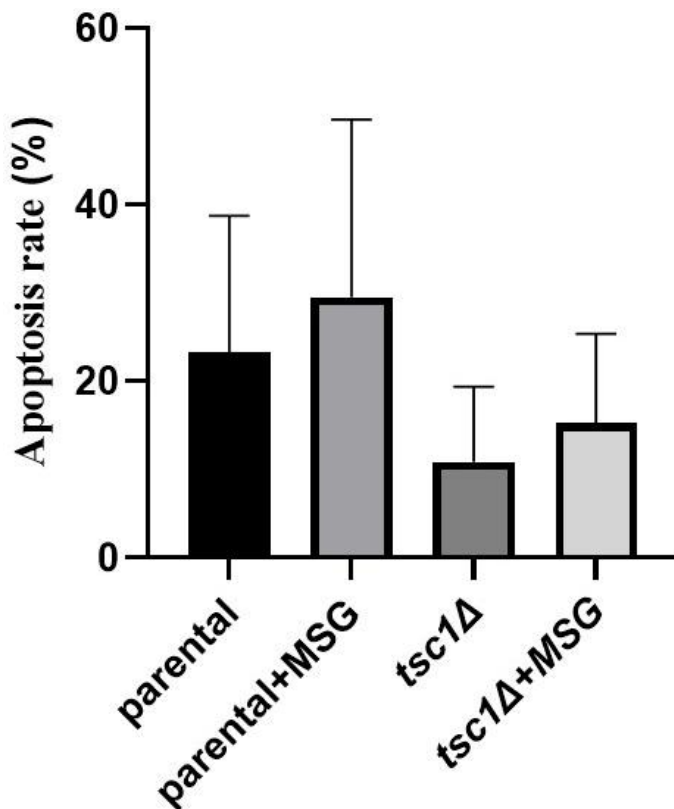


Fig. 5. The apoptosis rate of cells under the fluorescence microscope.

The TSC1 (hamartin) and TSC2 (tuberin) proteins form mTORC1, a TSC protein complex that functions as a tumor suppressor. A key component of the mTORC1 signaling pathway, the TSC complex integrates extracellular signals. The TSC complex suppresses tumor growth by adversely regulating the mTORC1 complex's activity (Rehbein et al., 2021). Pathogenic variants in genes encoding proteins of the mTORC1 signaling pathway lead to mTORopathies, which involve hyperactivity of this pathway. (Kim and Lee, 2019; Crino, 2020). Inactivation of either gene results in overactivation of mTOR signaling (Islam, 2021).

As part of a heterodimeric complex with tuberous sclerosis complex 2 (Tsc2), tuberous sclerosis complex 1 (Tsc1) controls several important processes including autophagy, cell survival and proliferation, protein synthesis, and lipid synthesis (Kim and Guan, 2019). Deletion of Tsc1 led to a pro-apoptotic phenotype in natural killer cells (Yang et al., 2016).

The PI3K/AKT/mTOR (PAM) signaling pathway is highly conserved in eukaryotic cells. As a result of TSC1/TSC2 mutation in TSC pathogenesis, the TSC protein complex is inactive, mTOR inhibition is lost, and the cell cycle and cell growth are disrupted (Mizuguchi et al., 2021). The cell cycle is disrupted by decreased inhibition of the mTOR pathway and this situation leads to abnormal cell proliferation and migration, which results in symptoms of TSC (Northrup et al., 2021; Fu et al., 2024). mTORC1 controls cell growth by controlling protein, lipid, and nucleotide synthesis, while also inhibiting autophagy (Ballesteros-Álvarez and Andersen, 2021). mTOR inhibition increases the activity of the autophagy-lysosomal pathway, which results in the degradation of damaged macromolecules and organelles (Johnson et al., 2015). In the present study, the *tsc1Δ* mutant cells showed more proliferation compared to other cells in both growth curve and spot analysis. These findings support that *tsc1* gene deletion causes an increase in cell

proliferation. At the level of gene expression, compared to the parental cells, *tor1* gene expression is higher in the *tsc1Δ* mutant cells, while *atg14* gene expression is lower. As expected, in the absence of hamartin, the product of the *tsc1* gene, which is a repressor of the mTOR complex, inhibition on mTOR1 was removed and an increase in the expression of the *tor1* gene was observed. Depending on this signaling pathway, a decrease in the expression of the autophagy-related *atg14* gene was observed, similar to the findings of Johnson et al. (Johnson et al., 2015).

Monosodium glutamate (MSG) is a globally used food additive found in many commercially processed foods. MSG use has increased significantly over the last 30 years. However, studies have identified MSG consumption as a significant contributing factor to the development and progression of syndromes such as hypertension, diabetes mellitus, cancer, and obesity. Additionally, Alzheimer's disease, brain damage, depression, addiction, anxiety, epilepsy, Parkinson's disease, and stroke are pathological disorders that can occur due to the neurotoxic effects of MSG. MSG has both positive and negative effects, depending on the amount consumed. Low doses of MSG have the potential to increase energy balance and homeostasis, while excessive consumption may cause genotoxic and cytotoxic effects that lead to metabolic disorders (Keshewani et al., 2024). Despite the controversy over the risks of MSG, its global consumption is still very high (Kayode et al., 2023).

Monosodium glutamate causes genotoxic effects *in vitro* and *in vivo* through both direct and indirect mechanisms. MSG can directly cause chromosomal aberrations, clumping, and stickiness of chromosomes. It indirectly causes oxidative stress in cells. Reactive free radicals cause functional and structural defects in genes. Molecular mechanisms such as changes in the levels of p53, TNF- $\alpha$ , gadd45, NF- $\kappa$ B, Bcl-2, and Bax have been associated with the genotoxic effects of MSG (Imam, 2019).

Oxidative stress due to reactive oxygen species causes apoptosis. Apoptosis is the normal physiological response of the cell to aging and cell damage and can be triggered by various factors such as oxidative stress (Li et al., 2021). High levels of Bax and low levels of Bcl-2 were seen in the kidneys and livers of MSG-treated rats, indicating significant induction of apoptosis (Kassab et al., 2022). It has been reported that MSG treatment induces apoptosis by causing downregulation of Bcl-2 protein in the thymus glands (Rezzani et al., 2003).

Many studies have supported the findings that MSG causes cell death (González-Burgos et al., 2001; Akataobi, 2020). MSG dose-dependently decreased thymocyte proliferation and increased cytotoxicity (Pavlovic, 2006). A study on human hepatoblastoma cell lines has shown that MSG causes cell damage and death by causing ROS accumulation. Additionally, mRNA upregulation of genes related to apoptosis and autophagy has been reported (Kakade et al., 2024). It has been shown that MSG increased DNA fragmentation and apoptosis in *Chlorella vulgaris* and *Spirulina platensis*. The study reported that MSG caused upregulation of caspase-3 and *Bax* genes and downregulation of *Bcl-2* gene expression. Oxidative stress and hepatic cell damage were triggered (Umbuzeiro et al., 2017).

In our fluorescence microscope examination, when MSG was treated, an increase in the apoptosis rate was observed in both parental and *tsc1Δ* mutant cells compared to the untreated control groups. In addition, it was observed under a fluorescence microscope that the cell density was higher in the *tsc1Δ* mutant cells than in the other cells cultured for the same time and initial concentrations. An increase in the expression of the *tsc1* gene

and *tor1* gene was observed when 8 mg/mL MSG was treated in the parental cells. There was a decrease in the expression of the *atg14* gene associated with autophagy. When MSG was treated to *tsc1Δ* mutant cells, a lesser increase in the *tor1* gene was observed compared to the parental cells, and a significant increase in the expression of the *atg14* gene was observed. The *tsc1* mutation results in the devoid of *tor1* inhibition, and when these cells were treated with MSG, there was a decrease in the increase of the *tor1* gene, independent of the absence of the *tsc1* gene. When MSG-treated *tsc1Δ* mutant cells were compared with MSG-treated parental cells, MSG treatment caused a decrease in the expression of the *tor1* gene in cells lacking the *tsc1* gene, and an increase in the expression of the autophagy-related *atg14* gene was observed, consistent with the flow of the signaling pathway. Despite the negative effects revealed in previous studies, there is no scientific evidence that requires a prohibition on MSG use. However, the ongoing debate about the negative effects of MSG and the lack of complete evidence about its harmlessness indicate that MSG may pose a health risk (Ataseven et al., 2016). Depending on the dosage used, MSG can be both beneficial and harmful. Considering the effects on cell viability, correct dosage adjustment is of great importance. In this study, the proliferation of cells treated with MSG (8 mg mL<sup>-1</sup>) increased less than in the control group. Additionally, it was seen that MSG caused an increase in the expression of the *tsc1* gene, and an increase in autophagy in conditions where the *tsc1* gene was deleted. The findings obtained in the study suggest that MSG acts via the mTOR signaling pathway. MSG may be disrupting cell homeostasis by affecting the TSC complex.

## 5. Conclusion

The results of the studies on MSG are controversial.

## References

- Adhikari, D., Zheng, W., Shen, Y., Gorre, N., Hämäläinen, T., Cooney, A. J., ... & Liu, K. (2010). Tsc/mTORC1 signaling in oocytes governs the quiescence and activation of primordial follicles. *Human Molecular Genetics*, *19*(3), 397-410.
- Agus, H. H., Sarp, C., & Cemiloglu, M. (2018). Oxidative stress and mitochondrial impairment mediated apoptotic cell death induced by terpinolene in *Schizosaccharomyces pombe*. *Toxicology Research*, *7*(5), 848-858.
- Akataobi, U. S. (2020). Effect of monosodium glutamate (MSG) on behavior, body and brain weights of exposed rats. *Environmental Disease*, *5*(1), 3-8.
- Aronica, E., Specchio, N., Luinburg, M. J., & Curatolo, P. (2023). Epileptogenesis in tuberous sclerosis complex-related developmental and epileptic encephalopathy. *Brain*, *146*(7), 2694-2710.
- Ataseven, N., Yuzbasioglu, D., Keskin, A. C., & Unal, F. (2016). Genotoxicity of monosodium glutamate. *Food and Chemical Toxicology*, *91*, 8-18.
- Awang, H., Aziz, A. S., R Azmi, N. N. A., Saad, N. S., Zamri, N. A. S., & Seman-Kamarulzaman, A. F. (2020). Effect of monosodium glutamate on the growth of solanum melongena. *Gading Journal for Science and Technology*, *3*(1), 52-59.
- Ballesteros-Álvarez, J., & Andersen, J. K. (2021). mTORC2: The other mTOR in autophagy regulation. *Aging cell*, *20*(8), e13431.
- Crino, P. B. (2020). mTORopathies: a road well-traveled. *Epilepsy currents*, *20*(6\_suppl), 64S-66S.
- Curatolo, P., Specchio, N., & Aronica, E. (2022). Advances in the genetics and neuropathology of tuberous sclerosis complex: edging closer to targeted therapy. *The Lancet Neurology*, *21*(9), 843-856.
- Curatolo, P., Scheper, M., Emberti Gialloreti, L., Specchio, N., & Aronica, E. (2024). Is tuberous sclerosis complex-associated autism a preventable and treatable disorder?. *World Journal of Pediatrics*, *20*(1), 40-53.
- Farombi, E. O., & Onyema, O. (2006). Monosodium glutamate-induced oxidative damage and genotoxicity in the rat: modulatory role of vitamin C, vitamin E and quercetin. *Human & experimental toxicology*, *25*(5), 251-259.
- Fingar, D. C., & Blenis, J. (2004). Target of rapamycin (TOR): an integrator of nutrient and growth factor signals and coordinator of cell growth and cell cycle progression. *Oncogene*, *23*(18), 3151-3171.
- Fonseca, B. D., Smith, E. M., Yelle, N., Alain, T., Bushell, M., & Pause, A. (2014). The ever-evolving role of mTOR in translation. In *Seminars in cell & developmental biology* (Vol. 36, pp. 102-112). Academic Press.
- Fu, J., Liang, P., Zheng, Y., Xu, C., Xiong, F., & Yang, F. (2024). A large deletion in TSC2 causes tuberous sclerosis complex by dysregulating PI3K/AKT/mTOR signaling pathway. *Gene*, *909*, 148312.
- Gonzalez-Burgos, I., Perez-Vega, M. I., & Beas-Zarate, C. (2001). Neonatal exposure to monosodium glutamate induces cell death and dendritic hypotrophy in rat prefrontocortical pyramidal neurons. *Neuroscience letters*, *297*(2), 69-72.
- Hoffman, C. S., Wood, V., & Fantès, P. A. (2015). An ancient yeast for young geneticists: a primer on the *Schizosaccharomyces pombe* model system. *Genetics*, *201*(2), 403-423.
- Holmes, G. L., Stafstrom, C. E., & Tuberous Sclerosis Study Group. (2007). Tuberous sclerosis complex and epilepsy: recent developments and future challenges. *Epilepsia*, *48*(4), 617-630.
- Huang, J., & Manning, B. D. (2008). The TSC1-TSC2 complex: a molecular switchboard controlling cell growth. *Biochem. J.*, *412*(2), 179-190.
- Imam, R. S. (2019). Genotoxicity of monosodium glutamate: a review on its causes, consequences and prevention. *Indian Journal of Pharmaceutical Education and Research*, *53*(4), S510-517.
- Islam, M. P. (2021). Tuberous sclerosis complex. In *Seminars in pediatric neurology* (Vol. 37, p. 100875). WB Saunders.
- Johnson, S. C., Sangesland, M., Kaerberlein, M., & Rabinovitch, P. S. (2015). Modulating mTOR in aging and health. *Aging and health-A systems biology perspective*, *40*, 107-127.
- Kakade, S. S., Bote, H. K., Sarvalkar, P. D., Sharma, K. K. K., & Pawar, P. K. (2024). Effects of Common Food Additives on HepG2 Cells: Accumulation of Reactive Oxygen Species and Induction of Cell Damage and Death. *ES Food & Agroforestry*, *17*, 1142.

- Kassab, R. B., Theyab, A., Al-Ghamdy, A. O., Algahtani, M., Mufti, A. H., Alsharif, K. F., ... & Elmasry, H. A. (2022). Protocatechuic acid abrogates oxidative insults, inflammation, and apoptosis in liver and kidney associated with monosodium glutamate intoxication in rats. *Environmental Science and Pollution Research*, 1-14.
- Kayode, O. T., Bello, J. A., Oguntola, J. A., Kayode, A. A., & Olukoya, D. K. (2023). The interplay between monosodium glutamate (MSG) consumption and metabolic disorders. *Heliyon*.
- Kazmi, Z., Fatima, I., Perveen, S., & Malik, S. S. (2017). Monosodium glutamate: Review on clinical reports. *International Journal of Food Properties*, 20(sup2), 1807-1815.
- Kesharwani, R., Bhoumik, S., Kumar, R., & Rizvi, S. I. (2024). Monosodium glutamate even at Low dose may affect oxidative stress, inflammation and neurodegeneration in rats. *Indian Journal of Clinical Biochemistry*, 39(1), 101-109.
- Kilic, E. (2021). Tuberoskleroz Kompleksi. *Turkiye Klinikleri Pediatric Genetic Diseases-Special Topics*, 2(2), 93-99.
- Kim, J., & Guan, K. L. (2019). mTOR as a central hub of nutrient signalling and cell growth. *Nature Cell Biology*, 21(1), 63-71.
- Kim, J. K., & Lee, J. H. (2019). Mechanistic target of rapamycin pathway in epileptic disorders. *Journal of Korean Neurosurgical Society*, 62(3), 272-287.
- Lee, M., & Nurse, P. (1988). Cell cycle control genes in fission yeast and mammalian cells. *Trends in Genetics*, 4(10), 287-290.
- Li, Z., Liu, Y., Wang, F., Gao, Z., Elhefny, M. A., Habotta, O. A., ... & Kassab, R. B. (2021). Neuroprotective effects of protocatechuic acid on sodium arsenate induced toxicity in mice: Role of oxidative stress, inflammation, and apoptosis. *Chemico-Biological Interactions*, 337, 109392.
- Mallela, K., & Kumar, A. (2021). Role of TSC1 in physiology and diseases. *Molecular and cellular biochemistry*, 476(6), 2269-2282.
- Man, A., Di Scipio, M., Grewal, S., Suk, Y., Trinari, E., Ejaz, R., & Whitney, R. (2024). The genetics of tuberous sclerosis complex and related mTORopathies: Current understanding and future directions. *Genes*, 15(3), 332.
- Merinas-Amo, T., Merinas-Amo, R., Alonso-Moraga, Á., Font, R., & Del Río Celestino, M. (2024). *In vivo* and *in vitro* studies assessing the safety of monosodium glutamate. *Foods*, 13(23), 3981.
- Mizuguchi, M., Ohsawa, M., Kashii, H., & Sato, A. (2021). Brain symptoms of tuberous sclerosis complex: pathogenesis and treatment. *International Journal of Molecular Sciences*, 22(13), 6677.
- Moavero, R., Mühlebner, A., Luinenburg, M. J., Craiu, D., Aronica, E., & Curatolo, P. (2022). Genetic pathogenesis of the epileptogenic lesions in Tuberous Sclerosis Complex: Therapeutic targeting of the mTOR pathway. *Epilepsy & Behavior*, 131, 107713.
- Nabbout, R., Belousova, E., Benedik, M. P., Carter, T., Cottin, V., Curatolo, P., ... & Pruna, D. (2019). Epilepsy in tuberous sclerosis complex: Findings from the TOSCA Study. *Epilepsia Open*, 4(1), 73-84.
- Nakashima, A., & Tamanoi, F. (2010). Conservation of the Tsc/Rheb/TORC1/S6K/S6 signaling in fission yeast. In *The Enzymes* (Vol. 28, pp. 167-187). Academic Press.
- Niu, W., Siciliano, B., & Wen, Z. (2024). Modeling tuberous sclerosis complex with human induced pluripotent stem cells. *World Journal of Pediatrics*, 20(3), 208-218.
- Northrup, H., Koenig, M. K., Pearson, D. A., & Au, K. S. (2021). Tuberous sclerosis complex. University of Washington, Seattle, Seattle (WA), 1-95.
- Pavlovic, V. (2006). The effect of monosodium glutamate on rat thymocyte proliferation and Bcl-2/bax protein expression. *Archives of Medical Science*, 2(4), 247.
- Petersen, J., & Russell, P. (2016). Growth and the environment of *Schizosaccharomyces pombe*. *Cold Spring Harbor Protocols*, 2016(3), pdb-top079764.
- Pfaffl, M. W. (2001). A new mathematical model for relative quantification in real-time RT-PCR. *Nucleic acids research*, 29(9), e45-e45.
- Rehbein, U., Prentzell, M. T., Cadena Sandoval, M., Heberle, A. M., Henske, E. P., Opitz, C. A., & Thedieck, K. (2021). The TSC complex-mTORC1 axis: from lysosomes to stress granules and back. *Frontiers in Cell and Developmental Biology*, 9, 751892.
- Rezzani, R., Corsetti, G., Rodella, L., Angoscini, P., Lonati, C., & Bianchi, R. (2003). Cyclosporine-A treatment inhibits the expression of metabotropic glutamate receptors in rat thymus. *Acta Histochemica*, 105(1), 81-87.
- Singh, S., Rekha, P. D., Arun, A. B., Huang, Y. M., Shen, F. T., & Young, C. C. (2011). Wastewater from monosodium glutamate industry as a low cost fertilizer source for corn (*Zea mays* L.). *Biomass and Bioenergy*, 35(9), 4001-4007.
- Singh, M., & Panda, S. P. (2024). The Role of Monosodium Glutamate (MSG) in Epilepsy and other Neurodegenerative Diseases: Phytochemical-based Therapeutic Approaches and Mechanisms. *Current Pharmaceutical Biotechnology*, 25(2), 213-229.
- Slegtenhorst, M. V., Hoogt, R. D., Hermans, C., Nellist, M., Janssen, B., Verhoef, S., ... & Kwiatkowski, D. J. (1997). Identification of the tuberous sclerosis gene TSC1 on chromosome 9q34. *Science*, 277(5327), 805-808.
- Umbuzeiro, G. D. A., Heringa, M., & Zeiger, E. (2017). In vitro genotoxicity testing: significance and use in environmental monitoring. *In vitro Environmental Toxicology-Concepts, Application and Assessment*, 59-80.
- Vadysirisack, D. D., & Ellisen, L. W. (2012). mTOR activity under hypoxia. *mTOR: Methods and Protocols*, 45-58.
- Vyas, A., Freitas, A. V., Ralston, Z. A., & Tang, Z. (2021). Fission yeast *Schizosaccharomyces pombe*: a unicellular “micromammal” model organism. *Current Protocols*, 1(6), e151.
- Wood, V., Harris, M. A., McDowall, M. D., Rutherford, K., Vaughan, B. W., Staines, D. M., ... & Oliver, S. G. (2012). PomBase: a comprehensive online resource for fission yeast. *Nucleic Acids Research*, 40(D1), D695-D699.
- Yang, M., Chen, S., Du, J., He, J., Wang, Y., Li, Z., ... & Dong, Z. (2016). NK cell development requires Tsc1-dependent negative regulation of IL-15-triggered mTORC1 activation. *Nature Communications*, 7(1), 12730.
- Zhao, Y., & Lieberman, H. B. (1995). *Schizosaccharomyces pombe*: a model for molecular studies of eukaryotic genes. *DNA and Cell Biology*, 14(5), 359-371.

**Cite as:** Yilmazer, M., & Kale, D. (2025). Monosodium glutamate induces *tsc1* gene expression in fission yeast. *Front Life Sci RT*, 6(1), 1-8.



Research article

## Microbiological changes of kefir traditionally produced from different milks according to storage time

Hilal Dogan Guney<sup>\*1</sup> , Ozlem Ozer Altundag<sup>2</sup> , Meryem Colak<sup>3</sup> 

<sup>1</sup> Safranbolu District Health Directorate, Nutrition and Diet Unit, 78100 Karabuk, Türkiye

<sup>2</sup> Karabuk University, Safranbolu Faculty of Tourism, Department of Gastronomy and Culinary Arts, 78100, Karabuk, Türkiye

<sup>3</sup> Karabuk University, Faculty of Medicine, Basic Medical Sciences, Medical Microbiology, 78100, Karabuk, Türkiye

### Abstract

Kefir is a fermented dairy product known for its positive effects on health. It has been reported to have positive effects on gastrointestinal diseases, hypertension, metabolic disorders, and the immune system due to its lactic acid bacteria, yeasts, and various bioactive compounds. The study aimed to investigate the microbiological properties of kefir produced from different milk types and pasteurization processes. Different types of milk were used in kefir production, such as UHT cow, pasteurized cow, open cow, and pasteurized goat. For each milk, kefir was produced with a 24-hour incubation period followed by microbial analysis on days 1, 7, 14, and 21. The microbial flora was assessed based on total bacterial counts, as well as specific enumeration of *Lactobacillus* sp., *Lactococcus* sp., coliform bacteria, molds, and yeasts. The pH levels of the kefir samples were also measured. The analysis showed that pH values decreased with increasing storage time in all kefir types. Especially the *Lactobacillus* sp. count of kefir produced from goat's milk was lower than other milk types and decreased until day 21. It was also observed that the number of coliform bacteria decreased faster in kefir produced with UHT milk, while it was not detected in other kefir after the 14<sup>th</sup> day. The study revealed that the microbial structure of kefir varied significantly according to milk type, pasteurization method, and storage time. Open cow's milk kefir produced by traditional methods were found to be richer in probiotic bacteria but at risk of contamination.

**Keywords:** Diet; kefir; kefir grain; traditional food

### 1. Introduction

Fermented products show positive effects on health thanks to various microorganisms and the compounds produced by these microorganisms. Microbial fermentation of kefir produces various bioactive compounds, vitamins, and minerals. Thanks to these compounds, kefir is known to have various health benefits such as antimicrobial, hypocholesterolemic, immunostimulant, and antitumor effects (Gokirmakli and Guzel-Seydim, 2022; Bozkir et al., 2024). Kefir is an acidic-alcoholic fermented milk beverage with unique characteristics such as its slightly sour and yeasty taste and viscous and creamy density. It is a food

characterized by its high nutritional, biological, and dietetic value and is recommended as an alternative option for gastrointestinal, metabolic, cancer, hypertension, cardiac, and allergic diseases (Aydin, 2023; Saleem et al., 2023; Cheng et al., 2024). It is especially recommended to be consumed by patients, the elderly, pregnant women, lactating women, infants, lactose intolerant individuals, and healthy people. Kefir consumption has increased worldwide in recent years, and the global kefir market is expected to at least double by 2030 (Tavsanlı et al., 2024).

Kefir grains are white to yellowish, irregularly shaped cauliflower-like grains traditionally used in kefir production

\* Corresponding author.

E-mail address: [hilaldogan21@gmail.com](mailto:hilaldogan21@gmail.com) (H. Dogan Guney).

<https://doi.org/10.51753/flsrt.1561917> Author contributions

Received 05 October 2024; Accepted 23 January 2025

Available online 30 April 2025

2718-062X © 2025 This is an open access article published by Dergipark under the [CC BY](https://creativecommons.org/licenses/by/4.0/) license.

(Yousefvand et al., 2022). The starter of kefir grain consists of lactic acid bacteria and yeast that produce lactic acid and alcohol. The quality of kefir is greatly influenced by the type of milk used, the amount of kefir grains, kefir grain microorganisms, and the incubation period (Arslan, 2015; Sulmiyati et al., 2019; de Souza et al., 2024). Kefir has a complex mixture of more than 50 bacteria and yeasts. Kefir grains contain *Lb. Kefir*, *Lb. Casei*, *Lb. Fermentum*, *Lb. Acidophilus*, *Lactococcus lactis*, *Streptococcus thermophilus*, and yeast species such as *Candida albicans*, *Saccharomyces cerevisiae*, *Kluyveromyces marxianus*, and *Pichia caribbica* (Sulmiyati et al., 2019; Saleem et al., 2023; Kalamaki et al., 2024).

Various kefir grains and kefir drinks have been evaluated in terms of microbiota and sensory composition. However, detailed microbial characterization studies examining kefir produced under home conditions and made with different milk types (different milk types such as goat, cow, and different pasteurization processes) have not yet been reported. The aim of this study was to investigate and compare the microbiological characteristics of kefir grains and traditional kefir made with different milk types and different pasteurization processes.

## 2. Materials and methods

### 2.1. Preparation of kefir samples

Kefir grains required for kefir production were obtained and activated at home using traditional methods. Sterile ultra-heat treated (UHT) cow milk, pasteurized cow milk, open cow milk, and pasteurized goat milk were used for kefir production. The kefir production process was carried out in the Karabuk University Gastronomy and Culinary Arts Application Kitchen and the samples were transferred to the Karabuk University Microbiology Laboratory for microbial analysis without breaking the cold chain. The kefir samples were coded as kefir produced with open cow's milk (K100), kefir produced with pasteurized cow's milk (K200), kefir produced with UHT cow's milk (K300), kefir produced with pasteurized goat's milk (K400), kefir produced with half pasteurized goat's milk and cow's milk (K500). In order to activate kefir grains, 5% kefir grains were added to cow's milk (300 ml), which was heat-treated at 90°C for 10 minutes to kefir to be produced with open cow's milk (K100). Then, it was left for incubation for 24 hours at room temperature. After incubation, kefir grains were filtered under hygienic conditions, and the activation of the grains was completed by repeating the same process one more time. This time, the activated grains were added to the milk, which was heat treated at 90°C for 10 minutes for kefir production and kept under the same incubation conditions. After incubation, the grains were separated from kefir under hygienic conditions, and the drinkable kefir was bottled for ripening and stored at +4°C for 24 hours. The production processes of K200, K300, K400, and K500 kefir samples were carried out in the same way. Inoculated samples were incubated at room temperature for 24 hours. After incubation, the grains were collected by passing through a sterile plastic strainer, and the same process was repeated once more to complete the activation of the grains. The activated grains were added to 5% kefir grains into 300 ml milk to ferment kefir and kept under the same incubation conditions. After incubation, the grains were separated from the kefir under hygienic conditions and the kefir in drinkable form was bottled and stored at +4°C for 24 hours for ripening.

### 2.2. Microbiological and physiological analyses

Microbiological analysis of kefir samples coded K100, K200, K300, K400, and K500 was carried out in the Microbiology laboratory of Karabuk University Faculty of Medicine. In order to determine the number of bacteria forming the microbial flora of kefir and their contamination status, each kefir sample was divided into four separate sterile tubes by paying attention to sterile conditions and kept at 4°C, which is the recommended condition for storage, and analyzed on the 1st day, 7<sup>th</sup> day, 14<sup>th</sup> day and 21<sup>st</sup> day. The pH values of kefir samples were determined using a pH meter (Thermo Orion Model-420A').

### 2.3. Preparation of media and dilution solution

In the samples obtained from kefir produced in all codes, 1 ml kefir was used for each analysis, and conventional methods were used in microbiological analyses. For this purpose, Milk Plate Count Agar (MCA) (Merck Millipore, Germany) was used for the determination of total viable bacteria count, M17 Agar (Merck Millipore, Germany) for the determination of Lactobacillus species and MRS Agar (Merck Millipore, Germany) for the determination of Bifidobacterium species. For the detection of contaminated microorganisms, VRB Agar (Merck Millipore, Germany) was used for the detection of coliform group bacteria, and Potato Dextrose Agar (Merck Millipore, Germany) was used for the detection of mold and yeast. Commercial powder/granule media were used in culture procedures and prepared with attention to sterility. The powder/granular media were stored in the original clamshell packaging in the dark, at ambient temperature, and in the refrigerator (MRS Agar) according to the manufacturer's instructions. They were sterilized in an autoclave at 121°C for 15 min and kept in a water bath at 47°C until use. Buffered Peptone Water was used as a dilution solution. 1 L of distilled water was added to 1 gram of solution and homogenized with a magnetic stirrer. It was divided into tubes at 9 ml per tube and sterilized. It was used after it was brought to ambient temperature.

### 2.4. Total viable bacteria, *Lactobacillus* sp. and *Bifidobacterium* sp. count (cfu/mL)

For the determination of the total number of viable bacteria; 1 ml of kefir samples was transferred to test tubes containing 9 ml of 0.1% Buffered Peptone Water. It was mixed in a vortex for 5-7 seconds. Inoculations of 1 ml were made from the tubes diluted at ratios of 1/1, 1/10, 1/100, 1/1000, 1/10000, 1/100000, 1/1000000. 10-12 ml Milk Plate Count Agar (MCA) (Merck Millipore, Germany) medium was added to the Petri dishes and allowed to solidify. Petri dishes were incubated at 37°C for 72 hours in an aerobic environment. At the end of incubation, colonies were counted and the total number of bacteria in 1 ml was determined. For *Lactobacillus* sp. analysis; 1 ml of kefir samples were transferred to test tubes containing 9 ml of 0.1% Buffered Peptone Water. It was mixed in a vortex for 5-7 seconds. The tubes were diluted at ratios of 1/1, 1/10, 1/100, 1/1000, 1/10000, 1/100000, 1/1000000 and inoculated with 1 ml. 20 ml of M17 Agar (Merck Millipore, Germany) medium was added to the Petri dishes and allowed to solidify. Petri dishes were incubated at 37°C for 72 hours in an aerobic environment. At the end of incubation, colonies were

counted and the number of *Lactobacillus* sp. bacteria in 1 ml was determined. For *Bifidobacterium* sp. analysis; 1 ml of kefir samples were transferred to test tubes containing 9 ml of 0.1% Buffered Peptone Water. After mixing for 5-7 seconds in the vortex, 1 ml was inoculated into tubes diluted at ratios of 1/1, 1/10, 1/100, 1/1000, 1/10000, 1/100000, 1/1000000. After 20 ml of MRSA (Merck Millipore, Germany) medium was added to the Petri dishes and allowed to solidify, the Petri dishes inoculated with the medium were placed in anaerobic jars, and anaerogenic kit was added and placed in an incubator and anaerobic incubation was performed at 37°C for 72 hours. At the end of incubation, the number of *Bifidobacterium* sp. in 1 ml was determined by counting the colonies formed. For the enumeration of *Lactobacillus* sp. and *Bifidobacterium* sp., 1 mL of kefir sample was transferred into test tubes containing 9 mL of 0.1% Buffered Peptone Water and vortexed for 5–7 seconds. Serial dilutions were prepared at 1/1, 1/10, 1/100, 1/1000, 1/10000, 1/100000, and 1/1000000, and 1 mL of each dilution was inoculated onto selective media. For *Lactobacillus* sp., M17 agar (Merck Millipore, Germany) was used, and plates were incubated aerobically at 37°C for 72 hours. For *Bifidobacterium* sp., MRSA medium (Merck Millipore, Germany) was used; the inoculated Petri dishes were placed in anaerobic jars with an anaerogenic kit and incubated anaerobically at 37°C for 72 hours. After incubation, colony counts were performed, and the number of viable *Lactobacillus* sp. and *Bifidobacterium* sp. per milliliter was determined.

**2.5. Coliform group bacteria and mold/yeast count (cfu/mL)**

For the detection of coliform group bacteria as a contamination indicator, 1 ml of kefir samples were inoculated without dilution. 20 ml VRB Agar (Merck Millipore, Germany) medium was added to the Petri dishes and allowed to solidify. In order to create a microaerophilic environment, 5-6 ml of medium was added again after the first layer of the medium solidified. Petri dishes were incubated at 37°C for 72 hours in an aerobic environment and the number of coliform group bacteria in 1 ml was determined by counting the colonies formed. For mold and yeast detection, 1 ml of kefir samples were inoculated without dilution. 20 ml of Potato Dextrose Agar (Merck Millipore, Germany) medium was added to the Petri dishes and the Petri dishes were incubated at 25°C for 72 hours in an aerobic environment. At the end of incubation, colonies were counted and the number of mold yeast in 1 ml was determined.

**2.6. Statistical analysis**

The data obtained were evaluated with the SPSS for Windows (Version 20.0, Statistical Package for Social Sciences) program. Descriptive statistics of continuous variables in the study were shown with mean and standard deviation values, and descriptive statistics of categorical variables were shown with frequency and percentage. The Pearson correlation coefficient was used to examine the relationship between dependent variables. In statistical analyses, measurements with a *p*-value below 0.05 (*p*<0.05) were accepted as significant.

**3. Results**

The distribution of total bacterial count values of K100, K200, K300, K400, and K500 coded products according to

storage periods under the same temperature and storage conditions are shown in Table 1. According to the results of the analysis, the total bacterial counts in kefir types showed a rapid decrease in K100 and K300 as the storage period prolonged compared to day 1, while this was not observed in K200, K400, and K500.

**Table 1**

Total bacterial count (cfu/ml) of kefir types according to temperature and storage periods.

Types of kefir	Day 1	Day 7	Day 14	Day 21
K100	63.10 <sup>^7</sup>	60.10 <sup>^7</sup>	15.10 <sup>^6</sup>	12.10 <sup>^6</sup>
K200	40.10 <sup>^7</sup>	60.10 <sup>^7</sup>	22.10 <sup>^6</sup>	24.10 <sup>^6</sup>
K300	57.10 <sup>^7</sup>	53.10 <sup>^7</sup>	37.10 <sup>^6</sup>	18.10 <sup>^6</sup>
K400	32.10 <sup>^7</sup>	26.10 <sup>^7</sup>	62.10 <sup>^6</sup>	20.10 <sup>^6</sup>
K500	35.10 <sup>^7</sup>	22.10 <sup>^7</sup>	47.10 <sup>^6</sup>	20.10 <sup>^6</sup>

When the correlation between the total bacterial counts of kefir types according to the storage periods was analyzed, it was observed that there was a significant difference at day 7 and a significant decrease in the total bacterial count at day 14 (*p*<0.05) (Table 2).

**Table 2**

Correlation between total bacteria values of kefir types at different storage days.

	1	2	3	4	5
1 Total bacteria count day 1	1				
2 Total bacteria count day 7	0.745	1			
3 Total bacteria count day 14	-0.713	-0.890*	1		
4 Total bacteria count day 21	-0.768	-0.246	0.342	1	
5 Kefir type	-0.734	-0.929*	0.869	0.433	1

\**p*<0.05

The effect of temperature and storage conditions on coliform group bacteria count changes of kefir types are shown in Table 3. According to the results of the analysis, there was a positive change in the number of coliform group bacteria in K100, K200, K300, and K400 kefir types between the 1<sup>st</sup> day and the 7<sup>th</sup>, 14<sup>th</sup>, and 21<sup>st</sup> days. It was determined that this situation developed due to the decrease in the pH level of the samples due to the prolongation of the storage period.

**Table 3**

Coliform group bacteria count (cfu/ml) of kefir types according to temperature and storage periods.

Types of kefir	Day 1	Day 7	Day 14	Day 21
K100	20.10 <sup>^1</sup>	10.10 <sup>^1</sup>	1.10 <sup>^1</sup>	0
K200	58.10 <sup>^1</sup>	2.10 <sup>^1</sup>	0	0
K300	7.10 <sup>^1</sup>	0	0	0
K400	3.10 <sup>^1</sup>	3.10 <sup>^1</sup>	0	0
K500	2.10 <sup>^2</sup>	6.10 <sup>^1</sup>	0	0

The effects of temperature and storage conditions on the *Lactococcus* sp. bacteria count changes of kefir types are shown in Table 4. According to the analysis results, there were differences between kefir samples and storage periods. It was observed that *Lactococcus* sp. bacteria content reached the highest levels in K300 and K500 on the 1st day and in K100, K200, and K400 on the 7<sup>th</sup> day during fermentation; *Lactococcus* sp. bacteria count showed a significant decrease in K300 and K500 on the 14<sup>th</sup> and 21<sup>st</sup> days compared to the 1st day.

When the correlation between the total *Lactococcus* sp. bacteria species according to the storage times of kefir types

were examined, it was observed that there was a significant negative difference in the 1st day values according to kefir types, and there was a significant positive difference between the 1<sup>st</sup> day and the 7<sup>th</sup> day for all kefir types ( $p<0.05$ ) (Table 5).

**Table 4**

*Lactococcus* sp. bacteria count (cfu/ml) of kefir types according to temperature and storage periods.

Types of kefir	Day 1	Day 7	Day 14	Day 21
K100	37.10 <sup>^7</sup>	50.10 <sup>^7</sup>	10.10 <sup>^6</sup>	3.10 <sup>^6</sup>
K200	37.10 <sup>^7</sup>	50.10 <sup>^7</sup>	12.10 <sup>^6</sup>	7.10 <sup>^6</sup>
K300	30.10 <sup>^7</sup>	25.10 <sup>^7</sup>	2.10 <sup>^6</sup>	1.10 <sup>^6</sup>
K400	21.10 <sup>^7</sup>	72.10 <sup>^6</sup>	15.10 <sup>^6</sup>	2.10 <sup>^6</sup>
K500	20.10 <sup>^7</sup>	18.10 <sup>^7</sup>	12.10 <sup>^6</sup>	1.10 <sup>^6</sup>

**Table 5**

Correlation between total *Lactococcus* spp. bacteria counts of kefir types depending on storage periods.

	1	2	3	4	5
1 Kefir type	1				
2 <i>Lactococcus</i> sp. bacteria count day 1	-.955*	1			
3 <i>Lactococcus</i> sp. bacteria count day 7	-0.875	.948*	1		
4 <i>Lactococcus</i> sp. bacteria count day 14	0.225	-0.307	-0.153	1	
5 <i>Lactococcus</i> sp. bacteria count day 21	-0.572	0.679	0.712	0.31	1

\* $p<0.05$

The effects of temperature and storage conditions on the *Lactobacillus* sp. bacteria count changes of kefir types are shown in Table 6. According to the results of the analysis of the products stored and analyzed in the same environment, it is seen that the highest level of *Lactobacillus* sp. species bacteria counts in the product coded K100 reached the highest level on the 7<sup>th</sup> day and the highest level on the 1st day in kefir samples produced with other milk types. It is seen that the prolongation of the storage period causes the number of *Lactobacillus* sp. bacteria to decrease.

**Table 6**

*Lactobacillus* sp. count (cfu/ml) of kefir types according to temperature and storage periods.

Types of kefir	Day 1	Day 7	Day 14	Day 21
K100	24.10 <sup>^7</sup>	26.10 <sup>^7</sup>	12.10 <sup>^6</sup>	11.10 <sup>^6</sup>
K200	16.10 <sup>^7</sup>	10.10 <sup>^7</sup>	9.10 <sup>^6</sup>	15.10 <sup>^6</sup>
K300	14.10 <sup>^7</sup>	22.10 <sup>^6</sup>	10.10 <sup>^6</sup>	6.10 <sup>^6</sup>
K400	11.10 <sup>^7</sup>	20.10 <sup>^6</sup>	5.10 <sup>^6</sup>	45.10 <sup>^5</sup>
K500	10.10 <sup>^7</sup>	3.10 <sup>^7</sup>	4.10 <sup>^6</sup>	35.10 <sup>^5</sup>

**Table 7**

Correlation between *Lactobacillus* sp. bacteria counts of kefir types during storage periods.

	1	2	3	4	5
1 Kefir type	1				
2 <i>Lactobacillus</i> sp. bacteria count day 1	-.937*	1			
3 <i>Lactobacillus</i> sp. bacteria count day 7	-0.833	.958*	1		
4 <i>Lactobacillus</i> sp. bacteria count day 14	-.933*	.887*	0.722	1	
5 <i>Lactobacillus</i> sp. bacteria count day 21	-0.83	0.67	0.617	0.66	1

\* $p<0.05$

The correlation between *Lactobacillus* sp. bacteria counts of kefir types in different storage periods is shown in Table 7. Day 1 *Lactobacillus* sp. bacteria counts showed a significant difference between kefir types. There was a significant negative correlation in the number of *Lactobacillus* sp. bacteria from kefir K100 to kefir K500. A significant negative relationship was also observed between kefir types on days 7 and 14 ( $p<0.05$ ).

According to the results of the analysis of the changes in mold and yeast bacteria counts of kefir types due to temperature and storage conditions, intense mold and yeast bacteria counts were observed in all kefir types between the 1<sup>st</sup> day and the 7<sup>th</sup>, 14<sup>th</sup>, and 21<sup>st</sup>-day counts. The prolongation of the storage period caused intense mold and yeast bacteria to be found in all kefir types.

The pH changes of kefir types due to temperature and storage conditions are shown in Table 8. According to the results of the analysis, a decrease in pH values was observed in all kefir types between the 1<sup>st</sup> day and the 7<sup>th</sup>, 14<sup>th</sup>, and 21<sup>st</sup> days.

**Table 8**

pH change of kefir types according to temperature and storage periods.

Types of kefir	Day 1	Day 7	Day 14	Day 21
K100	4.53	4.49	4.46	4.43
K200	4.5	4.47	4.42	4.38
K300	4.45	4.42	4.35	4.32
K400	4.5	4.48	4.44	4.43
K500	4.5	4.48	4.45	4.43

The correlation between the pH changes of kefir types depending on the storage periods is shown in Table 9. A significant correlation was observed in the pH values of all kefir types according to storage times ( $p<0.05$ ,  $p<0.001$ ).

**Table 9**

Correlation between pH changes of kefir types at different storage periods.

	1	2	3	4	5
1 Kefir type	1				
2 pH day 1	-0.329	1			
3 pH day 7	-0.057	.957*	1		
4 pH day 14	0	.944*	.993**	1	
5 pH day 21	0.162	0.866	.959*	.975**	1

\* $p<0.05$  \*\* $p<0.001$

#### 4. Discussion

The pH value, which is important in determining the quality of food, determines the acidity level by reflecting the activity of hydrogen ions. In kefir production, the fermentation process is usually completed in the pH range of 4.5-4.6. Changes in pH values during the storage of kefir are an indication of the shelf life of the product and the slow fermentation that occurs during the storage process (Putri et al., 2020; Acar, 2023; Li et al., 2024). In this study, microbiological analysis of traditional kefirs prepared with cow and goat milk with different pasteurization processes was evaluated. The pH measurements of kefir samples showed a statistically significant difference depending on the storage periods ( $p<0.05$ ). It was observed that the general average pH value was 4.49 on the 1st day of the research, and pH values decreased statistically significantly in all kefir types on the 7<sup>th</sup>, 14<sup>th</sup>, and 21<sup>st</sup> days of the research. It was understood that there was no significant difference in pH values between kefir samples obtained from cow or goat milk ( $p>0.05$ ). In the study conducted by Buran (2020), the pH values of kefir samples from cow's milk ranged between 4.39 and 4.47, while the pH values of samples from goat's milk ranged between 4.18 and 4.42 (Buran, 2020). In the study conducted by Acik et al., pH values in kefir samples were found in the range of 4.13-4.55 (Acik et al., 2020). Yousefvand et al. (2022) reported that the pH values of kefir samples measured after 1, 7, 14, and 21 days of storage at 4°C ranged between 4.49 and 4.53 on day 1

and gradually decreased throughout the storage period. The findings of the current study are consistent with this result. The differences in pH values are thought to be related to factors such as fermentation time and the type of milk used (Ektik, 2022; Li et al., 2024).

Buran (2020) found that *Lactococcus* sp. numbers in kefir produced with cow and goat milk varied between 7.15-7.93 and 7.00-8.30 log cfu/mL; Bakan (2021) found that *Lactococcus* sp. numbers of concentrated kefir types produced by different methods varied between 8.08-8.76 log cfu/g. In this study, it was understood that the *Lactococcus* sp. bacteria content reached the highest levels on day 1; K300 and K500 during fermentation and decreased as a result of fermentation in the following storage days.

While Bakan (2021) determined that the number of *Lactobacillus* sp. in concentrated kefir types produced by different methods ranged between 8.17 and 9.01 log cfu/g, da Costa et al. (2020) reported that the number of *Lactobacillus* sp. increased until the 14th day of storage in four out of six kefir samples, but then decreased, whereas in the remaining two samples, the decrease occurred on the 7th day. When the literature is examined, the results of some researchers indicate that the number of *Lactobacillus* sp. in kefir decreases during storage, while others indicate that it first increases and then decreases or remains constant (Sendogan et al., 2021; Yousefvand et al., 2022; Acar, 2023; Gulhan, 2023). This is thought to be due to the effects of fermentation metabolites on lactic acid bacteria resulting from microbiota differences in kefir. In this study, the number of *Lactobacillus* sp. bacteria in kefir samples was generally higher than the literature (Egea et al., 2022; Sánchez-Rodríguez et al., 2024; Onat et al., 2025). When the kefir types were evaluated within themselves, it was observed that the number of *Lactobacillus* sp. bacteria in kefirs made with goat milk was lower than the kefirs made with other milk types, and the increase was higher on the 21st day, while the number of *Lactobacillus* sp. bacteria of kefirs made with cow milk decreased gradually with the prolongation of the storage period. Yeasts are effective in the development of the taste and aroma of kefir and in the establishment of symbiosis between microorganisms. Buran (2020) reported that yeast results in kefir produced with cow and goat milk varied between 4.16-5.49 and 4.00-5.18 log cfu/mL, respectively. Ciftci and Oncul (2022) reported that they detected 2.37 and 3.08 log cfu/mL yeast in plain kefir and fruit kefir. In literature studies, the mold count in kefir samples produced by industrial method is below the detectable values (Yilmaz et al., 2022; Salik et al., 2023; Gulhan, 2023). In this study, intense mold and yeast were detected in all

kefir types starting from the 7th day.

Ciftci and Oncul (2022) found that the total number of coliform bacteria in the samples was below the detectable value as a result of total coliform bacteria count. In this study, the number of coliform group bacteria was not detected in kefir produced with UHT milk (K300) as of the 7th day, while no coliform group bacteria were detected after the 14th day in the other kefirs except K100, while no coliform group bacteria were detected only on the 21st day in kefir made with open cow's milk (K100). With the prolongation of the storage period, the pH values of kefirs decrease, and these low pH values negatively affect the ability of bacteria to survive. For this reason, all bacterial species may have decreased in number by being affected by the decreasing pH values due to the prolongation of the storage period.

## 5. Conclusion

When the data of the study are evaluated, it is seen that storage periods and the type of milk used in kefir production, as well as the pasteurization processes applied to the milk affect the microbial load of the kefirs obtained. As a result of the study, goat milk was found to be the most inefficient milk type in terms of probiotic bacteria in kefir production. The prolonged storage period causes a decrease in the number of probiotic bacteria in kefirs. As of day 7, *Lactobacillus* sp. and *Lactococcus* sp. bacteria species of all kefir types show a decrease. This may be due to decreasing pH values. In light of the data obtained, the highest probiotic bacteria species were found in open cow milk produced by traditional methods, while the lowest value was found in kefir produced with pasteurized goat milk. These results indicate that the production of kefir from cow milk with traditional methods for kefir production provides an advantage in terms of probiotic bacteria species, but poses a risk in terms of coliform bacteria species. This study is one of the rare studies that examined the difference between the microbial values of kefirs produced with the use of cow's milk and goat's milk which have undergone different pasteurization processes according to storage periods. It is thought that the study data will make a positive contribution to the literature.

**Conflict of interest:** The authors declare that they have no conflict of interests.

**Informed consent:** The authors declare that this manuscript did not involve human or animal participants and informed consent was not collected.

## References

- Acar, C. (2023). Kahveli kefirin kimyasal ve mikrobiyolojik özelliklerin belirlenmesi, Yüksek Lisans Tezi, (pp. 1-99). Aksaray Üniversitesi, Türkiye.
- Acik, M., Çakiroğlu, F. P., Altan, M., & Baybo, T. (2020). Alternative source of probiotics for lactose intolerance and vegan individuals: sugary kefir. *Food Science and Technology*, 40, 523-531.
- Arslan, S. (2015). A review: chemical, microbiological and nutritional characteristics of kefir. *CyTA-Journal of Food*, 13(3), 340-345.
- Aydin, E. (2023). *Saccharomyces boulardii* kullanarak kefir üretimi ve bazı özelliklerinin incelenmesi, Yüksek Lisans Tezi, (pp. 1-96). Ege Üniversitesi, Türkiye.
- Bakan, R. (2021). Türk mutfağındaki sütlü tatlıların değerlendirilmesi ve inovasyonu, Yüksek Lisans Tezi, (pp. 1-125). Pamukkale Üniversitesi, Türkiye.
- Bozkir, E., Yilmaz, B., Sharma, H., Esatbeyoglu, T., & Ozogul, F. (2024). Challenges in water kefir production and limitations in human consumption: A comprehensive review of current knowledge. *Heliyon*.
- Buran, I. (2020). Probiyotik ve prebiyotiklerin sinbiyotik kullanımının inekve keçi sütünden üretilen kefirlerin kalite özellikleri üzerine etkisi, Doktora Tezi, (pp. 1-187). Ankara Üniversitesi, Türkiye.
- Cheng, T., Zhang, T., Zhang, P., He, X., Sadiq, F. A., Li, J., ... & Gao, J. (2024). The complex world of kefir: Structural insights and symbiotic relationships. *Comprehensive Reviews in Food Science and Food Safety*, 23(4), e13364.
- da Costa, G. M., de Paula, M. M., Costa, G. N., Esmerino, E. A., Silva, R., de Freitas, M. Q., ... & Pimentel, T. C. (2020). Preferred attribute elicitation methodology compared to conventional descriptive analysis: A study using probiotic yogurt sweetened with xylitol and added with

- prebiotic components. *Journal of Sensory Studies*, 35(6), e12602.
- Ciftci, M., & Oncul, N. (2022). Ticari probiyotik içeceklerin bazı mikrobiyolojik özellikleri. *Akademik Ziraat Dergisi*, 11(1), 165-178.
- de Souza, H. F., Monteiro, G. F., Bogáz, L. T., Freire, E. N. S., Pereira, K. N., de Carvalho, M. V., ... & Kamimura, E. S. (2024). Bibliometric analysis of water kefir and milk kefir in probiotic foods from 2013 to 2022: A critical review of recent applications and prospects. *Food Research International*, 175, 113716.
- Egea, M. B., Santos, D. C. D., Oliveira Filho, J. G. D., Ores, J. D. C., Takeuchi, K. P., & Lemes, A. C. (2022). A review of nondairy kefir products: their characteristics and potential human health benefits. *Critical Reviews in Food Science and Nutrition*, 62(6), 1536-1552.
- Ektik, N. (2022). Klasik (olgunlaştırılmış) beyaz peynir üretiminin farklı aşamalarından laktik asit bakterilerinin izolasyonu, identifikasyonu ve teknolojik özelliklerinin belirlenmesi, Doktora Tezi, (pp. 1-128). Balıkesir Üniversitesi, Türkiye.
- Gokirmakli, C., & Guzel-Seydim, Z. B. (2022). Water kefir grains vs. milk kefir grains: Physical, microbial and chemical comparison. *Journal of Applied Microbiology*, 132(6), 4349-4358.
- Gulhan, A. (2023). Physicochemical, microbiological and sensory analyses of functional detox juices fermented with water kefir grains. *Gıda*, 48(4), 715-727.
- Kalamaki, M. S., Kakagianni, M. N., & Angelidis, A. S. (2024). Shifts in ovine (*Ovis aries*) bulk-tank milk microbiota as a function of cold-storage temperature and duration. *International Dairy Journal*, 158, 106032.
- Li, S., Liu, X., Wang, L., Wang, K., Li, M., Wang, X., ... & Wang, Z. (2024). Innovative beverage creation through symbiotic microbial communities inspired by traditional fermented beverages: Current status, challenges and future directions. *Critical Reviews in Food Science and Nutrition*, 64(28), 10456-10483.
- Onat, B., Nicin, R. T., Kanıbol, N. A., Cetin, E., Senturk, D. Z., & Simsek, O. (2025). Influence of Jerusalem artichoke on microbial and chemical characteristics of water kefir production. *International Journal of Gastronomy and Food Science*, 39, 101104.
- Putri, Y. D., Setiani, N. A., & Warya, S. (2020). The effect of temperature, incubation and storage time on lactic acid content, pH and viscosity of goat milk kefir. *Current Research on Biosciences and Biotechnology*, 2(1), 101-104.
- Saleem, K., Ikram, A., Saeed, F., Afzaal, M., Ateeq, H., Hussain, M., ... & Asif Shah, M. (2023). Nutritional and functional properties of kefir. *International Journal of Food Properties*, 26(2), 3261-3274.
- Salik, R. A., Bitim, E., Koprualan, O., Selcuk, E., Altay, O., & Ertekin, F. (2023). Encapsulation of olive leaf extract obtained by ultrasonic-assisted extraction method and use in kefir beverage. *The Journal of Food*, 48(1), 73-93.
- Sánchez-Rodríguez, R., Terriente-Palacios, C., García-Olmo, J., Osorio, S., & Rodríguez-Ortega, M. J. (2024). Combined Metabolomic and NIRS Analyses Reveal Biochemical and Metabolite Changes in Goat Milk Kefir under Different Heat Treatments and Fermentation Times. *Biomolecules*, 14(7), 816.
- Sulmiyati, S., Said, N. S., Fahrodi, D. U., Malaka, R., & Maruddin, F. (2019). The physicochemical, microbiology, and sensory characteristics of kefir goat milk with different levels of kefir grain. *Tropical Animal Science Journal*, 42(2), 152-158.
- Sendogan, G., Akan, E., Yerlikaya, O., Meric, S., & Kinik, O. (2021). Changes in benzoic acid content of goat milk kefir produced using different kefir cultures. *Mljekarstvo: časopis za unaprjeđenje proizvodnje i prerade mlijeka*, 71(1), 60-68.
- Tavsanlı, N., Yıldız, S., Caliskan, M., & Aydın, S. (2024). Evaluating the potential effect of microalgae on soymilk vegan kefir in terms of physical, chemical, microbiological properties. *Algal Research*, 82, 103630.
- Yilmaz, B., Elibol, E., Shangpliang, H. N. J., Ozogul, F., & Tamang, J. P. (2022). Microbial communities in home-made and commercial kefir and their hypoglycemic properties. *Fermentation*, 8(11), 590.
- Yousefvand, A., Huang, X., Zarei, M., & Saris, P. E. J. (2022). *Lactaseibacillus rhamnosus* GG survival and quality parameters in kefir produced from kefir grains and natural kefir starter culture. *Foods*, 11(4), 523.

**Cite as:** Dogan Guney, H., Ozer Altundag, O., & Colak, M. (2025). Microbiological changes of kefir traditionally produced from different milks according to storage time. *Front Life Sci RT*, 6(1), 9-14.



## Research article

# The effect of nutritional education on nutritional knowledge level and diet quality in volleyball players living in a disadvantaged area

Sevim Aytekin<sup>1</sup> , Bilge Meral Koc<sup>\*2</sup> 

<sup>1</sup> Bahcesehir University, Institute of Health Sciences, Department of Nutrition and Dietetics, 34353, Istanbul, Türkiye

<sup>2</sup> Izmir Democracy University Institute of Health Sciences, Department of Nutrition and Dietetics, 35140, Izmir, Türkiye

## Abstract

The aim of this study is to determine the effect of nutritional education (NE) planned for volleyball players who live in a socioeconomically disadvantaged area on the level of nutritional knowledge and diet quality. The study was conducted with volleyball players between the ages of 9 and 14 who were studying in schools in disadvantaged areas of Istanbul between July 2022 and August 2022. NE was applied in 3 separate modules. As a data collection tool, the General Information and Nutritional Habits Questionnaire, from which information about the hypothesis of the study will be obtained, was used both pre- and post-NE. A 1-day (24-hour) food consumption record was taken from the study group at the beginning and end of the study. Again, at the beginning of the study, the Diet Quality Index (DQI-I) of the food consumption records was calculated to analyze the current diet quality of the players at the end. The nutritional knowledge level of 40 volleyball players participating in the study increased post NE ( $p < 0.05$ ). There is no statistically significant difference in the weight parameters of the pre and post-NE ( $p > 0.05$ ). There is no statistically significant difference between the total DQI-I scores ( $p > 0.05$ ). The 3-week nutrition education given as a result of the study, which was planned to examine the effect of nutrition education on the nutritional knowledge level and diet quality of volleyball players living in disadvantaged areas, caused a significant increase in the level of nutrition knowledge, while it did not create significant changes in the DQI-I. It is thought that the reason for this situation is related to socioeconomic level, the availability of high nutritional value food, and the level of nutritional knowledge of families. There is a need for necessary practices in the dissemination of nutrition education in the adolescent period.

**Keywords:** Adolescents; exercise; nutrition education; volleyball

## 1. Introduction

The health of the people living in a society ensures the development of that society in terms of health and economy. Balanced and adequate nutrition is the most important parameter determining human health. Physical activity and healthy nutrition practices should be popularized in order to protect and improve the health of individuals and to lead a quality life (Rozanski, 2023). It is a scientific fact that when any of the nutrients are consumed inadequately or excessively, growth and development are hindered (Vlaardingerbroek, 2024).

Children and adolescents are not able to choose foods and beverages with high nutritional value because their nutritional knowledge is not sufficient. Adolescence is the period when the start of healthy eating habits is laid. The education conducted during adolescence period is important for adolescents on their way to becoming adults. Physical activity is indispensable for a quality life (Wu et al., 2024). Growth is affected by physical activity as much as external factors such as genetic structure, circadian rhythm, and diet. High physical activity in childhood reduces the likelihood of chronic diseases, especially obesity, in adulthood (Souilla et al., 2024).

\* Corresponding author.

E-mail address: [bilgemerall@gmail.com](mailto:bilgemerall@gmail.com) (B. Meral Koc).

<https://doi.org/10.51753/flsrt.1572464> Author contributions

Received 23 October 2024; Accepted 29 January 2025

Available online 30 April 2025

2718-062X © 2025 This is an open access article published by Dergipark under the [CC BY](https://creativecommons.org/licenses/by/4.0/) license.

According to the United Nations Educational, Scientific and Cultural Organization (UNESCO), disadvantaged individuals are defined as individuals who have less chance of social and economic integration because of their gender, economic status, political status, ethnic or religious origin (Atchoarena and Gasperini, 2003). Disadvantaged groups are those who have limited access to facilities such as health, education, and information that are easily accessible to most of society (Kazu, 2019). In a 2010 study conducted in Türkiye, it was concluded that the rate of healthy eating decreases as socioeconomic status worsens according to education level, employment status, and income factors (Simsek, 2010). Hatun et al. (2003) concluded that malnutrition is observed in children of families with low economic levels. It has been determined that the risk of Type-2 Diabetes Mellitus (T2DM) increases when individuals who are fed with limited food for a long time start to be fed with high-calorie and cheap foods. Therefore, T2DM and obesity are the most common diseases after infectious diseases in poor regions of the world. According to the World Health Organization (WHO) report, as poverty increases, the prevalence of low-weight, malnourished children increases (WHO, 2017). The consequences of malnutrition are short stature (stunting), weakened immune system, easy infection, and severe course of infection. Low socioeconomic status negatively affects maternal nutrition. Therefore, inequality between individuals starts during pregnancy (Nguyen, 2023).

Childhood and adolescence are important for the acquisition and maintenance of healthy lifestyle behaviors. Lifestyle and nutritional behaviors develop during adolescence, individuals have more control over their dietary choices, and dietary behaviors acquired during this period affect adulthood (Scheineder, 2016; Winpenny, 2018).

The aim of our study was to determine the effect of healthy nutrition education given to female volleyball players aged 9-14 years living in a socio-economically disadvantaged area on the nutritional knowledge level and diet quality.

## 2. Materials and methods

This study is a descriptive cross-sectional study. The data collection process of this planned research was carried out between 4 July 2022 and 18 August 2022 after the approval of Bahcesehir University Scientific Research and Publication Ethics Board dated 05.07.2022 and numbered E-20021704-604.01.02-36586. The population of the study consisted of female adolescents between the ages of 9-14 studying in schools located in disadvantaged areas of Istanbul, Turkey. These schools are located in Zeytinburnu, Sisli, Maltepe, Fatih, and Kagithane districts.

The power of the study was determined with the G\*Power (G\*Power 3.1.9.2, Duesseldorf, Germany) package program. Power analysis was performed in sample selection; type 1 error rate  $\alpha=0.05$  and type 2 error rate  $\beta=0.20$ , power of the test  $1-\beta=0.80$  and effect size 0.50 were calculated. In line with this information, it was shown that at least 34 individuals should be included in the study. The study sample was designed to include 40 female adolescents who signed the consent form, considering possible losses. Adolescents who used medication, had chronic diseases, and played sports other than volleyball were not included in the study.

Different methods were used as data collection tools to obtain information about the hypothesis of the study. General Information and Dietary Habits Questionnaire: With the General

Information and Nutrition Habits Questionnaire, information such as age, disease information, weight and height, dietary habits (number of main meals and snacks, frequency of fast-food consumption, etc.), nutritional knowledge level and fluid consumption were determined before the individuals were included in the study. The questionnaire was based on a similar study examining the effect of nutrition education on players' nutrition knowledge. The nutritional knowledge test consists of three parts; Multiple Choice: 12 questions, each with one correct answer (+1 point). Scores range from 0 to 12.

True/False: 8 questions, each with one correct answer (+1 point). Scores range from 0 to 8. Food Group Questions: 5 questions, with 25 foods to choose from. Correct answers (+1 point), wrong answers (-1 point). Highest score is +15, lowest is -10. (Akder, 2017). 24-hour food consumption record method: The 24-hour (1-day) food consumption record method was used to determine nutritional status. At the beginning of the study, a 24-hour food consumption record of the previous day was taken from the players. This method is recommended by the European Food Safety Authority (EFSA, 2014).

With this method, players were asked to indicate the foods they consumed at each meal the day before they participated in the study, along with detailed quantities, on the form sent to them. Household measurements (water glass, thin/thick slice, coffee/tea cup, matchbox, tablespoon/teaspoon, etc.) were used to indicate food measurements.

Food consumption records obtained from the players were entered into the Nutrition Information System (NIS) version 7.2 system and macro and micronutrients such as energy, protein, carbohydrate, fat, and fiber were determined. This study was conducted in accordance with the Principles of the Declaration of Helsinki.

Diet Quality Index (DQI-I): (DQI-I) of food consumption records was calculated to analyze the current diet quality of the players at the beginning and end of the study. The DQI-I is a diet quality measurement tool developed in line with the Recommended Dietary Allowance (RDA) recommendations for daily consumption of food and nutrients. The diet quality index consists of 4 main components. These components are diversity, adequacy, dietary moderation, and overall balance. The diversity component is scored between 0-20 points by evaluating the general nutrient diversity and diversity in terms of protein source. The adequacy component is scored between 0-40 points by comparing and scoring protein, grain, fruit, vegetable, pulp, vitamin C, calcium, and iron consumption according to RDA recommendations. The dietary moderation component is scored between 0-30 by evaluating and scoring cholesterol, saturated fatty acids, sodium, total fat, and empty energy nutrients according to RDA recommendations. The overall balance component is scored between 0-10 points by assessing the ratio of macronutrients and fatty acids. After the individual scores of all components are calculated, they are summed to form the DQI-I total score between 0-100. DQI-I is an internationally applicable index that enables the comparison of the nutritional status of developed and developing countries. The increase in the DQI-I indicates an increase in diet quality (Kim, 2003).

## 3. Results

### 3.1. Nutrition education

Healthy nutrition training was provided by the dietitian who conducted the study. This training consists of 3 modules.

Module 1. The importance of adequate and balanced nutrition and being at an ideal weight is mentioned. Nutrient, carbohydrate, protein, fat, vitamin, and mineral definitions were made. The benefits of nutrients and the foods in which they are found are given as examples. The importance of water is mentioned in this module. Module 2. The module aims to introduce food groups and explain them with examples. Faulty nutrition behaviors, obesity, causes of weakness, breakfast, and the importance of main meals and intermediate meals are also included in this module. Module 3. In the module, the importance of adequate and balanced nutrition in athletes is explained with examples and recommendations shared. Pre- and post-sport meal recommendations were given. General reinforcement of all modules was done interactively. Nutrition training was completed with a question-answer activity.

After data collection in the first week, the study lasted 4 weeks in total, including 3 weeks of training implementation, 1 time per week.

The General Information and Dietary Habits Questionnaire, 24-Hour Food Consumption Record, and DQI-I calculation, which were administered to the players at the beginning of the study, were also administered at the end of the training. The entire data collection process and training were conducted online.

### 3.2. Data evaluation

Body Mass Indexes of adolescents were calculated using the formula  $BMI = \text{weight (kg)} / \text{height}^2 \text{ (m}^2\text{)}$ . BMI, height and weight percentiles were evaluated according to the standards developed by Neyzi et al. (2015) for Turkish children.

The data obtained were statistically evaluated in SPSS 21.0 package program. Statistical significance was accepted as  $p < 0.05$  in all analyses. In descriptive statistics, numbers, percentages, mean, lower-upper value and standard deviation values will be included. The square test was applied in the analysis of qualitative variables. The conformity of the data to normal distribution was checked with the Kolmogorov-Smirnov test. The t-test was used to compare means. The distribution of anthropometric measurements of the players in the study is given in Table 1.

**Table 1**  
Distribution of anthropometric measurements of volleyball players.

	Average	Standard Deviation	Minimum	Maximum
<b>n=40</b>				
<b>Age</b>	12,70	0,883	9	14
<b>Body Weight (kg)</b>	50,38	12,382	37	93
<b>Height (cm)</b>	159,00	3,550	154	165
<b>BMI (kg/m<sup>2</sup>)</b>	19,38	3,93	14,17	32,17
<b>BMI Z Score</b>	-0,41	1	-1,73	2,84

A total of 40 players participated in the study. The average age of the players was 12.70 (SD=0.883). The youngest player was 11 years old and the oldest player was 14 years old. The mean body weight was 50.38 kg (SD=12.382). The weakest player weighed 37 kg, while the player with the highest body weight weighed 93 kg. The mean height was 159 cm (SD=3,550). The shortest player was 154 cm and the tallest player was 165 cm.

According to the percentile groups of anthropometric measurements of adolescents, 55% of the players in terms of

weight, 47.5% in terms of height and 42.5% in terms of BMI are in the 25-75 percentile range, which is the recommended percentile value. Although the rate of those below the 10th percentile according to weight was 7.5% and the rate of those below the 10th percentile according to height was 2.5%, those below the 25th percentile according to BMI levels constituted 40% of the population. Descriptive statistics of the players' dietary habits before / after the training are presented in Table 2.

**Table 2**  
Distribution of dietary habits of adolescents pre and post NE.

	Pre-NE	Post NE		P		
		N	(%)		N	(%)
<b>Number of main meals consumed</b>	1 Meal	-	-	1	2.5	0.227
	2 Meals	17	42.5	11	27.5	
	3 Meals	23	57.5	28	70.0	
<b>Number of snacks consumed</b>	1 Snack	7	17.5	6	15.0	1.000
	2 Snacks	22	55	22	55.0	
	3 Snacks	11	27.5	12	30.0	
<b>Skipping meals</b>	There is	27	67.5	25	62.5	0.804
	No	13	32.5	15	37.5	
	Evening	3	7.5	2	5.0	
	Snacks	11	27.5	9	22.5	
	Breakfast	7	17.5	6	15.0	
	Noon	8	20	9	22.5	

Before the NE, 57.5% of the players consumed 3 main meals in 3 days, while 42.5% consumed 2 main meals per day. After the training, the number of main meals increased and 70% of the players preferred 3 main meals. In addition, 55% consumed 2 snacks per day, 27.5% consumed 3 snacks per day, and 17.5% consumed 1 snack per day. After the NE, the preference for snacks increased and 30% of the players started to prefer 3 snacks. Those who skip meals are 67.5%. After the training, the rate of skipping meals decreased (62.5%). However, this decrease was not significant ( $p > 0.05$ ). The most frequently skipped meal was snacks (27.5%). Lunch was skipped by 20%, breakfast by 17.5% and dinner by 7.5%. The number of players skipping snacks decreased after the training.

Table 3 shows the statistics of the answers given to the questions about the players' dietary preferences before and after the training.

**Table 3**  
Distribution of nutrition preferences of adolescents.

Preferences	Pre-NE	Post NE		P		
		N	%		N	%
<b>Answer Category</b>	There is	37	92.5	37	92.5	1.0
	No	3	7.5	3	7.5	
	<b>Consumption of drinks with added sugar</b>	1 cup or less	23	57.5	20	
<b>Consumption of fast-food (hamburgers, pizza, pasta, etc. not prepared at home)</b>	2-3 cups of water	14	35	18	45.0	1.0
	Total	40	100	40	100.0	
	There is	34	85	35	87.5	
	No	6	15	5	12.5	
	2-3 times a month	25	62.5	26	65.0	
	2-3 times a week	8	20	7	17.5	
<b>prepared at home)</b>	4-6 times a week	2	5	2	5.0	1.0
	Every day	-	-	1	2.5	
	No	10	25	16	40.0	

When Table 3 is analyzed, 92.5% of the players consumed drinks with added sugar before and after the training. The number of sugar-containing beverages consumed was 1 cup or less for 57.5% of the players. While 35% consumed 2-3 cups of sugar-added beverages before the training, this rate increased to 45% after the training. While 85% of the players consumed fast-food before the training, 87.5% of them consumed fast-food after the training. While the frequency of fast-food consumption was 2-3 times a month for 62.5% of the players before the training, this frequency increased to 65% after the training.

While players preferred crackers, biscuits, and the like, fruit, and chocolate for snacks before the training, the number of those who preferred fruit increased after the training. Although the number of those who prefer chocolate, crackers, biscuits, and the like decreased, they are still the most preferred products for snacks.

Statistical analysis of the players' nutrition knowledge levels before and after the training is presented in Table 4.

**Table 4**  
Analysis of adolescents' nutrition knowledge level scores Pre- and Post-NE.

	Average	N	Standard Deviation	P
Pre-NE Knowledge Level	6.7750	40	1.16548	0.042
Post-NE Knowledge Level	7.9000	40	1.27702	

Statistically, there is a significant difference between the nutrition knowledge levels of the players before and after the

training ( $p < 0.05$ ). Therefore, the knowledge level of the players increased after the training.

The results of the analysis on whether there is a significant difference between the players' Diet Quality Index and its components before and after the NE are presented in Table 5. It was determined that NE had a significant effect on food diversity and vegetable intake.

#### 4. Discussion

This study aimed to evaluate the impact of a nutrition education program on volleyball players from socioeconomically disadvantaged areas, focusing on their nutritional knowledge and diet quality. By analyzing pre- and post-education assessments, the research explored changes in knowledge levels and food consumption patterns among players. Studies show that adolescents generally have unhealthy eating habits, especially skipping breakfast and consuming foods with high-calorie content frequently (Zahrah, 2023; Li et al., 2024). This increases the likelihood of obesity. Regular breakfast has been shown to support the protection of health (Xian, 2023). The habit of eating breakfast was found to be 51% in Istanbul.19,20 Considering the skipping of meals in adolescents in Turkey, it was found that 69.5% in Gaziantep and 81% in Bornova skipped meals. It was shown that breakfast was the most frequently skipped meal (Tanrıverdi, 2011).

In this study, the number of main meals increased after the training and 70% of the players preferred 3 main meals. The preference for snacks increased after the training and 30% of the

**Table 5**  
Results of the analyses of the differences of the diet quality index and its components of adolescents Pre- and Post -NE.

	Pre NE					Post NE					Mean	t	df	P
	N	Average	Std. Deviation	Min	Max	Average	Std. Deviation	Min	Max					
Food Diversity (0-15)	40	11.45	2.791	3	15	9.9	3.153	3	15	1.55	2.401	39	<b>0.021</b>	
Protein Diversity (0-5)	40	4.2	1.265	1	5	4.08	1.347	0	5	0.125	0.429	39	0.67	
Vegetable	40	1.28	0.933	0	3	0.9	0.632	0	3	0.375	2.199	39	<b>0.034</b>	
Fruit	40	2.53	2.05	0	5	3.1	1.865	0	5	-0.575	-1.518	39	0.137	
Grain	40	3.5	1.086	1	5	2.95	1.648	0	5	0.55	1.936	39	0.06	
Pulp	40	2.95	1.319	1	5	2.75	1.446	1	5	0.2	0.781	39	0.44	
Protein	40	5	0	5	5	4.9	0.441	3	5	0.1	1.433	39	0.16	
Iron	40	4.15	1.001	3	5	4.15	1.189	1	5	0	0	39	1	
Calcium	40	2.15	1.189	1	5	1.95	1.197	1	5	0.2	0.85	39	0.401	
Vitamin C	40	3.8	1.418	1	5	3.35	1.35	1	5	0.45	1.548	39	0.13	
Total Oil	40	0.15	0.662	0	3	0.15	0.662	0	3	0	0	39	1	
Saturated Fat	40	0.15	0.662	0	3	0	0	0	0	0.15	1.433	39	0.16	
Oil	40	0.15	0.662	0	3	0	0	0	0	0.15	1.433	39	0.16	
Cholesterol	40	3.15	2.537	0	6	4.28	2.242	0	6	-1.125	-1.955	39	0.058	
Sodium	40	2.63	2.467	0	6	3.23	2.577	0	6	-0.6	-0.984	39	0.331	
Empty	40	1.13	1.62	0	6	0.9	1.549	0	6	0.225	0.621	39	0.538	
Energised Feed.	40	0	0	0	0	0	0	0	0	0	0	0	-	
Carb/Pro/Oil	40	0	0	0	0	0	0	0	0	0	0	0	-	
Fatty Acids Ratio	40	0.35	1.001	0	4	0.5	1.177	0	4	-0.15	-0.595	39	0.555	
Diversity	40	15.65	3.773	4	20	13.98	4.252	3	20	1.675	1.957	39	0.058	
Competence	40	25.35	5.522	14	36	24.05	5.602	13	34	1.3	1.386	39	0.174	
Dietary Measurement.	40	7.2	4.339	0	15	8.55	4.163	0	18	-1.35	-1.311	39	0.198	
Total	40	7.2	4.339	0	15	8.55	4.163	0	18	-1.35	-1.311	39	0.198	
General Balance	40	0.35	1.001	0	4	0.5	1.177	0	4	-0.15	-0.595	39	0.555	
Total	40	0.35	1.001	0	4	0.5	1.177	0	4	-0.15	-0.595	39	0.555	
<b>DQI Total</b>	40	48.2000	8.02624	27	63	46.5750	7.65904	32	62	1.625	0.994	39	0.326	

players started to prefer 3 snacks. The rate of skipping meals decreased after the training (62.5%). The number of players skipping snacks decreased after the training. While the players preferred crackers, biscuits, and the like, fruit, and chocolate for snacks before the training, the number of those who preferred fruit increased after the training. Although the number of those who preferred chocolate, crackers, biscuits' and the like decreased, they were still the most preferred products for snacks. Positive effects of nutrition education on the number of main meals, snacks, and snack preferences were observed. Therefore, supplying healthy nutrition education practices during adolescence, when eating habits begin to form, is a strategy that positively affects public health (Ares et al., 2024). After the nutrition education, no positive effects were observed on the consumption of sugar-added beverages and fast-food in the study group. The ease of access to such foods and the difficulty in accessing healthy alternatives are thought to be one of the reasons for this result. Positive changes in the nutritional habits of the players after the training are promising for public health.

According to the DQI-I criteria, scores below 60 indicate poor diet quality, while scores above 60 indicate good diet quality. Improved diet quality in adolescents has positive effects such as decreasing obesity indicators, increasing cognitive functions, and improving mental health (Larruy-Garcia et al., 2024). Having parents with a high level of education, mothers with good nutritional knowledge, a healthy home environment, absence of distractions at breakfast, and regular physical activity are factors that improve diet quality (Arouca, 2019). According to a study conducted in the Balearic Islands of Spain, the average DQI-I value was 43.0.24 A study conducted in southern Spain showed that the DQI-I score was 56.3.25 The mean DQI-I values of Americans and Chinese were 59.1 and 60.5 points, respectively.15 In this study, the mean DQI-I score of adolescents was 48.2 before the training and 46.58 after the training. There was no statistically significant difference between the pre-training and post-training diet quality index measurements, except for food diversity and vegetable intake ( $p > 0.05$ ). It was determined that the adolescents participating in this study had poor diet quality both before and after the training. This result is not surprising when we consider that our study group resided in areas with low socioeconomic status. There is a need for practices that facilitate access to nutritious and healthy foods in disadvantaged areas (Veldwisch et al., 2024).

A systematic review provides evidence that school-based nutrition education interventions are effective in reducing BMI in children and adolescents, especially if the intervention period is longer than one school year (Mogre et al., 2024). In this study, there was no significant difference between the weights of the players before and after the intervention. This is thought to be due to the fact that the nutrition education we implemented was a short period of 3 weeks.

A healthy and balanced diet is essential for adequate and timely intake of energy and nutrients needed for growth, development, health maintenance, and improved quality of life (Keeley, 2019; Cerf, 2025). However, adolescent growth and nutrition are overlooked in the United Nations (UN) Decade of Action on Nutrition (Mariscal-Arcas, 2007). The Sustainable Development Goals for nutrition do not include adolescent-specific targets (WHO, 2017). Adolescence is a unique point of intervention because people in this age group are more susceptible to lifestyle changes (Bakraina, 2018). Adolescence

should be targeted to promote healthy eating and lifestyle habits as a foundation for community health (TUBER, 2015). A study in Libya showed a significant effect of socio-demographic variables on nutritional status in school-aged children. Schools are considered the best place for food education and childhood is a crucial period when eating habits are formed that continue into adulthood. The benefits of nutrition education as part of the curriculum will have significant impacts on healthy nutrition (Eljamay, 2022; Albin et al., 2024). There have, therefore, been numerous global calls for the integration of food and nutrition education into school curricula as a key strategy to prevent all forms of malnutrition and support the transformation of food systems (WHO, 2017; FAO, 2020).

Statistically, there is a significant difference between the nutrition knowledge levels of the players before and after the training ( $p < 0.05$ ). Therefore, the knowledge level of the players increased significantly after the training. However, when we examined the DQI-I score of adolescents living in disadvantaged areas, no significant increase was observed in parallel with the increased knowledge level after the training. The fact that the increased level of nutrition knowledge did not affect diet quality is thought to be due to the limited access to healthy foods for children living in disadvantaged areas.

#### 4. Conclusion

As a result of the study planned to investigate the effect of nutrition education on nutritional knowledge level and diet quality in female volleyball players living in disadvantaged areas, the 3-week nutrition education provided caused a significant increase in the level of nutritional knowledge but did not cause significant changes in the Diet Quality Index (DQI-I). Nutrition education can help adolescents gain the knowledge and skills they need to make healthy food choices and develop lifelong healthy eating patterns. The nutrition education also had positive effects on some eating habits such as skipping meals, paying attention to the presence of each food group on the plate, and food preferences in snacks, but it did not have a positive effect on the frequency of fast-food consumption. Nutrition education did not cause a significant change in body weight. It is thought that the reason why 3-week nutrition education applied to female adolescents living in disadvantaged regions did not have a positive effect on DQI-I scores and its components while increasing the level of knowledge is related to socioeconomic level, accessibility of nutritious foods, and nutritional knowledge levels of families.

The study has some limitations, including the relatively small sample size and the fact that it was conducted with participants from only one sport, which may limit the generalizability of the findings to other athletic disciplines.

**Acknowledgement:** We would like to thank Dear Ebrar Karakurt, the founder of Ebrar Karakurt Volleyball Academy, and all the volleyball players who participated.

**Conflict of interest:** The authors declare that they have no conflict of interests.

**Informed consent:** The authors declare that this manuscript did not involve human or animal participants and informed consent was not collected.

## References

- Akder, R. N. (2017). *Tabak modeli ile verilen beslenme eğitiminin ilköğretim ikinci sınıf öğrencilerinin beslenme bilgi ve alışkanlıklarına etkisi* (Master's thesis). Ankara University Institute of Health Sciences.
- Albin, J. L., Thomas, O. W., Marvasti, F. F., & Reilly, J. M. (2024). Perspective: There and back again: A 40-year perspective on physician nutrition education. *Advances in Nutrition*, 100230.
- Ares, G., De Rosso, S., Mueller, C., Philippe, K., Pickard, A., Nicklaus, S., ... & Varela, P. (2024). Development of food literacy in children and adolescents: Implications for the design of strategies to promote healthier and more sustainable diets. *Nutrition Reviews*, 82(4), 536-552.
- Arouca, A., Moreno, L. A., Gonzalez-Gil, E. M., Marcos, A., Widhalm, K., Molnár, D., ... & Michels, N. (2019). Diet as moderator in the association of adiposity with inflammatory biomarkers among adolescents in the HELENA study. *European Journal of Nutrition*, 58(5), 1947-1960.
- Atchoarena, D., & Gasperini, L. (2003). *Education for Rural Development towards New Policy Responses*. International Institute for Educational Planning (IIEP) UNESCO. 7-9 rue Eugene-Delacroix, 75116 Paris, France.
- Bakrania, S., Ghimire, A., & Balvin, N. (2018). *Bridging the gap to understand effective interventions for adolescent well-being: An evidence gap map on protection, participation, and financial and material well-being in low-and middle-income countries* (pp. 1-63). New York, NY, USA: UNICEF Office of Research-Innocenti.
- Cerf, M. E. (2025). Nutrition and health promotion: The life-course approach. In *Handbook of Concepts in Health, Health Behavior and Environmental Health* (pp. 1-21). Springer Nature Singapore.
- Eljamay, S. M., Elgebaily, E. S. M., Eljamay, F. M., & Younis, F. H. (2022). The rate of socioeconomic and demographic factors affecting body mass index (BMI) among teenagers in Derna City, Libya. *African Journal of Advanced Pure and Applied Sciences (AJAPAS)*, 91-97.
- EFSA, (2014). European Food Safety Authority, Guidance on the EU menu methodology. *EFSA Journal*, 12(12), 3944. <https://efsa.onlinelibrary.wiley.com/doi/epdf/10.2903/j.efsa.2014.3944>
- FAO, (2020). Food and Agriculture Organisation, School-based food and nutrition education: A white paper on the current state, principles, challenges, and recommendations for low- and middle-income countries, <https://openknowledge.fao.org/items/5d1441bb-8d1b-414d-93fb-6d8f48de0423>, Last accessed on February, 2025.
- Rozanski, A. (2023). New principles, the benefits, and practices for fostering a physically active lifestyle. *Progress in Cardiovascular Diseases*, 77, 37-49.
- Kazu, I. Y. (2019). The problems faced by socio-economically disadvantaged people during their education. *Journal of Dicle University Ziya Gökalp Faculty of Education*, 34, 38-47.
- Hatun, S., Etiler, N., & Gonullu, E. (2003). Poverty and its effects on children. *Journal of Pediatrics*, 46(4), 251-260.
- Keeley, B., Little, C., & Zuehlke, E. (2019). The State of the World's Children 2019: Children, Food and Nutrition--Growing Well in a Changing World. *UNICEF*.
- Kim, S., Haines, P. S., Siega-Riz, A. M., & Popkin, B. M. (2003). The Diet Quality Index-International (DQI-I) provides an effective tool for cross-national comparison of diet quality as illustrated by China and the United States. *The Journal of nutrition*, 133(11), 3476-3484.
- Larruy-García, A., Mahmood, L., Miguel-Berges, M. L., Masip, G., Seral-Cortés, M., De Miguel-Etayo, P., & Moreno, L. A. (2024). Diet quality scores, obesity, and metabolic syndrome in children and adolescents: A systematic review and meta-analysis. *Current Obesity Reports*, 1-34.
- Li, S., Li, X., Wang, J., Jiang, D., Zhang, Y., Lou, W., ... & Gong, Q. (2024). Associations between insufficient sleep, skipping breakfast, and depressive symptoms in children and adolescents: A school-based cross-sectional study in China. *Preventive Medicine*, 184, 107978.
- Mariscal-Arcas, M., Romaguera, D., Rivas, A., Feriche, B., Pons, A., Tur, J. A., & Olea-Serrano, F. (2007). Diet quality of young people in southern Spain evaluated by a Mediterranean adaptation of the Diet Quality Index-International (DQI-I). *British Journal of Nutrition*, 98(6), 1267-1273.
- Mogre, V., Sefogah, P. E., Adetunji, A. W., Olalekan, O. O., Gaa, P. K., Ayettey Anie, H. N., & Tayo, B. (2024). A school-based food and nutrition education intervention increases nutrition-related knowledge and fruit consumption among primary school children in northern Ghana. *BMC Public Health*, 24(1), 1739.
- Neyzi, O., Bundak, R., Gökçay, G., Günöz, H., Furman, A., Darendeliler, F., & Baş, F. (2015). Reference values for weight, height, head circumference, and body mass index in Turkish children. *Journal of Clinical Research in Pediatric Endocrinology*, 7(4), 280.
- Nguyen, G., Boath, A., & Heslehurst, N. (2023). Addressing inequalities and improving maternal and infant outcomes: The potential power of nutritional interventions across the reproductive cycle. *Proceedings of the Nutrition Society*, 82(3), 241-252.
- Schneider, B. C., Dumith, S. D. C., Lopes, C., Severo, M., & Assunção, M. C. F. (2016). How do tracking and changes in dietary pattern during adolescence relate to the amount of body fat in early adulthood?. *PLoS one*, 11(2), e0149299.
- Souilla, L., Larsen, A. C., Juhl, C. B., Skou, S. T., & Bricca, A. (2024). Childhood and adolescence physical activity and multimorbidity later in life: A systematic review. *Journal of Multimorbidity and Comorbidity*, 14, 26335565241231403.
- Simsek, H. G., Gunay, T., & Ucku, R. (2010). The effect of social inequalities on coronary heart disease risk factors: A population-based, cross-sectional study in Izmir. *Anatolian Journal of Cardiology/Anadolu Journal of Cardiology*, 10(3), 190-198.
- Tanrıverdi, S., Gonulluoglu, K., & Balık, Z. (2011). Investigation of eating attitudes, eating behaviors, and self-esteem of high school students. *Gaziantep Medical Journal*, 17(1), 33-39.
- TUBER. (2015). TC Sağlık Bakanlığı Yayın, ISBN : 978-975-590-608-9. 1-288.
- Veldwisch, G. J., Amerasinghe, P., Letema, S., & Wessels, M. T. (2024). The practices and politics of irrigated urban agriculture. *Water International*, 49(2), 129-143.
- Vlaardingerbroek, H., Joustra, S. D., Oostdijk, W., de Bruin, C., & Wit, J. M. (2024). Assessment of nutritional status in the diagnostic evaluation of the child with growth failure. *Hormone Research in Paediatrics*, 97(1), 11-21.
- Winpenny, E. M., van Sluijs, E. M., White, M., Klepp, K. I., Wold, B., & Lien, N. (2018). Changes in diet through adolescence and early adulthood: longitudinal trajectories and association with key life transitions. *International Journal of Behavioral Nutrition and Physical Activity*, 15, 1-9.
- Wu, Z. J., Han, C., Wang, Z. Y., & Li, F. H. (2024). Combined training prescriptions for improving cardiorespiratory fitness, physical fitness, body composition, and cardiometabolic risk factors in older adults: Systematic review and meta-analysis of controlled trials. *Science & Sports*, 39(1), 1-18.
- WHO, (2017). World Health Organization, Global targets 2025 to improve maternal, infant and young children nutrition. Geneva: World Health Organization, <https://pesquisa.bvsalud.org/portal/resource/pt/who-259188>, Last accessed on February, 2025
- Xian, X., Wang, C., Yu, R., & Ye, M. (2023). Breakfast frequency and sleep quality in college students: The multiple mediating effects of sleep chronotypes and depressive symptoms. *Nutrients*, 15(12), 2678.
- Zahrah, N. I., Fanani, M., & Ardyanto, T. D. (2023). The relationship between emotional eating, meal skipping and unhealthy food consumption pattern in adolescent girls. *The Indonesian Journal of Public Health*, 18(1), 47-58.

**Cite as:** Aytekin, S., & Meral Koc, B. (2025). The effect of nutritional education on nutritional knowledge level and diet quality in volleyball players living in a disadvantaged area. *Front Life Sci RT*, 6(1), 15-20.



## Research article

## Possible effect of E-SELECTIN (Ser128Arg), L-SELECTIN (Pro213Ser), P-SELECTIN (Thr715Pro) gene polymorphisms for COVID-19 disease severity

Nihan Bozkurt<sup>1</sup> , Figen Guzelgul<sup>2</sup> , Nejmiye Akkus<sup>3</sup> , Kubra Sahin<sup>1</sup> , Sadegul Savkin<sup>1</sup> ,  
Tuncay Yigit<sup>4</sup> 

<sup>1</sup> Tokat Gaziosmanpasa University, Faculty of Medicine, Department of Medical Biology, 60030, Tokat, Türkiye

<sup>2</sup> Tokat Gaziosmanpasa University, Faculty of Pharmacy, Department of Biochemistry, 60250, Tokat, Türkiye

<sup>3</sup> Tokat Gaziosmanpasa University, Faculty of Medicine, Department of Medical Genetics, 60030, Tokat, Türkiye

<sup>4</sup> Tokat Public Hospital, Department of Internal Medicine, 60030, Tokat, Türkiye

**Abstract**

COVID-19 is an inflammatory disease characterized by a severe immune response, the pathogenesis of which is mediated by many cytokines. It was determined that the cytokine storm that occurs during severe infection may trigger coagulopathy by disrupting the interaction between platelets, endothelium, and leukocytes. Selectins (P-SELECTIN, L-SELECTIN, E-SELECTIN) are active in the mammalian immune system, especially in tissues. They are important adhesion molecules that play a part in the formation of the inflammatory response and the healing process. In this study, the probable effects of L-SELECTIN, P-SELECTIN, and E-SELECTIN gene variations on the pathogenesis of COVID-19 (on the severity and course of the disease) were investigated. In this direction, 44 controls and 129 patients (45 mild symptoms, 30 ward patients, and 54 intensive care patients) were included in the study. Genotyping of selectin polymorphisms was performed by the PCR-Restriction Fragment-Length Polymorphism (RFLP) techniques. In E-SELECTIN, CC genotype and C allele frequency were higher in inpatients than in the control group. The allele frequency and AA genotype were higher in the control group ( $p = 0.0001$ ). No significant relationship was detected with P-SELECTIN and L-SELECTIN polymorphisms. In addition, the binary genotype distribution between the loci studied in our study and the control groups was also examined. Statistically significant differences were detected in P-SELECTIN/E-SELECTIN and E-SELECTIN/L-SELECTIN binary genotypes. Therefore, it was concluded that binary genotypes may affect disease severity or the course of the disease.

**Keywords:** COVID-19; E-SELECTIN; L-SELECTIN; P-SELECTIN; polymorphisms; susceptibility

**1. Introduction**

COVID-19, which has become a global health problem affecting the whole world and has been accepted as a pandemic by the World Health Organization, has caused many social, psychological, educational, and especially economic problems (Mohanty et al., 2020; Abdelmageed et al., 2025). The most important finding in the diagnosis of COVID-19 disease is high infection, but radiological images and pathological and clinical

findings are also necessary for definitive diagnosis (Agrati et al., 2021a). However, clinical findings vary from mild symptoms to severe symptoms and can sometimes be asymptomatic. In cases where severe symptoms are observed, the need for intensive care, respiratory failure, and multiple organ failure occur and result in death (Eketunde et al., 2020). In the early stages of COVID-19, cough, dyspnea, fever, and obstructive sleep apnea are common symptoms in the patient, while in the advanced stages, complaints such as metabolic irregularities,

\* Corresponding author.

E-mail address: [nihan.bozkurt08@gmail.com](mailto:nihan.bozkurt08@gmail.com) (N. Bozkurt).

<https://doi.org/10.51753/flsrt.1580594> Author contributions

Received 07 November 2024; Accepted 21 February 2025

Available online 30 April 2025

2718-062X © 2025 This is an open access article published by Dergipark under the [CC BY](https://creativecommons.org/licenses/by/4.0/) license.

thromboembolism, sepsis, kidney damage, and acute respiratory distress syndrome are observed (Attiq et al., 2024; Li et al., 2024). In addition to playing a role in hemostasis, immune response, and angiogenesis, endothelial cells can form different barrier structures and are effective in different physiological functions such as gas exchange, nutrient absorption, and organ protection (Wu et al., 2024). Conditions such as long-term infection, neuronal dysfunction, thromboembolism, and especially endothelial damage are also effective in the multifactorial pathogenesis of post-COVID syndrome (Maltezou, 2025). Studies show that the impairment of vascular endothelial function caused by COVID-19 may be permanent and that this damage is effective in vascular events that develop both during and after COVID-19 infection (Aljadah et al., 2024).

The most well-known cause of death during the COVID-19 epidemic is thromboembolic complications. Interrelated mechanisms such as coagulopathy, endotheliopathy, platelet activation, and enhanced adhesiveness to leukocytes and damaged endothelium have been linked to the hypercoagulability seen in COVID-19 (Watany et al., 2022). The anticoagulant system contributes to the complicated process of coagulopathy in COVID-19. An appropriate balance needs to be struck during this process, particularly concerning fibrinolytic, clotting, and endothelial components (Job et al., 2023; Sayyadi et al., 2023).

Selectins are an essential adhesion molecule in the immune system and inflammatory response, and they are linked to numerous illnesses and biological processes (Selvaraj et al., 2022). The significance of these adhesion molecules in the inflammatory response has been shown by their simultaneous release to the inflamed site (Agrati et al., 2021b).

Platelet cells and endothelial cells are the primary cells that express P-SELECTIN, a 140 kDa single-chain glycoprotein. Immune cells attaching to P-SELECTIN is the initial stage of the inflammatory process (Imhof and Dunon, 1995; Zlibut et al., 2019). P-SELECTIN expression increases depending on a stimulus (thrombin, etc.) and is stored in platelets (in alpha granules) and endothelial cells (in Weibel-Palade bodies) (Longo and Wakefield, 2007). E-SELECTIN, another member of the selectin family, is a 115 kDa adhesion protein that is expressed on the surface of endothelial cells and whose expression rises in response to endothelial cell damage. Shortly after the increase in expression, its levels fall to initial levels (Wong and Dorovini-Zis, 1996; Mantovani and Dejana, 1998). The last member of selectins, L-SELECTIN, is expressed in leukocytes, unlike other members. The main function of L-SELECTINS is to ensure the aggregation and migration of lymphocytes (Hirata, 2016). Research indicates that the degree of COVID-19 and thrombotic disorders is correlated with endothelial, platelet, and neutrophil activity (Petito et al., 2023).

The entry and replication of SARS-CoV-2 into cells, as well as the development of the immune response, are significantly influenced by genetic polymorphisms, which are known to be crucial in determining susceptibility or resistance to other viral diseases. Numerous genes and their combinations are believed to be involved in the pathophysiology of COVID-19 (Debnath et al., 2020; Dieter et al., 2022). As a result, the connection between COVID-19 and single nucleotide polymorphisms has been the subject of numerous investigations (Anastassopoulou et al., 2020; Debnath et al., 2020; Elhabyan et al., 2020; Ozturk et al., 2020; Dieter et al., 2022).

This study aims to explain the role of P, E, and L-SELECTIN gene polymorphisms, which are effective in the

inflammatory response and play a role in adhesion interactions in COVID-19 patients, in the susceptibility to this infection, as well as their possible relationship with the severity of the disease.

## 2. Materials and methods

### 2.1. Participants

This study included 129 COVID-19 patients with positive RT-PCR test results and 44 healthy controls with negative RT-PCR results, who applied to Tokat State Hospital between 2019-2020. Patients and controls who had previously had COVID-19 were not included in the study. The G\*Power version 3.1.9.4 program was used to determine the required sample size and it was determined that at least 30 patients and 30 controls were sufficient for the sample size (Power:0.95, effect size:1.086, margin of error:0.05). This study followed the rules of the Declaration of Helsinki. In addition, necessary permissions were obtained from Tokat Gaziosmanpasa University Non-invasive Clinical Research Ethics Committee (22-KAEK-211). Necessary consent forms were obtained from the participants in the control and patient groups. Volunteers in the study were divided into 3 groups according to the severity of the disease: those with a mild course, those needing intensive care, and inpatients (hospitalized patients).

The intensive care group (collected from patients hospitalized in Tokat Gaziosmanpasa University Intensive Care Unit) included individuals who were >18 years old, vaccinated or unvaccinated, had findings compatible with COVID-19 pneumonia on chest radiography or thoracic tomography and these findings could not be explained by another etiology and other etiologies were excluded, had dyspnea and respiratory distress, tachypnea (respiratory rate >30/min), increased O<sub>2</sub> requirement during follow-up, SpO<sub>2</sub><90%, PaO<sub>2</sub><70mmHg, PaO<sub>2</sub>/Fio<sub>2</sub>:<300 despite >5L/min oxygen support. The mild course group included individuals who were >18 years old, had not been hospitalized due to COVID-19, and were not vaccinated. The inpatient group consisted of individuals who were >18 years old had never been vaccinated and did not need intensive care but needed hospital care. The control group consisted of individuals who were >18 years old, unvaccinated, and had never had COVID-19. Patient and control samples were investigated in terms of E-SELECTIN, P-SELECTIN, and L-SELECTIN polymorphisms. All analyses were first examined among the total patient and control groups, and then subgroup (mild course, intensive care, inpatients, and control) analyses were performed.

### 2.2. Genotyping

Blood samples from both COVID-19 patients and controls were isolated using the PureLink™ Genomic DNA Mini Kit (USA). Polymerase Chain Reaction and Restriction Fragment Length Polymorphism (PCR-RFLP) techniques were utilized to establish the genotypes of L-SELECTIN Pro213Ser (rs2229569), P-SELECTIN Thr715Pro (rs6136) and E-SELECTIN Ser128Arg (rs7799039) polymorphisms. The PCR program, primers, restriction enzymes, and restriction products used in the determination of polymorphisms are shown in Table 1. The PCR and restriction products obtained were visualized using agarose gel electrophoresis. For doubtful results, we performed a second PCR-RFLP.

**Table 1**

Primer sequences, restriction enzymes, PCR program, PCR lengths, and restriction lengths for selectin polymorphisms.

Polymorphism	Primer sequence	PCR Product Lengths	PCR programme	Restriction enzyme	Restriction product size
E-SELECTIN Ser128Arg	5'AGAAAGAGGCAAGAACCAGACT-3' 5'AAAGGCACTCAGTATAAGCACA-3'	193 bp	95°C 5 min 94°C 20 sec 58°C 30 sec 72°C 45 sec 72°C 7 min 40 cycle	PstI	109+84 bp 193 bp
P-SELECTIN Thr715Pro	5'ATTGTACCTTGGCAGGTTGG-3' 5'TTTCTGCAGCTGTGAAATGC-3'	198 bp	94°C 5 min 94°C 30 sec 60°C 30 sec 72°C 30 sec 72°C 7 min 38 cycle	Eco91I (BstEII)	163+35 bp 198 bp
L-SELECTIN Pro213Ser	5'TGATTCACTGTGAGCCTTTG-3' 5'CTTGACAGGTTGGTTCTG-3'	186 bp	94°C 5 min 94°C 20 sec 55°C 30 sec 72°C 30 sec 72°C 7 min 40 cycle	HphI	141+45 bp 186 bp

**2.3. Statistical analysis**

SPSS 16.0 and OpenEpi statistical software were used to analyze allele and genotype frequencies. Genotype and allele frequencies in the patient and control groups were determined using the  $\chi^2$  test.  $p < 0.05$  values were considered statistically significant.  $\chi^2$  or Fischer's exact test was used to determine the combined genotypes of polymorphisms. Allele and genotype distributions were determined by Hardy-Weinberg equilibrium. 95% odds ratios (ORs) and confidence intervals (CIs) were used to assess risk factors.  $p$  values were interpreted as significant when they were less than 0.05, and all  $p$  values were two-tailed.

**3. Results**

The study included 129 patients (78 men and 51 women) infected with COVID-19 and 44 controls. The average age of the 129 patients with COVID-19 was 49.27±19.26 years and the average age of the 44 controls was 39.20±11.55 years.

When the genotype and allele distributions in COVID-19 patient and control groups were analyzed, no statistically significant association was determined between COVID-19 and E-SELECTIN gene in terms of genotype and haplotype distributions ( $p=0.28$  and  $p=0.13$ , respectively). When AA and AC+CC or AA+AC and CC were evaluated, no statistically significant relationship was detected between COVID-19 patients and controls in AA and AC+CC, but borderline significance was detected in AA+AC and CC ( $p=0.34$  and  $p=0.049$ , respectively) (Table 2).

L-SELECTIN polymorphism was examined in terms of genotype and allele distributions in COVID-19 patient and control groups, but no statistically significant result was obtained ( $p=0.36$  and  $p=0.94$ , respectively). When CC and TC+TT or CC+TC and TT were evaluated, no statistically significant difference was found between COVID-19 patients and controls ( $p=0.62$  and  $p=0.24$ , respectively).

In terms of P-SELECTIN polymorphism genotype distribution in the COVID-19 patient and control groups, it was seen that 92.43% of the patients had the AA genotype, 7.56% had the AC genotype, and no patient with the CC genotype was encountered. In the control group, 95.12% AA genotype and 4.87% AC genotype were detected, while no CC genotype was found. When P-SELECTIN polymorphism was analyzed in terms of allele distributions in COVID-19 patients and control

groups, no statistically significant result was found ( $p=0.61$ ). When AA vs AC+CC was appraised, no statistically significant difference was detected between COVID-19 patients and controls ( $p=0.6$ ). When AA+AC vs CC was evaluated, statistical analysis could not be performed because there were no patients or controls with the CC genotype.

**Table 2**

Genotype distributions and allele frequencies of E-SELECTIN polymorphism.

Gene (Polymorphism)	Patients n=129 (%)	Controls (n=44)	$p$	OR (95% CI)
<b>E-SELECTIN</b>				
<b>Ser128Arg</b>				
Genotypes				
AA	90 (%70)	34 (%77.2)	$p=0.2844$	
AC	26 (%20)	9 (%20.5)		
CC	13 (%10)	1 (%2.3)		
AA:AC+CC	90 (%70): 39 (%30)	34 (%77.2): 10 (% 22.8)	$p=0.3499$	0.9029 (0.7419-1.099)
AA+AC:CC	116 (%90): 13 (%10)	43 (%97.7): 1 (%2.3)	$p=0.049$	0.9201 (0.8551-0.9901)
Allel				
A	206 (%80)	77 (%)	$p=0.131$	
C	52 (%20)	11 (%9.8)		

In the analysis of subgroups as patients (mild course, intensive care unit, hospitalized patients) and controls, no statistically significant difference was detected in terms of allele frequencies and genotype distribution in E-SELECTIN polymorphism in both mild course and intensive care patients. However, the genotype distributions and allele frequencies of E-SELECTIN polymorphism in inpatients were statistically significant ( $p=0.0001$  and  $p=0.000000794$ , respectively). When AA vs AC+CC and AA+AC vs CC were evaluated, a statistically significant difference was determined among these groups ( $p=0.0002$  and  $p=0.0003$ , respectively) (Table 3).

Genotype distributions and allele frequencies of P and L-SELECTIN polymorphisms were not statistically significant in all three groups (mild, intensive care, inpatient) compared to the control group. When examined for all groups AA vs AC+CC and AA+AC vs CC in the P-SELECTIN polymorphism, no statistically meaningful difference was identified among the two

groups. Similarly, when CC vs TC+TT and CC+TC vs TT were examined for all groups in L-SELECTIN polymorphism, no statistically significant difference was determined between the two groups.

**Table 3**

Genotype distributions and allele frequencies of E-SELECTIN polymorphism at inpatients.

Gene (Polymorphism)	Patients (inpatients) n=30 (%)	Controls (n=44)	P	OR (95% CI)
<b>E-SELECTIN Ser128Arg</b>				
Genotypes				
AA	10 (%33.33)	34 (%77.2)	<b>0.0001</b>	1.15 (0.05-0.42)
AC	10 (%33.33)	9 (%20.45)		
CC	10 (%33.33)	1 (%2.27)		
AA:AC+CC	10 (%33.33): 20 (%66.66)	34 (%77.2): 10 (22.72)	<b>0.0002</b>	0.04 (0.002-0.31)
AA+AC:CC	20 (%66.66): 10 (%33.33)	43 (%97.72): 1 (%2.27)	<b>0.0003</b>	0.14 (0.06-0.32)
Allele				
A	30 (%50)	77 (%87.5)	<b>0.0000</b>	0.14 (0.06-0.32)
C	30 (%50)	11 (%12.5)		

COVID-19 groups and control groups were also compared in terms of binary genotype for E-SELECTIN and P-SELECTIN, P-SELECTIN and L-SELECTIN, and E-SELECTIN and L-SELECTIN regions. Results for the E-SELECTIN and P-SELECTIN binary study were obtained from 118 COVID-19 patients and 41 control samples. 1 out of 9 binary genotypes (AA/CC) was statistically different between the groups ( $p=0.0457$ ) (Table 4). Results for the E-SELECTIN and L-SELECTIN binary study were obtained from 115 COVID-19 patients and 41 control samples. No statistically significant difference was detected between COVID-19 patient and control groups in terms of E-SELECTIN and L-SELECTIN binary genotypes. Likewise, results for the P SELECTIN and L SELECTIN binary study were obtained from 110 COVID-19 patients and 41 control samples. No statistically significant difference was detected between the COVID-19 patient and control groups in terms of P-SELECTIN and L-SELECTIN binary genotypes.

In our study, binary genotyping was performed in the mild course, intensive care, and inpatient subgroups compared to the

**Table 5**

Comparative analysis of combined genotypes of E-SELECTIN and P-SELECTIN in mild course, intensive care, and inpatient.

Composite	Patients (mild course)	P (mild course E-P)	Patients (intensive care)	P (intensive care E-P)	Patients (inpatients)	P (inpatients E-P)	Control
Genotypes	n (%)		n (%)		n (%)		n (%)
E-SELECTIN/P-SELECTIN	n=41		n=51		n=25		n=41
AA/AA	33 (%80.48)	0.6072	40 (%78.43)	0.7533	8 (%32)	<b>0.0006</b>	31 (%75.60)
AA/AC	0	0.2469	4 (%7.84)	0.6080	3 (%12)	0.3390	2 (%4.87)
AA/CC	0		0		10 (%40)	<b>0.0000</b>	0
AC/AA	3 (%7.31)	0.1208	0	<b>0.001</b>	4 (%16)	0.7448	8 (%19.51)
AC/AC	4 (%9.75)	<b>0.0579</b>	7 (%13.72)		0		0
AC/CC							
CC/AA	1 (%2.43)	0.5	0		0		0
CC/AC							
CC/CC							

**Table 4**

Comparative analysis of combined genotypes of E-SELECTIN and P-SELECTIN.

Genotypes	Patients		Control		p
	n	%	n	%	
<b>E-SELECTIN/P-SELECTIN</b>					
AA/AA	81	68.6	31	75.60	0.41
AA/AC	8	6.77	2	4.87	0.71
AA/CC	10	8.47	0	0.000	<b>0.04</b>
AC/AA	14	11.86	8	19.51	0.24
AC/AC	4	3.38	0	0.000	0.29
AC/CC	0		0		NA
CC/AA	1	0.84	0	0.000	0.74
CC/AC	0		0		NA
CC/CC	0		0		

control group. Comparative analysis of E-SELECTIN and P-SELECTIN combined genotypes in mild course, intensive care, and inpatients revealed statistically significant genotypes in each group. Significant results were obtained for AC/AC ( $p=0.0579$ ) genotype in patients with a mild course, AC/AA ( $p=0.001$ ) genotype in the intensive care unit, and AA/AA ( $p=0.0006$ ) and AA/CC ( $p=0.00001$ ) genotypes in inpatients (Table 5). In the comparative analysis of P-SELECTIN and L-SELECTIN combined genotypes in mild course, intensive care, and inpatients, no statistically significant data were obtained compared to the control group. When the comparative analysis of E-SELECTIN and L-SELECTIN combined genotypes in patients with the mild course, intensive care, and inpatients were evaluated, statistically significant results were found for AA/TC, CC/TC, and CC/CC genotypes only in inpatients ( $p=0.0088$ ,  $p=0.0047$  and  $0.0305$ , respectively) (Table 6).

**4. Discussion**

COVID-19 infection is often related to thromboembolic events, particularly venous thrombosis (Srivastava et al., 2022). According to the results of independent studies conducted by many researchers, genetic factors appear to have an important place among the possible risk factors that may lead to COVID-19 susceptibility. However, the effect of genetic polymorphisms on the severity of COVID-19 has not yet been clarified. In this study, the possible role of E, P, and L-SELECTIN gene polymorphisms in disease severity was investigated by comparing 3 groups of COVID-19 patients with mild course, need for hospitalization, and need for intensive care with the control group who were not diagnosed with COVID-19.

**Table 6**

Comparative analysis of combined genotypes of E-SELECTIN and L-SELECTIN in mild course, intensive care, and inpatients.

Composite	Patients (mild course)	P (mild course E-L)	Patients (intensive care)	P (intensive care E-L)	Patients (inpatients)	P (inpatients E-L)	Control
Genotypes	n (%)		n (%)		n (%)		n
E-SELECTIN/L-SELECTIN	n=41		n=43		n=31		n=41
AA/TT	2 (%4.87)	0.6204	6 (%13.95)	0.0694	0	0.5694	1 (%2.43)
AA/TC	10 (%24.39)	0.1086	16 (%37.20)	0.6971	4 (%12.90)	<b>0.0088</b>	17 (%41.46)
AA/CC	21 (%51.21)	0.1923	17 (%39.53)	0.7866	7 (%22.58)	0.1619	15 (36.58)
AC/TT	0		0		1 (%3.22)	0.4306	0
AC/TC	1 (%2.43)	0.3657	1 (%2.32)	0.3425	4 (%12.90)	0.4614	3 (%7.31)
AC/CC	6 (%12.19)	0.7594	3 (%6.97)	0.4471	5 (%16.12)	0.6475	5 (%12.19)
CC/TT	0		0		0		0
CC/TC	0		0		6 (19.35)	<b>0.0047</b>	0
CC/CC	1 (2.43)	0.50	0		4 (%12.90)	<b>0.0305</b>	0

The three categories of the selectin family --E-, P-, and L- are calcium-dependent and contribute to immune cells' adherence to the endothelium as well as their admission into lymphoid organs and inflammatory areas. E-SELECTIN is expressed by endothelial cells, L-SELECTIN by leukocytes, and P-SELECTIN by platelets. (Agrati et al., 2021).

Leukocyte adhesion during inflammation is facilitated by the protein E-SELECTIN, which is expressed on the surface of endothelial cells (Zhang et al., 2023). It has been suggested that expression changes of these molecules may affect neutrophil adhesion during the inflammation process observed in COVID-19. It has been noted that increased infiltration by immature and/or inefficient neutrophils might lead to an imbalance in the lungs' immunological response, which exacerbates the condition (Bartolotti et al., 2021). Only a few studies have investigated how soluble (s) E-SELECTIN affects the rise in disease severity or death in COVID-19 patients (Smadja et al., 2020; Bartolotti et al., 2021; Birnhuber et al., 2021; Oliva et al., 2021; Spadaro et al., 2021; Vassiliou et al., 2021; Srivastava et al., 2022). In their study, Smadja et al. and Oliva et al. discovered that patients admitted to critical care had greater levels of sE-SELECTIN. They proposed that sE-SELECTIN expression levels could be employed as a biomarker as they were linked to an increase in the patient's requirement for critical care (Smadja et al., 2020; Oliva et al., 2021). Additionally, Vassiliou et al. (2021) found that sE-SELECTIN levels were higher in patients who passed away in critical care than in those who survived, suggesting that these levels could be used to predict mortality in COVID-19 patients. According to Birnhuber et al. (2021), critically ill COVID-19 patients had much greater levels of sE-SELECTIN than healthy controls.

Leukocyte adhesion to monocytes and neutrophils is facilitated by the membrane protein P-SELECTIN, which is expressed on active platelets and endothelium. It contributes to immunothrombosis by forming leukocyte-platelet and leukocyte-endothelial complexes during the inflammatory response. Elevated circulating P-SELECTIN plasma levels are thought to be a sign of platelet destruction. Studies have demonstrated elevated P-SELECTIN expression on the platelet surface in COVID-19 (Fenyves et al., 2021). P-SELECTIN levels and leukocyte-platelet aggregates on the platelet membrane surface of COVID-19 patients were found to be elevated in the Manne et al. (2020) investigation. Furthermore, the same study discovered that COVID-19 patients had faster platelet aggregation and higher collagen-fibrinogen diffusion. Agrati et al. (2021) discovered that COVID-19 patients had a

greater plasma P-SELECTIN level ( $p=0.0023$ ) than healthy controls. According to a study by Campo et al. (2021), P-SELECTIN levels were higher in patients who died and those who required critical care than in those who survived. Vassiliou et al. (2021) found that sP-SELECTIN and other endothelial markers were higher in critically ill COVID-19 patients admitted to the intensive care unit. Karsli et al. (2021) found that sP-SELECTIN levels were higher in mild-moderate and severe pneumonia groups diagnosed with COVID-19 compared to the control group. Similarly, in the study by Prihatni et al. (2023), it was determined that sP-SELECTIN levels were mostly increased in patients treated in intensive care, while sP-SELECTIN levels were mostly normal in the non-intensive care group. However, unlike the above studies, Spadaro et al. (2021) found that plasma levels of E-SELECTIN and P-SELECTIN did not differ between surviving and non-surviving COVID-19 patients with acute respiratory distress syndrome.

L-SELECTIN is a glycoprotein structurally expressed on the surface of certain types of leukocytes. It is responsible for the migration of leukocytes to the lymphoid tissue (from the blood) and communicates with the antigen there. Endothelial cells expressing L-SELECTIN ligands on their surface capture leukocytes with L-SELECTIN and allow them to migrate into the lymphoid tissue (Šmak et al., 2021; Golubeva, 2022). There are limited studies on COVID-19 and L-SELECTIN in the literature. In a study on children with COVID-19, it was reported that neutrophils of children with COVID-19 showed lower L-SELECTIN expression compared to healthy controls (Seery et al., 2021). In a study evaluating P, E, and L-SELECTIN levels as markers of thrombosis in hospitalized COVID-19 patients, a significant difference was found in serum soluble selectins (sL, sP and sE). It has been reported that sP, sL, and sE-SELECTIN levels in COVID-19 patients who developed thrombosis had approximately two times higher expression levels ( $p<0.001$ ) compared to healthy patients who did not develop thrombosis (Watany et al., 2022).

As seen in the above studies, the possible relationship between the selectin family and COVID-19 is mostly based on determining the expression level. To our knowledge, there is only one study that examined the association of single nucleotide polymorphisms (SNPs) of COVID-19 and the selectin family with COVID-19 susceptibility and disease severity. According to this study, significant differences were found in P-SELECTIN (rs6133) and E-SELECTIN (rs5361) SNPs between COVID-19 patients and healthy controls. In this study, Srivastava et al. (2022) suggested that P-SELECTIN and

E-SELECTIN polymorphisms are significantly associated with COVID-19 disease and that these polymorphisms may be prognostic genetic markers of COVID-19 susceptibility.

As far as we know, our study is the first to examine the relationship between P (rs6136) E (rs7799039), and L (rs2229569) SELECTIN polymorphisms and COVID-19. In our study, while there was no significant relationship in all three polymorphisms when examined as a total patient and control group when the subgroups and control group were examined, E-SELECTIN Ser128Arg polymorphism was statistically significant at both genotypic and allelic levels in the inpatient group (ward patient) ( $p=0.0001$ ).

This may be attributed to the relatively low and unequal sample size between the total patient and control groups in the study. In addition, in our study, the binary genotype distribution between the studied loci and control groups was also examined. According to the combined genotype results, statistically significant differences were detected in E-SELECTIN/P-SELECTIN and E-SELECTIN/L-SELECTIN binary genotypes.

When E-SELECTIN and P-SELECTIN combined analyses were examined, the AA/AA binary genotype frequency ( $p=0.006$ ) was found to be higher in controls than in hospitalized patients. In addition, the frequency of the AC/AA ( $p=0.001$ ) binary genotype was found to be higher in the control group than in the patient group receiving intensive care. It was thought that these dual genotype frequencies may have a protective effect against COVID-19. Furthermore, the AA/CC dual genotype frequency ( $p=0.00001$ ) and the AC/AC binary genotype frequency ( $p=0.05$ ) were found to be significantly higher in inpatients and mild course patients, respectively, compared to the control group. It was thought that these dual genotype frequencies may have effects on the susceptibility to COVID-19 and the severity of the disease.

When E-SELECTIN and L-SELECTIN combined genotypes were evaluated in combination, it was determined that the CC/TC ( $p=0.0047$ ) and CC/CC ( $p=0.0305$ ) dual genotype

frequencies in inpatients were statistically significant compared to the control group. The present study revealed that the AA/TC dual genotype frequency ( $p=0.0088$ ) was statistically significant in comparison with the inpatients in the control group.

It was hypothesized that the significance of the control group was important in terms of the severity of the disease in the COVID-19 epidemic and could affect the disease being milder. It was commented that CC/TC and CC/CC dual genotypes may have an impact on hospitalizations and increase the severity of the disease.

Data obtained from binary genotypes suggest that the relationship of polymorphisms with different polymorphisms belonging to the same gene family may also have an impact on diseases. As a matter of fact, in our study, while there was no significant relationship when the three loci were evaluated separately, significant relationships were found in dual genotypes, especially between the ward patients and the control group.

## 5. Conclusions

Although the impact of COVID-19 disease on individuals has now diminished, elucidating the genetic determinants of SARS-CoV-2 infection is important for understanding the pathophysiology of COVID-19 and interindividual variability in its severity; Thus, it can contribute to the development of updated vaccines and new antivirals.

**Ethical approval:** Blood samples taken from volunteers were used in the study and the Declaration of Helsinki was complied with. Necessary permissions were obtained by Tokat Gaziosmanpasa University Non-invasive Clinical Research Ethics Committee (22-KAEK-211).

**Conflict of interest:** The authors declare that they have no conflict of interests.

## References

- Abdelmageed, M., Guzelgul, F., Yalin, S., & Akkapulu, M. (2025). Determination of oxidative stress and copeptin levels of COVID-19 according to the clinical course. *Microbial Pathogenesis*, 199, 107263.
- Agrati, C., Bordoni, V., Sacchi, A., Petrosillo, N., Nicastrì, E., Del Nonno, F., ... & Bibas, M. (2021a). Elevated P-selectin in severe Covid-19: considerations for therapeutic options. *Mediterranean Journal of Hematology and Infectious Diseases*, 13(1), e2021016.
- Agrati, C., Sacchi, A., Tartaglia, E., Vergori, A., Gagliardini, R., Scarabello, A., & Bibas, M. (2021b). The role of P-selectin in COVID-19 coagulopathy: an updated review. *International Journal of Molecular Sciences*, 22(15), 7942.
- Aljadah, M., Khan, N., Beyer, A. M., Chen, Y., Blanker, A., & Widlansky, M. E. (2024). Clinical implications of COVID-19-related endothelial dysfunction. *JACC: Advances*, 3(8), 101070.
- Anastassopoulou, C., Gkizarioti, Z., Patrinos, G. P., & Tsakris, A. (2020). Human genetic factors associated with susceptibility to SARS-CoV-2 infection and COVID-19 disease severity. *Human Genomics*, 14(1), 40.
- Attiq, A., Afzal, S., Wahab, H. A., Ahmad, W., Kandeel, M., Almofti, Y. A., ... & Wu, Y. S. (2024). Cytokine Storm-Induced Thyroid Dysfunction in COVID-19: Insights into Pathogenesis and Therapeutic Approaches. *Drug Design, Development and Therapy*, 4215-4240.
- Birnhuber, A., Fliesser, E., Gorkiewicz, G., Zacharias, M., Seeliger, B., David, S., ... & Kwapiszewska, G. (2021). Between inflammation and thrombosis: endothelial cells in COVID-19. *The European Respiratory Journal*, 58(3), 2100377.
- Bortolotti, D., Gentili, V., Rizzo, S., Schiuma, G., Beltrami, S., Spadaro, S., Strazzabosco G., ... & Contoli, M. (2021). Increased sHLA-G is associated with improved COVID-19 outcome and reduced neutrophil adhesion. *Viruses*, 13(9), 1855.
- Campo, G., Contoli, M., Fogagnolo, A., Vieceli Dalla Sega, F., Zucchetti, O., Ronzoni, L., ... & Spadaro, S. (2021). Over time relationship between platelet reactivity, myocardial injury and mortality in patients with SARS-CoV-2-associated respiratory failure. *Platelets*, 32(4), 560-567.
- Debnath, M., Banerjee, M., & Berk, M. (2020). Genetic gateways to COVID-19 infection: implications for risk, severity, and outcomes. *The FASEB Journal*, 34(7), 8787-8795.
- Dieter, C., Brondani, L. D. A., Leitão, C. B., Gerchman, F., Lemos, N. E., & Crispim, D. (2022). Genetic polymorphisms associated with susceptibility to COVID-19 disease and severity: A systematic review and meta-analysis. *PLoS One*, 17(7), e0270627.
- Eketunde, A. O., Mellacheruvu, S. P., & Oreoluwa, P. (2020). A review of postmortem findings in patients with COVID-19. *Cureus*, 12(7).
- Elhabyan, A., Elyaacoub, S., Sanad, E., Abukhadra, A., Elhabyan, A., & Dinu, V. (2020). The role of host genetics in susceptibility to severe viral infections in humans and insights into host genetics of severe COVID-19: A systematic review. *Virus Research*, 289, 198163.
- Fenyves, B. G., Mehta, A., Kays, K. R., COVID, M., Goldberg, M. B., Hacoheh, N., & Filbin, M. R. (2021). Plasma P-selectin is an early marker of thromboembolism in COVID-19. *MedRxiv*.
- Golubeva, M. G. (2022). Role of P-Selectin in the Development of Hemostasis Disorders in COVID-19. *Biology Bulletin Reviews*, 12(4), 406-413.
- Hirata, T. (2016). Blood Vascular Endothelial Adhesion Molecules. *Encyclopedia of Immunobiology*, 3, 512-519.
- Job, M. S. B., Chacko, B., Selvarajan, S., Peter, J. V., Geevar, T., Dave, R.

- G., ... & Srivastava, A. (2024). Biomarkers of coagulation, endothelial, platelet function, and fibrinolysis in patients with COVID-19: a prospective study. *Scientific Reports*, 14(1), 2011.
- Imhof, B. A., & Dunon, D. (1995). Leukocyte migration and adhesion. *Advances in Immunology*, 58, 345-416.
- Karsli, E., Sabirli, R., Altintas, E., Canacik, O., Sabirli, G. T., Kaymaz, B., ... & Koseler, A. (2021). Soluble P-selectin as a potential diagnostic and prognostic biomarker for COVID-19 disease: a case-control study. *Life Sciences*, 277, 119634.
- Li, Z., Zeng, M., Wu, T., Wang, Z., Sun, Y., Zhang, Z., ... & Meng, F. (2024). Causal effects of COVID-19 on the risk of thrombosis: a two-sample Mendel randomization study. *Thrombosis and Haemostasis*, 124(08), 709-720.
- Longo, C., & Wakefield, T. W. (2007). Fundamental Mechanisms in Venous Thrombosis. In *The Vein Book* (pp. 331-338). Academic Press.
- Maltezou, H. C. (2025). Post-COVID syndrome in children compared with adults. *World Academy of Sciences Journal*, 7(2), 26.
- Manne, B. K., Denorme, F., Middleton, E. A., Portier, I., Rowley, J. W., Stubben, C., ... & Campbell, R. A. (2020). Platelet gene expression and function in patients with COVID-19. *Blood, The Journal of the American Society of Hematology*, 136(11), 1317-1329.
- Mantovani, A., & Dejana, E. (1998). *Endothelium, encyclopedia of immunology (Second Edition)*, pp. 802-806.
- Mohanty, S. K., Satapathy, A., Naidu, M. M., Mukhopadhyay, S., Sharma, S., Barton, L. M., ... & Parwani, A. V. (2020). Severe acute respiratory syndrome coronavirus-2 (SARS-CoV-2) and coronavirus disease 19 (COVID-19)—anatomic pathology perspective on current knowledge. *Diagnostic Pathology*, 15, 1-17.
- Oliva, A., Rando, E., Al Ismail, D., De Angelis, M., Cancelli, F., Miele, M. C., ... & Mastroianni, C. M. (2021). Role of serum E-selectin as a biomarker of infection severity in coronavirus disease 2019. *Journal of Clinical Medicine*, 10(17), 4018.
- Ozturk, R. (2020). COVID-19: pathogenesis, genetic polymorphism, clinical features and laboratory findings. *Turkish Journal of Medical Sciences*, 50(9), 638-657.
- Petito, E., Franco, L., Falcinelli, E., Guglielmini, G., Conti, C., Vaudo, G., ... & COVIR-Study Investigators. (2023). COVID-19 infection-associated platelet and neutrophil activation is blunted by previous anti-SARS-CoV-2 vaccination. *British Journal of Haematology*, 201(5), 851-856.
- Prihatni, D., Budianto, F. C., Andriyoko, B., & Trisa, S. (2023). The Correlation Between sP-Selectin and Platelet Count in COVID-19 Patients in Referral Hospital, West Java Indonesia. *Journal of Blood Medicine*, 555-561.
- Sayyadi, M., Hassani, S., Shams, M., & Dorgalaleh, A. (2023). Status of major hemostatic components in the setting of COVID-19: the effect on endothelium, platelets, coagulation factors, fibrinolytic system, and complement. *Annals of Hematology*, 102(6), 1307-1322.
- Seery, V., Raiden, S. C., Algieri, S. C., Grisolia, N. A., Filippo, D., De Carli, N., ... & Arruvito, L. (2021). Blood neutrophils from children with COVID-19 exhibit both inflammatory and anti-inflammatory markers. *EBioMedicine*, 67.
- Selvaraj, C., Abhirami, R., Vijayakumar, R., Alfaiz, F. A., & Singh, S. K. (2022). Immunological insights of selectins in human disease mechanism. *Advances in Protein Chemistry and Structural Biology*, 129, 163-188.
- Smadja, D. M., Guerin, C. L., Chocron, R., Yatim, N., Boussier, J., Gendron, N., ... & Diehl, J. L. (2020). Angiopoietin-2 as a marker of endothelial activation is a good predictor factor for intensive care unit admission of COVID-19 patients. *Angiogenesis*, 23, 611-620.
- Šmak, P., Chandrabose, S., Tvaroška, I., & Koča, J. (2021). Pan-selectin inhibitors as potential therapeutics for COVID-19 treatment: in silico screening study. *Glycobiology*, 31(8), 975-987.
- Spadaro, S., Fogagnolo, A., Campo, G., Zucchetti, O., Verri, M., Ottaviani, I., ... & Contoli, M. (2021). Markers of endothelial and epithelial pulmonary injury in mechanically ventilated COVID-19 ICU patients. *Critical Care*, 25, 1-9.
- Srivastava, S., Kumari, B., Garg, I., Dogra, V., Ghosh, N., Singh, Y., ... & Ganju, L. (2022). Gene variants in pro-coagulant and anti-coagulant genes could be prognostic genetic markers of COVID-19 susceptibility. *Heliyon*, 8(11).
- Vassiliou, A. G., Keskinidou, C., Jahaj, E., Gallos, P., Dimopoulou, I., Kotanidou, A., & Orfanos, S. E. (2021). ICU admission levels of endothelial biomarkers as predictors of mortality in critically ill COVID-19 patients. *Cells*, 10(1), 186.
- Watany, M. M., Abdou, S., Elkolaly, R., Elgharbawy, N., & Hodeib, H. (2022). Evaluation of admission levels of P, E and L selectins as predictors for thrombosis in hospitalized COVID-19 patients. *Clinical and Experimental Medicine*, 22(4), 567-575.
- Wong, D., & Dorovini-Zis, K. (1996). Regulation by cytokines and lipopolysaccharide of E-selectin expression by human brain microvessel endothelial cells in primary culture. *Journal of Neuropathology & Experimental Neurology*, 55(2), 225-235.
- Wu, X., Xiang, M., Jing, H., Wang, C., Novakovic, V. A., & Shi, J. (2024). Damage to endothelial barriers and its contribution to long COVID. *Angiogenesis*, 27(1), 5-22.
- Zhang, J., Zhang, S., Xu, S., Zhu, Z., Li, J., Wang, Z., ... & Liu, J. (2023). Oxidative stress induces E-selectin expression through repression of endothelial transcription factor ERG. *The Journal of Immunology*, 211(12), 1835-1843.
- Zlibut, A., Bocsan, I. C., & Agoston-Coldea, L. (2019). Pentraxin-3 and endothelial dysfunction. *Advances in Clinical Chemistry*, 91, 163-179.

**Cite as:** Bozkurt, N., Guzelgul, F., Akkus, N., Sahin, K., Savkin, S., & Yigit, T. (2025). Possible effect of E-SELECTIN (Ser128Arg), L-SELECTIN (Pro213Ser), P-SELECTIN (Thr715Pro) gene polymorphisms for COVID-19 disease severity. *Front Life Sci RT*, 6(1), 21-27.



## Research article

# The effect of paclitaxel on cachexia-related gene *AZGP1* expression during adipocyte differentiation

Ozlem Agirel<sup>1</sup> , Ceyda Okudu<sup>\*2</sup> 

<sup>1</sup> Halic University, Faculty of Health Sciences, Department of Nutrition and Dietetics, 34060, Istanbul, Türkiye

<sup>2</sup> Atlas University, Faculty of Engineering and Natural Sciences, Department of Molecular Biology and Genetics, 34403, Istanbul, Türkiye

## Abstract

Cancer cachexia, a syndrome characterized by involuntary weight loss, affects skeletal muscles and leads to adipose tissue loss. Activation of adipose tissue during cancer cachexia may contribute to cachexia through mechanisms like ZAG, a biomarker for adipose atrophy. This study aimed to analyze the effect of paclitaxel on adipogenesis and cachexia-related genes in cancer cachexia. The study involved human preadipocyte cells grown in a commercial medium, with 50 nM paclitaxel applied on different days for differentiation. The 15th day, marking the completion of differentiation was analyzed for lipid accumulation and *PPAR $\gamma$*  and *AZGP1* gene expression. The study found that paclitaxel during adipogenesis suppressed differentiation and lipid accumulation in human preadipocytes. It was determined that there was no change in the expression level of the *AZGP1* gene in day 3 preadipocytes given paclitaxel starting from the 3rd day of differentiation. It was determined that *PPAR $\gamma$*  gene expression was suppressed in day 0 preadipocytes given paclitaxel starting from the first day of differentiation compared to the control group. As a result, it has been determined that paclitaxel may contribute to adipose tissue loss in cancer cachexia by suppressing the differentiation of preadipocytes and lipid accumulation during adipogenesis. The change caused by paclitaxel in the expression of genes such as *AZGP1* and *PPAR $\gamma$*  during adipogenesis needs to be analyzed in further studies.

**Keywords:** Adipogenesis; cachexia; paclitaxel; *AZGP1*; *PPAR $\gamma$*

## 1. Introduction

Loss of fat and skeletal muscle mass characterizes cachexia, a multifactorial illness that progresses into functional impairment and is not entirely reversible with standard dietary support (Ni and Zhang, 2020). It is a multifaceted systemic illness affecting various organs and tissues (Peixoto da Silva et al., 2020). Cancer cachexia lowers quality of life, lowers responsiveness to treatment, decreases response to anticancer therapy, lowers performance status, and lowers survival (Muliawati et al., 2012).

Primary tumor treatment or anticancer treatments like surgery, chemotherapy, and radiotherapy can contribute to

cachexia by altering nutritional and metabolic status and causing tumor-specific damage (Laviano et al., 2011). However, there is conflicting evidence on the direct effect of anticancer drugs on cachexia (Cabrera et al., 2025).

Most cancer patients experience body composition changes the disease. Patients receiving chemotherapy for breast cancer and prostate cancer, for instance, acquire adipose tissue and lose skeletal muscle, which is linked to a higher risk of clinical comorbidities and cancer recurrence. On the other hand, patients with advanced colorectal and lung cancer may lose skeletal muscle in addition to adipose tissue, which is linked to a worse prognosis and a reduced response to treatment (Sebastiano and Mourtzakis, 2012; Choi et al., 2025; Khan et al., 2025).

\* Corresponding author.

E-mail address: [ceydaokudu@gmail.com](mailto:ceydaokudu@gmail.com) (C. Okudu).

<https://doi.org/10.51753/flsrt.1609937> Author contributions

Received 30 December 2024; Accepted 13 March 2025

Available online 30 April 2025

2718-062X © 2025 This is an open access article published by Dergipark under the [CC BY](https://creativecommons.org/licenses/by/4.0/) license.

Several studies with tumor-bearing animals have reported brown adipose tissue activation via lipolysis during cancer cachexia (Panagiotou et al., 2025). Adipose tissue plays a critical role in the pathophysiology of cancer cachexia, particularly through enhanced lipolysis, browning, and thermogenesis during the early stages of the disease. Although brown adipose tissue contributes to energy expenditure and may exacerbate cachexia, the specific mechanisms and overall role of adipose tissue in human cancer cachexia remain inadequately understood (Mota et al., 2024).

Cancer cachexia involves the remodeling of adipose tissue due to various genetic, metabolic, and inflammatory mechanisms. It's unclear if tumor-derived compounds or the tumor itself cause the loss of adipose tissue. *In vitro* studies show that co-culturing Lewis lung carcinoma cells inhibits adipogenesis in mouse precursor adipocytes, promoting lipid droplet volume reduction (Lopes et al., 2018). Adipocytes and tumor cells secrete pro-inflammatory cytokines and downregulate adipogenic genes, suggesting that tumor cells may interfere with adipocyte formation by inducing an inflammatory response. This could significantly influence metabolic and functional alterations in cachectic adipose tissue (Mannelli et al., 2020).

*PPAR $\gamma$*  (Peroxisome proliferator-activated receptor gamma) is a crucial regulator of adipogenesis, increasing the expression of adipocyte differentiation markers and lipid accumulation. It plays a significant role in both brown and white adipose tissue differentiation in various regions. *PPAR $\gamma$*  may contribute to the pathogenesis of diseases with irregular lipid metabolism (Kim et al., 2024). The activation of *PPAR $\gamma$*  in white adipose tissue may depend on the NF- $\kappa$ B pathway, potentially modulating inflammation in white adipose tissue, possibly due to cancer cachexia (Mannelli et al., 2020).

ZAG (zinc- $\alpha$ 2-glycoprotein) is a secretory protein and is encoded by the *AZGP1* ( $\alpha$ 2 zinc glycoprotein 1, zinc-binding) gene (Pendás et al., 1994). *AZGP1* plays a crucial role in regulating energy homeostasis and glucose/lipid metabolism by acting on hypothalamic POMC neurons, and its regulation pathway is being investigated in several types of cancer (Yun et al., 2024; Qin et al., 2024; Qiu et al., 2024). ZAG is one of the proteins involved in regulating body weight, glucose levels, and body fat (Zimowska et al., 2024). ZAG's association with metabolic syndrome, including obesity, hypertension, and dyslipidemia, underscores its broader implications for human health (Zhou et al., 2024). The relationship between serum ZAG protein and serum zinc is not fully explained but ZAG levels have regulatory effects on insulin resistance and plasma glucose levels are mediated by zinc and acylated ghrelin (Kurtulus et al., 2024). ZAG is involved in metabolism through various pathways. Recent studies have demonstrated the role of ZAG in energy and lipid metabolism, as well as a possible connection

with exercise (Unver et al., 2024). It promotes the browning of white adipose tissue, raising energy expenditure and reducing body weight and fat tissue (Elattar et al., 2018). ZAG supports the proliferation of 3T3-L1 mouse preadipocytes by inhibiting the expression of *PPAR $\gamma$*  and *C/ERB $\alpha$*  (Zhu et al., 2013). Enhanced expression of ZAG in adipose tissue has been linked to elevated lipolytic activity, contributing to fat depletion and body weight reduction. As a key lipid-mobilizing factor, ZAG plays a pivotal role in the metabolic alterations observed in cachectic individuals (Martínez-Navarro et al., 2024). Moreover, increased circulating levels of ZAG protein may serve as a potential biomarker for the early detection of cancer-associated cachexia characterized by adipose tissue wasting (Yeung et al., 2009; Senyigit et al., 2024; Wen et al., 2024). ZAG is upregulated in cachectic people and animal models, and elevated amounts of free fatty acids in the bloodstream have been linked to the acceleration of muscle protein breakdown in cancer cachexia (Burgi and Schmid, 1961).

The study investigated the impact of chemotherapeutic agent paclitaxel on adipogenesis and adipose tissue loss in cancer cachexia. The aim was to determine how effective chemotherapy agents are on the molecular infrastructure of the cachectic state that occurs in cancer. It examined gene expression, lipid accumulation, and cachexia-related gene expression. Results showed that paclitaxel suppressed adipogenesis and preadipocyte differentiation, highlighting the relationship between chemotherapeutic agents and adipose tissue loss.

## 2. Materials and methods

### 2.1. Preparation of paclitaxel concentrations

The study used 1 mg paclitaxel (Taxol<sup>®</sup>, Sigma Aldrich) and prepared a concentration of 1.25 mM main stock and 5  $\mu$ M intermediate stock for human preadipocyte cells. During differentiation, 1  $\mu$ L of intermediate stock was applied to cells, with a final concentration of 50 nM, ensuring DMSO did not exceed 0.05% in each well (Choron et al., 2015).

### 2.2. Culture of human preadipocyte cells

Human preadipocyte cells (HPAD) used in the research were provided by Dr. Sevgin Degirmencioglu. Cells stored as stock at -196°C were cultured in a human preadipocyte growth medium (Thermo Fisher, USA) under appropriate conditions (at 37°C with 5% CO<sub>2</sub>). When the cells were fully confluent, they were passaged and multiplied until they reached the ideal number for the experiment.

### 2.3. Application of paclitaxel and differentiation of preadipocyte cells

**Table 1**

The experimental groups treated with paclitaxel.

Experimental Groups	Treatment 1	Treatment 2	Treatment 3	Treatment 4	Treatment 5
Day 0	PTX+DM	PTX+DM	PTX+DM	PTX+DM	PTX+DM
Day 3	DM	PTX+DM	PTX+DM	PTX+DM	PTX+DM
Day 6	DM	DM	PTX+DM	PTX+DM	PTX+DM
Day 9	DM	DM	DM	PTX+DM	PTX+DM
Day 12	DM	DM	DM	DM	PTX+DM
Control DMSO (+)	DM+DMSO	DM+DMSO	DM+DMSO	DM+DMSO	DM+DMSO
Control (-)	DM	DM	DM	DM	DM

PTX: paclitaxel DM: differentiation medium DMSO: Dimethyl sulfoxide.

The seeded cells were followed until sufficient density was reached in the culture dishes. To determine the effect of paclitaxel on adipogenesis at the determined concentration, the differentiation stage of human preadipocyte cells into mature adipocyte cells was chosen as a model. For this, HPAD cells were counted,  $10^5$  cells/well in 12-well culture dishes and seeded with 1 ml of growth medium. The cells were incubated and checked regularly until they were 90% confluent. When the cells were 90% confluent, the growth medium was then aspirated from the wells and 1 mL of human adipocyte differentiation medium used to differentiate cells was added. After removing the old medium, 50 nM paclitaxel and 1 mL of fresh human adipocyte differentiation medium were replaced every 3 days for 15 days (Table 1).

## 2.4. Analysis of gene expression

Following paclitaxel application and the time required for differentiation, cells were collected on day 15 for total RNA isolation, cDNA synthesis, and PCR analyses. Total RNA was obtained from total RNA with the isolation kit (GeneJet RNA Purification Kit, Thermo Scientific, USA) following the manufacturer's recommendations. Purity and concentration analysis of the obtained RNAs was performed using a spectrophotometer (Thermo Scientific, USA). The concentrations of all RNAs were adjusted to 1000 ng/ $\mu$ l. To determine the gene expression level, cDNA synthesis using 1  $\mu$ g RNA was performed using a commercially available kit (RevertAid First Strand cDNA Synthesis Kit, Thermo Scientific, USA). PCR cycling conditions for cDNA synthesis: 10 min at 25°C, 15 min at 42°C, and 5 min at 85°C. The expression levels of the genes whose primer sequences are given in Table 2 were examined with the cDNAs obtained. *PPAR $\gamma$*  and *AZGP1* genes and *GAPDH* gene primer sequences as internal control are given in Table 2 and were synthesized by Oligomer Biotechnology (Turkey). SyberGreen Master Mix kit (Real Q Plus 2X Master Mix Green, Amplicon, Denmark) was prepared under the manufacturer's recommendations, and 40 cycles in the quantitative real-time polymerase chain reaction was performed using a 30 sec at 95°C, 30 sec at 55°C, 30 sec 72°C heat program. The level of expression of each gene compared to control cells was examined using the formula  $2^{-\Delta\Delta Ct}$ .

## 2.5. Determination of lipid accumulation

Determination of lipid accumulation in cells was done by the Oil Red O Staining method. To analyze the effect of paclitaxel on lipid accumulation during the adipocyte differentiation process, 105 cells/well of human preadipocyte cells were passaged into 12-well cell culture plates and paclitaxel was applied at the determined concentration every 3 days for the 15 days required for differentiation into mature adipocytes. On day 15, the procedure previously described by

You et al. (2014) was applied with minor modifications. Cells were washed 2 times with 1 ml of PBS after the medium was collected. Cells were fixed by incubation for 1 hour with 1 ml of 10% formalin. Following this, the cells were washed 2 times with 1.5ml ddH<sub>2</sub>O and incubated for 5 min. It was treated with 1ml of 60% isopropanol. The isopropanol was then withdrawn and left to dry. When drying was observed, it was kept in an Oil Red O (Merck, Germany) working solution for 30 min. Oil Red O dye was aspirated and cells were washed with 1.5 ml of ddH<sub>2</sub>O. Cells were photographed under a 10X inverted microscope. After photographing, 1 ml of 60% isopropanol was added to each well and the absorbance of the dye solution at 570 nm was measured in a spectrophotometer.

## 2.6. Statistical analysis of data

Two-tailed distribution and two-sample homoscedastic t-test analysis were used for data analysis. The statistical significance of the results obtained was evaluated over a p-value of 0.05, and values with a p-value of  $\leq 0.05$  were considered reliable.

## 3. Result

### 3.1. Paclitaxel reduced lipid accumulation

As a result of the analysis of 50 nM paclitaxel applied to preadipocytes with Oil Red O staining, it was determined that lipid accumulation was reduced in the group compared to the control group (Fig. 1A). After staining, the absorbance measurements of the dye obtained from the cells were normalized with the absorbance value of the control cells. Preadipocytes differentiated by administering paclitaxel were compared with those in the control group. Considering that paclitaxel was applied to the cells in the day 0 group throughout the differentiation period, it was determined that paclitaxel suppressed lipid accumulation, and the day 0 group was followed by the cells in the days 3, 6, 9, and 12 group, respectively. According to the results, absorbance measurements were obtained at values of 0.67, 0.86, 0.87, 1.05, and 1.19 on days 0, 3, 6, 9, and 12, respectively. The results were found to be statistically significant for all groups ( $p < 0.05$ ). (Fig. 1B).

### 3.2. Effect of paclitaxel on *AZGP1* and *PPAR $\gamma$* gene expression

It was observed that there was no change in the expression level of the *AZGP1* gene in day 3 preadipocytes given 50 nM paclitaxel starting from the 3rd day of differentiation, compared to the control group (cells that were not treated with any substance). When the on days 0, 6, 9, and 12 preadipocyte groups were compared with the control group, it was observed that gene expression levels were suppressed up to 0.44, 0.42, 0.5,

**Table 2**

Primer sequences used for RT-PCR.

Gene	Primer Sequences	Temperature of Annealing (°C)	GC Content (%)
<i>AZGP1</i>	Forward (F)	5'-TACAACGACAGTAACGGGTCT-3'	58
	Reverse (R)	5'-TATTCCAGAATGCTCCGCTG-3'	58
<i>PPAR<math>\gamma</math></i>	Forward (F)	5'-TCGGTTTCAGAAATGCCTTG-3'	55
	Reverse (R)	5'-AGGTCAGCGGACTCTGGATT-3'	59
<i>GAPDH</i>	Forward (F)	5'-CGAGATCCCTCCAAAATCAA-3'	55
	Reverse (R)	5'-TTCACACCCATGACGAACAT-3'	55

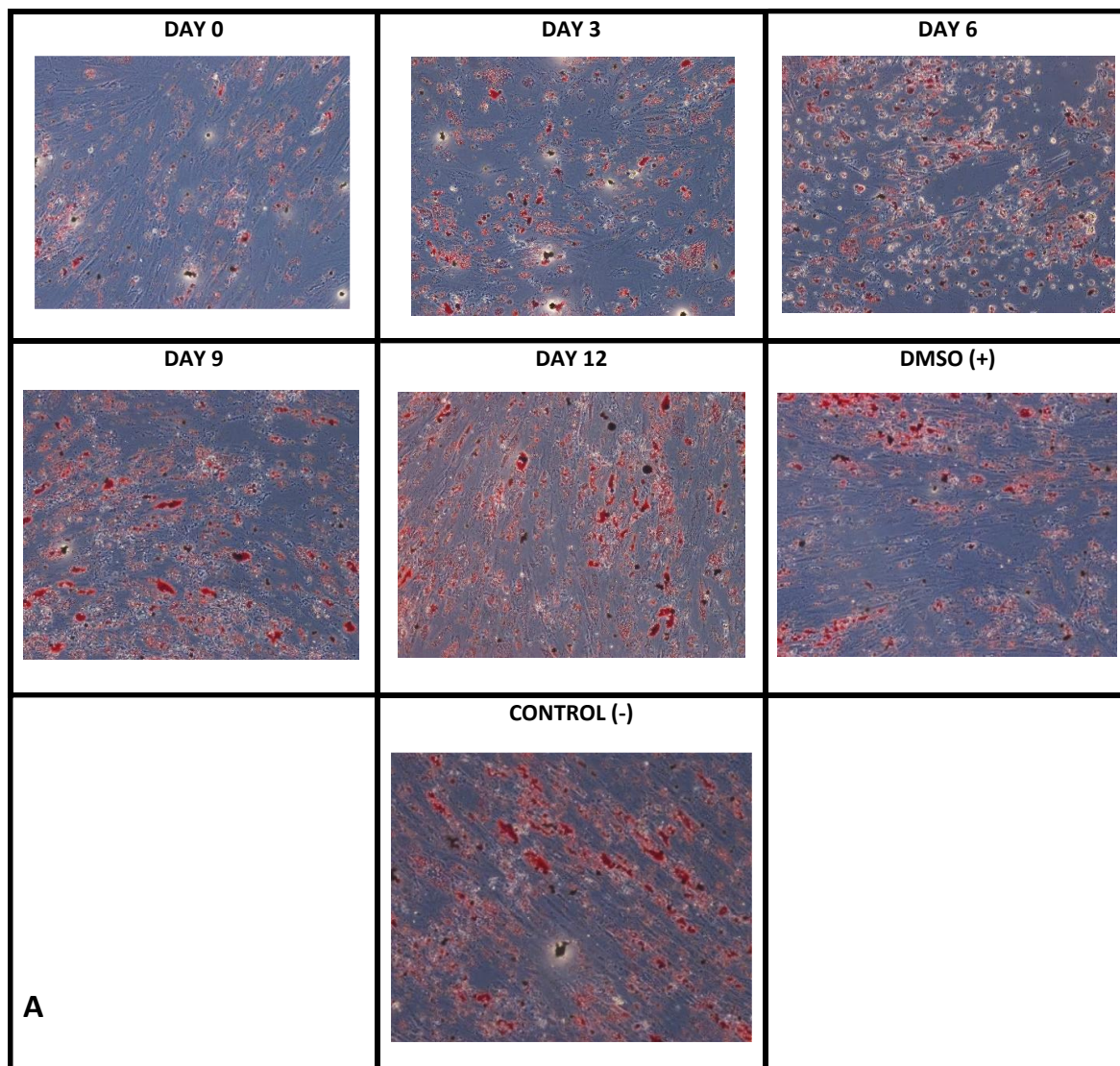


**Fig. 1A.** Effect of paclitaxel on differentiation of human preadipocyte cells. Lipid accumulation was detected by Oil Red O staining. (A) Microscope images of differentiated adipocytes after Oil Red O staining (scale bar=100  $\mu$ m).

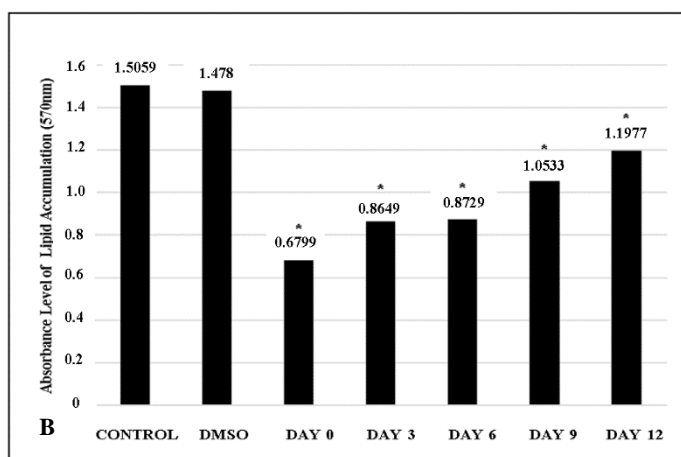


**Fig. 1B.** Effect of paclitaxel on differentiation of human preadipocyte cells. Lipid accumulation was detected by Oil Red O staining. (B) Comparison of optical absorbance values at 570 nm of the dye recollected from adipocytes.

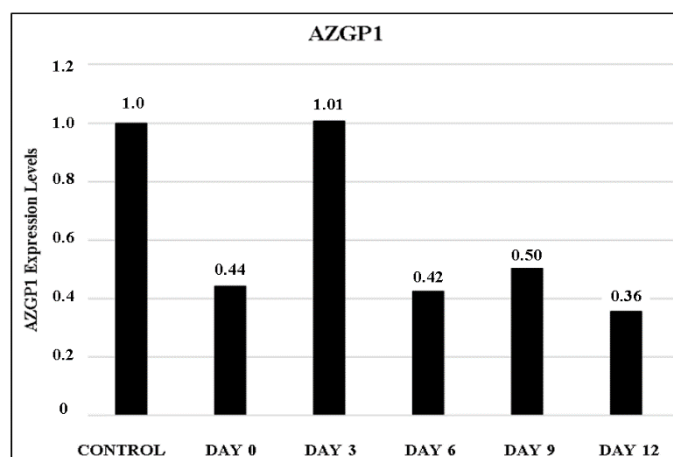


**Fig. 2.** AZGP1 gene expression level (\*: statistically significant).

and 0.36, respectively (Fig. 2). p values were found to be 0.12, 0.78, 0.703, 0.177, and 0.068 for on days 0, 3, 6, 9 and 12, respectively.

When comparing day 0 preadipocytes given 50 nM paclit-

axel from the first day of differentiation with the control group (cells not applied any substance), it was determined that *PPAR $\gamma$*  gene expression was suppressed (p=0.000). In the day 3 and day 6 preadipocyte groups, gene expression levels were observed to be suppressed up to 0.65 and 0.9, respectively, when compared to the control group (0.100, 0.604, respectively). However, it was observed that gene expression levels in day 9 and day 12

preadipocyte cells increased to 2.29 and 3.99, respectively, compared to the control group ( $p=0.015$ ,  $0.003$ , respectively) (Fig. 3).

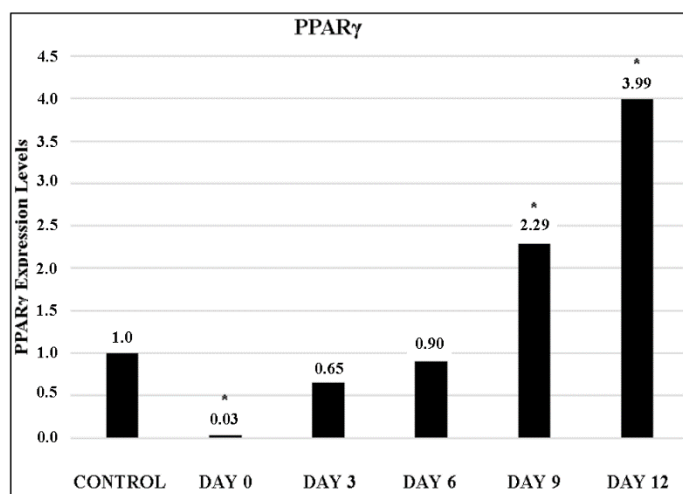


Fig. 3. *PPAR $\gamma$*  gene expression level (\*: statistically significant).

#### 4. Discussion

Cancer cachexia is a syndrome characterized by involuntary weight loss, affecting skeletal muscles and adipose tissue (Fearon et al., 2011). Chemotherapeutic agents also cause body weight loss (Huang et al., 2019). ZAG, a marker of fat catabolism and cachexia, is highly expressed in cachectic patients and promotes browning of adipocytes, triggers fat oxidation, increases energy expenditure, and inhibits adipocyte differentiation by inhibiting *PPAR $\gamma$*  and *C/ERB $\alpha$*  expression in preadipocytes (Mracek et al., 2011; Zhu et al., 2013).

Cancer cachexia can impair the regulation of adipogenesis and adipogenic factors (Batista et al., 2013; Bing et al., 2006). A study found that co-culture of lung carcinoma cells with mouse preadipocyte 3T3-L1 cells negatively affected adipogenesis by promoting reduced lipid accumulation and volume, leading to downregulation of adipogenic and lipolytic gene expressions (Lopes et al., 2018). Another study found that the downregulation of ZAG was accompanied by a decrease in lipid droplet formation, thus suggesting that inhibition of ZAG may reduce lipid synthesis in colorectal cancer cells (Xu et al., 2024). This is the first study to examine the effects of paclitaxel on the differentiation of human preadipocyte cells, adipogenesis, and cachexia-related genes like *AZGP1* in cancer cachexia.

Chemotherapeutic agents can disrupt adipogenesis in adipose tissue by inhibiting the differentiation of human adipocyte stem cells (Ebadi and Mazurak, 2014). In our study, paclitaxel administered to human preadipocyte cells suppressed lipid accumulation and adipogenesis. The study conducted by Choron et al. (2015) demonstrated that treatment with 1  $\mu$ M paclitaxel significantly inhibited adipogenesis in human adipose-derived stem cells (hASCs). Although adipose tissue-derived mesenchymal stem cells (ADSC) could differentiate into adipocytes, asteroids, and chondrocytes, their adipogenic differentiation ability was significantly reduced after cisplatin treatment (Dasari and Tchounwou, 2014). Chang et al. (2017) studied the ability of ADSCs to differentiate *in vivo* after 9 receiving chemotherapy based on cisplatin, finding that chemotherapy significantly decreased the donor capacity to differentiate into adipogenic, osteogenic, and chondrogenic cells. However, combinations of radiotherapy, chemotherapy,

and surgical intervention are used in cancer treatment, and *in vitro* chemotherapeutic agent treatments may not fully represent the clinical situation of cachectic patients (Dasari and Tchounwou, 2014).

Bao et al. (2005) found that ZAG mRNA levels increased gradually after induction and peaked on the 8th day, regulated through TNF- $\alpha$  and *PPAR $\gamma$*  receptors. Zhu et al. (2013) reported that after ZAG expression plasmid transfection into 3T3-L1 mouse preadipocytes, lipid accumulation decreased, adipocyte differentiation was inhibited, and ZAG down-regulated *PPAR $\gamma$*  and *C/EBP $\alpha$*  mRNA levels in the middle and late differentiation phases. In intrahepatic cholangiocarcinoma treated with the anticancer agent lenvatinib, it has been shown that low expression of *AZGP1* is associated with a poor prognosis in patients (Deng et al., 2023).

In our study, paclitaxel applied from day 3 of differentiation did not change *AZGP1* expression in human preadipocytes compared to the control but reduced *AZGP1* expression from day 0, day 6, day 9, and day 12. More *in vitro* and *in vivo* studies are needed to determine the molecular pathways involved in cancer cachexia and to better analyze these findings at the gene level by determining the change in ZAG protein level and possible cachexia pathways.

Recent studies have shown that *PPAR* agonists may be a useful adjuvant therapy to preserve tissue mass (Langer et al., 2024; Beluzi et al., 2015; Goncalves et al. 2018). Our study found that paclitaxel, given from day 0 of differentiation, significantly reduced *PPAR $\gamma$*  expression in human preadipocyte cells, suggesting that chemotherapeutic agents may be effective in developing cancer cachexia. This is in line with the theory that factors involved in downregulating genes involved in adipocyte differentiation may play a key role in metabolic and functional changes in cachectic adipose tissue. *PPAR $\gamma$*  is a transcription factor required for adipogenesis and maintenance of the differentiated state (Chu et al., 2014). In the late stage of adipocyte differentiation, there is an increase in the expression of *PPAR $\gamma$*  and *CEBP $\alpha$* , necessary for the completion of differentiation. Suppression of *PPAR $\gamma$*  reduces triglyceride accumulation in adipocytes (Chu et al., 2014). However, paclitaxel significantly increased *PPAR $\gamma$*  expression in the late stage of differentiation compared to the control. This increase may be due to *PPAR $\gamma$*  being active in the late stage of adipogenesis or paclitaxel application. Further studies are needed to determine the possible effects of paclitaxel and other chemotherapeutic agents on adipogenesis in the setting of cachexia.

#### 5. Conclusion

This study was conducted to provide a better understanding of how chemotherapeutic agents affect adipose tissue at the molecular level during cachexia. The expression of the adipogenesis-related gene *PPAR $\gamma$*  and the cachexia biomarker *AZGP1* was examined the effects of paclitaxel administered at each stage of preadipocyte differentiation into mature adipocytes. It decreased *PPAR $\gamma$*  expression and lipid accumulation in a dose-dependent manner. The results demonstrated that paclitaxel when employed as a chemotherapeutic treatment for cachectic tumors, has a negative effect on adipocyte differentiation that is dose dependent. It is thought that these findings contribute to the literature for further analysis. Basic data has been provided for the steps to be taken to increase the quality of life of cachectic cancer patients.

**Conflict of interest:** The authors declare that they have no conflict of interests.

**Informed consent:** The authors declare that this manuscript did not involve human or animal participants and informed consent was not collected.

## References

- Bao, Y., Bing, C., Hunter, L., Jenkins, J. R., Wabitsch, M., & Trayhurn, P. (2005). Zinc- $\alpha$ 2-glycoprotein, a lipid mobilizing factor, is expressed and secreted by human (SGBS) adipocytes. *FEBS letters*, 579(1), 41-47.
- Batista Jr, M. L., Oliván, M., Alcantara, P. S. M., Sandoval, R., Peres, S. B., Neves, R. X., ... & Seelaender, M. (2013). Adipose tissue-derived factors as potential biomarkers in cachectic cancer patients. *Cytokine*, 61(2), 532-539.
- Beluzi, M., Peres, S. B., Henriques, F. S., Sertie, R. A., Franco, F. O., Santos, K. B., ... & Batista Jr, M. L. (2015). Pioglitazone treatment increases survival and prevents body weight loss in tumor-bearing animals: possible anti-cachectic effect. *PLoS one*, 10(3), e0122660.
- Bing, C., Russell, S., Becket, E., Pope, M., Tisdale, M. J., Trayhurn, P., & Jenkins, J. R. (2006). Adipose atrophy in cancer cachexia: morphologic and molecular analysis of adipose tissue in tumour-bearing mice. *British journal of cancer*, 95(8), 1028-1037.
- Burgi, W., & Schmid, K. (1961). Preparation and properties of Zn- $\alpha$ 2-glycoprotein of normal human plasma. *Journal of Biological Chemistry*, 236(4), 1066-1074.
- Cabrera, A. R., Parker, K., Snoke, D. B., Hammig, B., & Greene, N. P. (2025). Landscape of Clinical Trials in Cancer Cachexia: Assessment of Trends From 1995-2024. *medRxiv*, 2025-03.
- Chang, Y. H., Liu, H. W., Chu, T. Y., Wen, Y. T., Tsai, R. K., & Ding, D. C. (2017). Cisplatin-impaired adipogenic differentiation of adipose mesenchymal stem cells. *Cell Transplantation*, 26(6), 1077-1087.
- Choi, J. Y., Kim, Y. J., Shin, J. S., Choi, E. B., Kim, Y., Kim, M. G., ... & Kim, J. G. (2025). Integrative metabolic profiling of hypothalamus and skeletal muscle in a mouse model of cancer cachexia. *Biochemical and Biophysical Research Communications*, 151766.
- Choron, R. L., Chang, S., Khan, S., Villalobos, M. A., Zhang, P., Carpenter, J. P., ... & Liu, Y. (2015). Paclitaxel impairs adipose stem cell proliferation and differentiation. *Journal of Surgical Research*, 196(2), 404-415.
- Chu, D. T., Malinowska, E., Gawronska-Kozak, B., & Kozak, L. P. (2014). Expression of adipocyte biomarkers in a primary cell culture models reflects preweaning adipobiology. *Journal of Biological Chemistry*, 289(26), 18478-18488.
- Dasari, S., & Tchounwou, P. B. (2014). Cisplatin in cancer therapy: molecular mechanisms of action. *European journal of pharmacology*, 740, 364-378.
- Deng, L., Bao, W., Zhang, B., Zhang, S., Chen, Z., Zhu, X., ... & Chen, G. (2023). AZGP1 activation by lenvatinib suppresses intrahepatic cholangiocarcinoma epithelial-mesenchymal transition through the TGF- $\beta$ 1/Smad3 pathway. *Cell Death & Disease*, 14(9), 590.
- Di Sebastiano, K. M., & Mourtzakis, M. (2012). A critical evaluation of body composition modalities used to assess adipose and skeletal muscle tissue in cancer. *Applied Physiology, Nutrition, and Metabolism*, 37(5), 811-821.
- Ebadi, M., & Mazurak, V. C. (2014). Evidence and mechanisms of fat depletion in cancer. *Nutrients*, 6(11), 5280-5297.
- Elattar, S., Dimri, M., & Satyanarayana, A. (2018). The tumor secretory factor ZAG promotes white adipose tissue browning and energy wasting. *The FASEB Journal*, 32(9), 4727.
- Fearon, K., Strasser, F., Anker, S. D., Bosaeus, I., Bruera, E., Fainsinger, R. L., ... & Baracos, V. E. (2011). Definition and classification of cancer cachexia: an international consensus. *The lancet oncology*, 12(5), 489-495.
- Huang, T. H., Wu, T. H., Guo, Y. H., Li, T. L., Chan, Y. L., & Wu, C. J. (2019). The concurrent treatment of *Scutellaria baicalensis* Georgi enhances the therapeutic efficacy of cisplatin but also attenuates chemotherapy-induced cachexia and acute kidney injury. *Journal of Ethnopharmacology*, 243, 112075.
- Goncalves, M. D., Hwang, S. K., Pauli, C., Murphy, C. J., Cheng, Z., Hopkins, B. D., ... & Cantley, L. C. (2018). Fenofibrate prevents skeletal muscle loss in mice with lung cancer. *Proceedings of the National Academy of Sciences*, 115(4), E743-E752.
- Khan, M. S., Butler, J., & Anker, M. (2025). Weight gain among cancer patients receiving chemotherapy—facts and numbers. *Journal of Cachexia, Sarcopenia and Muscle*, 16(1), e13694.
- Kim, H. Y., Jang, H. J., Muthamil, S., Shin, U. C., Lyu, J. H., Kim, S. W., Go, Y., Park, S. H., Lee, H. G., & Park, J. H. (2024). Novel insights into regulators and functional modulators of adipogenesis. *Biomedicine & pharmacotherapy = Biomedecine & pharmacotherapie*, 177, 117073.
- Kurtulus, E. M., Karis, D., Ercan, A. M., & Konukoglu, D. (2024). Zinc Alpha-2 Glycoprotein, Acylated Ghrelin, and Zinc Levels in Prediabetics. *in vivo*, 38(2), 975-981.
- Langer, H. T., Ramsamooj, S., Dantas, E., Murthy, A., Ahmed, M., Ahmed, T., ... & Goncalves, M. D. (2024). Restoring adiponectin via rosiglitazone ameliorates tissue wasting in mice with lung cancer. *Acta Physiologica*, e14167.
- Laviano, A., Seelaender, M., Sanchez-Lara, K., Gioulbasanis, I., Molfino, A., & Fanelli, F. R. (2011). Beyond anorexia-cachexia. Nutrition and modulation of cancer patients' metabolism: supplementary, complementary or alternative anti-neoplastic therapy?. *European Journal of Pharmacology*, 668, S87-S90.
- Lopes, M. A., Franco, F. O., Henriques, F., Peres, S. B., & Batista, M. L. (2018). LLC tumor cells-derived factors reduces adipogenesis in co-culture system. *Heliyon*, 4(7).
- Mannelli, M., Gamberi, T., Magherini, F., & Fiaschi, T. (2020). The adipokines in cancer cachexia. *International Journal of Molecular Sciences*, 21(14), 4860.
- Martinez-Navarro, I., Vilchis-Gil, J., Cossio-Torres, P. E., Hernández-Mendoza, H., Klünder-Klünder, M., Layseca-Espinosa, E., Galicia-Cruz, O. G., & Rios-Lugo, M. J. (2024). Serum Zinc-Alpha-2 Glycoprotein and Zinc Levels and Their Relationship with Insulin Resistance and Biochemical Parameters in Overweight and Obese Children. *Biological trace element research*. Advance online publication.
- Mracek, T., Stephens, N. A., Gao, D., Bao, Y., Ross, J. A., Ryden, M., ... & Bing, C. (2011). Enhanced ZAG production by subcutaneous adipose tissue is linked to weight loss in gastrointestinal cancer patients. *British Journal of Cancer*, 104(3), 441-447.
- Mota, I. N. R., Satari, S., Marques, I. S., Santos, J. M. O., & Medeiros, R. (2024). Adipose tissue rearrangement in cancer cachexia: The involvement of  $\beta$ 3-adrenergic receptor associated pathways. *Biochimica et biophysica acta. Reviews on cancer*, 1879(3), 189103.
- Muliawati, Y., Haroen, H., & Rotty, L. W. (2012). Cancer anorexia-cachexia syndrome. *pathogenesis*, 5(5), 154-162.
- Ni, J., & Zhang, L. (2020). Cancer cachexia: definition, staging, and emerging treatments. *Cancer Management and Research*, 5597-5605.
- Panagiotou, G., Babazadeh, D., Mazza, D. F., Azghadi, S., Cawood, J. M., Rosenberg, A. S., ... & Chondronikola, M. (2025). Brown adipose tissue is associated with reduced weight loss and risk of cancer cachexia: A retrospective cohort study. *Clinical Nutrition*, 45, 262-269.
- Peixoto da Silva, S., Santos, J. M., Costa e Silva, M. P., Gil da Costa, R. M., & Medeiros, R. (2020). Cancer cachexia and its pathophysiology: links with sarcopenia, anorexia and asthenia. *Journal of Cachexia, Sarcopenia and Muscle*, 11(3), 619-635.
- Pendás, A. M., Matilla, T., Uría, J. A., Freije, J. P., Fueyo, A., Estivill, X., & López-Otín, C. (1994). Mapping of the human Zn- $\alpha$ 2-glycoprotein gene (AZGP1) to chromosome 7q22 by *in situ* hybridization. *Cytogenetic and Genome Research*, 66(4), 263-266.
- Senyigit, A., Durmus, S., Tabak, O., Oruc, A., Uzun, H., & Ekinci, I. (2024). The Associations between Asprosin, Clusterin, Zinc Alpha-2-Glycoprotein, Nuclear Factor Kappa B, and Peroxisome Proliferator-Activated Receptor Gamma in the Development of Complications in Type 2 Diabetes Mellitus. *Journal of clinical medicine*, 13(20), 6126.
- Qiu, S., Wu, Q., Wang, H., Liu, D., Chen, C., Zhu, Z., ... & Yang, M. (2024). AZGP1 in POMC neurons modulates energy homeostasis and metabolism through leptin-mediated STAT3 phosphorylation. *Nature*

- Communications*, 15(1), 3377.
- Qin, H., Yuan, Y., Yuan, M., Wang, H., & Yang, Y. (2024). Degradation of AZGP1 suppresses the progression of breast cancer cells via TRIM25. *Environmental Toxicology*, 39(2), 882-889.
- Unver, S., Biyik, I., Akman, T., Simsek, E., Kucuk, H., Kaplan, A., ... & Cayci, Y. T. (2024). Effect of acute anaerobic performance on zinc alpha 2 glycoprotein, apelin and lipasin levels. *PeerJ*, 12, e18093.
- Wen, R. M., Qiu, Z., Marti, G. E. W., Peterson, E. E., Marques, F. J. G., Bermudez, A., Wei, Y., Nolley, R., Lam, N., Polasko, A. L., Chiu, C. L., Zhang, D., Cho, S., Karageorgos, G. M., McDonough, E., Chadwick, C., Ginty, F., Jung, K. J., Machiraju, R., Mallick, P., ... Brooks, J. D. (2024). AZGP1 deficiency promotes angiogenesis in prostate cancer. *Journal of translational medicine*, 22(1), 383.
- Xu, M., Jin, X., & Shen, Z. (2024). ZAG promotes colorectal cancer cell proliferation and epithelial–mesenchymal transition by promoting lipid synthesis. *Open Life Sciences*, 19(1), 20221007.
- Yeung, D. C., Lam, K. S., Wang, Y., Tso, A. W., & Xu, A. (2009). Serum zinc- $\alpha$ 2-glycoprotein correlates with adiposity, triglycerides, and the key components of the metabolic syndrome in Chinese subjects. *The Journal of Clinical Endocrinology & Metabolism*, 94(7), 2531-2536.
- You, J. S., Lee, Y. J., Kim, K. S., Kim, S. H., & Chang, K. J. (2014). Anti-obesity and hypolipidaemic effects of Nelumbo nucifera seed ethanol extract in human pre-adipocytes and rats fed a high-fat diet. *Journal of the Science of Food and Agriculture*, 94(3), 568-575.
- Yun, H., Jeong, H. R., Kim, D. Y., You, J. E., Lee, J. U., Kang, D. H., ... & Jin, D. H. (2024). Degradation of AZGP1 suppresses apoptosis and facilitates cholangiocarcinoma tumorigenesis via TRIM25. *Journal of Cellular and Molecular Medicine*, 28(3), e18104.
- Zhu, H. J., Ding, H. H., Deng, J. Y., Pan, H., Wang, L. J., Li, N. S., ... & Gong, F. Y. (2013). Inhibition of preadipocyte differentiation and adipogenesis by zinc- $\alpha$ 2-glycoprotein treatment in 3T3-L1 cells. *Journal of Diabetes Investigation*, 4(3), 252-260.
- Zhou, X., Deng, C., Chen, L., Lei, L., Wang, X., Zheng, S., ... & Yang, J. (2024). Zinc-alpha2-glycoprotein modulates blood pressure by regulating renal lipid metabolism reprogramming-mediated urinary Na<sup>+</sup> excretion in hypertension. *Cardiovascular Research*, 120(16), 2134-2146.
- Zimowska, M., Rolbiecka, M., Antoniuk-Pietrynczak, K., Jaskulak, M., & Zorena, K. (2024). Dynamics of Serum Inflammatory Markers and Adipokines in Patients: Implications for Monitoring Abnormal Body Weight: Preliminary Research. *Metabolites*, 14(5), 260.

**Cite as:** Agirel, O., & Okudu, C. (2025). The effect of paclitaxel on cachexia-related gene *AZGP1* expression during adipocyte differentiation. *Front Life Sci RT*, 6(1), 28-34.



## Research article

## Analysis of potential fire and explosion incidents in an LNG terminal in a port area using the FRAM method

Ahmet Gokcan<sup>\*1</sup> , Hacer Handan Demir<sup>2</sup> , Rabia Akdogan<sup>3</sup> , Fahri Oluk<sup>4</sup> , Goksel Demir<sup>1</sup> 

<sup>1</sup> University of Health Science Türkiye, Hamidiye Faculty of Health Sciences, Occupational Health and Safety Department, 34668, Istanbul, Türkiye

<sup>2</sup> University of Health Science Türkiye, Hamidiye Faculty of Health Sciences, Emergency Aid and Disaster Management Department, 34668, Istanbul, Türkiye

<sup>3</sup> University of Health Science Türkiye, Hamidiye Institute of Health Sciences, Health Management Department, 34668, Istanbul, Türkiye

<sup>4</sup> Cankiri Karatekin University, Social Sciences Vocational School, Property Protection and Security Department, 18100, Cankiri, Türkiye

### Abstract

The commercialization of liquefied natural gas (LNG) offers significant benefits to various industries; however, its chemical properties pose substantial risks, potentially resulting in catastrophic incidents. The transportation, storage, and utilization of flammable substances like LNG can lead to industrial accidents, such as fires and explosions, if not adequately controlled. To mitigate these risks, conducting a comprehensive hazard and risk analysis at the worksite and implementing appropriate safety measures are essential. This study focuses on analyzing potential fire and explosion scenarios that may arise in a port area engaged in LNG operations, employing the Functional Resonance Analysis Method (FRAM). Accident processes are examined through functional analysis, identifying 20 distinct functions. Of these, 7 functions were categorized as high risk, 5 as medium risk, and 8 as low risk. Based on the findings, this study provides recommendations for safety measures aimed at safeguarding both occupational health and environmental integrity.

**Keywords:** Explosion; FRAM; liquefied natural gas; safety measures; occupational health and safety

### 1. Introduction

The global energy demand continues to grow as it plays a crucial role in enhancing the well-being of populations worldwide. Among the various energy sources available, fuel oil and natural gas have been preferred choices, particularly since the 20th century. Natural gas is recognized as one of the cleanest fossil fuels due to its high hydrogen-to-carbon ratio and low sulfur content, provided it is commercialized (Wu et al., 2023). Its composition includes gases such as methane, ethane, butane, propane, carbon dioxide, oxygen, and nitrogen, with methane

being the primary component (Akpınar and Basibuyuk, 2011).

Due to the uneven distribution of natural gas production, transportation over long distances are essential. For this purpose, natural gas must be converted into a liquefied form (liquefied natural gas-LNG) at -162°C and atmospheric pressure. In its liquefied state, natural gas occupies 1/625th of its original volume and has a density of approximately 45%, making it suitable for long-distance transport and storage in commercial seaports via sea transportation (Avci et al., 1995; Shirazi et al., 2019). The increasing utilization for commercial purposes has led to a growing demand for this energy resource in recent years

\* Corresponding author.

E-mail address: [ahmet.gokcan@sbu.edu.tr](mailto:ahmet.gokcan@sbu.edu.tr) (A. Gokcan).

<https://doi.org/10.51753/flsrt.1612860> Author contributions

Received 03 January 2025; Accepted 14 April 2025

Available online 30 April 2025

2718-062X © 2025 This is an open access article published by Dergipark under the [CC BY](https://creativecommons.org/licenses/by/4.0/) license.

(Pospisil et al., 2019). According to data from the International Energy Agency, the rising LNG demand in Asian countries has contributed significantly to overall market growth (Akpınar and Basibuyuk, 2011).

From an environmental perspective, the use of LNG as a fuel offers a promising solution to reducing emissions. To accommodate the growing demand, high-capacity tanks (160,000 m<sup>3</sup> and above) have been developed to store LNG reserves. However, despite the advantages LNG offers to various industries, its chemical properties pose significant risks, potentially leading to catastrophic incidents (Baalisampang et al., 2019). Methane, the primary component of LNG, can detonate when it forms a gaseous mixture with air at concentrations of 5-15%. Loss of control during the transportation, storage, or utilization of LNG could result in severe accidents, including fires and explosions (Animah and Shafiee, 2020).

Particularly, LNG stored in tanks can evaporate and form explosive vapors in the event of a leak. Historical analyses of explosion disasters have identified LNG vapor leaks as a frequent cause of such incidents. To mitigate the risks of fires and explosions in workplaces handling LNG, hazard and risk analyses must be conducted, and appropriate safety measures should be implemented (Animah and Shafiee, 2020; Huffman et al., 2024).

Risk assessment, a relatively young scientific discipline developed 30-40 years ago, is widely applied across various industries, including healthcare, engineering, infrastructure, transportation, security, defense, and the social and legal sectors (Aven, 2016). While traditional risk analysis methods focus on investigating the direct consequences of accidents, modern methods such as the Functional Resonance Analysis Method (FRAM) and Systems-Theoretical Accident Modeling and Processes (STAMP) have gained prominence. These approaches aim to analyze the complex nature of accidents and understand how seemingly normal operations can lead to accidents (Patriarca et al., 2020; De Carvalho, 2011).

FRAM examines how a system operates as a whole, identifies potential disruptions in its functionality, and determines ways to enhance flexibility in response to such disruptions. Unlike traditional methods, FRAM focuses on system-level interactions rather than the direct outcomes of accidents (Bal Besikci and Sihmantepe, 2020). Initially, FRAM was applied in the aviation sector to investigate accidents and has since been adopted across various industrial domains (Patriarca et al., 2017).

In this study, a scenario involving a potential fire and explosion in an LNG tank located in a designated shipyard area was developed, and the hazards and risks were analyzed using the FRAM method. This approach enabled the identification of all potential hazards, risks, and related variable factors as an integrated system. The relationships between seemingly independent events were also examined. The findings will be presented using the FRAM model to provide a comprehensive understanding of the system's vulnerabilities and potential disruptions.

## 2. Materials and methods

### 2.1. Functional resonance analysis method (FRAM)

FRAM analysis, which is used to create potential accident scenarios that may occur in work environments, was introduced

by Hollnagel (2016) and developed in the following years (Hollnagel, 2016). FRAM is a systemic analysis method that tries to explain the non-linear relationships and interactions between different functions in a system. FRAM focuses more on the explanation of complex interactions in the system. By analyzing the activities of a normal system, it takes into account functional variables and disturbances between variables (Naeini and Nadeau, 2022). The functions in a planned system, scenario, or simulation are defined functionally, and by characterizing each variable in the determined functions, it enables the interpretation of the interactions between them and the provision of recommendations for taking the necessary safety measures in case of the emergence of an unexpected variable (Furniss et al., 2016). The goal of FRAM analysis is to find out how the components of the functions affect the events and how the results will change with the changing conditions. FRAM is an analysis method that requires the use of imagination. It considers the system as a whole, not in parts, and provides the person who does it with a clue, not an answer (Franca et al., 2021). The main purpose of FRAM analysis is to find the connections between the variables of the function and to examine the system function by analyzing how they affect the system. FRAM is a new risk analysis method and therefore it is a long and difficult analysis method to prepare. The main steps of FRAM analysis are;

- Determine the main goal of the model and define the event to be analyzed,
- Determine and characterize the main functions of the process according to input, output, preconditions, resources, time and control,
- Characterize the actual/potential variability of the functions,
- Identify functional resonances based on potential connections between functions, considering both normal and worst-case variability,
- Provide ways to monitor and minimize performance variability (Hollnagel, 2012).

The Functional Resonance Analysis Method is based on four basic principles: the basic principle of success and failure, the principle of approximate adjustments, the principle of emergence, and the principle of functional resonance. FRAM analysis takes place in four main stages (Hollnagel et al., 2014; Koruklu and Ozay, 2021).

- Defining functions
- Determine variability
- Bringing variability together
- Managing variability

The first stage of FRAM analysis is to create the functions and determine the parameters of the functions. In FRAM analysis, functions provide the connection between each other. A function can have six parameters. Not all these parameters have to be in a function (Rosa et al., 2015).

Function Parameters;

- Input (I)
- Output (O)
- Control (C)
- Time (T)
- Source (S)

- Prerequisite (P)

For each function determined in the risk analysis, the parameters in Fig. 1 are created and a connection is established between the determined functions. In the FRAM analysis, each function can be connected to a single module or a connection can be established on more than one module. In the FRAM analysis, the common performance value that reveals the factors affecting the system and how the system operation is affected is revealed. In this context, the common performance value is classified as sufficient, insufficient, and unpredictable. Common performance evaluation criteria are given in Table 1.

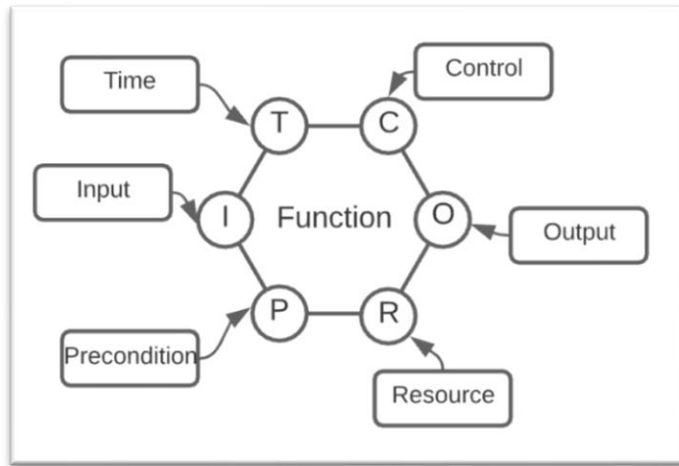


Fig. 1. Function parameters.

Table 1  
FRAM common performance evaluation criteria.

Common Performance Value	Probability of Risk Occurrence
Adequate	Very Low
Inadequate	High
Unpredictable	Very High

The changes that may occur between the specified functions and performance values are divided into 4 categories. These categories explain the fluctuations that occur between the functions and performance values. The performance-based changes in the specified functions are evaluated in 4 categories and are given in Table 2.

Table 2  
Performance-based change.

Performance Based Fluctuations	Common Performance Value
Random Functional Module	Unpredictable $\geq$ 3 or Inadequate $\geq$ 8
Opportunity Functional Module	Unpredictable=2 or Inadequate $\geq$ 6
Tactical Functional Module	Unpredictable=1 or Inadequate $\geq$ 4
Strategy Functional Module	Unpredictable=0 or Inadequate $\leq$ 3

The categories in Table 2 describe the fluctuations in the determined functions. The random functional module in these categories is the module with the largest fluctuations, and the random evaluation of one of the determined functions explains why the error occurs very easily and creates functional resonance (Ozsayan and Barlas, 2023). While creating the FRAM analysis, the FRAM Model Visualizer (FMV) software tool introduced by Hill and Hollnagel (2016) is used. The determined functions are entered into the software system with the FRAM analysis stages and the connection between the

functions is created (Hill and Slater, 2024). Fig. 2 shows an example of FRAM obtained from the software system.

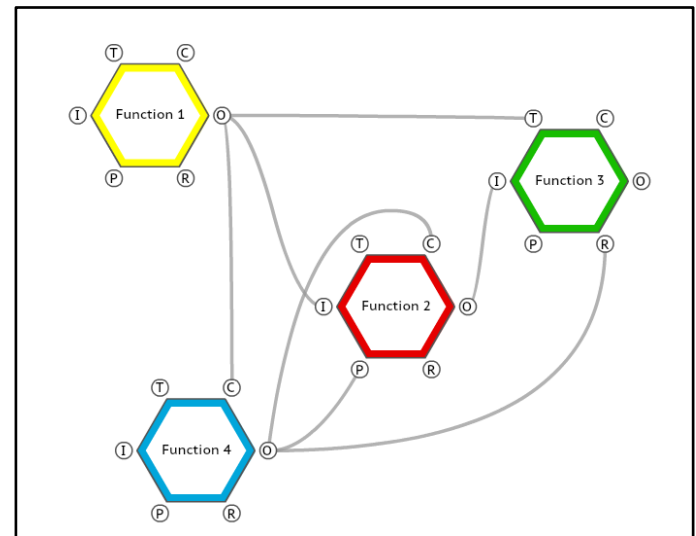


Fig. 2. FRAM connection example.

In this study, a port area located in the Marmara Region of Turkey and having an LNG terminal was determined. This area is an important area in terms of maritime transportation and employment and approximately 150,000 people are employed. The location of the LNG tank in the area is given in Fig. 3.



Fig. 3. Port area location.

A case study was conducted on occupational health and safety regarding a possible fire and explosion in an LNG tank used for commercial purposes. This analysis aimed to adopt proactive approaches in the field of occupational health and safety, to combat risks at source by detecting possible hazards in advance and to take necessary precautions to increase the health and safety of employees, and in this context, a possible fire and explosion in an LNG tank was analyzed using the FRAM analysis method. Before starting the FRAM analysis, a scenario was prepared for the possible fire and explosion process.

## 2.2. Scenario

While storing 40,000 m<sup>3</sup> of LNG for commercial use on a chemical tanker ship at the LNG terminal in the Marmara Region, an LNG leak occurred due to an unnoticed and invisible crack in the tanker supply pipeline. The leak continued because the gas detectors on the ship did not activate and the LNG, which had turned from liquid to gas, began to accumulate in a closed area. Methane, which turned into gas and is an important component of LNG, began to form an explosive vapor cloud.

**Table 3**  
Functions and variables related to functions.

	Function	FD	Variable	Description
F1	LNG tanker vessel leaks due to crack in supply pipeline	F1D1	The leak was detected early.	The risk of fire or explosion due to leakage has been eliminated.
		F1D2	The leak went unnoticed.	Explosion and fire occurred due to the methane gas in the leaking LNG reaching the explosion percentage.
F2	The gas detector on board failed to activate and the leaking LNG entered the gas phase, creating a flammable gas cloud	F2D1	The flammable gas cloud intervened before it reached the explosion percentage	The methane in LNG was intervened before it reached the explosion percentage, thus eliminating the risk of explosion and fire.
		F2D2	The flammable gas cloud could not be intervened.	Explosion and fire occurred due to the methane in LNG reaching the explosion percentage.
F3	An explosion occurred on the ship when the methane in the flammable gas cloud reached the explosion percentage.	F3D1	It happened during the day.	The shipyard has many employees.
		F3D2	It happened at night.	At the shipyard, there are only shift workers and those on duty for the transfer process.
		F3D3	There was a small explosion.	It only requires intervention to the LNG tanker and the workers on board.
		F3D4	There was a very violent explosion.	It requires immediate intervention to the LNG tanker vessel being worked on, the surrounding vessels and the workers on board.
		F3D5	Temperature high	The risk of a post-explosion fire is increased and the environment in which it can impact is larger.
		F3D6	Temperature low	The risk of fire occurring after the explosion has decreased and the environment it will affect is limited.
F4	The explosion released methane gas into the environment.	F4D1	Low impact on workers and the environment.	No emergency intervention required for workers and the environment.
		F4D2	Highly impacted employees and the environment.	Immediate intervention is required for workers and the environment.
F5	Fire caused by explosion	F5D1	The fire is under control.	The fire was prevented from growing. Measures were taken to minimize the impact on people and the environment.
		F5D2	The fire grew.	The fire could not be brought under control. People and the environment have been greatly affected. Because of this impact, people and the environment need urgent intervention.
F6	Safety valve on tanker vessel activated	F6D1	The safety valve activated without any problems.	That is what is necessary.
		F6D2	The safety valve failed to activate.	It was activated manually.
F7	The electrical system has been disabled.	F7D1	The electrical system was automatically deactivated.	That is what is necessary.
		F7D2	The electrical system could not be deactivated.	The system was manually deactivated.
F8	An emergency alert was issued at the shipyard.	F8D1	Emergency alert has been issued.	People in the area were informed of the emergency. Early precautions were also taken in the neighborhood.
		F8D2	The emergency alarm didn't work.	People in the area could not be informed about the emergency. Early measures could not be taken due to the lack of information about the situation.
F9	The shipyard's emergency response team arrived at the scene.	F9D1	Emergency teams arrived on the scene just in time.	Emergency intervention happens just in time.
		F9D2	Emergency crews did not arrive on the scene in time.	Intervention is disrupted.
F10	Employees were directed to assembly areas for evacuation.	F10D1	The emergency plan was adhered to and the area was quickly evacuated.	Evacuation and intervention happen just in time.
		F10D2	There was chaos because the employees panicked.	Evacuation is delayed, exposing workers to another explosion and more toxic gases.
F11	Entrances and exits to the scene were closed.	F11D1	Entrances and exits were closed after checking that no one was left at the scene.	That is what is necessary.
		F11D2	The entrances and exits were closed, but due to lack of control, some people remained at the scene.	The scene is checked again. Workers remaining in the area will continue to be exposed to the explosion and toxic gases.
F12	The injured were treated at the scene.	F12D1	Those injured at the scene were treated just in time.	The injured received first aid on time and were transferred to ambulances on time.
		F12D2	Response to the injured at the scene was delayed.	The first aid and ambulance transport of the injured was not timely. Their condition deteriorated.
F13	Emergency responders were called.	F13D1	Emergency responders were notified just in time.	The explosion and fire were intervened from the sea at the right time.
		F13D2	Emergency responders were notified late.	Response to the explosion and fire from the sea was delayed. The time to bring the situation under control has increased.

F14	General control was carried out in the bay with boats by the teams.	F14D1	The controls were carried out correctly.	That is what is necessary.
		F14D2	Checks detected deficiencies.	Areas not checked by the teams could not be intervened. Checks are carried out again and completely.
		F14D3	While the controls were taking place, the boats malfunctioned, and the controls were interrupted.	An emergency response team is called to the boats and the team that will provide controls is sent to the place of the malfunctioning boat.
F15	The teams started to intervene with the necessary equipment to prevent the spread. They made sure the incident was under control.	F15D1	The intervention was timely and correct.	The incident was contained.
		F15D2	During the intervention, a malfunction occurred, and the intervention could not be carried out.	The incident grew and there was an increase in the number of people affected. A team was dispatched to fix the fault early.
F16	The incident was under control.	F16D1	The situation is under control.	That is what is necessary.
		F16D2	The situation could not be contained.	The incident has escalated and there has been an increase in those affected. The scene has been asked to be checked again.
F17	Cooling work has begun.	F17D1	The cooling works were successfully realized.	The environment has been adapted to eliminate the risk of explosion and fire recurrence.
		F17D2	The cooling work could not be carried out in a complete and timely manner.	The environment could not be made safe. There is a risk of explosion and fire recurrence.
F18	Debris removal has begun.	F18D1	Debris removal was carried out safely.	Hazards such as falling and being trapped under the material were eliminated and a new accident was prevented.
		F18D2	Debris removal could not be carried out safely.	An accident occurred while debris was being removed. Teams were deployed to ensure ambient safety.
F19	Cleanup operations have started for the LNG leaking into the sea.	F19D1	LNG cleaning operations were carried out thoroughly and accurately.	The danger of methane gas for marine life and the atmosphere has been eliminated.
		F19D2	LNG cleaning operations could not be carried out.	Methane gas is dangerous for living things and the environment. Methane gas should be measured in the environment and cleanup should be carried out completely and correctly as soon as possible.
F20	Damage assessment work has begun.	F20D1	The team started damage assessment on time.	Timely loss assessment for the enterprise is important for economy and sustainability.
		F20D2	The team was late in starting the damage assessment.	Delays in damage assessment have a negative impact on the economy and sustainability. Damage assessment should be carried out as soon as possible.

The explosive vapor cloud formed in the region reached 5%-15% degrees and caused an explosion in the terminal. The explosion that could have occurred according to the scenario created was analyzed with FRAM and explained in the findings section.

### 3. Results

Functions were determined for the hazards and risks that may arise by analyzing the possible explosion of the LNG tank in the shipyard port area by the FRAM analysis method. The functions are indicated with the letter “F” and the parameters that should occur for each function are explained and given in Table 3.

The parameters of the functions are determined separately for each function in Table 3. After the parameters of the functions were determined, the next step was to determine the variables. Variables were determined for each function and the variables were numbered with the letter D and explanations were made including the actions to be taken regarding the determined variables.

Within the scope of the analysis, 20 functions were defined and the impact of each function on security was evaluated. In this analysis, the functions were classified according to their risk levels; %35 (n=7) of them were determined as high risk, %25 (n=5) as medium risk and %40 (n=8) as low risk and are given in Fig. 4.

As a result of the analysis, the functions were examined one by one, and it was seen that the function coded F3 “An explosion occurred on the ship when the methane in the flammable gas cloud reached the explosion percentage” was the strongest function in the analysis. A visual analysis of the

function is given in Fig. 5. This function is explained below to provide an example of how the result of the analysis is interpreted.

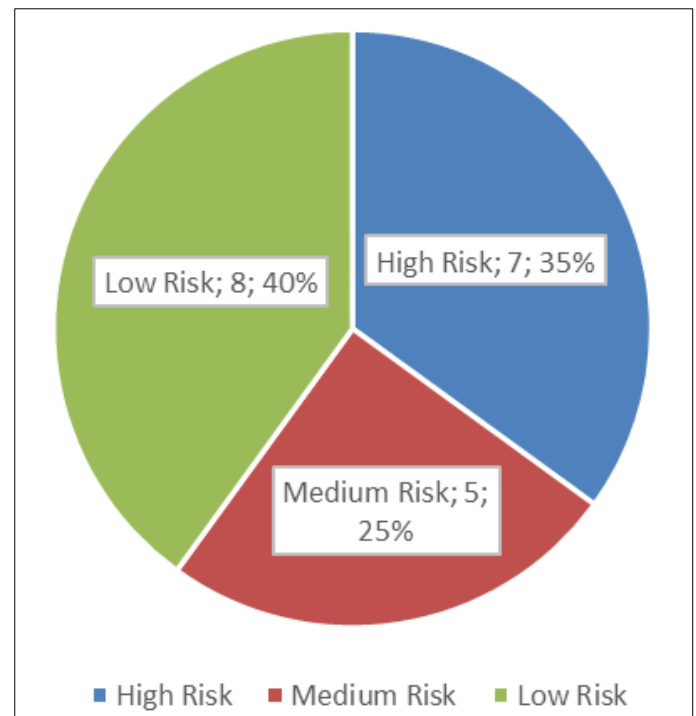


Fig. 4. Risk levels.

The F3 function has 2 inputs: “F1- A leak occurred due to a crack in the supply pipeline on the LNG tanker ship”, “F2- The

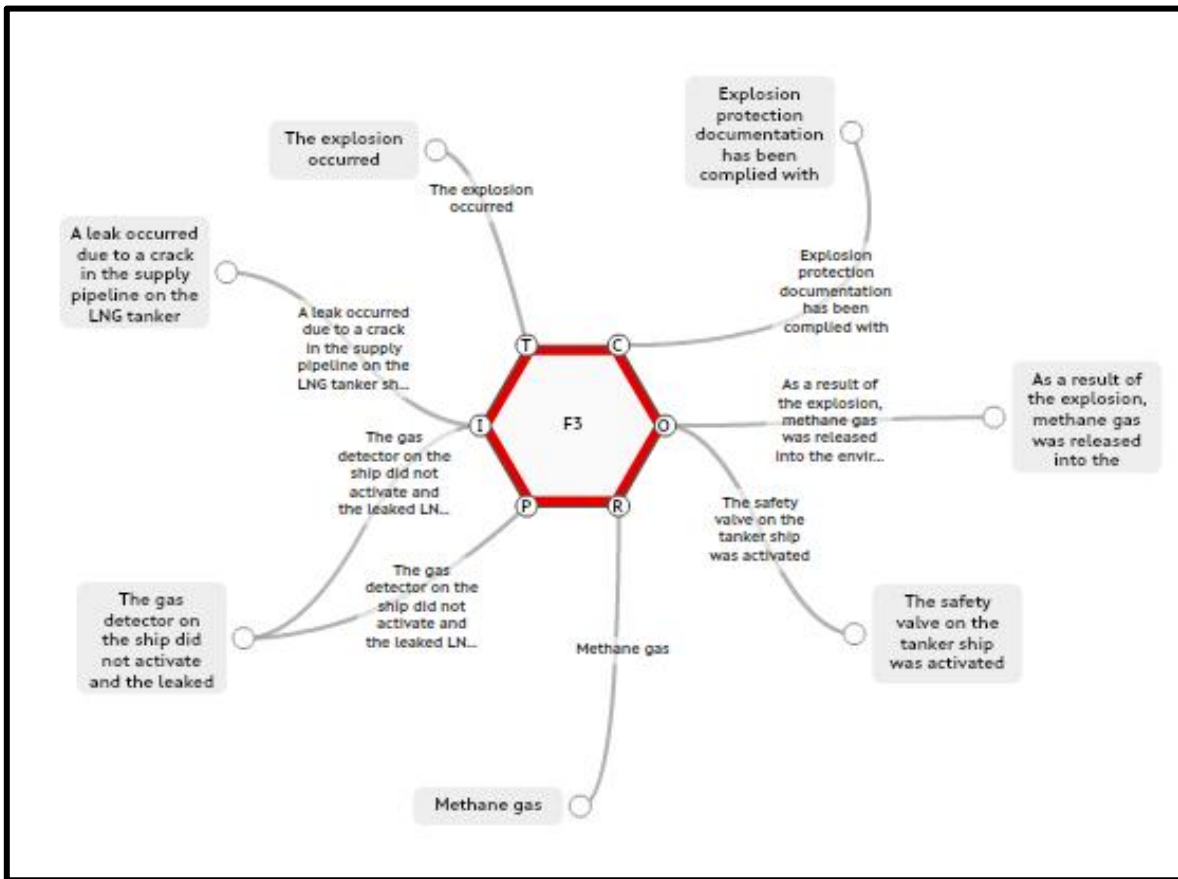


Fig. 5. Analysis image of F3 function.

gas detector on the ship did not activate and the leaked LNG passed into the gas phase and formed a flammable gas cloud”, 3 outputs: “F4- Methane gas was released into the environment as a result of the explosion”, “F5- A fire occurred as a result of the explosion”, “F6- The safety valve on the tanker ship was activated”, 1 precondition as “F2- The gas detector on the ship did not activate and the leaked LNG passed into the gas phase and formed a flammable gas cloud”, 1 source as “Methane gas”, 1 control as “Explosion protection document was complied with” and 1-time parameter as “Explosion occurred”.

The function F3 can have 6 variables. F3D1- May occur during the day. Since there will be a lot of human circulation (current employees, daily subcontractors, guests, deliverers) during working hours in the shipyard during the daytime and due to the intensity of hazardous work, the number of people affected by an explosion that may occur will be high. This situation will affect the response time and evacuation operations of the emergency teams in the shipyards “F9, F10, F12, and F15”.

F3D2- It may occur at night. According to this variable, the number of people affected by the explosion that may occur will be at a minimum level since the human circulation (night shift workers and transfer workers) and the intensity of dangerous work will decrease. However, toxic smoke from explosions and fires may affect people in the immediate vicinity. The precautions and interventions to be taken should be planned by considering these situations.

F3D3- Explosion may be of low intensity. People outside the transfer area may be moderately affected by the explosion. The damage that may occur because of the explosion is at a level that will not harm the business. Necessary evacuation and emergency response methods should be planned as employees located close to the LNG tanker will be affected.

F3D4- The explosion may be very violent. Since people in both the transfer area and other work areas can feel the explosion violently, it may cause panic. In this case, it is of great importance that an effective intervention plan is immediately put into effect to prevent the effect from growing and to manage the crisis correctly. People and employees in the vicinity should be taken to the assembly area quickly and safely. Effective and correct intervention should be carried out for people and the environment affected by the methane gas formed as a result of the explosion that may occur. Emergency intervention is required for the LNG tanker ship in question, the surrounding ships, and the employees there. The area of activity is greatly damaged and therefore the customer who makes the operation and investment suffers economic losses. This variability will be applied to the “F4, F5, F6, F7, F8, F9, F10, F11, F12, F13, F14, F15, F16, F17, F18, F19, F20” functions.

Therefore, variations in the F3 function may affect “F4, F5, F6, F7, F8, F9, F10, F11, F12, F13, F14, F15, F16, F17, F18, F19, F20” functions, may cause changes in intervention methods or may require the addition of new functions.

F3D5- Temperature may be high. The risk of fire after the explosion has increased and the area that the fire can affect is growing. Fire extinguishers must be in the correct position and ready for use to intervene in time for the fire that may occur. The intervention should be started by the fire extinguishing team determined in the shipyard. If the team is insufficient, the fire brigade should be called urgently.

F3D6- The temperature may be low. The risk of fire following the explosion is reduced and the area that the fire can affect remains limited. Attention should be paid to the risk of fire spread due to wind. Fire extinguishers must be in the correct position and ready for use in order to be able to intervene in time

for the fire that may occur. It should be intervened by the fire extinguishing team determined in the shipyard.

Fig. 6 shows the areas that may be affected as a result of a possible explosion in the shipyard area.

The red area is the first area to be affected when the explosion occurs and is the area where the hazard severity will be seen at the highest level. It is important to take appropriate safety measures for this area. The areas shown in yellow color are the areas where the hazard level will be seen at a high level, although they are of medium risk. Green areas are the areas where the effects of the explosion will be less than the red and yellow areas.



Fig. 6. Areas to be affected by the explosion.

In the next stage of the FRAM method, the relationship between the parameters determined for the functions was analyzed. The visual output of the analysis resulting from the

analysis is shown in Fig. 7. In the FRAM visual, it is seen how the parameters affect each other and how a parameter can be the parameter of many functions.

#### 4. Discussion

According to the *Regulation on Workplace Hazard Classes Regarding Occupational Health and Safety*, which came into effect in Türkiye in 2012, commercial LNG storage activities are classified as “very hazardous workplaces” due to their critical implications for occupational health and safety. Increasingly, scientific studies are being conducted to assess the potential explosion and fire risks associated with the oil and gas industry (Ma and Huang, 2019).

This study aims to conduct a risk analysis using the Functional Resonance Analysis Method (FRAM) to evaluate potential explosion and fire hazards in an LNG tanker within a designated shipyard port area. The study focuses on identifying the functions and variability parameters associated with these hazards and examining the relationships between them. A process comprising 20 functions was defined for the explosion scenario involving an LNG tank leak in the shipyard.

Three functions were identified as particularly critical, representing high accident risk in LNG tanker operations:

**F1:** A leak occurred due to a crack in the supply pipeline of the LNG tanker.

**F2:** The gas detector on the ship failed to activate, allowing the leaked LNG to vaporize and form a flammable gas cloud.

**F3:** An explosion occurred when the methane in the flammable gas cloud reached its explosive concentration.

Other functions identified were associated with processes occurring after the explosion event. The analysis revealed that

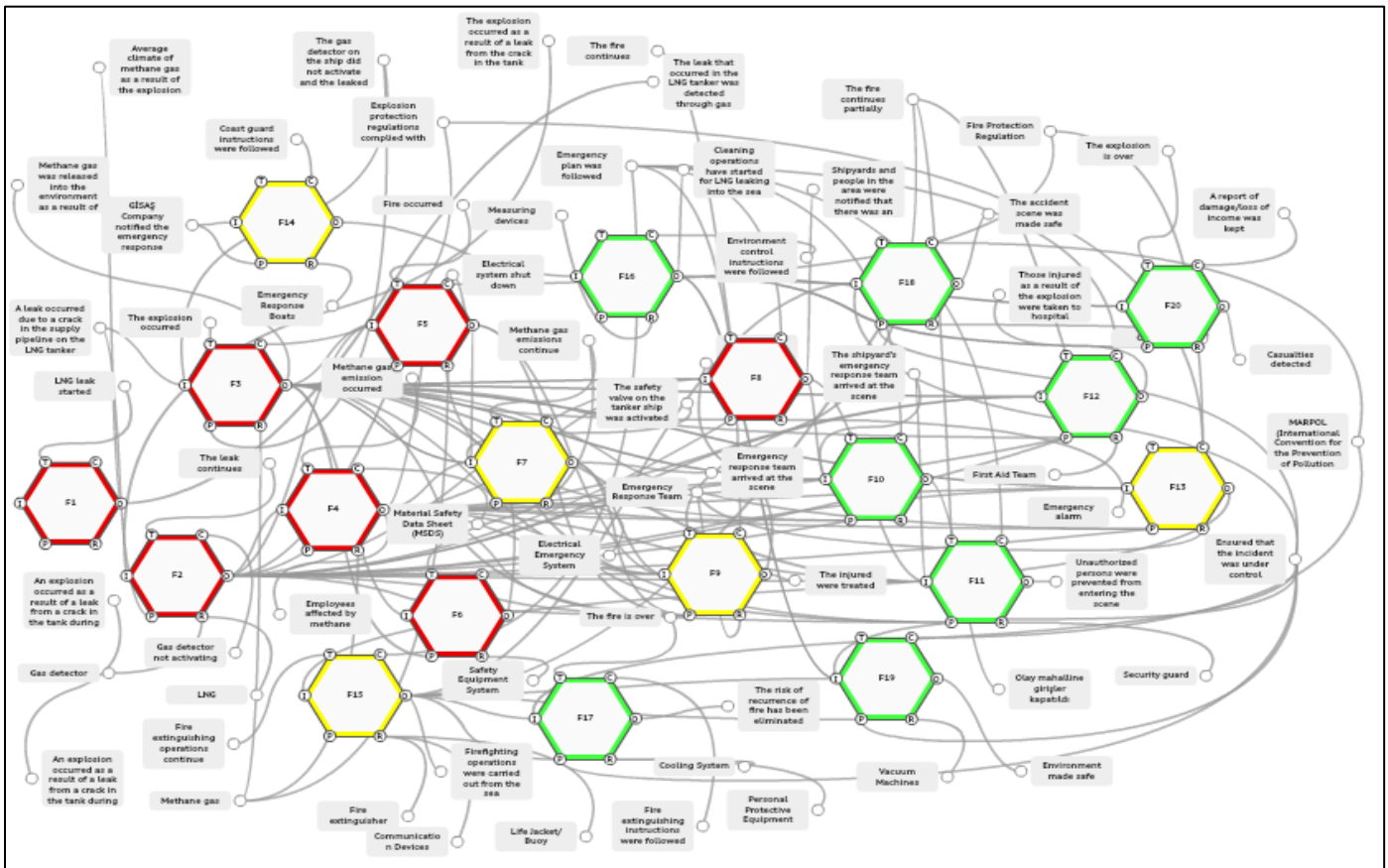


Fig. 7. FRAM analysis visualization.

all functions are interconnected, meaning that the failure of one function adversely impacts others.

The consequences of such an explosion are severe. Potential outcomes include injuries, loss of limbs, and fatalities among workers. Additionally, the hazardous chemicals in LNG can mix with the air, leading to significant air pollution. The chemical decomposition of LNG during an explosion releases a substantial amount of carbon dioxide, contributing to increased greenhouse gas levels and exacerbating climate change. Moreover, the explosion generates thermal radiation, posing a risk to individuals in the vicinity of the accident.

Environmental impacts are also significant. If LNG spills into the sea, it will result in marine pollution, endangering aquatic ecosystems. Economically, explosions in LNG operations can lead to substantial financial losses due to the high cost of LNG tanks and ship manufacturing in shipyards. Such incidents may disrupt operations, halting work until the hazardous situation is resolved, and further impacting the economy on a national scale.

An examination of extant literature reveals that...In a study by Dan et al. (2014), a quantitative risk analysis of the liquefaction system of an LNG-FPSO in an offshore environment was performed. Fire and explosion events in the upper part of the floating platform were modeled using PHAST software, and the most critical scenarios were evaluated in detail. The study also emphasized that system design in accordance with SIL (Safety Integrity Level) levels offers an effective strategy for risk management. In the present study, a qualitative analysis method, namely FRAM, was employed to examine and model fire and explosion incidents at LNG terminals. FRAM diverges from conventional failure analysis methodologies by adopting a more holistic approach, encompassing the natural functioning and failures of the system in question.

In a study by Nubli et al. (2022), CFD (Computational Fluid Dynamics) technology was used to assess the impact of LNG (Liquefied Natural Gas) on accidents. Deterministic and probabilistic methods were applied in LNG gas release and VCE (Vapor Cloud Explosions) analyses; critical zones were defined according to flammability limits. The VCE analysis guided equipment placement by examining the factors affecting the explosion pressure. CFD and FRAM methods can be complementary; one analyzes physical processes and numerical details in depth, while the other evaluates system operation and failures in a broader context.

In the study by Li and Huang (2012), the fire and explosion hazard index (F&EI) method developed by DOW was employed for the analysis of fire and explosion risks in LNG (Liquefied Natural Gas) operations. The study emphasized that the risk level, initially assessed as "very high", could be reduced to "slight" following the implementation of safety measures and substantial reductions in the hazard radius and impact area. Furthermore, simulations utilizing VCE (Vapor Cloud Explosion) and BLEVE (Boiling Liquid Expanding Vapor Explosion) models quantitated the deleterious impacts of explosions on surrounding structures, equipment and human health, thereby demonstrating the efficacy of safety measures in mitigating risks during such events.

The analysis of fire and explosion risks in LNG operations can be approached in a holistic manner through the utilization of both quantitative and qualitative methodologies. The former encompasses the application of mathematical and statistical techniques to assess risk, while the latter involves the use of

qualitative methods, such as the FRAM (Functional Resonance Analysis Model). Quantitative methods calculate the impact and magnitude of specific risks by providing numerical data through detailed modeling of physical processes. For instance, CFD (Computational Fluid Dynamics) can be utilized to mathematically simulate the propagation of gas leaks, the effects of blast radiation, and the size of damaged areas. Conversely, VCE (Vapor Cloud Explosion) and BLEVE (Boiling Liquid Expanding Vapor Explosion) models quantitatively analyze the potential consequences of fire and explosion events, providing concrete measures to reduce risks.

Conversely, the FRAM method offers a more comprehensive approach by qualitatively examining the variability of functions within the system and the interactions between these functions. The FRAM approach seeks to elucidate the interconnections between critical functions and the systemic ramifications of their failure. In the context of LNG operations, FRAM employs a more holistic approach to events such as a gas detector failure or a crack in a pipeline. This approach encompasses human factors, environmental conditions, and dynamics in system design, rather than focusing solely on physical processes.

Quantitative methods are employed to shape risk mitigation strategies by measuring the impact of specific processes; however, the FRAM method allows for the understanding of the complex interactions in the system and the wider-scale consequences of potential failures. The integration of these two approaches, when employed in tandem, facilitates a dual-faceted analysis in the risk assessment of LNG operations, thereby enabling a more comprehensive risk management strategy. The integration of these approaches has the potential to enhance the efficacy of security measures and to provide more detailed insights into the overall functioning of the system.

## 5. Conclusion

Today, LNG is a critical energy resource, and measures are being implemented to ensure its transportation and storage are as safe as those of other liquid fuels. However, the storage of cryogenic liquids remains a complex issue that is not yet fully understood. Historical incidents provide valuable insights into the risks associated with LNG. Notably, a major incident occurred in Cleveland, Ohio, in 1944, which significantly hindered the development of the U.S. LNG industry for nearly two decades. Another incident in 1979 involved the failure of an electrical seal in an LNG pump, which allowed gas to accumulate in a closed building, leading to an explosion triggered by an unidentified ignition source.

Although LNG does not exhibit flammable or explosive properties in its liquefied state, its rapid phase transition characteristic presents significant risks. At ambient temperatures, LNG quickly vaporizes, and the accumulation of the resulting gas in confined spaces can form flammable gas clouds. Methane, which constitutes a significant portion of LNG, is flammable within a concentration range of 5-15%. When this gas cloud meets an ignition source, it can lead to combustion and explosions due to the pressure generated (Foss et al., 2003).

Given the potential risks, particularly in industrial areas, it is crucial to implement and rigorously enforce safety measures to protect worker health, ensure operational safety, and prevent economic disruptions stemming from LNG-related incidents.

Measures that can be taken in terms of occupational health and safety are as follows;

LNG facilities must be equipped with comprehensive safety systems to mitigate risks associated with potential gas leaks and fires. These measures include the installation of advanced warning systems, such as gas detectors, fire detectors, and integrated security systems designed to detect and manage gas leaks effectively. Additionally, an automated emergency circuit disconnection system should be implemented to eliminate ignition sources arising from electrical systems during potential gas leaks.

Given that gas leaks frequently occur in gas transfer lines, the use of appropriate, high-quality materials and equipment in these systems is critical. Furthermore, periodic inspections of gas transfer lines by qualified specialists should be mandated to ensure their reliability and safety.

Alarm systems should be installed to promptly detect fires, and appropriate fire suppression systems must be designed to enable rapid intervention during emergencies. In addition, storage tanks should be equipped with safe discharge systems capable of automatically activating under high-pressure conditions. All safety measures should align with national and international standards to ensure a systematic and effective risk management approach.

A comprehensive risk assessment must be conducted in the work environment using an appropriate risk analysis methodology. This assessment should identify potential hazards and risks, and necessary precautions should be implemented accordingly.

## References

- Akpınar, E., & Basibuyuk, A. (2011). Jeoekonomik önemi giderek artan bir enerji kaynağı: doğalgaz. *Electronic Turkish Studies*, 6(3).
- Animah, I., & Shafiee, M. (2020). Application of risk analysis in the liquefied natural gas (LNG) sector: An overview. *Journal of Loss Prevention in the Process Industries*, 63, 103980.
- Avci, A., Can, M., & Kilic, M. Doğal gaz sıvılaştırma yöntemleri, sıvılaştırılmış doğal gazın (lng) nakli ve depolanması üzerine bir inceleme. *Pamukkale Üniversitesi Mühendislik Bilimleri Dergisi*, 1(3), 137-144.
- Aven, T. (2016). Risk assessment and risk management: Review of recent advances on their foundation. *European journal of operational research*, 253(1), 1-13.
- Baalısampang, T., Abbassi, R., Garaniya, V., Khan, F., & Dadashzadeh, M. (2019). Modelling an integrated impact of fire, explosion and combustion products during transitional events caused by an accidental release of LNG. *Process Safety and Environmental Protection*, 128, 259-272.
- Besikci, E. B., & Sihmantepe, A. (2020). Deniz kazalarının çözümlenmesine güncel bir bakış: fram yöntemi ile analiz örneği. *Dokuz Eylül Üniversitesi Denizcilik Fakültesi Dergisi*, 12, 69-90. DOI: 10.18613/deudfd.740159.
- Dan, S., Lee, C. J., Park, J., Shin, D., & Yoon, E. S. (2014). Quantitative risk analysis of fire and explosion on the top-side LNG-liquefaction process of LNG-FPSO. *Process Safety and Environmental Protection*, 92(5), 430-441.
- De Carvalho, P. V. R. (2011). The use of Functional Resonance Analysis Method (FRAM) in a mid-air collision to understand some characteristics of the air traffic management system resilience. *Reliability Engineering & System Safety*, 96(11), 1482-1498.
- Foss, M. M., Delano, F., Gulen, G., & Makaryan, R. (2003). LNG safety and security. *Center for Energy Economics (CEE)*.
- Franca, J. E., Hollnagel, E., dos Santos, I. J. L., & Haddad, A. N. (2021). Analysing human factors and non-technical skills in offshore drilling operations using FRAM (functional resonance analysis method). *Cognition, Technology & Work*, 23(3), 553-566.
- Furniss, D., Curzon, P., & Blandford, A. (2016). Using FRAM beyond safety: a case study to explore how sociotechnical systems can flourish or stall. *Theoretical Issues in Ergonomics Science*, 17(5-6), 507-532.
- Hill, R., & Slater, D. (2024). Using a metadata approach to extend the functional resonance analysis method to model quantitatively, emergent behaviours in complex systems. *Systems*, 12(3), 90.
- Hollnagel, E. (2012). An application of the Functional Resonance Analysis Method (FRAM) to risk assessment of organisational change. 1-87.
- Hollnagel, E., Hounsgaard, J., & Colligan, L. (2014). *FRAM-the Functional Resonance Analysis Method: a handbook for the practical use of the method*. Centre for Quality, Region of Southern Denmark. 1-22.
- Hollnagel, E. (2016). *Barriers and accident prevention*. Routledge. 1-242.
- Huffman, M., Hutchison, V., Ranganathan, S., Noll, G., Baxter, C., Hildebrand, M., & Wang, Q. (2024). A comparative bibliometric study of the transport risk considerations of liquefied natural gas and liquefied petroleum gas. *The Canadian Journal of Chemical Engineering*, 102(6), 2019-2038.
- Koruklu, M. S., & Ozay, M. E. (2021). Bir alışveriş merkezinin deprem sonrası müdahale aşamasının fonksiyonel rezonans analiz metodu ile analizi. *International Journal of Pure and Applied Sciences*, 7(1), 63-77.
- Li, J., & Huang, Z. (2012). Fire and explosion risk analysis and evaluation for LNG ships. *Procedia Engineering*, 45, 70-76.
- Ma, G., & Huang, Y. (2019). Safety assessment of explosions during gas stations refilling process. *Journal of Loss Prevention in the Process Industries*, 60, 133-144.
- Naeini, A. M., & Nadeau, S. (2022). Application of FRAM to perform risk analysis of the introduction of a data glove to assembly tasks. *Robotics and Computer-Integrated Manufacturing*, 74, 102285.
- Nubli, H., Fajri, A., Prabowo, A. R., & Sohn, J. M. (2022). CFD implementation to mitigate the LNG leakage consequences: A review of explosion accident calculation on LNG-fueled ships. *Procedia Structural Integrity*, 41, 343-350.
- Ozsayan, S., & Barlas, B. (2023). Tersanelerde Vinç ile Yük Elleçleme Operasyonları ve FRAM Yöntemi Kullanılarak Risk Analizi. *Gemi ve Deniz Teknolojisi*, (223), 13-28.

- Patriarca, R., Di Gravio, G., & Costantino, F. (2017). A Monte Carlo evolution of the Functional Resonance Analysis Method (FRAM) to assess performance variability in complex systems. *Safety Science*, 91, 49-60.
- Patriarca, R., Di Gravio, G., Woltjer, R., Costantino, F., Praetorius, G., Ferreira, P., & Hollnagel, E. (2020). Framing the FRAM: A literature review on the functional resonance analysis method. *Safety Science*, 129, 104827.
- Pospišil, J., Charvát, P., Arsenyeva, O., Klimeš, L., Špiláček, M., & Klemeš, J. J. (2019). Energy demand of liquefaction and regasification of natural gas and the potential of LNG for operative thermal energy storage. *Renewable and Sustainable Energy Reviews*, 99, 1-15.
- Rosa, L. V., Haddad, A. N., & de Carvalho, P. V. R. (2015). Assessing risk in sustainable construction using the Functional Resonance Analysis Method (FRAM). *Cognition, Technology & Work*, 17, 559-573.
- Shirazi, L., Sarmad, M., Rostami, R. M., Moein, P., Zare, M., & Mohammadbeigy, K. (2019). Feasibility study of the small scale LNG plant infrastructure for gas supply in north of Iran (Case Study). *Sustainable Energy Technologies and Assessments*, 35, 220-229.
- Wu, Y., Sun, J., Yang, G., Cui, L., Wang, Z., & Wang, M. (2023). Research on digital twin based temperature field monitoring system for LNG storage tanks. *Measurement*, 215, 112864.

**Cite as:** Gokcan, A., Demir, H. H., Akdogan, R., Oluk, F., & Demir, G. (2025). Analysis of potential fire and explosion incidents in an LNG terminal in a port area using the FRAM method. *Front Life Sci RT*, 6(1), 35-44.



## Research article

# Assessing the performance of multivariate data analysis for predicting solar radiation using alternative meteorological variables

Mustafa Ozbuldu<sup>\*1</sup> , Yunus Emre Sekerli<sup>1</sup> 

<sup>1</sup> Hatay Mustafa Kemal University, Faculty of Agriculture, Department of Biosystems Engineering, 31060, Hatay, Türkiye

## Abstract

This research analyses how well the Partial Least Squares Regression models could predict the monthly average daily global solar radiation for seven stations in the Mediterranean region of Türkiye. Five model scenarios were created with the SARA3 satellite dataset from 2005 to 2023 and using ERA5-AG meteorological variables. These included maximum and minimum temperature configurations, dew point temperature, precipitation, wind speed, and vapor pressure. Different models were examined for their prediction success by using different criteria and assessing the models with varying performance evaluation benchmarks. Based on the results, the models were accurate, mainly when all the predictor variables were used. The highest predictive performance was observed at Burdur station with KGE=0.937, NSE=0.901, and RSR=0.322. The greater regional variations showcased the specific meteorological parameters' relevancy. The results also support the adequacy of the ERA5-AG dataset for climate modelling and resource evaluation purposes. Unlike traditional regression approaches, this study demonstrates the efficiency of PLSR in handling high-dimensional climatic datasets for solar radiation prediction. These findings support the reanalysis of data in renewable energy and agricultural applications, particularly in data-limited regions.

**Keywords:** ERA5-AG; Mediterranean region; partial least squares regression; solar radiation prediction

## 1. Introduction

Solar radiation and climate data are crucial to understanding agricultural productivity, renewable energy, and environmental systems. Accurate modeling and forecasting of these factors are critical as climate change and its repercussions threaten food security and energy sustainability (Bai et al., 2024). The evolution of remote sensing with reanalysis datasets and compiled statistics gives rise to numerous opportunities that make predicting and analyzing solar radiation and climate elements possible (Farbo et al., 2024). Other recent studies also highlight the limitless future of Artificial Intelligence (AI) technology in calculating solar radiation across various locations (Rabault et al., 2025).

Solar radiation is the primary driver of photosynthesis, affecting plant growth, yield, and biomass accumulation (Fraga

et al., 2024). According to studies, more than 50% of agricultural yield variation is directly due to climatic factors such as solar radiation and precipitation (Munnoli et al., 2023). Furthermore, the utilization efficiency of solar radiation is critical for maximizing crop biomass production. The capture and conversion of solar radiation into biomass are significantly influenced by factors such as leaf area index (LAI) and spatial distribution of plants (Koester et al., 2014; Sgarbossa et al., 2018; Kaur et al., 2024). For example, studies on maize showed that optimizing plant arrangement increased the efficiency of solar radiation use, leading to higher yields (Sgarbossa et al., 2018). Similarly, sugarcane and rice demonstrated a positive relation between higher solar radiation and yield values (Marin and Carvalho, 2012; Wang et al., 2016). These findings highlight the need for precise solar radiation data that can be used in crop modeling and management practices to successfully

\* Corresponding author.

E-mail address: [mustafaozbuldu@mku.edu.tr](mailto:mustafaozbuldu@mku.edu.tr) (M. Ozbuldu).

<https://doi.org/10.51753/flsrt.1590684> Author contributions

Received 24 November 2024; Accepted 19 April 2025

Available online 30 April 2025

2718-062X © 2025 This is an open access article published by Dergipark under the [CC BY](https://creativecommons.org/licenses/by/4.0/) license.

optimize agricultural outputs (Castro et al., 2018; Perdinan et al., 2021). In addition, understanding the sensitivity of vegetation to radiation and soil moisture changes is another vital issue in regions facing water scarcity (Liu et al., 2025).

Remote sensing is essential in solar radiation analysis because it provides comprehensive spatial and temporal coverage. High-resolution solar radiation data, which is critical for various applications ranging from crop modeling to renewable energy system optimization, can be obtained with satellite-derived datasets, such as SARA and Himawari-8 (Kaskaoutis and Polo, 2019; Hama et al., 2020; Ghazouani et al., 2021; Kong et al., 2024; Pfeifroth et al., 2024).

Reanalysis data like ERA5 provide comprehensive, high-quality datasets by integrating ground-based observations with model outputs. These datasets help agricultural decision-making, hydrological modeling, and climate research by addressing data gaps in remote and under-monitored regions (Katsepor et al., 2024; Soci et al., 2024). For instance, since reanalysis data can effectively represent weather conditions, it can help in runoff simulations and irrigation planning in mountainous regions where data is scarce (Wang et al., 2024). In addition, it can be used in agricultural systems ranging from predicting evapotranspiration to optimizing growing seasons and evaluating the effects of climate on crop yield (Ishak et al., 2010; Hama et al., 2020; Pelosi et al., 2020; Araújo et al., 2022).

In cases where data sets have high dimensionality and multicollinearity, Partial Least Square Regression (PLSR) is a versatile technique that can predict complex interactions between variables. The PLSR technique differs from traditional regression techniques by allowing efficient dimensionality reduction without losing predictive accuracy by removing latent variables that maximize the covariance between predictors and response variables (Wangeci et al., 2024). This aspect makes PLSR ideal for climatic and agricultural studies where large and highly correlated datasets must be analyzed (Wu et al., 2022; Li et al., 2023; Dai et al., 2024). For instance, PLSR was successfully used in a study on rice genotypes to examine how different sowing dates influenced spikelet formation about solar radiation and temperature (Wang et al., 2019). In another study for the assessment of biophysical parameters of grassland, PLSR was used alongside reflectance data to improve the prediction of solar radiation effects on vegetation (Sakowska et al., 2016).

Moreover, these findings prove further use in remote sensing and reanalysis, thus enhancing agricultural resource management and decision-making. The distinctions become clear when assessing the performance and applicability of traditional station-based techniques to remote sensing methods for solar radiation and climate data. Classical methods using ground measurements, such as pyranometers and solarimeters, can determine solar radiation values for a given location with high precision and accuracy. These methods capture acceptable temporal variations and changes like direct and scattered components (Teke et al., 2015). However, these methods are geographically limited to a specific location. They require networks with multiple stations to transmit data to large areas, which can be logistically challenging and require high investment costs. Moreover, local conditions may affect ground measurement, such as the shading of close buildings or greenery, which are not typical of the regional environment (Harmsen et al., 2014; Olpenda et al., 2018).

In contrast, remote sensing techniques provide extensive spatial and temporal access, unlike traditional station-based methods, allowing continuous large-scale solar radiation

monitoring. These techniques use satellite imagery and complex models of the atmosphere to predict radiation over many terrains, thus filling essential gaps in regions not covered by ground-based systems (Irvem and Ozbuldu, 2018; Polo and Kaskaoutis, 2023). More excellent remote sensing coverage benefits agriculture and renewable energy in areas with limited ground-based infrastructure (Kosmopoulos et al., 2018; Hama et al., 2020).

Remote sensing techniques are associated with disadvantages such as atmospheric conditions (cloud cover, haze, and aerosols) that create uncertainty in the radiation prediction, reducing accuracy. Such problems often encourage combining remote sensing data with classical ground-based measurements to increase the precision of radiation measurements. Studies emphasize that the combination of these techniques provides an ideal solution due to the adequacy and unlimited coverage of satellite data and the sensitivity of ground-based methods for agricultural and renewable energy systems (Zhou et al., 2017; Wang et al., 2021). In addition to these accuracy-enhancement methods, the use of remote sensing along with advanced machine learning (ML) post-processing procedures can also help solve these issues (Rabault et al., 2025).

The applications of solar radiation data in agriculture extend to renewable energy systems. In this research, the combining of remote sensing reanalysis datasets and PLSR was examined to improve solar radiation prediction from climatic variables. Using these tools, it was aimed to enhance the agricultural productivity, optimize energy systems, and deepen the understanding of climatic processes. Although the application of machine learning and statistical techniques to predict solar radiation is on the rise, there is limited research on evaluating PLSR using reanalysis datasets. In order to fill this gap, the present work tested the prediction performance of PLSR against ERA5-AG and SARA-3 datasets, assessing its effectiveness with high-dimensional climate variables under varying meteorological conditions in the Mediterranean region.

## 2. Materials and methods

### 2.1. Study area and dataset

This work was carried out using the average monthly solar radiation data of the provincial centers of Adana, Hatay, Osmaniye, Antalya, Mersin, Isparta, and Burdur in the Mediterranean region of Türkiye. The data was retrieved from the European Exploitation of Meteorological Satellites Organization's (EUMETSAT) SARA-3 (Surface Radiation Data Set-Heliosat 3) dataset for the years 2005-2023. The study area is shown in Fig. 1. The SARA data set is critical in understanding the solar radiation dynamics of Europe, and therefore, is an integral part of the solar radiation European system (CM SAF).

Compared to its predecessors, SARA-3 is enhanced by lower-resolution solar radiation data from the METEOSAT satellite series. This data is supplied with a spatial resolution of 0.05°. The surface radiation value is calculated using the Heliosat technique (Thomas et al., 2023).

Data has undergone processing, cross-referencing satellite images and using ground truthing algorithms to ascertain precision on the data being analyzed (Mikelsons et al., 2022). With the satellite's ground observation, it was possible to create more reliable, optimized datasets critical for climate monitoring and modelling (Pfeifroth et al., 2018; Manara et al., 2020).

Inclusion for its systematic nature makes the dataset's accessibility and comprehensiveness unparalleled for most researchers and analysts, including policymakers and the industry (Kothe et al., 2017). The selected SARA3 solar radiation data, with its corresponding metadata, can be found at the JRC website (JRC, 2024). The solar radiation data from SARA3 was analysed and tested for quality using the Kolmogorov-Smirnov data normalization tests individually per station in R Studio. Statistical granularity of the presented test results and data sets is highlighted in Table 1. Normality tests reported that all stations met the requirements,  $p < 0.05$  reported (Azad et al., 2024). ERA5-AG and SARA3 were chosen due to their long-term availability, high geographical accuracy, and spatial detail. Their reliability has been previously proven by comparing them with *in situ* measurements.

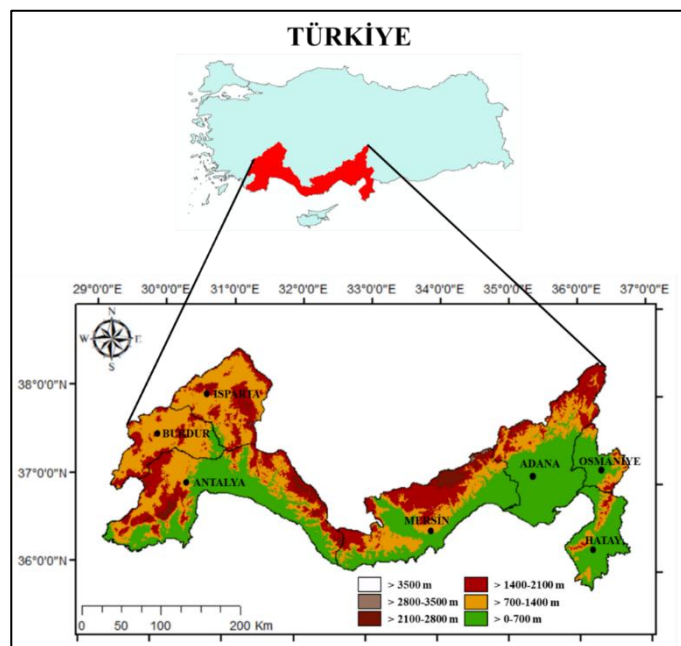


Fig. 1. Location of the study areas.

Table 1

Descriptive statistical values of monthly average solar radiation ( $\text{kWh m}^{-2} \text{day}^{-1}$ ) data.

Station	Average	Standard Deviation	Max.	Min.	Kolmogorov-Smirnov p value
Adana	5.03	1.97	8.09	1.84	0.002
Hatay	5.18	2.24	8.46	1.36	0.001
Osmaniye	4.86	1.93	8.11	1.81	0.003
Mersin	5.07	1.98	8.19	1.76	0.001
Antalya	5.21	2.07	8.44	1.97	0.001
Burdur	5.10	2.10	8.60	1.85	0.003
Isparta	4.84	2.03	8.45	1.57	0.006

## 2.2. Model inputs and creation of scenarios

In the study, maximum temperature ( $T_{\max}$ ), minimum temperature ( $T_{\min}$ ), average dew point temperature ( $T_{\text{dew}}$ ), precipitation (P), wind speed (WS) and vapor pressure (VP) were used as predictor variables to be used in the models that will predict the monthly average solar radiation. The ERA5-AG reanalysis dataset is a notable improvement in climate data as it contains high-resolution meteorological data from ECMWF's 5th generation of atmospheric reanalysis (ERA5)-a new and improved version. It benefits agricultural, hydrological, and

environmental studies because it covers a wide area and has a high spatial resolution of  $0.1^\circ \times 0.1^\circ$  (about 10 km) (Zhou and Ismael, 2020). Simanjuntak et al. (2022) claimed that the dataset is essential for agriculture because it contains wind, solar, and other parameters for studying and modeling the environment or weather-changing factors. This research acquired the required ERA5-AG data from Google Earth Engine for the corresponding study areas. Five scenarios concerning model inputs were structured with the data discussed above to predict the impact of climate parameters. The model scenarios are presented in Table 2. Initial tests showed that wind speed had little impact in the stable climate regions, while precipitation had more significant impacts in the coastal areas. Atmospheric conditions (with accompanying changes in wind speeds) could considerably affect energy production, which indicates that under more stable conditions (low variability in wind), the wind speed does not have much impact. Furthermore, in areas with changing precipitation patterns, precipitation can diminish solar radiation by obstructing light in the region (Vizzo et al., 2021; Pérez et al., 2023).

Table 2

Model input scenarios.

Model Scenarios	Input variables
M1	$T_{\max} + T_{\min} + T_{\text{dew}} + P + WS + VP$
M2	$T_{\max} + T_{\min} + T_{\text{dew}}$
M3	$T_{\max} + T_{\min} + T_{\text{dew}} + P$
M4	$T_{\max} + T_{\min} + T_{\text{dew}} + VP$
M5	$T_{\max} + T_{\min} + T_{\text{dew}} + WS$

## 2.3. Multivariate data analysis

The data were analyzed to assess the potential for predicting solar radiation based on climatic variables, including  $T_{\min}$ ,  $T_{\max}$ ,  $T_{\text{dew}}$ , WS, and VP. Regression analysis were conducted using the Partial Least Squares Regression method, implemented in the multivariate statistical software UnScrambler (version 9.7, Camo, Oslo, Norway). The PLS method was selected as more suitable than other classical techniques (such as Multiple Linear Regression and Principal Component Regression) for datasets with highly correlated variables (Esbensen, 2009). In the PLS analysis, 70% of the data (from 2005 to 2017) were used for model calibration, while the remaining 30% (from 2018 to 2023) served as the validation set.

## 2.4. Criteria for evaluating model performance

In this study, the results received from the PLS regression model were evaluated using five separate performance assessment metrics. The coefficient of determination ( $R^2$ ) is one of the most important criteria used to evaluate the regression model's goodness of fit. As stated in (Kasuya, 2018), "A higher  $R^2$  value indicates a better fit." Root Mean Square Error (RMSE) has emerged as one of the most common metrics used to evaluate the accuracy of predictive models. It captures the discrepancies between predicted values ( $M_i$ ) and observed values ( $O_i$ ) and assesses the overall effectiveness of the model (Chai and Draxler, 2014). It is widely accepted that lower RMSE values suggest improved model performance. However, the actual value of this parameter depends on data dataset size. On the contrary, the Root Mean Standard Deviation Ratio (RSR) was introduced by (Singh et al., 2005) as a model comparison

statistic that improves the interpretability of these values. RSR adjusts the RMSE values by the standard deviation of the observations to produce a constant value.

As for the calculation of the NSE, its coefficient is a metric to measure the predictive power of a model. The coefficient can take any value lower than 1, preferably zero or higher. Closer to 1 suggests that the model prediction result is satisfactory (Moriassi et al., 2007). The KGE is one of the most common metrics used for model evaluation, especially for hydrological models. KGE is composed of three main components: the correlation coefficient ( $r$ ), the variability ratio ( $\alpha$ ) and the mean bias ( $\beta$ ), making the model evaluation much more informative (Smit and Van Tol, 2022). These model performance metrics are derived from the results calculated in Equations 1-5. The quantitative results from these equations were benchmarked against the qualitative evaluations listed in Table 3 and Table 4.

$$R^2 = \left( \frac{\sum_{i=1}^n (O_i - \bar{O}) \times (M_i - \bar{M})}{\sqrt{\sum_{i=1}^n (O_i - \bar{O})^2} \times \sqrt{\sum_{i=1}^n (M_i - \bar{M})^2}} \right)^2 \tag{1}$$

$$RMSE = \sqrt{\frac{1}{n} \sum_{i=1}^n (O_i - M_i)^2} \tag{2}$$

$$RSR = \frac{RMSE}{\sigma_{obs}} \tag{3}$$

$$NSE = 1 - \frac{\sum_{i=1}^n (O_i - M_i)^2}{\sum_{i=1}^n (O_i - \bar{O})^2} \tag{4}$$

$$KGE = 1 - \sqrt{(r - 1)^2 + (\alpha - 1)^2 + (\beta - 1)^2} \tag{5}$$

**Table 3**  
NSE and RSR performance evaluation table (Singh et al., 2005; Moriassi et al., 2007).

Performance	NSE	RSR	R <sup>2</sup>
Very good	0.75 < NSE ≤ 1.00	0.00 < RSR ≤ 0.50	0.90 < R <sup>2</sup> ≤ 1.00
Good	0.65 < NSE ≤ 0.75	0.50 < RSR ≤ 0.60	0.75 < R <sup>2</sup> < 0.90
Satisfactory	0.50 < NSE ≤ 0.65	0.60 < RSR ≤ 0.70	0.50 < R <sup>2</sup> < 0.75
Unsatisfactory	NSE ≤ 0.50	RSR > 0.70	0.50 > R <sup>2</sup>

**Table 4**  
KGE performance evaluation table (Towner et al., 2019).

Performance	KGE
Good	KGE > 0.75
Intermediate	0.5 < KGE < 0.75
Poor	0 < KGE < 0.5
Very poor	KGE < 0

### 3. Result and discussion

This study evaluated PLS regression prediction models for their ability to predict average monthly solar radiation at seven different stations in the Mediterranean region of Türkiye under five different input scenarios. In the models created using variables obtained from the ERA5-AG reanalysis dataset, 70% of the dataset (2005-2017) was used as training and 30% (2018-2023) as a test dataset. The performance results of the test period, monthly average daily global solar radiation predictions obtained from the models for all stations, are given in Table 5.

Table 5 shows that the models generally have high values for KGE and NSE and low values for RSR. This indicates that

the error rate of the models is low, and they have a good prediction performance. The M1 model showed the best performance in most of the stations. This is since model includes all variables ( $T_{max}$ ,  $T_{min}$ ,  $T_{dew}$ ,  $P$ ,  $WS$ ,  $VP$ ) and therefore represents the atmospheric conditions most comprehensively. The fact that M1 has higher KGE and NSE values emphasizes the importance of considering meteorological components together. Among the other models, performance decreases were generally observed when the number of variables was reduced. The model M2 with only temperature variables typically produced lower KGE and NSE values.

Considering the results obtained on a station basis, the M4 model stands out with the highest KGE (0.907) and NSE (0.854) values at Adana station. Moreover, the lowest RSR value (0.356) shows that the model minimizes the error rate. This result can be attributed to Adana’s high humidity and low wind speed variability. Therefore,  $VP$  is considered to be more critical in solar radiation prediction. On the other hand, the results show that the exclusion of  $WS$  and  $P$  variables from the prediction model may be less effective for Adana.

**Table 5**  
Prediction performances of the models based on different input scenarios.

Stations	MODELS	KGE	NSE	RSR
Adana	M1	0.911	0.851	0.363
	M2	0.892	0.842	0.365
	M3	0.906	0.843	0.372
	<b>M4</b>	<b>0.907</b>	<b>0.854</b>	<b>0.356</b>
	M5	0.878	0.833	0.369
Antalya	<b>M1</b>	<b>0.873</b>	<b>0.760</b>	<b>0.459</b>
	M2	0.851	0.725	0.480
	M3	0.875	0.758	0.465
	M4	0.863	0.743	0.471
	M5	0.861	0.748	0.462
Burdur	<b>M1</b>	<b>0.937</b>	<b>0.901</b>	<b>0.322</b>
	M2	0.914	0.832	0.398
	M3	0.929	0.859	0.367
	M4	0.921	0.843	0.389
	M5	0.933	0.879	0.349
Hatay	<b>M1</b>	<b>0.927</b>	<b>0.928</b>	<b>0.249</b>
	M2	0.818	0.685	0.496
	M3	0.808	0.660	0.514
	M4	0.792	0.665	0.495
	M5	0.935	0.902	0.296
Isparta	M1	0.875	0.816	0.390
	M2	0.873	0.778	0.434
	M3	0.871	0.776	0.435
	M4	0.879	0.786	0.429
	<b>M5</b>	<b>0.917</b>	<b>0.861</b>	<b>0.353</b>
Mersin	M1	0.901	0.862	0.346
	M2	0.872	0.852	0.346
	M3	0.890	0.844	0.366
	<b>M4</b>	<b>0.910</b>	<b>0.861</b>	<b>0.357</b>
	M5	0.844	0.854	0.331
Osmaniye	M1	0.907	0.881	0.318
	M2	0.898	0.848	0.360
	M3	0.899	0.846	0.363
	M4	0.899	0.848	0.361
	<b>M5</b>	<b>0.912</b>	<b>0.884</b>	<b>0.316</b>

The most successful model at Antalya station was M1 (KGE=0.873, NSE=0.760, RSR=0.459). This model, in which all inputs were included, was able to reflect the complex meteorological structure of Antalya in the best way. Because Antalya is in a geography, where coastal and mountainous areas

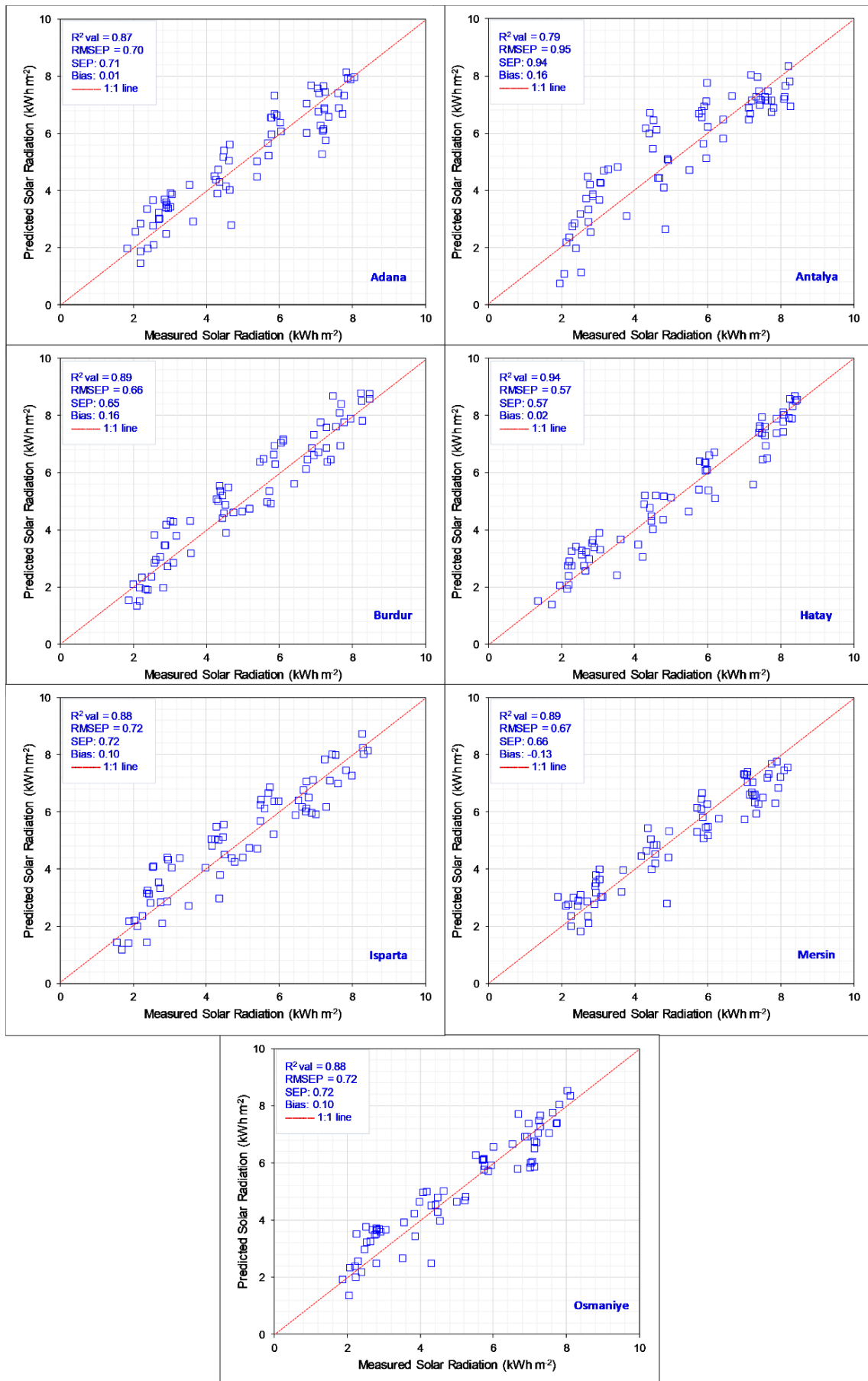


Fig. 2. Scatter plots of monthly average daily global solar radiation predictions obtained for each station for the test period.

merge, parameters such as wind speed and precipitation are important factors affecting solar radiation. Therefore, the inclusion of all parameters in M1 provided better performance of the model.

In Burdur station, the M1 model showed the best performance (KGE=0.937, NSE=0.901, RSR=0.322). It is known that Burdur is under the influence of a terrestrial climate and has low humidity levels. Therefore, the effect of parameters such as  $T_{dew}$ , VP, and WS on solar radiation becomes more noticeable. Because M1 includes all parameters, it provided high accuracy at this station. The most successful model at Hatay station was M1 (KGE=0.927, NSE=0.928, RSR=0.249). Although Hatay has a Mediterranean climate similar to Adana, the inclusion of all parameters produced a more successful result due to geographical differences. Including all inputs in M1 improved the performance of the model, particularly if factors such as precipitation and wind speed affect solar radiation.

The M5 model provided the highest performance at Isparta station (KGE=0.917, NSE=0.861, RSR=0.353). The M5 model considered WS instead of VP. Although Isparta is under the influence of a continental climate, it is seen that the land structure makes the changes in wind speed more important for solar radiation prediction. This shows that WS is a more effective parameter for predicting solar radiation in this region.

The M4 model provided the best performance at Mersin station (KGE=0.910, NSE=0.861, RSR=0.357). The inclusion of vapor pressure in M4 indicates that humidity levels in Mersin are a determining factor in solar radiation prediction. The most successful model at Osmaniye station was M5 (KGE=0.912, NSE=0.884, RSR=0.316). The inclusion of wind speed in the M5 model indicates that the meteorological conditions in Osmaniye play a determining role in solar radiation. The main reason for the differences in the performance of the models is the variations in each station's meteorological, geographical, and environmental conditions. In humid and hot regions such as Adana, vapor pressure is critical for prediction performance. In contrast, the effect of wind speed may be more pronounced in areas with terrestrial climate characteristics, such as Burdur. Similarly, in coastal regions such as Antalya and Hatay, the effect of high humidity and wind speed should be considered together. Scatter plots generated according to the predictions obtained from the most successful models for each station are given in Fig. 2. The performance differences among stations may be linked to their geographical and meteorological characteristics. For instance, Burdur's stable conditions enhanced model accuracy, whereas Antalya's coastal variability led to slightly lower performance.

In general, the predicted values are in good agreement with the measured data. In particular, the predictions obtained for the models at Hatay, Mersin, and Burdur stations are very close to the 1:1 line, indicating that over- or under-predicted values are limited. According to the scatter plots, it is concluded that the predicted values of monthly average global solar radiation have a high level of accuracy.

The  $R^2$  values obtained from the models (0.79-0.94) show that the model predictions are highly accurate. According to the RMSE results (0.57-0.95), it was determined that the models predicted the monthly average daily global solar radiation with

a very low error amount. In similar modelling studies where solar radiation prediction models were evaluated, Mohammadi et al. (2015) calculated the performance of the regression prediction model as  $R^2=0.84$  in their research in Iran. Shamshirband et al. (2016) calculated  $R^2=97.37$  and  $RMSE=0.18$  in their study using machine learning in Iran. Karaman et al. (2021) calculated the RMSE value as 0.0297 and the  $R^2$  value as 0.99 in their prediction model using ANN in Karaman province in Türkiye. Soria et al. (2022) used a multiple linear regression model in their study in Peru and found the  $R^2$  value as 0.556. These results show that the PLS regression model method is much more successful than the models created with traditional regression approaches, although not as successful as ANN and machine learning based approaches. In addition, the findings of this study show that the ERA5-AG reanalysis dataset can be used for solar radiation prediction in developing countries such as Türkiye, where the meteorological observation gauge network is sparse.

#### 4. Conclusion

This study created models for solar radiation prediction using PLSR from climate variables of ERA5-AG reanalysis datasets in different scenarios. The prediction success of these models was evaluated based on various criteria. The study conducted in the seven Türkiye's Mediterranean Region stations found that PLSR models effectively processed high-dimensional and multicollinear climate data. Among all the evaluated models, those that included all features (temperature, dew point, wind speed, and vapor pressure) provided the best predicted solar radiation accuracy as indicated by KGE, NSE,  $R^2$ , and low RSR values. The findings also highlight the role of local climate and topographic features in the prediction model developing process. Indicating this, including wind speed and precipitation variables, is essential in coastal regions such as Antalya and Hatay. In contrast, wind speed data has become particularly important in Isparta, which has a more continental climate. This study underscores PLSR models' versatility in fitting regional datasets, which provide a reasonable balance between precision and model complexity when combined with classical regression and sophisticated machine learning techniques. According to study results, the ERA5-AG dataset can be a valid resource for predicting solar radiation in regions with limited data availability. This research helps to reduce the gaps created by insufficient meteorological observation networks, while also helping to maximize solar energy use and improve agricultural productivity. These results are crucial in optimizing photovoltaic energy use in areas where data is scarce. Accurate solar radiation prediction also helps support climate resilience strategies and enhances agricultural planning by predicting the potential crop yields.

**Conflict of interest:** The authors declare that they have no conflict of interests.

**Informed consent:** The authors declare that this manuscript did not involve human or animal participants and informed consent was not collected.

#### References

Araújo, C. S. P., Silva, I. A. C., Ippolito, M., & Almeida, C. D. G. C. (2022). Evaluation of air temperature estimated by ERA5-Land reanalysis using

surface data in Pernambuco, Brazil. *Environmental Monitoring and Assessment*, 194(5), 381.

- Azad, M. A. K., Mallick, J., Islam, A. R. M. T., Ayen, K., & Hasanuzzaman, M. D. (2024). Estimation of solar radiation in data-scarce subtropical region using ensemble learning models based on a novel CART-based feature selection. *Theoretical and Applied Climatology*, 155, 349-369.
- Bai, J. M., Xiao-Wei, W., Arslan, E., & Zong, X. (2024). Global solar radiation and its interactions with atmospheric substances and their effects on air temperature change in Ankara province. *Climate*, 12(3), 35.
- Castro, J. R., Cuadra, S. V., Pinto, L. B., Souza, J. M. H., Santos, M. P., & Heinemann, A. B. (2018). Parametrization of models and use of estimated global solar radiation data in the irrigated rice yield simulation. *Revista Brasileira de Meteorologia*, 33(2), 238-246.
- Chai, T., & Draxler, R. R. (2014). Root mean square error (RMSE) or mean absolute error (MAE)? – Arguments against avoiding RMSE in the literature. *Geoscientific Model Development*, 7(3), 1247-1250.
- Dai, Y., Yu, S., Ma, T., Ding, J., Chen, K., Zeng, G., & Zhang, M. (2024). Improving the estimation of rice above-ground biomass based on spatio-temporal uav imagery and phenological stages. *Frontiers in Plant Science*, 15.
- Esbensen, K. H. (2009). *Multivariate data analysis—In practice* (5th ed.). Camo Software AS.
- Farbo, A., Trombetta, N. G., Palma, L. d., & Mondino, E. B. (2024). Estimation of intercepted solar radiation and stem water potential in a table grape vineyard covered by plastic film using sentinel-2 data: a comparison of ols-, mlr-, and ml-based methods. *Plants*, 13(9), 1203.
- Fraga, H., Freitas, T. R., Moriondo, M., Molitor, D., & Santos, J. A. (2024). Determining the climatic drivers for wine production in the cda region (portugal) using a machine learning approach. *Land*, 13(6), 749.
- Ghazouani, N., Bawadekji, A., El-Bary, A. A., Elewa, M. M., Becheikh, N., Alassaf, Y., & Hassan, G. (2021). Performance evaluation of temperature-based global solar radiation models—case study: Arar City, KSA. *Sustainability*, 14, 35.
- Hama, A., Tanaka, K., Mochizuki, A., Tsuruoka, Y., & Kondoh, A. (2020). Improving the UAV-based yield estimation of paddy rice by using the solar radiation of geostationary satellite Himawari-8. *Hydrological Research Letters*, 14(1), 56-61.
- Harmsen, E. W., Cruz, P. T., & Mecikalski, J. R. (2014). Calibration of selected pyranometers and satellite-derived solar radiation in Puerto Rico. *International Journal of Renewable Energy Technology*, 5(1), 43-54.
- Irvem, A., & Ozbuldu, M. (2018). Accuracy of satellite-based solar data to estimate solar energy potential for Hatay Province, Turkey. *Bitlis Eren University Journal of Science*, 7(2), 361-369.
- Ishak, A., Bray, M., Remesan, R., & Han, D. (2010). Estimating reference evapotranspiration using numerical weather modelling. *Hydrological Processes*, 24(24), 3490-3509.
- JRC. (2024). Official Website of The Joint Research Centre: EU Science Hub, <https://joint-research-centre.ec.europa.eu/>, Last Accessed on March, 2025.
- Karaman, Ö. A., Tanyıldız Agir, T., & Arsel, İ. (2021). Estimation of solar radiation using modern methods. *Alexandria Engineering Journal*, 60, 2447-2455.
- Kaskaoutis, D., & Polo, J. (2019). Editorial for the special issue “solar radiation, modeling, and remote sensing”. *Remote Sensing*, 11(10), 1198.
- Kasuya, E. (2018). On the use of r and r squared in correlation and regression. *Ecological Research*, 34(1), 235-236.
- Katsekpor, J. T., Greve, K., Yamba, E. I., & Amoah, E. G. (2024). Comparative analysis of satellite and reanalysis data with ground-based observations in northern ghana. *Meteorological Applications*, 31(4), e2226.
- Kaur, N., Snider, J. L., Paterson, A. H., Virk, G., Parkash, V., Roberts, P. M., & Li, C. (2024). Genotypic variation in functional contributors to yield for a diverse collection of field-grown cotton. *Crop Science*, 64(3), 1846-1861.
- Koester, R. P., Skoneczka, J. A., Cary, T. R., Diers, B. W., & Ainsworth, E. A. (2014). Historical gains in soybean (*Glycine max* Merr.) seed yield are driven by linear increases in light interception, energy conversion, and partitioning efficiencies. *Journal of Experimental Botany*, 65(12), 3311-3321.
- Kong, H., Wang, J., Cai, L., Cao, J., Zhou, M., & Fan, Y. (2024). Surface solar radiation resource evaluation of Xizang region based on station observation and high-resolution satellite dataset. *Remote Sensing*, 16(8), 1405.
- Kosmopoulos, P. G., Kazadzis, S., El-Askary, H. M., Taylor, M., Gkikas, A., Proestakis, E., Kontoes, C. H., & El-Khayat, M. M. (2018). Earth-observation-based estimation and forecasting of particulate matter impact on solar energy in Egypt. *Remote Sensing*, 10(12), 1870.
- Kothe, S., Pfeifroth, U., Cremer, R., Trentmann, J., & Hollmann, R. (2017). A satellite-based sunshine duration climate data record for Europe and Africa. *Remote Sensing*, 9(5), 429.
- Li, Q., Bessafi, M., & Li, P. (2023). Mapping prediction of surface solar radiation with linear regression models: case study over Reunion Island. *Atmosphere*, 14(9), 1331.
- Liu, Y., Xiao, J., Li, X., & Li, Y. (2025). Critical soil moisture detection and water-energy limit shift attribution using satellite-based water and carbon fluxes over China. *Hydrology and Earth System Sciences*, 29, 1241-1258.
- Manara, V., Stocco, E., Brunetti, M., Diolaiuti, G., Fugazza, D., Pfeifroth, U., & Maugeri, M. (2020). Comparison of surface solar irradiance from ground observations and satellite data (1990–2016) over a complex orography region (Piedmont—northwest Italy). *Remote Sensing*, 12(23), 3882.
- Marin, F. R., & Carvalho, G. L. (2012). Spatio-temporal variability of sugarcane yield efficiency in the state of São Paulo, Brazil. *Pesquisa Agropecuária Brasileira*, 47(2), 149-156.
- Mikelsons, K., Wang, M., Kwiatkowska, E., Jiang, L., Dessailly, D., & Gossn, J. I. (2022). Statistical evaluation of sentinel-3 OLCI ocean color data retrievals. *IEEE Transactions on Geoscience and Remote Sensing*, 60, 1-19.
- Mohammadi, K., Shamshirband, S., Anisi, M. H., Alam, K. A., & Petković, D. (2015). Support vector regression based prediction of global solar radiation on a horizontal surface. *Energy Conversion and Management*, 91, 433-441.
- Moriassi, D. N., Arnold, J. G., Van Liew, M. W., Bingner, R. L., Harmel, R. D., & Veith, T. L. (2007). Model evaluation guidelines for systematic quantification of accuracy in watershed simulations. *Transactions of the American Society of Agricultural and Biological Engineers*, 50(3), 885-900.
- Munnoli, S., Shivashankar, K., & Golshetti, A. (2023). Influences of changes in rainfall and solar radiation on performance of kharif sorghum. *International Journal of Environment and Climate Change*, 13(6), 186-193.
- Olpenda, A., Stereńczak, K., & Będkowski, K. (2018). Modeling solar radiation in the forest using remote sensing data: a review of approaches and opportunities. *Remote Sensing*, 10(5), 694.
- Pelosi, A., Terribile, F., D'Urso, G., & Chirico, G. B. (2020). Comparison of ERA5-Land and UERRA MESCAN-SURFEX reanalysis data with spatially interpolated weather observations for the regional assessment of reference evapotranspiration. *Water*, 12(6), 1669.
- Perdinan, Winkler, J. A., & Andresen, J. A. (2021). Evaluation of multiple approaches to estimate daily solar radiation for input to crop process models. *Atmosphere*, 12(1), 8.
- Pérez, C., Rivero, M., Escalante, M., Ramirez, V., & Guilbert, D. (2023). Influence of atmospheric stability on wind turbine energy production: A case study of the coastal region of Yucatan. *Energies*, 16(10), 4134.
- Pfeifroth, U., Sánchez-Lorenzo, A., Manara, V., Trentmann, J., & Hollmann, R. (2018). Trends and variability of surface solar radiation in Europe based on surface- and satellite-based data records. *Journal of Geophysical Research: Atmospheres*, 123(3), 1735-1754.
- Pfeifroth, U., Drücke, J., Kothe, S., Trentmann, J., Schröder, M., & Hollmann, R. (2024). SARAH-3 – satellite-based climate data records of surface solar radiation. *Earth System Science Data*, 16, 5243-5265.
- Polo, J., & Kaskaoutis, D. (2023). Editorial on new challenges in solar radiation, modeling and remote sensing. *Remote Sensing*, 15(10), 2633.
- Rabault, J., Sætra, M. L., Dobler, A., Eastwood, S., & Berge, E. (2025). Data fusion of complementary data sources using Machine Learning enables higher accuracy Solar Resource Maps. *Solar Energy*, 290, 113337.
- Sakowska, K., Juszcak, R., & Gianelle, D. (2016). Remote sensing of grassland biophysical parameters in the context of the Sentinel-2 satellite mission. *Journal of Sensors*, 2016, 1-16.
- Sgarbossa, J., Scherz, F., Elli, E., Tibolla, L., Schmidt, D., & Caron, B. (2018). Agroforestry systems and their effects on the dynamics of solar radiation and soybean yield. *Comunicata Scientiae*, 9(3), 492-502.
- Shamshirband, S., Mohammadi, K., Tong, C. W., Zamani, M., Motamedi, S., & Ch, S. (2016). A hybrid SVM-FFA method for prediction of monthly mean global solar radiation. *Theoretical and Applied Climatology*, 125(1-2), 53-65.
- Simanjuntak, C., Gaiser, T., Ahrends, H. E., & Srivastava, A. K. (2022). Spatial and temporal patterns of agrometeorological indicators in maize producing provinces of South Africa. *Scientific Reports*, 12(1), 12072.
- Singh, J., Knapp, H. V., Arnold, J. G., & Demissie, M. (2005). Hydrologic modeling of the Iroquois River watershed using HSPF and SWAT. *Journal of the American Water Resources Association*, 41(2), 361-375.
- Smit, E., & Van Tol, J. (2022). Impacts of soil information on process-based hydrological modelling in the Upper Goukou Catchment, South Africa. *Water*, 14(3), 407.
- Soci, C., Hersbach, H., Simmons, A. J., Poli, P., Bell, B., Berrisford, P., & Thépaut, J. (2024). The era5 global reanalysis from 1940 to 2022. *Quarterly Journal of the Royal Meteorological Society*, 150(764), 4014-4048.
- Soria, J. J., Poma, O., Sumire, D. A., Rojas, J. H. F., & Chipa, S. M. R. (2022). Multiple linear regression model of environmental variables, predictors of global solar radiation in the area of East Lima, Peru. *IOP Conference Series: Earth and Environmental Science*, 1006(1), 012009.

- Teke, A., Yildirim, H. B., & Celik, O. (2015). Evaluation and performance comparison of different models for the estimation of solar radiation. *Renewable and Sustainable Energy Reviews*, 50, 1097-1107.
- Thomas, C., Nyamsi, W. W., Arola, A., Pfeifroth, U., Trentmann, J., Dorling, S., & Alexandr, A. (2023). Smart approaches for evaluating photosynthetically active radiation at various stations based on MSG Prime satellite imagery. *Atmosphere*, 14(8), 1259.
- Towner, J., Cloke, H. L., Zsoter, E., Flamig, Z., Hoch, J. M., Bazo, J., ... & Stephens, E. M. (2019). Assessing the performance of global hydrological models for capturing peak river flows in the Amazon basin. *Hydrology and Earth System Sciences*, 23(7), 3057-3080.
- Vizzo, J. I., Cabrerizo, M. J., Helbling, E. W., & Villafañe, V. E. (2021). Extreme and gradual rainfall effects on winter and summer estuarine phytoplankton communities from Patagonia (Argentina). *Marine Environmental Research*, 163, 105235.
- Wangeci, A., Adén, D., Nikolajsen, T., Greve, M. H., & Knadel, M. (2024). Combining laser-induced breakdown spectroscopy and visible near-infrared spectroscopy for predicting soil organic carbon and texture: a Danish national-scale study. *Sensors*, 24(14), 4464.
- Wang, D., Laza, M. R. C., Cassman, K. G., Huang, J., Nie, L., Ling, X., Centeno, G. S., Cui, K., Wang, F., Li, Y., & Peng, S. (2016). Temperature explains the yield difference of double-season rice between tropical and subtropical environments. *Field Crops Research*, 198, 303-311.
- Wang, Y., Wang, L., Chen, H., Xiang, J., Zhang, Y., Shi, Q., Zhu, D., & Zhang, Y. (2019). Sowing dates have different effects on spikelet formation among different photoperiod-sensitive rice genotypes. *Agronomy Journal*, 111(5), 2263-2275.
- Wang, Y., Zhou, T., & Zhou, W. (2021). Solar radiation distribution method for a photovoltaic greenhouse based on the maximization of annual economic benefits. *Research Square*.
- Wang, X., Zhou, J., Ma, J., Luo, P., Fu, X., Feng, X., Zhang, X., Jia, Z., Wang, X., & Huang, X. (2024). Evaluation and comparison of reanalysis data for runoff simulation in the data-scarce watersheds of alpine regions. *Remote Sensing*, 16(5), 751.
- Wu, X., Liu, H., Hartmann, H., Ciais, P., Kimball, J. S., Schwalm, C. R., Camarero, J. J., Chen, A., Gentile, P., Yang, Y., Zhang, S., Li, X., Xu, C., Zhang, W., Li, Z., & Chen, D. (2022). Timing and order of extreme drought and wetness determine bioclimatic sensitivity of tree growth. *Earth's Future*, 10(7), e2021EF002530.
- Zhou, Q., Flores, A., Glenn, N., Walters, R., & Han, B. (2017). A machine learning approach to estimation of downward solar radiation from satellite-derived data products: an application over a semi-arid ecosystem in the U.S. *PLoS One*, 12(8), e0180239.
- Zhou, Q., & Ismaeel, A. (2020). Seasonal cropland trends and their nexus with agrometeorological parameters in the Indus River plain. *Remote Sensing*, 13(1), 41.

**Cite as:** Ozbuldu, M., & Sekerli, Y. E. (2025). Assessing the performance of multivariate data analysis for predicting solar radiation using alternative meteorological variables. *Front Life Sci RT*, 6(1), 45-52.



## Review article

## Exploring the antioxidant and protective effects of usnic acid: Opportunities and challenges

Tubanur Aslan Engin\*<sup>1</sup> <sup>1</sup> *Yalova University, Faculty of Health Sciences, Department of Physiotherapy and Rehabilitation, 77200, Yalova, Türkiye*

### Abstract

Lichens are symbiotic organisms that produce a variety of secondary metabolites, including the well-known usnic acid (C<sub>18</sub>H<sub>16</sub>O<sub>7</sub>), which has garnered attention for its diverse biological activities and potential applications. Usnic acid, primarily found in lichen species such as *Usnea* and *Cladonia*, is a yellowish-green compound with notable antimicrobial, antiviral, and anti-inflammatory properties. Its antioxidant activity is particularly significant, with the ability to neutralize free radicals, inhibit lipid peroxidation, and stabilize cell membranes. Usnic acid, a secondary metabolite found in various lichen species, is recognized for its potent antioxidant properties. Its structure, characterized by a dibenzofuran backbone and phenolic hydroxyl groups, allows it to neutralize free radicals and inhibit lipid peroxidation, protecting cells from oxidative stress. Usnic acid can also chelate metal ions like iron and copper, preventing them from catalyzing reactions that produce harmful reactive oxygen species. This antioxidant capacity is of interest in both pharmaceutical and cosmetic fields. Usnic acid's ability to reduce oxidative damage makes it a promising ingredient in sunscreens and anti-aging products, where it protects the skin from ultraviolet (UV) radiation and environmental pollutants. Additionally, its potential to modulate antioxidant enzymes like superoxide dismutase (SOD) and catalase may further enhance its protective effects against oxidative stress-related damage, including inflammation and cell aging. Usnic acid effectively neutralizes free radicals, and its ability to prevent lipid peroxidation is comparable to that of vitamin E. However, this may vary depending on specific conditions. Vitamin C is particularly potent against ROS types in aqueous environments, but its ability to directly prevent lipid peroxidation is more limited compared to vitamin E or usnic acid. However, the practical use of usnic acid is limited by its potential hepatotoxicity at high concentrations, particularly in systemic applications. Despite these challenges, usnic acid remains a valuable compound for ongoing research, especially for topical products aimed at combating oxidative stress and protecting against skin damage.

**Keywords:** *Antioxidant properties; free radicals; inflammation; lichens; oxidative stress; pharmaceutical applications; usnic acid*

### 1. Introduction

Lichens are fascinating organisms that result from a symbiotic relationship between fungi and either algae or cyanobacteria. They are unique because they are not just one organism, but a combination of two or sometimes three different types of organisms living together (Morillas et al., 2022). Lichens consist of a fungal component (called the mycobiont) and a photosynthetic partner, either algae or cyanobacteria

(called the photobiont). The fungus provides structure and protection, while the algae or cyanobacteria produce food through photosynthesis (Honegger, 2009). There are three main types based on their growth forms. Crustose lichens form flat, crust-like structures that are tightly attached to the surface. Foliose lichens are leaf-like lichens that have a flat, leafy appearance and are attached to the surface loosely. Fruticose lichens have a bushy or hair-like appearance and are often three-dimensional, standing out from the surface they grow on

\* Corresponding author.

E-mail address: [tubanur.engin@yalova.edu.tr](mailto:tubanur.engin@yalova.edu.tr) (T. Aslan Engin).

<https://doi.org/10.51753/flsrt.1572004> Author contributions

Received 22 October 2024; Accepted 20 January 2025

Available online 30 April 2025

2718-062X © 2025 This is an open access article published by Dergipark under the [CC BY](https://creativecommons.org/licenses/by/4.0/) license.

(Armstrong and Bradwell, 2010; Grube, 2024).

Lichens can grow in a wide variety of environments, from tree bark and rocks to extreme locations like deserts and the Arctic. They are very resilient and can survive in harsh conditions where many other organisms cannot. Lichens play several important roles in ecosystems. They help break down rocks into soil, provide food for some animals, and are indicators of air quality since they are sensitive to pollution (Asplund and Wardle, 2017; Toksoz, 2023). Lichens grow slowly, often just a few millimeters per year, but they can live for a long time, sometimes hundreds or even thousands of years. Lichens reproduce in two main ways: by producing spores (from the fungal part) or by fragmenting and dispersing pieces that contain both the fungal and photosynthetic partners (Garrido-Benavent and Pérez-Ortega, 2017).

Lichens produce a wide range of secondary metabolites, many of which are unique to them. These metabolites serve various functions, including protection against environmental stressors, herbivores, and microbial infections (Yildirim et al., 2012a). Some of these compounds are also valuable in pharmaceutical and industrial applications (Yildirim et al., 2012b; Emsen et al., 2013; Gokalsin et al., 2020). Lichen metabolites can be broadly classified into two categories. Primary metabolites are essential for the growth and survival of the lichen and include basic compounds like carbohydrates, proteins, and lipids. Secondary metabolites are not directly involved in growth but play important ecological roles. The majority of lichen metabolites fall into this category and include various unique compounds (Boustie and Grube, 2005). Lichens often grow in exposed environments where they receive high levels of sunlight. Metabolites and certain phenolic compounds help absorb UV light and protect the lichen's cells from damage. Lichen metabolites have strong antimicrobial properties, helping lichens fend off bacteria, fungi, and viruses (Shah et al., 2024). Some lichen compounds are toxic or unpalatable to herbivores, providing protection from being eaten. Some lichens release chemicals into the environment that inhibit the growth of other plants or organisms nearby, allowing them to reduce competition for resources (Yildirim et al., 2012b; Emsen et al., 2015; 2016; Bhagarathi et al., 2023).

Many lichen metabolites are being studied for their potential therapeutic effects. They have shown promise in treating infections, inflammation, and even cancer (Aslan Engin et al., 2023). Some lichen compounds are used in skincare products for their antioxidant and anti-inflammatory properties (Turkez et al., 2014; Emsen et al., 2017). Historically, some lichen metabolites were used as natural dyes, especially in traditional textile industries (Rather et al., 2018).

The primary aim of our study is to explore the unique biology, ecological roles, and chemical properties of lichens, emphasizing their symbiotic structure, environmental resilience, and the significance of their metabolites in ecological, pharmaceutical, and industrial applications.

## 2. Main classes of lichen secondary metabolites

Many lichen species produce phenolic acids, which provide protection against UV radiation and oxidative stress (Xu et al., 2016; Furmanek et al., 2024). Depsides and depsidones are large groups of compounds, such as atranorin and gyrophoric acid, known for their antioxidant and antimicrobial properties (Ureña-Vacas et al., 2023). The most abundant and structurally diverse class of lichen compounds are polyketides. Many of

these have antibiotic, antiviral, and anti-inflammatory properties. Usnic acid inside polyketides ( $C_{18}H_{16}O_7$ ) is one of the most studied lichen metabolites, with strong antimicrobial, antiviral, and anti-inflammatory activities (Piska et al., 2018; Antonenko et al., 2019; Bangalore et al., 2019; Tripathi et al., 2021).

## 3. General information about usnic acid

Usnic acid is one of the most well-known and widely studied secondary metabolites produced by lichens. It is a yellowish-green compound that has attracted attention due to its diverse biological activities and potential applications in various fields, particularly in pharmaceuticals and cosmetics. Usnic acid ( $C_{18}H_{16}O_7$ ) is a dibenzofuran derivative with two phenolic hydroxyl groups (Nie et al., 2024). This structure contributes to its strong antioxidant and antimicrobial properties. Usnic acid exists in two enantiomeric forms, (+)-usnic acid and (–)-usnic acid. Both forms are commonly found in lichens but may have different biological activities. (Cocchietto et al., 2002; Luzina and Salakhutdinov, 2018).

Usnic acid is found in a variety of lichen species, including genera such as *Usnea*, *Cladonia*, *Evernia*, *Lecanora*, and *Ramalina* (Elkhateeb et al., 2022). It serves as a photoprotective compound in these lichens, helping them survive in exposed and extreme environments. The content of usnic acid can vary significantly among species and environmental conditions. For example, lichens growing in high-altitude or high-UV environments often have higher concentrations of this compound (Rojas et al., 2016; Salian et al., 2021).

Usnic acid possesses a range of biological activities, making it an attractive compound for medical and cosmetic research. Usnic acid has potent antibacterial and antifungal properties. It is particularly effective against Gram-positive bacteria like *Staphylococcus aureus* and *Bacillus subtilis*. It also shows activity against several fungi and yeasts, including *Candida* species (Cansaran et al., 2006; Bangalore et al., 2019).

Preliminary studies suggest that usnic acid may have antiviral effects, particularly against some viruses like the Herpes Simplex Virus (HSV). Usnic acid has demonstrated anti-inflammatory properties, making it a candidate for treating skin conditions and inflammatory diseases (Hassan et al., 2019). Usnic acid has shown cytotoxic effects against certain cancer cell lines, including breast cancer, melanoma, and leukemia cells. Its ability to induce apoptosis (programmed cell death) in cancer cells is of particular interest in oncology research (Galanty et al., 2017; Emsen et al., 2018; Ozben and Cansaran-Duman, 2020).

## 4. Antioxidant properties of usnic acid

Usnic acid exhibits significant antioxidant activity, which makes it a compound of interest in both pharmaceutical and cosmetic fields (Luzina and Salakhutdinov, 2018). Its antioxidant properties stem from its ability to neutralize free radicals, prevent oxidative damage to cells, and inhibit lipid peroxidation. These actions are vital for protecting biological systems from oxidative stress, which is implicated in aging, cancer, and various chronic diseases (Martin-Cordero et al., 2012).

Usnic acid's antioxidant activities can be attributed to several mechanisms (Araújo et al., 2015). Usnic acid has a structure rich in phenolic groups, which allows it to donate

hydrogen atoms or electrons to free radicals, neutralizing their reactivity. This helps in preventing cellular damage caused by reactive oxygen species (ROS) such as superoxide anions, hydroxyl radicals, and peroxy radicals (Ingólfssdóttir, 2002; Araújo et al., 2015).

Lipid peroxidation refers to the oxidative degradation of lipids, particularly in cell membranes, which can lead to cell damage or death (Gaschler and Stockwell, 2017; Recknagel et al., 2020). Usnic acid helps inhibit this process by neutralizing the free radicals that initiate and propagate lipid peroxidation, protecting cellular membranes (Kwong and Wang, 2020; Gulcin and Alwaseel, 2023).

Usnic acid may chelate metal ions like iron and copper, which catalyze the formation of free radicals through Fenton reactions (Kováčik et al., 2018). By binding these metal ions, usnic acid reduces the generation of free radicals. Some studies suggest that usnic acid may influence the activity of endogenous antioxidant enzymes such as SOD, catalase, and glutathione peroxidase. These enzymes play critical roles in detoxifying reactive oxygen species within the body (White et al., 2014; Fernández-Moriano et al., 2017). SOD converts superoxide radicals into less reactive hydrogen peroxide ( $H_2O_2$ ).

Usnic acid, with its phenolic hydroxyl groups, may directly scavenge superoxide radicals or inhibit the generation of ROS. This could reduce the burden on SOD by lowering the superoxide levels in the cellular environment (Mittal et al., 2021). Catalase breaks down hydrogen peroxide into water and oxygen. By scavenging ROS and reducing oxidative stress, usnic acid may indirectly decrease  $H_2O_2$  levels, affecting catalase activity. Alternatively, it may assist catalase by preventing the accumulation of toxic hydrogen peroxide (Beckett et al., 2021). GPx neutralizes lipid peroxides and hydrogen peroxide using glutathione. Usnic acid might reduce lipid peroxidation, thereby lowering the substrate levels for GPx. However, its direct interaction with the glutathione system remains unclear (Fernández-Moriano et al., 2017).

## 5. Antioxidant capacity measurement

Various experimental assays are used to measure the antioxidant capacity of usnic acid. Some of the most common methods include: 2,2-diphenyl-1-picrylhydrazyl (DPPH) radical scavenging assay measures the ability of usnic acid to scavenge the DPPH radical (Popovici et al., 2018). Usnic acid shows significant activity in reducing DPPH radicals, reflecting its hydrogen-donating ability. Similar to the DPPH assay, this method uses 2,2'-Azino-bis(3-ethylbenzothiazoline-6-sulfonic acid) (ABTS) radicals to evaluate antioxidant potential. Usnic acid can effectively neutralize ABTS radicals, showing its capacity to quench reactive radicals (Verma et al., 2012; Cakmak and Gulcin, 2019).

Ferric reducing antioxidant power (FRAP) method assesses the ability of antioxidants to reduce ferric ions ( $Fe^{3+}$ ) to ferrous ions ( $Fe^{2+}$ ) (Ananthi et al., 2015). Usnic acid demonstrates reducing power in this assay, indicating its electron-donating capacity. Lipid peroxidation inhibition assay measures the ability of usnic acid to prevent the oxidation of lipids. It shows strong inhibition of lipid peroxidation in various biological and artificial membranes, which is crucial for maintaining cell integrity (Suwalsky et al., 2015).

The antioxidant activity of usnic acid is closely related to its chemical structure, particularly its phenolic hydroxyl groups. These groups are capable of donating hydrogen atoms to

neutralize free radicals (Kocer et al., 2014). The dibenzofuran backbone of usnic acid enhances its stability after donating hydrogen atoms, making it an effective antioxidant. The presence of hydroxyl groups in the structure allows usnic acid to act as a hydrogen donor, neutralizing radicals (Millot et al., 2016). The dibenzofuran core structure contributes to the delocalization of electrons, which helps stabilize the radical form of usnic acid after it donates a hydrogen atom (Yousuf and Choudhary, 2014).

Usnic acid has been compared to other well-known antioxidants such as vitamin C, vitamin E, and synthetic antioxidants like butylated hydroxytoluene. While its antioxidant capacity is notable, its activity may vary depending on the experimental conditions and the specific assay used (Balanco et al., 2019; Ayusman et al., 2020).

In some studies, usnic acid has shown antioxidant activity comparable to that of vitamin C and vitamin E, particularly in lipid peroxidation inhibition (Thakur et al., 2023). However, its radical scavenging ability may be lower than these vitamins in some assays. Nonetheless, the unique combination of antimicrobial and antioxidant properties makes usnic acid an attractive compound for skin care, where oxidative stress and microbial infections are common issues (Shcherbakova et al., 2021; Kocovic et al., 2022).

## 6. Biological and pharmaceutical significance

The antioxidant properties of usnic acid have significant implications across various fields of study. Due to its ability to neutralize free radicals and prevent oxidative damage, usnic acid is a potential ingredient in sunscreens and anti-aging products. Its antioxidant activity helps protect the skin from damage caused by UV radiation and environmental pollutants (Galanty et al., 2021).

Oxidative stress is closely linked to inflammation. By reducing oxidative damage, usnic acid may also reduce inflammatory responses in tissues, contributing to its potential as an anti-inflammatory agent (Su et al., 2014). Oxidative stress plays a key role in neurodegenerative diseases such as Alzheimer's and Parkinson's. Some studies have suggested that usnic acid's antioxidant properties could be harnessed to protect neurons from oxidative damage (Fernández-Moriano et al., 2017). Since oxidative stress is involved in cancer progression, the antioxidant properties of usnic acid have sparked interest in its potential role in cancer prevention or treatment. Its ability to induce apoptosis in cancer cells, combined with its antioxidant activity, makes it a compound of interest for future research in oncology (Kumar et al., 2020; Azhamuthu et al., 2024).

While usnic acid has potent antioxidant properties, there are some challenges and concerns regarding its use. Usnic acid can be hepatotoxic at high concentrations, especially when taken orally (Gao et al., 2024). This limits its use in systemic antioxidant therapies and highlights the need for careful dosing in topical applications. Animal studies have demonstrated that high doses of usnic acid can induce liver damage, characterized by elevated liver enzymes (ALT and AST), oxidative stress, and histopathological changes such as hepatocyte necrosis and inflammation (Kwong and Wang, 2020). Cases of liver toxicity in humans have been reported, particularly in individuals using dietary supplements containing usnic acid for weight loss. Symptoms include jaundice, fatigue, and in severe cases, acute liver failure requiring transplantation (Sanchez et al., 2006). These findings underscore the need for stricter regulations and

comprehensive safety evaluations of usnic acid-containing products. The proposed mechanism involves mitochondrial dysfunction, where usnic acid disrupts oxidative phosphorylation, leading to excessive ROS generation and ATP depletion. Usnic acid's stability can be affected by environmental factors such as light and temperature, which may reduce its effectiveness in some formulations. Encapsulation techniques or combining it with stabilizing agents might be necessary to maintain its antioxidant efficacy in cosmetic and pharmaceutical products (Brugnoli et al., 2024; Fadhila et al., 2024).

At higher concentrations, usnic acid can exhibit pro-oxidant behavior, generating excessive ROS and exacerbating oxidative stress. This paradoxical effect may contribute to cellular damage, including lipid peroxidation, protein modification, and DNA fragmentation (Popovici et al., 2021). High doses of usnic acid can impair mitochondrial function by disrupting oxidative phosphorylation. This results in ATP depletion, increased ROS production, and apoptosis or necrosis, particularly in hepatocytes, leading to liver toxicity (Croce et al., 2022). Systematic investigations into the concentration-dependent effects of usnic acid in different cell types and animal models are essential. These studies should focus on defining the thresholds for beneficial vs. harmful effects (Araújo et al., 2015).

Usnic acid is used in products designed to combat oxidative stress and protect the skin from premature aging. Its antioxidant properties are particularly beneficial in sunscreens, moisturizers, and anti-aging creams (Ramaraj and Narayan, 2024). While not widely used yet due to safety concerns, usnic acid is being studied for its antioxidant potential in treating conditions related to oxidative stress, such as chronic inflammation and neurodegenerative diseases (Cazarin et al., 2021; Al Rihani et al., 2024).

## 7. Anticancer properties and cosmetic usage

Usnic acid inhibits the proliferation of cancer cells and induces apoptosis (programmed cell death), which is a key mechanism in preventing cancer cell survival. Usnic acid has been shown to trigger apoptosis in cancer cells by increasing cellular stress and DNA damage (Singh et al., 2013). This process leads to cancer cell death. Usnic acid facilitates apoptosis by altering the expression of pro-apoptotic and anti-apoptotic proteins, promoting the death of cancer cells. Usnic acid can affect the expression of proteins from the Bcl-2 family, such as Bcl-2 and Bax, which regulate cell death. By altering the balance of these proteins, usnic acid promotes the apoptosis of cancer cells (Erdogan et al., 2023).

Usnic acid influences the regulation of the cell cycle, which is critical for cancer cell division and proliferation. It inhibits the progression of cancer cells through the cell cycle, thus preventing cell division. Usnic acid can arrest cancer cells in the G1 phase of the cell cycle, preventing them from proceeding to DNA replication and cell division. This effectively halts cancer cell growth. Usnic acid may reduce the expression of key proteins involved in cell cycle regulation, such as Cyclin D1 and Cyclin-Dependent Kinases (CDK). This disruption inhibits cancer cell growth and proliferation (Gimła and Herman-Antosiewicz, 2024).

Another crucial anticancer property of usnic acid is its ability to inhibit metastasis—the spread of cancer to other parts of the body. Usnic acid can inhibit Matrix Metalloproteinases

(MMPs), enzymes that play a key role in the invasion of cancer cells into surrounding tissues. By blocking MMP activity, usnic acid helps prevent cancer cells from spreading and metastasizing. Usnic acid reduces the ability of cancer cells to invade adjacent tissues, a crucial step in metastasis. This anti-invasive effect can limit the spread of cancer (Wu et al., 2022).

Usnic acid also exhibits anti-inflammatory and antioxidant properties, which contribute to its anticancer activity. Chronic inflammation is often associated with cancer progression. Usnic acid can reduce the production of pro-inflammatory cytokines such as TNF- $\alpha$  and IL-6, which are involved in cancer development. By modulating these inflammatory signals, usnic acid can limit tumor progression (Paździora et al., 2023). Usnic acid can exert influence on genetic and epigenetic processes, which are crucial in cancer development. It has been shown to help repair DNA damage in cancer cells. DNA damage is a hallmark of cancer cell proliferation. By promoting DNA repair mechanisms, usnic acid may help to reduce the likelihood of mutations that drive cancer progression (Shukla et al., 2023). Usnic acid may affect DNA methylation and histone modification processes, which can regulate gene expression. These epigenetic changes can result in the silencing of oncogenes and activation of tumor suppressor genes, ultimately limiting cancer cell growth (Reddy et al., 2016). Usnic acid may also interact with hormonal and neurogenic pathways in certain types of cancer. Some studies suggest that usnic acid can influence estrogen receptors, which are important in the growth of estrogen-related cancers (e.g., breast cancer). This interaction could be beneficial in managing these types of cancers (Unver et al., 2019).

Usnic acid has been studied for its various potential applications in cosmetics due to its beneficial properties for skin care. Usnic acid has strong antimicrobial properties, making it useful in treating skin conditions caused by bacteria and fungi. Due to its antibacterial properties, usnic acid can help reduce acne by inhibiting the growth of *Propionibacterium acnes*, the bacteria responsible for acne breakouts. Usnic acid can help in treating fungal skin infections, such as ringworm or athlete's foot, by preventing the growth of harmful fungi (Sepahvand et al., 2021). By reducing oxidative stress, usnic acid helps protect the skin from premature aging, fine lines, and wrinkles. Its antioxidant effects can promote skin regeneration and improve the overall appearance of the skin (Ramakrishnan et al., 2020).

## 8. Usnic Acid's safety profile and potential toxicity

Usnic acid has been most notably associated with hepatotoxicity (liver damage) when consumed orally, particularly in dietary supplements marketed for weight loss, detoxification, or fat burning. Several cases of liver toxicity have been reported, leading to liver failure and, in some cases, requiring liver transplantation (Gao et al., 2024). The mechanism behind this toxicity is believed to involve mitochondrial dysfunction, as usnic acid can inhibit mitochondrial respiration, leading to oxidative stress and cellular damage (Demir et al., 2025). There have been documented cases where individuals experienced symptoms such as fatigue, jaundice, abdominal pain, and elevated liver enzymes after taking products containing usnic acid. While such severe cases are rare, they underscore the potential risks associated with prolonged or excessive use (Pandit et al., 2024).

Although studies on the bioaccumulation of usnic acid are limited, it is known that topical products containing usnic acid

can lead to gradual accumulation in the skin. This may increase the likelihood of sensitization or allergic reactions with prolonged use, especially if the skin is exposed to usnic acid regularly or in large amounts. This is why proper usage and adherence to recommended guidelines are important (de Souza et al., 2024).

## 9. Conclusion

In conclusion, usnic acid stands out as a remarkable bioactive compound produced by lichens, offering immense potential across diverse fields such as dermatology, anti-aging treatments, neuroprotection, and cancer therapies. Its potent antioxidant properties, along with its antimicrobial and anti-inflammatory activities, make it a versatile agent with significant implications for both pharmaceutical and cosmetic applications. However, the practical application of usnic acid is not without challenges. Notably, issues such as its toxicity, formulation stability, and the need for optimized delivery systems represent critical hurdles that must be addressed to fully harness its potential.

This review underscores the importance of bridging the gaps in current knowledge regarding usnic acid's mechanisms of action and safety profile. While its efficacy in addressing oxidative stress and microbial infections is well-documented, further investigations are essential to ensure its safe and effective use. For instance, studies focusing on dose optimization, long-term safety evaluations, and innovative formulation approaches could pave the way for its broader adoption in clinical and commercial settings. Additionally, the exploration of usnic acid's role in combating oxidative stress-

related conditions highlights its relevance in addressing pressing health challenges. By mitigating cellular damage caused by free radicals, usnic acid holds promise in advancing therapeutic strategies for chronic inflammatory diseases, skin health, and neurodegenerative disorders. Similarly, its application in cosmetic products, particularly in anti-aging and skin protection formulations, aligns with the growing demand for natural and effective solutions in the industry.

The review also emphasizes the dual nature of usnic acid's impact, balancing its substantial benefits with the necessity to manage potential risks. Addressing its toxicity and enhancing formulation stability are pivotal for realizing its full potential. Future research should prioritize innovative delivery systems, such as encapsulation techniques, to minimize adverse effects and improve bioavailability.

In summary, usnic acid represents a compelling avenue for future exploration, with promising applications that extend beyond its current scope. By addressing key challenges through targeted research and development, its potential can be maximized, contributing to advancements in medicine and industry. This review provides a foundation for guiding future studies and underscores the need for interdisciplinary collaboration to unlock the full spectrum of benefits that usnic acid offers.

**Conflict of interest:** The author declares that she has no conflict of interests.

**Informed consent:** The author declares that this manuscript did not involve human or animal participants and informed consent was not collected.

## References

- Al Rihani, S. B., Elfakhri, K. H., Ebrahim, H. Y., Al-Ghraiyyah, N. F., Alkhalifa, A. E., El Sayed, K. A., & Kaddoumi, A. (2024). The usnic acid analogue 4-FPBUA enhances the blood-brain barrier function and induces autophagy in Alzheimer's disease mouse models. *ACS Chemical Neuroscience*, 15(17), 3152-3167.
- Ananthi, R., Tinabaye, A., & Selvaraj, G. (2015). Antioxidant study of usnic acid and its derivative usnic acid diacetate. *International Journal of Research in Engineering and Technology*, 4(2), 356-366.
- Antonenko, Y. N., Khailova, L. S., Rokitskaya, T. I., Nosikova, E. S., Nazarov, P. A., Luzina, O. A., Salakhutdinov, N. F., & Kotova, E. A. (2019). Mechanism of action of an old antibiotic revisited: Role of calcium ions in protonophoric activity of usnic acid. *Biochimica et Biophysica Acta - Bioenergetics*, 1860(4), 310-316.
- Araújo, A. A. S., de Melo, M. G. D., Rabelo, T. K., Nunes, P. S., Santos, S. L., Serafini, M. R., Santos, M. R. V., Quintans-Júnior, L. J., & Gelain, D. P. (2015). Review of the biological properties and toxicity of usnic acid. *Natural Product Research*, 29(23), 2167-2180.
- Armstrong, R., & Bradwell, T. (2010). Growth of crustose lichens: a review. *Geografiska Annaler: Series A, Physical Geography*, 92(1), 3-17.
- Aslan Engin, T., Emsen, B., Yilmaz Ozturk, R., Cakir Koc, R., Inan, B., & Ozcimen, D. (2023). Cytotoxicity of *Usnea longissima* Ach. extracts and its secondary metabolite, usnic acid on different cells. *Anatolian Journal of Botany*, 7(2), 140-145.
- Asplund, J., & Wardle, D. A. (2017). How lichens impact on terrestrial community and ecosystem properties. *Biological Reviews*, 92(3), 1720-1738.
- Ayusman, S., Duraivadivel, P., Gowtham, H. G., Sharma, S., & Hariprasad, P. (2020). Bioactive constituents, vitamin analysis, antioxidant capacity and  $\alpha$ -glucosidase inhibition of *Canna indica* L. rhizome extracts. *Food Bioscience*, 35, 100544.
- Azhimuthu, T., Kathiresan, S., Senkuttuvan, I., Asath, N. A. A., Ravichandran, P., & Vasu, R. (2024). Usnic acid alleviates inflammatory responses and induces apoptotic signaling through inhibiting NF- $\kappa$ B expressions in human oral carcinoma cells. *Cell Biochemistry and Function*, 42(4), e4074.
- Balanco, J. M. F., Sussmann, R. A. C., Verdager, I. B., Gabriel, H. B., Kimura, E. A., & Katzin, A. M. (2019). Tocopherol biosynthesis in *Leishmania* (L.) amazonensis promastigotes. *FEBS Open Bio*, 9(4), 743-754.
- Bangalore, P. K., Vagolu, S. K., Bollikanda, R. K., Veeragoni, D. K., Choudante, P. C., Misra, S., ... & Kantevari, S. (2019). Usnic acid enaminone-coupled 1, 2, 3-triazoles as antibacterial and antitubercular agents. *Journal of Natural Products*, 83(1), 26-35.
- Beckett, R. P., Minibayeva, F., Solhaug, K. A., & Roach, T. (2021). Photoprotection in lichens: adaptations of photobionts to high light. *The Lichenologist*, 53(1), 21-33.
- Bhagarathi, L. K., DaSilva, P. N. B., Subramanian, G., Maharaj, G., Kalika-Singh, S., Pestano, F., Phillips-Henry, Z., & Cossiah, C. (2023). An integrative review of the biology and chemistry of lichens and their ecological, ethnopharmacological, pharmaceutical and therapeutic potential. *GSC Biological and Pharmaceutical Sciences*, 23(3), 92-119.
- Boustie, J., & Grube, M. (2005). Lichens-a promising source of bioactive secondary metabolites. *Plant Genetic Resources*, 3(2), 273-287.
- Brunoli, B., Perna, G., Alfano, S., Piozzi, A., Galantini, L., Axioti, E., Taresco, V., Mariano, A., Scotto d'Abusco, A., & Vecchio Cipriotti, S. (2024). Nanostructured poly-L-lactide and polyglycerol adipate carriers for the encapsulation of usnic acid: a promising approach for hepatoprotection. *Polymers*, 16(3), 427.
- Cakmak, K. C., & Gulcin, I. (2019). Anticholinergic and antioxidant activities of usnic acid-an activity-structure insight. *Toxicology Reports*, 6, 1273-1280.
- Cansaran, D., Kahya, D., Yurdakulol, E., & Atakol, O. (2006). Identification and quantitation of usnic acid from the lichen *Usnea* species of Anatolia and antimicrobial activity. *Zeitschrift Für Naturforschung C*, 61(11-12), 773-776.
- Cazarin, C. A., Dalmagro, A. P., Gonçalves, A. E., Boeing, T., da Silva, L. M., Corrêa, R., Klein-Júnior, L. C., Pinto, B. C., Lorenzetti, T. S., & da Costa Sobrinho, T. U. (2021). Usnic acid enantiomers restore cognitive

- deficits and neurochemical alterations induced by A $\beta$ 1-42 in mice. *Behavioural Brain Research*, 397, 112945.
- Cocchietto, M., Skert, N., Nimis, P., & Sava, G. (2002). A review on usnic acid, an interesting natural compound. *Naturwissenschaften*, 89, 137-146.
- Croce, N., Pitaro, M., Gallo, V., & Antonini, G. (2022). Toxicity of usnic acid: A narrative review. *Journal of Toxicology*, 2022(1), 8244340.
- de Souza, J. B., de Lacerda Coriolano, D., dos Santos Silva, R. C., da Costa Júnior, S. D., de Almeida Campos, L. A., Cavalcanti, I. D. L., ... & Cavalcanti, I. M. F. (2024). Ceftazidime and Usnic acid encapsulated in chitosan-coated liposomes for oral administration against colorectal cancer-inducing *Escherichia coli*. *Pharmaceuticals*, 17(6), 802.
- Demir, S., Alemdar, N. T., Yulug, E., Demir, E. A., Durmus, T. B., Mentese, A., & Aliyazicioglu, Y. (2025). Usnic acid suppresses inflammation and endoplasmic reticulum stress in a methotrexate-induced pulmonary toxicity model via modulating Nrf2 pathway. *South African Journal of Botany*, 177, 572-578.
- Elkhateeb, W. A., El-Ghwas, D. E., & Daba, G. M. (2022). Lichens uses surprising uses of lichens that improve human life. *Journal of Biomedical Research and Environmental Sciences*, 3(2), 189-194.
- Emsen, B., Aslan, A., Togar, B., & Turkez, H. (2016). In vitro antitumor activities of the lichen compounds olivetoric, physodic and psoromic acid in rat neuron and glioblastoma cells. *Pharmaceutical Biology*, 54(9), 1748-1762.
- Emsen, B., Aslan, A., Turkez, H., Taghizadehghalehjoughi, A., & Kaya, A. (2018). The anti-cancer efficacies of diffractaic, lobaric, and usnic acid: in vitro inhibition of glioma. *Journal of Cancer Research and Therapeutics*, 14(5), 941-951.
- Emsen, B., Aslan, A., Yildirim, E., & Ercisli, S. (2013). Toxicity effects of some lichen species extracts against the Colorado potato beetle, *Leptinotarsa decemlineata* Say (Coleoptera: Chrysomelidae). *Egyptian Journal of Biological Pest Control*, 23(2), 193-199.
- Emsen, B., Turkez, H., Togar, B., & Aslan, A. (2017). Evaluation of antioxidant and cytotoxic effects of olivetoric and physodic acid in cultured human amnion fibroblasts. *Human and Experimental Toxicology*, 36(4), 376-385.
- Emsen, B., Yildirim, E., & Aslan, A. (2015). Insecticidal activities of extracts of three lichen species on *Sitophilus granarius* (L.) (Coleoptera: Curculionidae). *Plant Protection Science*, 51(3), 156-161.
- Erdogan, O., Abas, B. I., & Cevik, O. (2023). Usnic Acid Exerts Antiproliferative and Apoptotic Effects by Suppressing NF-B p50 in DU145 Cells. *European Journal of Biology*, 82(2), 251-257.
- Fadhila, M., Effendy, S., & Siregar, S. H. (2024). Inclusion complexation of usnic acid-hydroxypropyl- $\beta$ -cyclodextrin: physicochemical characterization and dissolution rate studies. *Research Journal of Pharmacy and Technology*, 17(5), 2206-2212.
- Fernández-Moriano, C., Divakar, P. K., Crespo, A., & Gómez-Serranillos, M. P. (2017). Protective effects of lichen metabolites evernic and usnic acids against redox impairment-mediated cytotoxicity in central nervous system-like cells. *Food and Chemical Toxicology*, 105, 262-277. <https://doi.org/10.1016/j.fct.2017.04.030>
- Furmanek, Ł., Czarnota, P., Tekiel, A., Kapusta, I., & Seaward, M. R. D. (2024). A spectrophotometric analysis of extracted water-soluble phenolic metabolites of lichens. *Planta*, 260(2), 40.
- Galanty, A., Koczurkiewicz, P., Wnuk, D., Paw, M., Karnas, E., Podolak, I., Węgrzyn, M., Borusiewicz, M., Madeja, Z., Czyż, J., & Michalik, M. (2017). Usnic acid and atranorin exert selective cytostatic and anti-invasive effects on human prostate and melanoma cancer cells. *Toxicology In Vitro*, 40, 161-169.
- Galanty, A., Popiół, J., Paczkowska-Walendowska, M., Studzińska-Sroka, E., Paśko, P., Cielecka-Piontek, J., Pękala, E., & Podolak, I. (2021). (+)-Usnic acid as a promising candidate for a safe and stable topical photoprotective agent. *Molecules*, 26(17), 5224.
- Gao, X., Campasino, K., Yourick, M. R., Cao, Y., Yourick, J. J., & Sprando, R. L. (2024). Oxidative DNA damage contributes to usnic acid-induced toxicity in human induced pluripotent stem cell-derived hepatocytes. *Journal of Applied Toxicology*, 44(9), 1329-1346.
- Garrido-Benavent, I., & Pérez-Ortega, S. (2017). Past, present, and future research in bipolar lichen-forming fungi and their photobionts. *American Journal of Botany*, 104(11), 1660-1674.
- Gaschler, M. M., & Stockwell, B. R. (2017). Lipid peroxidation in cell death. *Biochemical and Biophysical Research Communications*, 482(3), 419-425.
- Gimla, M., & Herman-Antosiewicz, A. (2024). Multifaceted properties of usnic acid in disrupting cancer hallmarks. *Biomedicines*, 12(10), 2199.
- Gokalsin, B., Berber, D., Hur, J. S., & Sesal, N. C. (2020). Quorum sensing inhibition properties of lichen forming fungi extracts from *Cetrelia* species against *Pseudomonas aeruginosa*. *Frontiers in Life Sciences and Related Technologies*, 1(1), 22-27.
- Grube, M. (2024). Lichens. In *Fungal Associations* (pp. 145-179). Springer.
- Gulcin, İ., & Alwasel, S. H. (2023). DPPH radical scavenging assay. *Processes*, 11(8), 2248.
- Hassan, S. T. S., Šudomová, M., Berchová-Bímová, K., Šmejkal, K., & Echeverría, J. (2019). Psoromic acid, a lichen-derived molecule, inhibits the replication of HSV-1 and HSV-2, and inactivates HSV-1 DNA polymerase: shedding light on antiherpetic properties. *Molecules*, 24(16), 2912.
- Honegger, R. (2009). Lichen-forming fungi and their photobionts. In *Plant Relationships* (pp. 307-333). Springer.
- Ingólfssdóttir, K. (2002). Usnic acid. *Phytochemistry*, 61(7), 729-736.
- Kocer, S., Urus, S., Cakir, A., Gulluce, M., Digrak, M., Alan, Y., Aslan, A., Tumer, M., Karadayı, M., Kazaz, C., & Dal, H. (2014). The synthesis, characterization, antimicrobial and antimutagenic activities of hydroxyphenylimino ligands and their metal complexes of usnic acid isolated from *Usnea longissima*. *Dalton Transactions*, 43(16), 6148-6164.
- Kocovic, A., Jeremic, J., Bradic, J., Sovrljic, M., Tomovic, J., Vasiljevic, P., Andjic, M., Dragicin, N., Grujovic, M., Mladenovic, K., Jakovljevic, V., & Manojlovic, N. (2022). Phytochemical analysis, antioxidant, antimicrobial, and cytotoxic activity of different extracts of *Xanthoparmelia stenophylla* lichen from Stara Planina, Serbia. *Plants*, 11(13), 1624.
- Kováčik, J., Dresler, S., Peterková, V., and Babula, P. (2018). Metal-induced oxidative stress in terrestrial macrolichens. *Chemosphere*, 203, 402-409.
- Kumar, K., Mishra, J. P. N., & Singh, R. P. (2020). Usnic acid induces apoptosis in human gastric cancer cells through ROS generation and DNA damage and causes up-regulation of DNA-PKcs and  $\gamma$ -H2A.X phosphorylation. *Chemico-Biological Interactions*, 315, 108898.
- Kwong, S. P., & Wang, C. (2020). Usnic acid-induced hepatotoxicity and cell death. *Environmental Toxicology and Pharmacology*, 80, 103493.
- Luzina, O. A., & Salakhutdinov, N. F. (2018). Usnic acid and its derivatives for pharmaceutical use: a patent review (2000-2017). *Expert Opinion on Therapeutic Patents*, 28(6), 477-491.
- Martin-Cordero, C., Jose Leon-Gonzalez, A., Manuel Calderon-Montano, J., Burgos-Moron, E., & Lopez-Lazaro, M. (2012). Pro-oxidant natural products as anticancer agents. *Current Drug Targets*, 13(8), 1006-1028.
- Millot, M., Dieu, A., & Tomasi, S. (2016). Dibenzofurans and derivatives from lichens and ascomycetes. *Natural Product Reports*, 33(6), 801-811.
- Mittal, S., Ashhar, M. U., Ahuja, A., Ali, J., & Baboota, S. (2021). Role of natural bioactives and their nanocarriers for overcoming oxidative stress induced cancer. *Current Medicinal Chemistry*, 28(36), 7477-7512.
- Morillas, L., Roales, J., Cruz, C., & Munzi, S. (2022). Lichen as multipartner symbiotic relationships. *Encyclopedia*, 2(3), 1421-1431.
- Nie, W. Z., Shen, Q. K., Quan, Z. S., Guo, H. Y., & Li, Y. M. (2024). Bioactivities and Structure-Activity Relationships of Usnic Acid Derivatives: A Review. *Mini Reviews in Medicinal Chemistry*, 24(14), 1368-1384.
- Ozben, R., & Cansaran-Duman, D. (2020). The expression profiles of apoptosis-related genes induced usnic acid in SK-BR-3 breast cancer cell. *Human and Experimental Toxicology*.
- Pandit, S., Kim, M.-A., Jung, J.-E., Choi, H.-M., & Jeon, J.-G. (2024). Usnic acid brief exposure suppresses cariogenic properties and complexity of *Streptococcus mutans* biofilms. *Biofilm*, 8, 100241.
- Paździora, W., Podolak, I., Grudzińska, M., Paśko, P., Grabowska, K., & Galanty, A. (2023). Critical assessment of the anti-inflammatory potential of usnic acid and its derivatives—A review. *Life*, 13(4), 1046.
- Piska, K., Galanty, A., Koczurkiewicz, P., Żmudzki, P., Potaczek, J., Podolak, I., & Pękala, E. (2018). Usnic acid reactive metabolites formation in human, rat, and mice microsomes. Implication for hepatotoxicity. *Food and Chemical Toxicology*, 120, 112-118.
- Popovici, V., Bucur, L., Popescu, A., Caraiane, A., & Badea, V. (2018). Determination of the content in usnic acid and polyphenols from the extracts of *Usnea barbata* L. and the evaluation of their antioxidant activity. *Farmacia*, 66(2), 337-341.
- Popovici, V., Matei, E., Cozaru, G. C., Aschie, M., Bucur, L., Rambu, D.,

- Costache, T., Cucolea, I. E., Vochita, G., & Gherghel, D. (2021). Usnic acid and *Usnea barbata* (L.) FH wigg. dry extracts promote apoptosis and DNA damage in human blood cells through enhancing ROS levels. *Antioxidants*, 10(8), 1171.
- Ramakrishnan, V., Aiswarya, P. S., Pallavi, K., Husain, R. S. A., & Ahmed, S. S. S. J. (2020). Photoaging and anti-photoaging activity of compounds derived from marine origin. *Encyclopedia of Marine Biotechnology*, 3, 1641-1657.
- Ramaraj, J. A., & Narayan, S. (2024). Anti-aging strategies and topical delivery of biopolymer-based nanocarriers for skin cancer treatment. *Current Aging Science*, 17(1), 31-48.
- Rather, L. J., Jameel, S., Ganie, S. A., & Bhat, K. A. (2018). Lichen derived natural colorants: history, extraction, and applications. *Handbook of Renewable Materials for Coloration and Finishing*, 1, 103-114.
- Recknagel, R. O., Glende, E. A., & Britton, R. S. (2020). Free radical damage and lipid peroxidation. In *Hepatotoxicology* (pp. 401-436). CRC press.
- Reddy, R. G., Veeraval, L., Maitra, S., Chollet-Krugler, M., Tomasi, S., Dévéhat, F. L. Le, Boustie, J., & Chakravarty, S. (2016). Lichen-derived compounds show potential for central nervous system therapeutics. *Phytomedicine*, 23(12), 1527-1534.
- Rojas, J., Londoño, C., & Ciro, Y. (2016). The health benefits of natural skin UVA photoprotective compounds found in botanical sources. *International Journal of Pharmacy and Pharmaceutical Sciences*, 8(3), 13-23.
- Salian, A., Dutta, S., & Mandal, S. (2021). A roadmap to UV-protective natural resources: classification, characteristics, and applications. *Materials Chemistry Frontiers*, 5(21), 7696-7723.
- Sanchez, W., Maple, J. T., Burgart, L. J., & Kamath, P. S. (2006). Severe hepatotoxicity associated with use of a dietary supplement containing usnic acid. *Mayo Clinic Proceedings*, 81(4), 541-544.
- Sepahvand, A., Studzińska-Sroka, E., Ramak, P., & Karimian, V. (2021). *Usnea* sp.: Antimicrobial potential, bioactive compounds, ethnopharmacological uses and other pharmacological properties; a review article. *Journal of Ethnopharmacology*, 268, 113656.
- Shah, A. A., Badshah, L., Muhammad, M., Basit, A., Ullah, I., Mohamed, H. I., & Khan, A. (2024). Secondary metabolites of lichens and their application. In *Fungal Secondary Metabolites* (pp. 91-115). Elsevier.
- Shcherbakova, A., Strömstedt, A. A., Göransson, U., Gnezdilov, O., Turanov, A., Boldbaatar, D., Kochkin, D., Ulrich-Merzenich, G., & Koptina, A. (2021). Antimicrobial and antioxidant activity of *Evernia prunastri* extracts and their isolates. *World Journal of Microbiology and Biotechnology*, 37(8), 129.
- Shukla, A. K., Yadav, V. K., Mishra, R. K., Kumar, M., Sharma, M., Dev, S. K., & Maurya, R. (2023). Role of Usnic acid and its derivatives in the management of cancer. *Asian Journal of Pharmacy and Pharmacology*, 9(1), 6-12.
- Singh, N., Nambiar, D., Kale, R. K., & Singh, R. P. (2013). Usnic acid inhibits growth and induces cell cycle arrest and apoptosis in human lung carcinoma A549 cells. *Nutrition and Cancer*, 65(sup1), 36-43.
- Su, Z. Q., Mo, Z. Z., Liao, J. Bin, Feng, X. X., Liang, Y. Z., Zhang, X., Liu, Y. H., Chen, X. Y., Chen, Z. W., Su, Z. R., & Lai, X. P. (2014). Usnic acid protects LPS-induced acute lung injury in mice through attenuating inflammatory responses and oxidative stress. *International Immunopharmacology*, 22(2), 371-378.
- Suwalsky, M., Jemiola-Rzeminska, M., Astudillo, C., Gallardo, M. J., Staforelli, J. P., Villena, F., & Strzalka, K. (2015). An in vitro study on the antioxidant capacity of usnic acid on human erythrocytes and molecular models of its membrane. *Biochimica et Biophysica Acta-Biomembranes*, 1848(11), 2829-2838.
- Thakur, M., Kasi, I. K., Islary, P., & Bhatti, S. K. (2023). Nutritional and health-promoting effects of lichens used in food applications. *Current Nutrition Reports*, 12(4), 555-566.
- Toksoz, O. (2023). Geçmişten günümüze potansiyel hammadde kaynağı: Likenler. *Frontiers in Life Sciences and Related Technologies*, 4(S1), 38-44.
- Tripathi, A. H., Negi, N., Gahtori, R., Kumari, A., Joshi, P., Tewari, L. M., Joshi, Y., Bajpai, R., Upreti, D. K., & Upadhyay, S. K. (2021). A review of anti-cancer and related properties of lichen-extracts and metabolites. *Anti-Cancer Agents in Medicinal Chemistry*, 22(1), 115-142.
- Turkez, H., Aydin, E., & Aslan, A. (2014). Role of aqueous *Bryoria capillaris* (Ach.) extract as a genoprotective agent on imazalil-induced genotoxicity *in vitro*. *Toxicology and Industrial Health*, 30(1), 33-39.
- Unver, H., Berber, B., Demirel, R., & Koparal, A. T. (2019). Design, synthesis, anti-proliferative, anti-microbial, anti-angiogenic activity and in silico analysis of novel hydrazone derivatives. *Anti-Cancer Agents in Medicinal Chemistry*, 19(13), 1658-1669.
- Ureña-Vacas, I., González-Burgos, E., Divakar, P. K., & Gómez-Serranillos, M. P. (2023). Lichen depsides and tridepsides: progress in pharmacological approaches. *Journal of Fungi*, 9(1), 116.
- Verma, N., Behera, B. C., & Sharma, B. O. (2012). Glucosidase inhibitory and radical scavenging properties of lichen metabolites salazinic acid, sekikaic acid and usnic acid. *Hacettepe Journal of Biology and Chemistry*, 40(1), 7-21.
- White, P. A. S., Oliveira, R. C. M., Oliveira, A. P., Serafini, M. R., Araújo, A. A. S., Gelain, D. P., Moreira, J. C. F., Almeida, J. R. G. S., Quintans, J. S. S., & Quintans-Junior, L. J. (2014). Antioxidant activity and mechanisms of action of natural compounds isolated from lichens: a systematic review. *Molecules*, 19(9), 14496-14527.
- Wu, Y., Gan, D., Leng, X., He, W., Zhang, X., Li, C., Gu, X., Hu, Y., Du, S., & Han, Y. (2022). Anti-ageing and anti-lung carcinoma effects of vulpinic acid and usnic acid compounds and biological investigations with molecular modeling study. *Journal of Oleo Science*, 71(2), 247-255.
- Xu, M., Heidmarsson, S., Olafsdottir, E. S., Buonfiglio, R., Kogej, T., & Omarsdottir, S. (2016). Secondary metabolites from cetrarioid lichens: chemotaxonomy, biological activities and pharmaceutical potential. *Phytomedicine*, 23(5), 441-459.
- Yildirim, E., Aslan, A., Emsen, B., Cakir, A., & Ercisli, S. (2012b). Insecticidal effect of *Usnea longissima* (Parmeliaceae) extract against *Sitophilus granarius* (Coleoptera: Curculionidae). *International Journal of Agriculture and Biology*, 14(2), 303-306.
- Yildirim, E., Emsen, B., Aslan, A., Bulak, Y., & Ercisli, S. (2012a). Insecticidal activity of lichens against the maize weevil, *Sitophilus zeamais* Motschulsky (Coleoptera: Curculionidae). *Egyptian Journal of Biological Pest Control*, 22(2), 151-156.
- Yousuf, S., & Choudhary, M. I. (2014). Lichens: chemistry and biological activities. *Studies in Natural Products Chemistry*, 43, 223-259.

**Cite as:** Aslan Engin, T. (2025). Exploring the antioxidant and protective effects of usnic acid: opportunities and challenges. *Front Life Sci RT*, 6(1), 53-59.



## Review article

# Telomerase reverse transcriptase promoter mutations in non-small cell lung cancer: Biology and clinical significance

Onur Dulger\*<sup>1</sup> <sup>1</sup> *Istanbul University, Aziz Sancar Institute of Experimental Medicine, Department of Molecular Medicine, 33300, Istanbul, Türkiye*

## Abstract

About 85% of all lung cancers are non-small cell lung cancers (NSCLC), which are common, have a high death rate, and are usually diagnosed at an advanced stage. Recent studies have shown that mutations in the *TERT* promoter in NSCLC may be a noninvasive biomarker, enhance possible treatment approaches, and predict prognosis, especially in inoperable cases. This review comprehensively examines the present state of *TERT* promoter mutations in NSCLC, highlighting their clinical relevance, treatment approaches, challenges, and key considerations. *TERT* promoter mutations in NSCLC may offer new perspectives on the molecular pathogenesis of patients. For this reason, summarized *TERT* promoter mutations in NSCLC and current treatment strategies targeting *TERT*. Understanding the *TERT* effect on NSCLC may pave the way for new personalized treatment approaches.

**Keywords:** *Clinical significance; non-small cell lung cancer; promoter mutations; TERT*

## 1. Introduction

Lung cancer remains the most common cause of cancer-related mortality worldwide among all malignant neoplasms. (Lin and Park, 2024). The precise pathways leading to the development of most lung cancers are not yet fully understood. (Bertolaccini et al., 2024). It can be related to environmental variables, circle of relatives' records, tobacco smoke, and genetic elements consisting of aberrant oncogene and tumor suppressor gene law, according to analysis (Nigro et al., 2015; Qiu et al., 2019; Yu et al., 2019).

Up to 69% of patients with advanced non-small cell lung cancer are thought to have several gene alterations that can be treated (Fois et al., 2021). Based on histological capabilities, most lung cancers are split into principal subgroups: small-mobile lung cancers (SCLC) and non-small-mobile lung cancers (NSCLC) (Braicu et al., 2019). About 85% of lung cancers are within the NSCLC histology. (Sher et al., 2008). The majority of patients, however, are diagnosed at an advanced stage and need thorough care. These patients generally have poor

prognoses and a brief average survival time (Spiro and Silvestri, 2005; Ma and Wang, 2024). Despite improvements in remedies, surgical procedures, and clinical processes, the five-year survival fee for NSCLC patients remains low at 10%-15% (Tan et al., 2016; Smith et al., 2017; Yeh et al., 2018; Zhang et al., 2020).

Cancer molecular biomarkers are increasingly being used to diagnose, monitor, and treat cancer (Passaro et al., 2024). Over 150 prognostic factors have been described for non-small cell lung cancer (NSCLC). The most important factors affecting survival include tumor stage at presentation, weight loss, tumor doubling time, and molecular markers (Johnson, 1995; Brundage et al., 2002; Bremnes et al., 2003). Some of this data may not be available, especially in cases of inoperable NSCLC. Therefore, research on non-invasive prognostic markers continues. Treatment for NSCLC has significantly changed with a focus on treatment strategies guided by the molecular profiles of tumor cells (Morgenstern et al., 2024). Numerous mutations that might be targeted with specific treatments were recognized through the molecular characterization of tumor cells (Alamgeer

\* Corresponding author.

E-mail address: [onurdulger0@gmail.com](mailto:onurdulger0@gmail.com) (O. Dulger).<https://doi.org/10.51753/flsrt.1576211> Author contributions

Received 30 October 2024; Accepted 29 January 2025

Available online 30 April 2025

2718-062X © 2025 This is an open access article published by Dergipark under the [CC BY](https://creativecommons.org/licenses/by/4.0/) license.

et al., 2013, Onur et al., 2025). Molecular targeted therapies are more effective and less toxic than treatments that conventional oncological drugs (Cheng et al., 2010; Hirsch et al., 2010; Dacic, 2011). Accordingly, molecular markers have become improving treatment strategies for NSCLC (Planchard et al., 2018).

Comprising a protein complex called Shelterin and repetitive nucleotide sequences (TTAGGG), telomeres are specialized systems observed at the ends of chromosomes. To keep genomic stability and integrity, they protect chromosome ends from deterioration and fusion with nearby chromosomes. The enzyme telomerase reverse transcriptase (*TERT*) aids in retaining the ends of telomeres (Yoo et al., 2015).

Mutations inside the *TERT* promoter location can cause expanded telomerase expression, maintaining telomere length and genomic balance, allowing cancer cells to keep away from senescence or apoptosis and keep dividing (Griewank et al., 2013). In normal cells, telomeres shorten after each cell division, and when they emerge as seriously brief, cells prevent dividing, and senescence is triggered. This is a powerful human tumor suppressor mechanism (Campisi, 2013; Inada et al., 2019; Muneer and Minhas, 2019). However, maximum tumor cells grow to be immortalized, expressing or reactivating telomerase, hence stopping senescence and permitting non-stop cell division (Kim et al., 1994).

The first promoter region of the *TERT* mutations was diagnosed in melanomas and has since been identified in various types of cancer, consisting of hepatocellular cancer, bladder most cancers, glioblastoma, and thyroid most cancers (Huang et al., 2013; Horn et al., 2013; Liu et al., 2013, El Zarif et al., 2024). The association of lung cancers and *TERT* promoter mutations has been a significant research topic in recent years.

## 2. Telomerase reverse transcriptase gene and protein

*TERT* is the catalytic subunit of the telomerase enzyme, which, at the side of the telomerase RNA portion of the telomerase RNP enzyme, forms the most essential unit in the telomerase complex (Kageler et al., 2024). The model created for the structure of *TERT* likens the *TERT* protein to a semi-open right hand. This model's protein includes palm, thumb, and finger areas. The RNA portion of the enzyme complicated, located within the palm region and complementary to at least 1.5 telomeric repeats, features within the extension of the G3' give up of DNA. The *TERT* gene, which is located at 5p15.33, codes for the catalytic subunit of telomerase, a specialized ribonucleoprotein enzyme necessary for eukaryotic organisms to extend their telomeres and add hexamer repeats to the ends of chromosomes for replication. Human telomerase reverse transcriptase (*hTERT*) is encoded by it (Aubert et al., 2012).

This function is essential for continuous cell division and plays a role in cellular immortality. The *TERT* gene is tightly repressed, which consequently leads to the silencing of telomerase. Cancer patients exhibit higher telomerase function, which protects telomeres and allows tumors to evade aging (Smogorzewska and de Lange, 2004).

### 2.1. *TERT* promoter mutations in non-small cell lung cancer

The *TERT* promoter region is a 260-base-pair (bp) region located between -1,800 and +2,300 relative to the ATG start codon. *TERT* promoter mutations predominantly occur at two hotspot mutation points, C228T and C250T, which mutate more frequently than other DNA regions based on genomic

coordinates. The C228T region and the C250T region are located 124 bp and 146 bp upstream of the ATG region, which is the first codon of the *TERT* gene coding region, respectively (Fig.1) (Ma et al., 2014). This region is rich in GC content and lacks TATA or TCCA boxes. However, it contains multiple binding sites that regulate the transcriptional activity of *TERT* and telomerase activation (Heidenreich and Kumar, 2017). Somatic mutations in the *TERT* promoter are among the most common non-coding cancer mutations (Stern et al., 2015). In an analysis of 31 cancer types from The Cancer Genome Atlas, 27% of the samples contained these promoter mutations (Barthel et al., 2017).

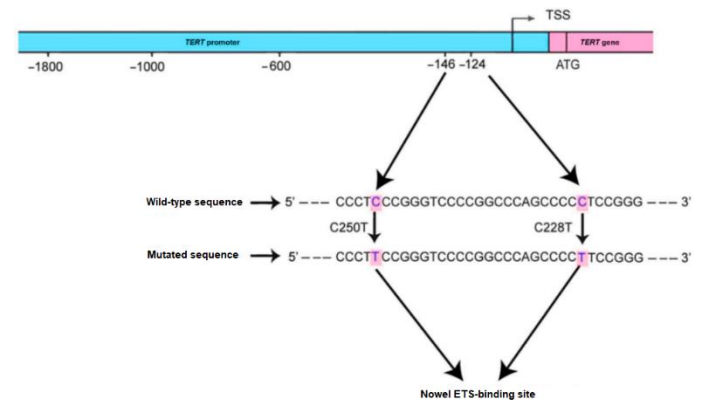


**Fig. 1.** *TERT* gene promoter binding sites and common promoter mutation points. ATG is the first codon, and the pink region is the coding region of the *TERT* gene. The blue region represents the *TERT* promoter region. TSS: Transcription start site. The new EST region occurs primarily at two hotspot regions, C228T and C250T, to create transcription factors. This region is located on the *TERT* promoter. TSS: transcription start site, EST: new binding site (Yang et al., 2021).

Cancer patients tend to have higher telomerase activity, which helps protect telomeres and allows tumors to evade aging. *TERT* promoter mutations generally lead to increased activity of *TERT* and telomerase in tumors (Smogorzewska and de Lange, 2004). Core promoter mutations create new ETS binding motifs, which in turn induce the upregulation of *TERT* (Wang et al., 2015). This results in the extension of telomeres in DNA sequences, enabling aging cells to bypass the Hayflick limit and, in some cases, achieve immortality, much like cancer cells. These *TERT* promoter mutations mainly occur at two hotspots, C228T and C250T, which are more frequently mutated than other regions of the genome (Hsu et al., 2006). Over 85% of *TERT* promoter mutations in various malignancies occur at these two canonical positions (Ma et al., 2014). Some reports indicate that exhibiting either mutation often demonstrates elevated levels of *TERT* and enhanced telomerase activity, implying a stimulatory effect on *TERT* expression (Barthel et al., 2017).

*TERT* promoter mutations activate telomerase expression, maintaining telomere length and genomic stability, allowing cells to continue dividing while avoiding senescence or apoptosis (Griewank et al., 2013). However, telomerase activity has also been observed in certain cancer types lacking *TERT* promoter mutations, suggesting alternative mechanisms might be at play. *TERT* promoter mutations were first identified in melanoma and subsequently found in cancers of the central nervous system, thyroid, and bladder (Akincilar et al., 2016). The frequency of these mutations varies across different cancer types. For example, liver, melanoma, and brain tumors exhibit a higher prevalence of these mutations, while they appear less

frequently in other cancers.

*TERT* promoter mutations have been linked to poor prognosis and lower survival rates in some cancers (Yuan et al., 2016; Spurr et al., 2024). In particular, studies indicate that these mutations are rare (~2.2-5.8%) in non-small cell lung cancer (NSCLC) patients and are typically found in older patients (Smogorzewska and de Lange, 2004; Yuan et al., 2016; Jung et al., 2017; El Zarif et al., 2024; Werr et al., 2024). Some studies have demonstrated that these mutations are associated with poor prognoses and lymph node infiltration (Jung et al., 2017). In addition, single nucleotide polymorphisms (SNPs), consisting of rs2853669, are found in the *TERT* promoter location and are connected to telomere length and survival in NSCLC patients with *EGFR* mutations (Yuan et al., 2019; Chen et al., 2024).

## 2.2. Current status of *TERT* promoter mutation therapies and therapeutic strategies

There are numerous treatment strategies concentrated on *TERT* promoter mutations. The primary technique is based on the strategy of directly inhibiting *TERT* expression (Mender et al., 2018). For this, antisense oligonucleotides that bind mainly to the mutated *TERT* promoter series are used. In this way, the transcription of the *TERT* gene is blocked and telomerase expression is reduced (Ningarhari et al., 2021). Researchers are investigating this method to lower telomerase activity in cells with *TERT* promoter mutations in NSCLC malignancies (Jafri et al., 2016). It has also been reported that *TERT* mRNA can be targeted for degradation by RNA interference (RNAi) techniques using small interfering RNAs (siRNAs) that prevent telomerase production (Fekri Aval et al., 2016). Even though they are still in the early phases of research, RNAi-based treatments show a great deal of promise in preventing *TERT* expression.

Utilizing small molecule inhibitors, which target certain transcription sites that attach to the mutant *TERT* promoter and prevent telomerase overexpression, is an additional strategy (Brennan et al., 2013; Asangani et al., 2014). In addition, inhibitors containing JQ1, which belongs to the bromodomain and extra-terminal domain (BET) kinship circle, can prevent the assembly of transcription complexes at the mutated promoter location and thus inhibit *TERT* transcription (Filippakopoulos et al., 2010). This method focuses on disrupting the interaction between the mutated promoter and transcriptional activators.

One option is to use CRISPR/Cas9 technology to target mutations in the *TERT* promoter (Wen et al., 2020). *TERT* promoter mutations in NSCLC can be corrected by gene editing techniques targeting specific mutation sites, such as C228T or C250T, to reduce *TERT* overexpression and telomerase activity (Zhan et al., 2019). While this approach minimizes off-goal results, it has demanding situations in delivering CRISPR properly and efficiently to cancer cells (Liang et al., 2015).

Epigenetic cures aimed at the chromatin structure associated with the mutant *TERT* promoter may additionally have the ability to mitigate *TERT* expression (Barthel et al., 2017). Histone deacetylase (HDAC) and DNA methyltransferase (DNMT) inhibitors may additionally exchange chromatin accessibility and lessen *TERT* transcriptional activation. DNMT inhibitors like azacitidine and HDAC inhibitors like vorinostat, which are already used in different cancers, are being explored for their ability to regulate telomerase expression in NSCLC (Lewis and Tollefsbol, 2016).

Immunotherapy strategies also are being considered

(Dosset et al., 2020). *TERT*-primarily based most cancer vaccines could assist the immune device become aware of and wreck *TERT*-expressing tumor cells, particularly in sufferers with *TERT* promoter mutations (Gridelli et al., 2020). Additionally, adoptive T-cell treatment plans involve modifying T-cells to target *TERT*-expressing tumor cells with the aid of recognizing neoantigens from *TERT* promoter mutations or by identifying *TERT*-derived peptides on the surface of cancer cells (Zanetti, 2017).

Lastly, the efficacy of *TERT* promoter mutation treatments may be increased by combining therapies. Telomerase inhibition may increase the susceptibility of cancer cells to immunological assaults or DNA damage when combined with traditional therapies like chemotherapy or immune checkpoint inhibitors (such as PD-1/PD-L1 inhibitors) (Yi et al., 2022). Additionally, telomerase suppression may make cancer cells more susceptible to radiation, which would hinder their ability to repair telomere damage caused by the treatment (Ali and Walter, 2023).

## 2.3. Challenges and considerations for therapeutic strategies targeting *TERT*

There are several challenges and concerns predicted for treatment strategies targeting *TERT*. Tumor heterogeneity means that not all NSCLC tumors harbor *TERT* promoter mutations, and even the ones that do could have other mutations that power resistance to telomerase-centered healing procedures (Guterres and Villanueva, 2020).

Therapeutic specificity is also an issue as concentrating on the *TERT* promoter without affecting ordinary stem cells, which depend upon telomerase for renewal, is a significant challenge. Moreover, cancer cells may develop resistance mechanisms by bypassing telomerase inhibition through alternative lengthening of telomeres (ALT), complicating the long-term efficacy of these therapies (Dilley & Greenberg, 2015). In addition, some methods for direct targeting of *TERT* present challenges in delivering the agent (e.g. CRISPR) directly and efficiently to tumor cells.

## 3. Conclusions

In NSCLC, mutations in the *TERT* promoter are linked to elevated production of telomerase, an enzyme that preserves telomere length and promotes the longevity of cancer cells. Therefore, targeting mutations of *TERT* promoter is a crucial area of therapeutic study in NSCLC. Most therapies that target mutations in the *TERT* promoter are currently in preclinical or early clinical development in clinical trials. Small molecule inhibitors and immunotherapy have entered early-stage studies for NSCLC and other malignancies. *TERT* promoter mutations may be used as predictive biomarkers in biomarker potential to find individuals who would benefit from telomerase-targeted treatments. Although research on how to best optimize these medicines for clinical usage continues, targeting *TERT* promoter mutations in NSCLC remains experimental but represents a potential area in cancer treatment.

**Conflict of interest:** The author declares that he has no conflict of interests.

**Informed consent:** The author declares that this manuscript did not involve human or animal participants and informed consent was not collected.

## References

- Akincilar, S. C., Unal, B., & Tergaonkar, V. (2016). Reactivation of telomerase in cancer. *Cellular and Molecular Life Sciences*, 73, 1659-1670.
- Alamgeer, M., Ganju, V., & Watkins, D. N. (2013). Novel therapeutic targets in non-small cell lung cancer. *Current Opinion in Pharmacology*, 13(3), 394-401.
- Ali, J. H., & Walter, M. (2023). Combining old and new concepts in targeting telomerase for cancer therapy: transient, immediate, complete and combinatory attack (TICCA). *Cancer Cell International*, 23(1), 197.
- Asangani, I. A., Dommeti, V. L., Wang, X., Malik, R., Cieslik, M., Yang, R., ... & Chinnaiyan, A. M. (2014). Therapeutic targeting of BET bromodomain proteins in castration-resistant prostate cancer. *Nature*, 510(7504), 278-282.
- Aubert, G., Baerlocher, G. M., Vulto, I., Poon, S. S., & Lansdorp, P. M. (2012). Collapse of telomere homeostasis in hematopoietic cells caused by heterozygous mutations in telomerase genes. *PLoS Genetics*, 8(5), e1002696.
- Barthel, F. P., Wei, W., Tang, M., Martinez-Ledesma, E., Hu, X., Amin, S. B., ... & Verhaak, R. G. (2017). Systematic analysis of telomere length and somatic alterations in 31 cancer types. *Nature Genetics*, 49(3), 349-357.
- Bertolaccini, L., Casiraghi, M., Uslenghi, C., Maiorca, S., & Spaggiari, L. (2024). Recent advances in lung cancer research: unravelling the future of treatment. *Updates in Surgery*, 76(6), 2129-2140.
- Braicu, C., Zimta, A. A., Harangus, A., Iurca, I., Irimie, A., Coza, O., & Berindan-Neagoe, I. (2019). The function of non-coding RNAs in lung cancer tumorigenesis. *Cancers*, 11(5), 605.
- Bremnes, R. M., Sundstrom, S., Aasebø, U., Kaasa, S., Hatlevoll, R., Aamdal, S., & Norwegian Lung Cancer Study Group. (2003). The value of prognostic factors in small cell lung cancer: results from a randomised multicenter study with minimum 5 year follow-up. *Lung Cancer*, 39(3), 303-313.
- Brennan, C. W., Verhaak, R. G., McKenna, A., Campos, B., Nounshmehr, H., Salama, S. R., ... & Davidsen, T. (2013). The somatic genomic landscape of glioblastoma. *Cell*, 155(2), 462-477.
- Brundage, M. D., Davies, D., & Mackillop, W. J. (2002). Prognostic factors in non-small cell lung cancer: a decade of progress. *Chest*, 122(3), 1037-1057.
- Campisi, J. (2013). Aging, cellular senescence, and cancer. *Annual Review of Physiology*, 75(1), 685-705.
- Chen, Z., Vallega, K. A., Wang, D., Quan, Z., Fan, S., Wang, Q., ... & Sun, S. Y. (2024). Inhibition of hTERT/telomerase/telomere mediates therapeutic efficacy of osimertinib in EGFR mutant lung cancer. *Journal of Experimental Medicine*, 221(11), e20240435.
- Cheng, H., Xu, X., Costa, D. B., Powell, C. A., & Halmos, B. (2010). Molecular testing in lung cancer: the time is now. *Current Oncology Reports*, 12, 335-348.
- Dacic, S. (2011). Molecular diagnostics of lung cancer. *Archives of Pathology & Laboratory Medicine*, 135, 623-829.
- Dilley, R. L., & Greenberg, R. A. (2015). ALTERNATIVE telomere maintenance and cancer. *Trends in Cancer*, 1, 145-156.
- Dosset, M., Castro, A., Carter, H., & Zanetti, M. (2020). Telomerase and CD4 T cell immunity in cancer. *Cancers*, 12(6), 1687.
- El Zarif, T., Machaalani, M., Nawfal, R., Nassar, A. H., Xie, W., Choueiri, T. K., & Pomerantz, M. (2024). TERT promoter mutations frequency across race, sex, and cancer type. *The Oncologist*, 29(1), 8-14.
- Fekri Aval, S., Akbarzadeh, A., Yamchi, M. R., Zarghami, F., Nejati-Koshki, K., & Zarghami, N. (2016). Gene silencing effect of SiRNA-magnetic modified with biodegradable copolymer nanoparticles on hTERT gene expression in lung cancer cell line. *Artificial Cells, Nanomedicine, and Biotechnology*, 44(1), 188-193.
- Filippakopoulos, P., Qi, J., Picaud, S., Shen, Y., Smith, W. B., Fedorov, O., ... & Bradner, J. E. (2010). Selective inhibition of BET bromodomains. *Nature*, 468(7327), 1067-1073.
- Fois, S. S., Paliogiannis, P., Zinellu, A., Fois, A. G., Cossu, A., & Palmieri, G. (2021). Molecular epidemiology of the main druggable genetic alterations in non-small cell lung cancer. *International Journal of Molecular Sciences*, 22(2), 612.
- Gridelli, C., Ciuleanu, T., Domine, M., Szczesna, A., Bover, I., Cobo, M., ... & Vx-001-201 trial team. (2020). Clinical activity of a htert (vx-001) cancer vaccine as post-chemotherapy maintenance immunotherapy in patients with stage IV non-small cell lung cancer: final results of a randomised phase 2 clinical trial. *British Journal of Cancer*, 122(10), 1461-1466.
- Griewank, K. G., Murali, R., Schilling, B., Schimming, T., Möller, I., Moll, I., ... & Hillen, U. (2013). TERT promoter mutations are frequent in cutaneous basal cell carcinoma and squamous cell carcinoma. *PLoS one*, 8(11), e80354.
- Guterres, A. N., & Villanueva, J. (2020). Targeting telomerase for cancer therapy. *Oncogene*, 39(36), 5811-5824.
- Heidenreich, B., & Kumar, R. (2017). TERT promoter mutations in telomere biology. *Mutation Research/Reviews in Mutation Research*, 771, 15-31.
- Hirsch, F. R., Wynes, M. W., Gandara, D. R., & Bunn Jr, P. A. (2010). The tissue is the issue: personalized medicine for non-small cell lung cancer. *Clinical Cancer Research*, 16(20), 4909-4911.
- Horn, S., Figl, A., Rachakonda, P. S., Fischer, C., Sucker, A., Gast, A., ... & Kumar, R. (2013). TERT promoter mutations in familial and sporadic melanoma. *Science*, 339(6122), 959-961.
- Hsu, C. P., Hsu, N. Y., Lee, L. W., & Ko, J. L. (2006). Ets2 binding site single nucleotide polymorphism at the hTERT gene promoter—effect on telomerase expression and telomere length maintenance in non-small cell lung cancer. *European Journal of Cancer*, 42(10), 1466-1474.
- Huang, F. W., Hodis, E., Xu, M. J., Kryukov, G. V., Chin, L., & Garraway, L. A. (2013). Highly recurrent TERT promoter mutations in human melanoma. *Science*, 339(6122), 957-959.
- Inada, E., Saitoh, I., Kubota, N., Iwase, Y., Kiyokawa, Y., Shibasaki, S., ... & Sato, M. (2019). piggy Bac transposon-based immortalization of human deciduous tooth dental pulp cells with multipotency and non-tumorigenic potential. *International Journal of Molecular Sciences*, 20(19), 4904.
- Jafri, M. A., Ansari, S. A., Alqahtani, M. H., & Shay, J. W. (2016). Roles of telomeres and telomerase in cancer, and advances in telomerase-targeted therapies. *Genome Medicine*, 8(1), 69. <https://doi.org/10.1186/s13073-016-0324-x>
- Johnson, B. E. (1995). Biologic and molecular prognostic factors—impact on treatment of patients with non-small cell lung cancer. *Chest*, 107(6), 287S-290S.
- Jung, S. J., Kim, D. S., Park, W. J., Lee, H., Choi, I. J., Park, J. Y., & Lee, J. H. (2017). Mutation of the TERT promoter leads to poor prognosis of patients with non-small cell lung cancer. *Oncology Letters*, 14(2), 1609-1614.
- Kageler, L., & Aquilanti, E. (2024). Discovery of telomerase inhibitors: existing strategies and emerging innovations. *Biochemical Society Transactions*, 52(4), 1957-1968.
- Kim, N. W., Piatyszek, M. A., Prowse, K. R., Harley, C. B., West, M. D., Ho, P. L., ... & Shay, J. W. (1994). Specific association of human telomerase activity with immortal cells and cancer. *Science*, 266(5193), 2011-2015.
- Lewis, K. A., & Tollefsbol, T. O. (2016). Regulation of the telomerase reverse transcriptase subunit through epigenetic mechanisms. *Frontiers in Genetics*, 7, 83.
- Liang, P., Xu, Y., Zhang, X., Ding, C., Huang, R., Zhang, Z., ... & Huang, J. (2015). CRISPR/Cas9-mediated gene editing in human triploid zygotes. *Protein & Cell*, 6(5), 363-372.
- Lin, H. Y., & Park, J. Y. (2024). Epidemiology of cancer. In *Anesthesia for oncological surgery* (pp. 11-16). Cham: Springer International Publishing.
- Liu, X., Bishop, J., Shan, Y., Pai, S., Liu, D., Murugan, A. K., ... & Xing, M. (2013). Highly prevalent TERT promoter mutations in aggressive thyroid cancers. *Endocrine-Related Cancer*, 20(4), 603-610.
- Ma, X., Gong, R., Wang, R., Pan, Y., Cai, D., Pan, B., ... & Chen, H. (2014). Recurrent TERT promoter mutations in non-small cell lung cancers. *Lung Cancer*, 86(3), 369-373.
- Ma, S., & Wang, L. (2024). Prognostic factors and predictive model construction in patients with non-small cell lung cancer: a retrospective study. *Frontiers in Oncology*, 14, 1378135.
- Mender, I., LaRanger, R., Luitel, K., Peyton, M., Girard, L., Lai, T. P., ... & Shay, J. W. (2018). Telomerase-mediated strategy for overcoming non-small cell lung cancer targeted therapy and chemotherapy resistance. *Neoplasia*, 20(8), 826-837.
- Morgenstern Kaplan, D., Kareff, S. A., Gandhi, N., Elliott, A., Magistri, M., Sumarriva, D., ... & Rodriguez, E. (2024). The genomic, transcriptomic,

- and immunological profile of patients with recurrent/refractory NSCLC.
- Muneer, A., & Minhas, F. A. (2019). Telomere biology in mood disorders: an updated, comprehensive review of the literature. *Clinical Psychopharmacology and Neuroscience*, 17(3), 343.
- Nigro, E., Imperlini, E., Scudiero, O., Monaco, M. L., Polito, R., Mazzarella, G., ... & Daniele, A. (2015). Differentially expressed and activated proteins associated with non small cell lung cancer tissues. *Respiratory Research*, 16, 1-10.
- Ningarhari, M., Caruso, S., Hirsch, T. Z., Bayard, Q., Franconi, A., Védie, A. L., ... & Zucman-Rossi, J. (2021). Telomere length is key to hepatocellular carcinoma diversity and telomerase addition is an actionable therapeutic target. *Journal of Hepatology*, 74(5), 1155-1166.
- Onur, D., İlhan, Y., & Büge, Ö. (2025). Association between PD-L1 expression with EGFR, ALK, and ROS1 driver oncogene mutations in non-small cell lung cancer. *Indian Journal of Pathology and Microbiology*, 68(1), 36-41.
- Passaro, A., Al Bakir, M., Hamilton, E. G., Diehn, M., André, F., Roy-Chowdhuri, S., ... & Peters, S. (2024). Cancer biomarkers: emerging trends and clinical implications for personalized treatment. *Cell*, 187(7), 1617-1635.
- Planchard, D., Popat, S. T., Kerr, K., Novello, S., Smit, E. F., Faivre-Finn, C., ... & ESMO Guidelines Committee. (2018). Metastatic non-small cell lung cancer: ESMO Clinical Practice Guidelines for diagnosis, treatment and follow-up. *Annals of Oncology*, 29, iv192-iv237.
- Qiu, M., Chen, Y. B., Jin, S., Fang, X. F., He, X. X., Xiong, Z. F., & Yang, S. L. (2019). Research on circadian clock genes in non-small-cell lung carcinoma. *Chronobiology International*, 36(6), 739-750.
- Sher, T., Dy, G. K., & Adjei, A. A. (2008, March). Small cell lung cancer. In *Mayo Clinic Proceedings*, 83(3), 355-361.
- Smith, R. A., Andrews, K. S., Brooks, D., Fedewa, S. A., Manassaram-Baptiste, D., Saslow, D., ... & Wender, R. C. (2017). Cancer screening in the United States, 2017: a review of current American Cancer Society guidelines and current issues in cancer screening. *CA: a Cancer Journal for Clinicians*, 67(2), 100-121.
- Smogorzewska, A., & de Lange, T. (2004). Regulation of telomerase by telomeric proteins. *Annual Review of Biochemistry*, 73(1), 177-208.
- Spiro, S. G., & Silvestri, G. A. (2005). One hundred years of lung cancer. *American Journal of Respiratory and Critical Care Medicine*, 172(5), 523-529.
- Spurr, L. F., & Pitroda, S. P. (2024). Clinical and molecular correlates of tumor aneuploidy in metastatic non-small cell lung cancer. *Scientific Reports*, 14(1), 19375.
- Stern, J. L., Theodorescu, D., Vogelstein, B., Papadopoulos, N., & Cech, T. R. (2015). Mutation of the TERT promoter, switch to active chromatin, and monoallelic TERT expression in multiple cancers. *Genes & Development*, 29(21), 2219-2224.
- Tan, W. L., Jain, A., Takano, A., Newell, E. W., Iyer, N. G., Lim, W. T., ... & Tan, D. S. (2016). Novel therapeutic targets on the horizon for lung cancer. *The Lancet Oncology*, 17(8), e347-e362.
- Werr, L., Bartenhagen, C., Rosswog, C., Cartolano, M., Voegelé, C., Sex-ton-Oates, A., ... & Lung NEN Network. (2025). TERT expression and clinical outcome in pulmonary carcinoids. *Journal of Clinical Oncology*, 43(2), 214-225.
- Wang, K., Liu, T., Liu, C., Meng, Y., Yuan, X., Liu, L., ... & Xu, D. (2015). TERT promoter mutations and TERT mRNA but not FGFR3 mutations are urinary biomarkers in Han Chinese patients with urothelial bladder cancer. *The Oncologist*, 20(3), 263-269.
- Wen, L., Zhao, C., Song, J., Ma, L., Ruan, J., Xia, X., ... & Xu, J. (2020). CRISPR/Cas9-mediated TERT disruption in cancer cells. *International Journal of Molecular Sciences*, 21(2), 653.
- Yang, L., Li, N., Wang, M., Zhang, Y. H., Yan, L. D., Zhou, W., ... & Cai, J. (2021). Tumorigenic effect of TERT and its potential therapeutic target in NSCLC. *Oncology Reports*, 46(2), 1-12.
- Yeh, J., Marrone, K. A., & Forde, P. M. (2018). Neoadjuvant and consolidation immuno-oncology therapy in stage III non-small cell lung cancer. *Journal of Thoracic Disease*, 10(Suppl 3), S451.
- Yi, M., Zheng, X., Niu, M., Zhu, S., Ge, H., & Wu, K. (2022). Combination strategies with PD-1/PD-L1 blockade: current advances and future directions. *Molecular Cancer*, 21(1), 28.
- Yoo, S. S., Do, S. K., Choi, J. E., Lee, S. Y., Cha, S. I., Kim, C. H., & Park, J. Y. (2015). TERT polymorphism rs2853669 influences lung cancer risk in the Korean population. *Journal of Korean Medical Science*, 30, 1423-1428.
- Yu, X. J., Chen, G., Yang, J., Yu, G. C., Zhu, P. F., Jiang, Z. K., ... & Zhong, F. M. (2019). Smoking alters the evolutionary trajectory of non-small cell lung cancer. *Experimental and Therapeutic Medicine*, 18(5), 3315-3324.
- Zhang, X. H., Hao, S., Gao, B., Tian, W. G., Jiang, Y., Zhang, S., ... & Luo, D. L. (2016). A network meta-analysis for toxicity of eight chemotherapy regimens in the treatment of metastatic/advanced breast cancer. *Oncotarget*, 7(51), 84533.
- Yuan, P., Huang, S., Bao, F. C., Cao, J. L., Sheng, H. X., Shi, L., ... & Hu, J. (2019). Discriminating association of a common telomerase reverse transcriptase promoter polymorphism with telomere parameters in non-small cell lung cancer with or without epidermal growth factor receptor mutation. *European Journal of Cancer*, 120, 10-19.
- Zanetti, M. (2017). A second chance for telomerase reverse transcriptase in anticancer immunotherapy. *Nature reviews Clinical oncology*, 14(2), 115-128.
- Zhan, T., Rindtorff, N., Betge, J., Ebert, M. P., & Boutros, M. (2019, April). CRISPR/Cas9 for cancer research and therapy. In *Seminars in cancer biology* (Vol. 55, pp. 106-119). Academic Press.
- Zhang, X. X., Yu, X. Y., Xu, S. J., Shi, X. Q., Chen, Y., Shi, Q., & Sun, C. (2024). rs2736098, a synonymous polymorphism, is associated with carcinogenesis and cell count in multiple tissue types by regulating TERT expression. *Heliyon*, 10(6).
- Zhang, Y., Shen, W. X., Zhou, L. N., Tang, M., Tan, Y., Feng, C. X., ... & Chen, M. B. (2020). The Value of Next-Generation Sequencing for Treatment in Non-Small Cell Lung Cancer Patients: The Observational, Real-World Evidence in China. *BioMed Research International*, 2020(1), 9387167.

**Cite as:** Dulger, O. (2025). Telomerase reverse transcriptase promoter mutations in non-small cell lung cancer: Biology and clinical significance. *Front Life Sci RT*, 6(1), 60-64.



Review article

## The effects of mesenchymal stem cells on asthma

Kemal Yuce<sup>\*1</sup> <sup>1</sup> Agri Ibrahim Cecen University, Medicine Faculty, Physiology Department of Basic Medical Science, 04100, Agri, Türkiye

### Abstract

Asthma is an inflammatory disease of the respiratory system characterized by cough, shortness of breath, wheezing, sputum, obstruction and bronchial hyperactivity. Asthma leads to disruption of epithelial structure, subepithelial fibrosis, inflammation, and ultimately airway reorganization. MSCs migrate into inflammatory tissue and settle there. Once in the tissue, the MSCs suppress inflammation and improve the internal structure of the tissue. These effects are achieved by transforming into tissue cells, producing anti-inflammatory and growth factors, and releasing microRNAs and extracellular vesicles. The effect of MSCs on asthma is based mostly on *in vivo* experimental animal models and *in vitro* studies of airway cells. While ovalbumin, cockroach extract and house dust mite are mostly used for *in vivo* experimental animal models, airway smooth muscle cells are mostly used for *in vivo* studies. This study aims to objectively present the information obtained from reliable articles about whether MSCs can be used in the treatment of asthma, a chronic inflammatory lung disease.

**Keywords:** Asthma models; identification of MSCs; inflammatory disease; mesenchymal stem cells

### 1. Introduction

Asthma affects more than 300 million people worldwide (Di Cicco et al., 2023). Airway remodeling and inflammation occur in patients with asthma. In addition, asthma-induced structural changes include disruption of epithelial structure, goblet cell hyperplasia, subepithelial fibrosis and increased smooth muscle hypertrophy. These changes lead to airway obstruction, cough, sputum production, hyperreactivity and impaired lung function (Lambrecht et al., 2017; Banno et al., 2020). Therefore, while the most common treatments for asthma are mainly anti-inflammatory agents and bronchodilators (Xie et al., 2018), new treatments and therapeutic targets are needed to better control symptoms and exacerbations in patients with severe asthma and to protect them from the side effects of medications (Cevhertas et al., 2020).

Mesenchymal stem cells (MSCs) have been shown to localize mostly in the lungs after intravenous injection (Brychtova et al., 2019). MSCs provide therapeutic effects for asthma, an inflammatory lung disease, by controlling cellular

activity or releasing bioactive factors (Bonfield et al., 2010). Airway hyperresponsiveness (AHR) and bronchoalveolar lavage fluid counts in mice sensitized with ovalbumin (OVA) were considerably reduced by both single and double human mesenchymal stem cell (hMSC) treatments. Furthermore, a single hMSC treatment significantly reduced allergic airway inflammation. However, inflammatory cell infiltration and TH2 cytokine levels were further elevated by repeated treatment with hMSCs during OVA sensitization and challenge (Hur et al., 2020). Both *in vitro* and *in vivo* (by inhalation), MSC-EV treatment encouraged macrophage polarization toward an M2 phenotype. The activity of MSC-EVs against acute lung injury (ALI) was linked to immunological and redox mediators, such as TLR4, ARG1, and HO-1, according to RNA sequencing (Zhao et al., 2022). Administration of normoxic human umbilical cord MSC-EVs (Nor-EVs) or hypoxic MSC-derived EVs (Hypo-EVs) to animals with OVA-induced asthma significantly improved pro-inflammatory mediators (IL-4 and IL-13), eosinophils, and bronchoalveolar lavage fluid (BALF) total cells (Liyang Dong et al., 2021). In conclusion, asthma,

\* Corresponding author.

E-mail address: [yuce2020@hotmail.com](mailto:yuce2020@hotmail.com) (K. Yuce).<https://doi.org/10.51753/flsrt.1567487> Author contributions

Received 15 October 2024; Accepted 13 March 2025

Available online 30 April 2025

2718-062X © 2025 This is an open access article published by Dergipark under the [CC BY](https://creativecommons.org/licenses/by/4.0/) license.

which has not yet been fully treated, is an inflammatory disease and MSCs have anti-inflammatory and immunomodulatory effects. Therefore, this study aims to evaluate the effect of MSCs on asthma, a respiratory system disease, and to provide information to researchers and physicians about whether MSCs can be an alternative treatment for asthma.

## 2. The effect of mesenchymal stem cells on asthma

### 2.1. *In vivo* studies

#### 2.1.1. Ovalbumin-induced asthma model

OVA makes up more than half of egg white. OVA contains 386 amino acid residues with acetylated glycine at the N-terminal end and proline at the C-terminal end. Thirty percent of OVA's amino acid residues are acidic, and fifty percent are hydrophobic. In addition, OVA contains four free sulfhydryl groups, one disulfide connection, and six cysteine residues. Moreover, OVA may exhibit antioxidant properties thanks to its ability to bind metal ions and may cause allergies (Rostamabadi et al., 2023). OVA is used to create an experimental animal asthma model. For this purpose, OVA can be administered intravenously, intraperitoneally, intratracheally and intranasally (Leite-Santos et al., 2023).

**Studies on the direct use of MSCs:** MSCs are thought to be effective in the treatment of asthma, an inflammatory disease, due to their immunomodulatory properties. Airway inflammation and remodeling were found to be evident in asthmatic mice. In addition, low levels of IL-12, fewer CD4+CD25+ regulatory T cells, and high levels of IL-4, IL-13, OVA-specific IgE, IgG2a, and IgG1 were detected in the asthmatic group. The use of BM-MSCs for transplantation notably reduced airway remodeling and inflammation, the level of OVA-specific IgE, OVA-specific IgG1, and IL-4, but increased the number of CD4+CD25+ regulatory T cells and the level of IL-12 in asthmatics. BM-MSCs did not support lung regeneration and IFN- $\gamma$ , IL-13, and IL-10 levels were not significantly affected by BM-MSCs (Ge et al., 2013). In a study comparing the effects of BM-MSCs and AD-MSCs, hBM-MSC treatment significantly reduced airway hyperresponsiveness, but hAD-MSC treatment did not. Although both MSCs decreased airway inflammation, the effects of hBM-MSCs were typically more significant. Treatment with hBM-MSCs decreased Th2-cytokine levels, but not with hAD-MSCs. Serum resistin-like molecule- $\beta$  level was found to be lower in asthma patients than in controls, but increased in both treatment groups (Choi et al., 2022). Intravenous Human umbilical cord-derived mesenchymal stem cells (hUC-MSCs) administration decreased mucus production, inflammation and airway resistance in a mouse model of asthma. hUC-MSCs not only attenuated Th17 cells and Th2 cells, but also enhanced regulatory T cells (Tregs). In addition, hUC-MSCs successfully inhibited ILC2s by down-regulating key regulators of ILC2s, such as *Tcf7* and *Gata3* (Innate to lymphoid cells). As a result, hUC-MSCs decreased the total quantity of macrophages, particularly the percentage of the population composed of macrophages produced from monocytes. Upon closer inspection of monocyte-derived macrophages, hUC-MSCs were found to lower M2c and M2a populations (Ahmadi et al., 2017; Kang et al., 2017; Mo et al., 2022) (Table 1). Methacholine-bronchial hyperresponsiveness and eosinophil count in bronchoalveolar lavage fluid cells significantly decreased upon administration of huMSCs. In a

similar way, following huMSC injection, lung and spleen tissues produced significantly fewer Th2 cytokines (IL-5, IL-13, and IL-4) and IgG1 and IgE levels, and additionally, the proportion of regulatory T cells increased (Kang et al., 2017). It was noted that rBM-MSCs restored the synthesis of INF- $\gamma$ , IL-12, IL-5, VCAM-1, and ICAM-1 to normal levels and significantly reduced pathological injuries in lung samples of asthmatic rats (Rahbarghazi et al., 2019). When gum-derived mesenchymal stem cells were used in another study, they found that MSCs greatly reduced eosinophil infiltration by blocking the growth of CD11b+CD11c+ proinflammatory dendritic cells (DCs) and the differentiation of Th2 cells. It was also revealed that gingival-derived mesenchymal stem cells' production of hepatocyte growth factor effectively reduced airway inflammation (Fang et al., 2024). In lung tissue, MSC injection was observed to significantly inhibit macrophage M2 polarization. Additionally, in a chronic allergy mouse model caused by OVA, MSC treatment decreased oxidative stress, ER stress, and nuclear translocation of NF- $\kappa$ B p65. MSC treatment stopped OVA-induced chronic airway remodeling through these processes (Yu et al., 2024). To sum up, MSCs allowed inflammatory cells to infiltrate and controlled the pathogenic milieu brought on by asthma (He et al., 2024).

**Studies on the use of MSC conditioned media (CM):** MSCs secrete various cytokines, growth factors and extracellular vesicles into the conditioned medium in which they are grown. Therefore, CMs are expected to have therapeutic effects, and various studies have been conducted to reveal these effects. It was found that systemic administration of CM in repeated dosages can notably decrease pathological injuries through modulation of GATA-3 and T-bet expression in lung tissues and interleukin levels. In contrast, CM administered in a single dose did not provide any beneficial effects (Keyhanmanesh et al., 2018). In asthmatic groups, it was demonstrated that both CM and BM-MSCs altered the synthesis of IL-10 and IL-4 to a level comparable to control rats. Histopathological examination showed that the administration of CM, and particularly mesenchymal stem cells, significantly decreased the amount of lung damage in asthmatic rats (Rahbarghazi et al., 2019) (Table 1). Systemic injection of rBM-MSCs, but not CM, reduced the levels of IL-13, IL-10, IL-4, miRNA155, miRNA133, and pathological changes. The result of the current study demonstrated the potential role of MSCs, but not CM, in decreasing pathological changes during asthma changes, probably through the modulation of miRNA133 and miRNA155 (Ahmadi et al., 2018).

**Studies on the use of MSC exosomes:** MSC-derived exosomes constitute an important source of the therapeutic effects of MSCs. Therefore, MSC-Exosomes can be used for therapeutic purposes. MSC-Exo can significantly expand spleen-derived lung IL-10-producing IMs and thus contribute to protection against allergic asthma in mice. After intranasal administration of MSC-derived exosomes, lung IM rates increased significantly and high levels of IL-10 were produced (Ren et al., 2021). *In vitro*, hypo-EV therapy enhanced the expression of ZO-1 and E-cadherin proteins and markedly improved the rise in airway cell permeability. Hypo-EV therapies were found to significantly increase caveolin-1 (CAV-1). The positive effects of Hypo-EVs on airway inflammation and remodeling in asthmatic mice were substantially eliminated when CAV-1 was reduced. It was discovered that nebulizing Hypo-EVs could treat other barrier-problem disorders and improve airway epithelial barrier abnormalities in asthma by

**Table 1**  
The effect of MSCs on asthma.

The type of MSC or product being used	The effect of MSCs on asthma	References
hUC-MSCs	hUC-MSCs administration decreased mucus production, inflammation and airway resistance in a mouse model of asthma. hUC-MSCs not only attenuated Th17 cells and Th2 cells, but also enhanced regulatory T cells (Tregs). Histopathological examination showed that the administration of CM, and particularly mesenchymal stem cells, significantly decreased the amount of lung damage in asthmatic rats	(Ahmadi et al., 2017; Kang et al., 2017; Mo et al., 2022).
CM, and MSCs	Compared to Nor-EVs, hypo-EVs were more successful in suppressing the chronic allergic airway remodeling in mice, as evidenced by decreased levels of collagen-1, the pro-fibrogenic markers alpha-smooth muscle actin (alpha-SMA), and the TGF- $\beta$ 1-p-smad2/3 signaling pathway	(Rahbarghazi et al., 2019).
hypo-EVs and nor-EVs	Induced pluripotent stem cell-derived MSC (iPSC-MSC) transplantation was found to significantly reduce T helper 2 cytokines, attenuate mitochondrial malfunction in epithelial cells and reduce asthma inflammation. Multiple doses of MSCs reduced lung inflammation and remodeling, while inducing immunosuppression in allergic asthma brought on by HDM.	(Liyang Dong et al., 2021).
iPSC-MSC		(Yao et al., 2018)
MSCs		(Castro et al., 2020)

supplying CAV-1 to decrease p-STAT6 expression (Luo et al., 2024). It was found that giving hUC-MSC migrasomes-recently discovered extracellular vesicles that promote intercellular communication-significantly reduced the symptoms of mucus production and airway inflammation in asthmatic mice. Furthermore, dendritic cell (DC) activation was prevented, and Th2 cytokine production (IL-4, IL-5, and IL-13) was decreased (Gu et al., 2025). It was found that miR-223-3p, which is highly abundant in exosomes, may promote airway remodeling and have protective effects on asthma by regulating the ASC/Caspase-1/GSDMD signaling pathway (Tortosa-Martinez et al., 2023). An inverse relationship was observed between asthma induction and BM-MSC transplantation. A substantial correlation was found between Mmu-miR-21a-3p and the Type IIA immune regulatory activin receptor (Acvr2a). mmu-miR-21a-3p was significantly correlated with immune regulatory activin Areceptor, Type IIA (Acvr2a). Mmu-miR-21a-3p had the opposite correlation with Acvr2a after BM-MSC treatment and asthma. MiR-21a binding sites were present in Acvr2a in both humans and mice. This indicated that the miR-21/Acvr2a axis was conserved between humans and mice. mmu-miR-21a-3p was found to negatively regulate Acvr2a transcript (Tang et

al., 2016). In summary, administering MSC-EVs improves a variety of asthma pathology-related factors. Additionally, the source, dosage, frequency, and timing of MSC-EV administration affect the therapy's outcome (Firouzabadi et al., 2024).

**Studies on the use of pre-treated MSCs and MSC secretomes:** Pre-treatment of MSCs affects the survival time of MSCs, their oxidative-antioxidative systems, their adhesion ability and the cytokines and extracellular vesicles they secrete. Changes in these factors are reflected in the therapeutic effects of MSCs. MSC proliferation, extracellular vesicle release, and self-renewal are all influenced by oxygen content. Therefore, the anti-asthma effect of MSCs can be enhanced under hypoxic conditions. Administration of Hypo-EVs or Nor-EVs notably improved eosinophils, pro-inflammatory mediators (IL-4 and IL-13), and BALF total cells in asthmatic mice. In asthmatic mice, hypo-EVs were often more effective than nor-EVs at reducing airway inflammation. Compared to Nor-EVs, hypo-EVs were more successful in suppressing the chronic allergic airway remodeling in mice, as evidenced by decreased levels of collagen-1, the pro-fibrogenic markers alpha-smooth muscle actin (alpha-SMA), and the TGF- $\beta$ 1-p-smad2/3 signaling pathway. Hypo-EVs inhibited the expression of p-smad2/3, alpha-SMA, and collagen-1 in human lung fibroblasts (HLF-1 cells) that were activated by TGF- $\beta$ 1 *in vitro* (Liyang Dong et al., 2021) (Table 1).

MSC-associated immunomodulatory effects may be enhanced by inflammatory cytokines. For this purpose, studies have been conducted to determine how IFN- $\gamma$  and tumor necrosis factor- $\alpha$  (TNF- $\alpha$ ) may affect the therapeutic effects of MSCs. Treg and Th9 cells show anti- and pro- allergic activity, respectively. Th9- and Treg-related parameters did not differ significantly between untreated asthmatic mice and those treated with uninduced MSCs. Compared with the untreated asthmatic group, treatment with IFN- $\gamma$ -induced MSCs notably decreased lung expression of PU.1 and IL-9 and serum IL-9 levels, and increased lung expression of FOXP3 and serum IL-35 levels. Treatment with TNF- $\alpha$ -derived MSCs significantly reduced serum IL-9 levels and lung expression of IL-9. All examined Treg and Th9-related parameters were substantially impacted by treatment with "IFN- $\gamma$ +TNF- $\alpha$ "-derived MSCs. Compared with mice treated with uninduced MSCs, serum IL-9 levels were significantly reduced in mice treated with "IFN-gamma+TNF-alpha"-induced MSCs. IFN- $\gamma$  and "IFN- $\gamma$ +TNF- $\alpha$ "-treated MSCs were more effective than TNF- $\alpha$ -exposed MSCs (Dong et al., 2021). In comparison to untreated MSC groups, calcitriol-treated MSCs dramatically raised IL-12, TGF- $\beta$ , and IFN- $\gamma$  levels in a study. Additionally, MSCs treated with and without calcitriol decreased IL-4 and IL-17 levels more than the asthmatic groups did. Histopathological analysis revealed that, in comparison to the asthma group, calcitriol-treated MSCs decreased the formation of inflammatory cells and the thickness of the bronchial wall (Ghalavand et al., 2023). Some of the studies that aim to enhance the therapeutic effects of MSCs are based on pre-treatment of MSCs with certain drugs. For this purpose, a study was conducted on the treatment of MSCs with the anti-fibrotic drug serelaxin (RLN). Combined administration of MSC and RLN further reversed OVA-induced airway inflammation and airway/lung fibrosis and further increased MMP-9 levels compared to treatment alone. RLN enhanced MSCs' therapeutic outcomes in a chronic illness context which was most likely due to RLN's capacity to restrict matrix production triggered by TGF- $\beta$ 1 (Royce et al., 2015).

**Studies on the use of recombinant MSCs and MSC secretomes:** Released into the cytosol or extracellular environment, a variety of metabolic products and mitochondrial constituents can act as damage-associated molecular models and induce inflammation (Marchi et al., 2023). Excreted mitochondrial products and elements may encourage inflammation when associated with damage and suppress inflammation when healthy. In this context, mitochondrial transfer from bone marrow MSCs to damaged epithelial cells may result in reduced acute lung injury in mice. Induced pluripotent stem cell-derived MSC (iPSC-MSC) transplantation was found to significantly reduce T helper 2 cytokines, attenuate mitochondrial malfunction in epithelial cells and reduce asthma inflammation. The formation of tunneling nanotubes (TNTs) occurred between iPSC-MSCs and epithelial cells, and it was discovered that iPSC-MSCs transferred mitochondria to epithelial cells both *in vivo* and *in vitro* using TNTs. Connexin 43 was found to mediate mitochondrial transfer between iPSC-MSCs and epithelial cells, and the modulation of TNT synthesis was significantly influenced by it (Yao et al., 2018) (Table 1). However, administration of iPSC-MSCs before inflammation occurred also led to protective effects. Mice treated with human iPSC-MSC systemic injection before developing asthma were shielded from the negative effects of long-term allergic airway inflammation, particularly fibrosis and improved remodeling of the airways (Zhong et al., 2019).

Downregulated miR-138 alleviated the inflammatory response and promoted wound healing in diabetic foot ulcer rats by activating the hTERT and PI3K/AKT pathway. After suppression of miR-138, the level of inflammatory cytokines decreased, while the amount of healing factors and anti-inflammatory increased *in vitro* and *in vivo* (Wang et al., 2022). In a study on whether there is a connection between miR-138 and the effect of MSCs on asthma, binding between miR-138-4p and SIRT1 was determined. SIRT1 was upregulated upon inhibition of miR-138-5p. Inhibition of miR-138-5p caused hMSCs to elicit an attenuated inflammatory response after TNF- $\alpha$  and IL-6 stimulation, leading to the release of histamine and ovalbumin-specific IgG, as well as allergic symptoms in mice. hMSCs with miR-138-5p inhibition demonstrated features of active SIRT1 and repressed the TLR4/HMGB1 pathway (Tang et al., 2021). MSCs transfected to express the *IL-35 gene* were able to control allergic asthma symptoms significantly better than MSCs lacking IL-35 (Bao et al., 2023).

### 2.1.2. Cockroach extract (CRE)-induced asthma model

For almost 60 years, cockroach allergies have been linked to the onset of asthma. Beginning in the 1990s, the determination of allergens in cockroaches led to the current listing of 20 confirmed allergy categories in the World Health Organization and International Union of Immunological Societies (WHO/IUIS) allergen nomenclature database, and this process is ongoing. Cockroach allergens are used in experimental animal models of asthma and can be administered intranasally, intratracheally and intraperitoneally (Pomes and Arruda, 2023).

While the macrophage M1 phenotype is pro-inflammatory, the M2 phenotype has an anti-inflammatory characteristic. MSCs significantly decreased mRNA levels of IL-1 $\beta$ , NOS2, and IL-6 as M1 markers, while notably increased mRNA levels of selected M2 markers such as FIZZ1, YM-1, and ARG-1. Furthermore, it was shown that aryl hydrocarbon receptor (AhR) signaling notably increased throughout the pathogenesis of

asthma. It was also shown that high AhR signaling could alleviate the onset of asthma. The use of an AhR antagonist (CH223191) led to significant inhibition of AhR signaling and increased expression of M2 markers, but elevated expression of M1 markers in the CRE-induced asthma model. MSC were shown to be able to modulate macrophage polarization through activation of AhR signaling during CRE-induced asthma (Cui et al., 2020). MSCs not only had an anti-inflammatory effect in asthma by supporting macrophage polarization towards M2, but also increased tissue regeneration and repair by activating TGF- $\beta$ 1 signaling. TGF- $\beta$ 1 signaling was observed to be more activated in MSCs treated with CRE. Transforming growth factor beta 1 had an important effect on the collection of stem cells for tissue regeneration, repair and remodeling. When Tbr1 inhibitors or TGF- $\beta$ 1 neutralizing Ab substantially reduced MSC migration, TGF- $\beta$ 1 neutralizing Ab prevented MSC recruitment stimulated by CRE but encouraged inflammation of the airways (Xu et al., 2014). Compared with mice used as controls, the lungs' tissues from mice with asthma exhibited a higher synthesis of active RhoA. Another way that MSCs repair the devastating effects of asthma was through differentiation into damaged epithelial cells and collagen. RhoA-L63 expression promoted MSC development into fibroblasts and myofibroblasts, while differentiation toward epithelial cells was changed by RhoA-19 expression (Ke et al., 2019). In conclusion, MSCs created an anti-inflammatory and regenerative effect in animals with cockroach-induced asthma.

### 2.1.3. House dust mite (HDM)-induced asthma model

It has been demonstrated that HDMs are significant sources of indoor allergens linked to allergies, including asthma. *D. farinae* (Df), *D. pteronyssinus* (Dp), *B. tropicalis* (Bt), and *E. maynei* (Em) are the most prevalent dust mite species found in the world (Milián and Díaz, 2004). House dust mites are used in experimental animal models of asthma and are administered to the animal intratracheally or intranasally.

Since MSCs have immunomodulatory qualities and the host's ability to tolerate them, they may be used therapeutically to treat asthma, but previous evidence indicates that blood-borne progenitor cells may participate in airway remodeling. MSCs were found to localize to the lungs and rapidly reduce airway inflammation in association with increased T-helper-1 lung cytokines. However, this effect was diminished under constant allergen challenge despite the permanent presence of MSCs. Therapeutic MSC infusion in experimental mouse asthma did not create undesirable side effects and was able to improve airway hyperresponsiveness and contractile tissue remodeling (Marinas-Pardo et al., 2014). hUC-MSC administration alleviated lung type 2 (Type 2 and th2 innate lymphoid cell) inflammation in both diesel exhaust particle (DEP)/HDM-induced and alternaria alternata-induced asthma models. These consequences, however, could only be proven with certain treatment regimens and schedules. *In vitro* co-culture revealed that hUC-MSC down-regulated IL-13 and IL-5 synthesis of peripheral blood mononuclear cells and differentiated mouse Th2 cells taken from people with asthma. Thus, these findings suggested that hUC-MSCs could improve asthma by decreasing the generation of asthmagenic cytokines by effector cells (Shin et al., 2021). However, how many doses of MSCs should be administered is also an important issue. In a study conducted to investigate this, two and three MSC dosages reduced lung inflammation, IL-13, eotaxin and IL-4 levels, CD4+ T cell,

eosinophil and total leukocyte counts in bronchoalveolar lavage fluid, and total leukocyte counts in spleen, mediastinal lymph nodes and bone marrow. Two and three MSC dosages also reduced TGF- $\beta$  levels and collagen fiber content in lung tissue, but the three-dosage frequency worked better, reducing these parameters to control levels while also reducing alpha-actin content in lung tissue. Multiple doses of MSCs reduced lung inflammation and remodeling, while inducing immunosuppression in allergic asthma brought on by HDM (Castro et al., 2020) (Table 1). In a study, a medium that produced CATT7-MIF-licensed MSCs with elevated VEGF levels (CATT7-MIF MSC CM) greatly accelerated the migration and proliferation of bronchial epithelial wounds *in vitro*. This impact was eliminated by using mitomycin C or blocking VEGFR2. Furthermore, upon HDM exposure, CATT7-MIF MSC CM markedly decreased goblet cell hyperplasia *in vivo*. The application of an anti-human VEGF neutralizing antibody eliminated this impact, confirming that it was VEGF-dependent (Dunbar et al., 2025).

## 2.2. *In vitro* studies

Some of the studies investigating the effect of mesenchymal stem cells on asthma are *in vitro* studies. How these *in vitro* studies are organized is up to the creativity of the individual. MSCs and Tregs are powerful immune modulators. The development of asthma is significantly influenced by Treg proliferation and abnormal function. MSC exosomes were found to increase TGF- $\beta$ 1 and IL-10 from peripheral blood mononuclear cells (PBMCs), thus promoting the immunosuppressive capacity and proliferation of Tregs. In this study, antigen-presenting cells (APCs), not the CD4+T cells-dependent pathway, were shown to be the likely mechanism involved in MSC exosome-mediated regulation (Du et al., 2018). The underlying reason for this may be that MSCs have high levels of miR-1470 because it was shown that exosomal miR-1470 of MSCs can increase the proportion of CD4+CD25+FOXP3+ regulatory T cells in patients with asthma. In addition, mechanistic studies indicated that miR-1470 can improve the up-regulation of P27KIP1 by specifically aiming for the *c-Jun mRNA*'s 3' region. Mimic transfection of miR-1470 notably increased the proportion of CD4+CD25+FOXP3+Tregs in CD4+T cells. siRNA-mediated suppression of P27KIP1 inhibited the increase in the proportion of CD4+CD25+FOXP3+ Tregs induced by miR-1470 overexpression. This shows that miR-1470 stimulates the differentiation of CD4+CD25+FOXP3+ Tregs through P27KIP1 (Zhuansun et al., 2019). MSCs suppressed the proliferation of PBMCs exposed to DM (Dust mite) in allergic asthmatic subjects, but not in allergic subjects without asthma. MSCs prevented the maturation of dendritic cells but did not affect regulatory T cells (Kapoor et al., 2012).

Airway smooth muscle (ASM) cells play an important role in the pathogenesis of asthma through cellular changes. ASM has the capacity to contribute to symptoms of asthma, such as asthmatic hyperplasia (proliferative phenotype), inflammation (synthetic phenotype), and bronchoconstriction (contractile phenotype). In this context, how a healthy airway smooth muscle cell becomes diseased is important. The synthesis functions of ASMs in culture from non-asthmatic and asthmatic donors differ. These differences include increased production of extracellular matrix proteins, proinflammatory mediators, and

adhesion receptors. ASMs taken from asthmatic subjects are capable of modifying their environment, actively participating in repair processes, and functionally responding to changes in their microenvironment (Wright et al., 2013). Therefore, joint studies on MSCs and ASMs are important in revealing the effect of MSCs on asthma. Exosomes derived from AD-MSCs can be efficiently taken up by ASMs. Exosomal miR-301a-3p significantly suppressed platelet-derived growth factor-BB (PDGF-BB)-derived proliferation and migration of ASMs, increased apoptosis and decreased secretion of inflammatory factors. The 3'UTR region of *STAT3* was the direct target of MiR-301a-3p.

The increased expression of STAT3 reversed exosomal miR-301a-3p's repressive impact in ASMs stimulated by PDGF-BB. Expression of STAT3 and miR-301a-3p were negatively correlated in samples from asthmatic patients. It was found that exosomal miR-301a-3p produced from AD-MSCs may significantly ameliorate PDGF-BB-induced inflammation and remodeling of ASMs by targeting STAT3 (Feng et al., 2022).

## 3. Limitations and risk factors for the use of MSCs in asthma treatment

Very promising results have been obtained for the use of MSCs in asthma treatment and no negative side effects of MSC applications other than mild fever have been detected. All MSCs, especially UC-MSCs, reduce mucus production, inflammation, airway resistance, IgG1 and IgE levels and provide tissue healing. However, the donor's age, the *in vitro* culture conditions, the storage time, the injection period, and the timing of the injection are some of the variables that could adversely impact the treatment's outcome if this is not taken into account.

## 4. Conclusion

Asthma is an inflammatory respiratory disease, in which tissue structure is impaired. MSCs suppress the inflammatory response caused by asthma and provide tissue remodeling and repair. Such studies are based on the direct use of MSCs, recombinant MSCs and pretreated MSCs, the use of their conditioned media and their exosomes. In studies on the direct use of MSCs, AD-MSCs, BM-MSCs and UC-MSCs can be used. We believe that the best results are obtained from UC-MSCs. When we compare the use of MSCs and MSC conditioned media, the direct use of MSCs gives better results. When we compare Hypo-EVs with Nor-EVs, Hypo-EVs give better results. When we compare normal MSCs with recombinant MSCs, it can be said that recombinant MSCs generally give better results. Of course, it should not be forgotten that the recombinantly modified gene is also important.

As a result, the use of MSCs in asthma treatment is promising and it is important to take this information into consideration when determining which MSCs to use.

**Conflict of interest:** The author declares that he has no conflict of interests.

**Informed consent:** The author declares that this manuscript did not involve human or animal participants and informed consent was not collected.

## References

- Ahmadi, M., Rahbarghazi, R., Aslani, M. R., Shahbazfar, A. A., Kazemi, M., & Keyhanmanesh, R. (2017). Bone marrow mesenchymal stem cells and their conditioned media could potentially ameliorate ovalbumin-induced asthmatic changes. *Biomedicine & Pharmacotherapy*, 85, 28-40. doi:10.1016/j.biopha.2016.11.127
- Ahmadi, M., Rahbarghazi, R., Shahbazfar, A. A., Baghban, H., & Keyhanmanesh, R. (2018). Bone marrow mesenchymal stem cells modified pathological changes and immunological responses in ovalbumin-induced asthmatic rats possibly by the modulation of miRNA155 and miRNA133. *General Physiology and Biophysics*, 37(3), 263-74. doi:10.4149/gpb\_2017052
- Banno, A., Reddy, Aravind T., Lakshmi, Sowmya P., & Reddy, Raju C. (2020). Bidirectional interaction of airway epithelial remodeling and inflammation in asthma. *Clinical Science*, 134(9), 1063-1079. doi:10.1042/cs20191309
- Bao, X. H., Gao, F., Athari, S. S., & Wang, H. (2023). Immunomodulatory effect of IL-35 gene-transfected mesenchymal stem cells on allergic asthma. *Fundamental & Clinical Pharmacology*, 37(1), 116-124. doi:10.1111/fcp.12823
- Bonfield, T. L., Koloze, M., Lennon, D. P., Zuchowski, B., Yang, S. E., & Caplan, A. I. (2010). Human mesenchymal stem cells suppress chronic airway inflammation in the murine ovalbumin asthma model. *American Journal of Physiology-Lung Cellular and Molecular Physiology*, 299(6), L760-L770. doi:10.1152/ajplung.00182.2009
- Brychtova, M., Thiele, J.-A., Lysak, D., Holubova, M., Kralickova, M., & Vistejnova, L. (2019). Mesenchymal stem cells as the near future of cardiology medicine--truth or wish? *Biomedical Papers of the Medical Faculty of Palacky University in Olomouc*, 163(1).
- Castro, L. L., Kitoko, J. Z., Xisto, D. G., Olsen, P. C., Guedes, H. L., Morales, M. M., ... & Rocco, P. R. (2020). Multiple doses of adipose tissue-derived mesenchymal stromal cells induce immunosuppression in experimental asthma. *Stem Cells Translational Medicine*, 9(2), 250-260. doi:10.1002/sctm.19-0120
- Cevhertas, L., Ogulur, I., Maurer, D. J., Burla, D., Ding, M., Jansen, K., ... Akdis, C. A. (2020). Advances and recent developments in asthma in 2020. *Allergy*, 75(12), 3124-3146.
- Choi, J. Y., Hur, J., Jeon, S., Jung, C. K., & Rhee, C. K. (2022). Effects of human adipose tissue-and bone marrow-derived mesenchymal stem cells on airway inflammation and remodeling in a murine model of chronic asthma. *Scientific Reports*, 12(1), 12032. doi:10.1038/s41598-022-16165-8
- Cui, Z., Feng, Y., Li, D., Li, T., Gao, P., & Xu, T. (2020). Activation of aryl hydrocarbon receptor (AhR) in mesenchymal stem cells modulates macrophage polarization in asthma. *Journal of Immunotoxicology*, 17(1), 21-30. doi:10.1080/1547691X.2019.1706671
- Di Cicco, M., Ghezzi, M., Kantar, A., Song, W.-J., Bush, A., Peroni, D., & D'Auria, E. (2023). Pediatric obesity and severe asthma: Targeting pathways driving inflammation. *Pharmacological Research*, 188, 106658.
- Dong, L., Wang, Y., Zheng, T., Pu, Y., Ma, Y., Qi, X., ... Mao, C. (2021). Hypoxic hUCMSC-derived extracellular vesicles attenuate allergic airway inflammation and airway remodeling in chronic asthma mice. *Stem Cell Research & Therapy*, 12(1).
- Dong, L., Wang, Y., Zheng, T., Pu, Y., Ma, Y., Qi, X., ... & Mao, C. (2021). Hypoxic hUCMSC-derived extracellular vesicles attenuate allergic airway inflammation and airway remodeling in chronic asthma mice. *Stem Cell Research & Therapy*, 12, 1-14.
- Du, Y. M., Zhuansun, Y. X., Chen, R., Lin, L., Lin, Y., & Li, J. G. (2018). Mesenchymal stem cell exosomes promote immunosuppression of regulatory T cells in asthma. *Experimental Cell Research*, 363(1), 114-120. doi:10.1016/j.yexcr.2017.12.021
- Dunbar, H., Hawthorne, I. J., Tunstead, C., Dunlop, M., Volkova, E., Weiss, D. J., ... & English, K. (2025). The VEGF-Mediated Cytoprotective Ability of MIF-Licensed Mesenchymal Stromal Cells in House Dust Mite-Induced Epithelial Damage. *European Journal of Immunology*, 55(1), e202451205. doi:10.1002/eji.202451205
- Fang, Q., Wu, W., Xiao, Z., Zeng, D., Liang, R., Wang, J., ... & Zheng, S. G. (2024). Gingival-derived mesenchymal stem cells alleviate allergic asthma inflammation via HGF in animal models. *Iscience*, 27(5). doi:10.1016/j.isci.2024.109818.
- Feng, C. Y., Bai, S. Y., Li, M. L., Zhao, J. Y., Sun, J. M., Bao, H. J., ... Su, X. M. (2022). Adipose-Derived Mesenchymal Stem Cell-Derived Exosomal miR-301a-3p Regulates Airway Smooth Muscle Cells During Asthma by Targeting STAT3. *Journal of Asthma and Allergy*, 15, 99-110. doi:10.2147/JAA.S335680
- Firouzabadi, S. R., Mohammadi, I., Ghafourian, K., Kiani, A., & Hashemi, S. M. (2024). Mesenchymal Stem Cell-Derived Extracellular Vesicle Therapy for Asthma in Murine Models: A Systematic Review and Meta-analysis. *Stem Cell Reviews and Reports*, 20(5), 1162-1183. doi:10.1007/s12015-024-10704-8
- Ge, X., Bai, C., Yang, J., Lou, G., Li, Q., & Chen, R. (2013). Effect of mesenchymal stem cells on inhibiting airway remodeling and airway inflammation in chronic asthma. *Journal of Cellular Biochemistry*, 114(7), 1595-1605. doi:10.1002/jcb.24501
- Ghalavand, M., Gouvarchin Ghaleh, H. E., Khafaei, M., Paryan, M., Kondori, B. J., Nodoushan, M. M., ... & Mohammadi-Yeganeh, S. (2023). Effect of calcitriol treated mesenchymal stem cells as an immunomodulation micro-environment on allergic asthma in a mouse model. *Endocrine, Metabolic & Immune Disorders-Drug Targets (Formerly Current Drug Targets-Immune, Endocrine & Metabolic Disorders)*, 23(8), 1096-1103. doi:10.2174/1871530323666230127115847
- Gu, W., Zheng, T., Li, W., Luo, X., Xu, X., Wang, Y., ... & Dong, L. (2025). Migrasomes derived from human umbilical cord mesenchymal stem cells: a new therapeutic agent for ovalbumin-induced asthma in mice. *Stem Cell Research & Therapy*, 16(1), 26. doi:10.1186/s13287-025-04145-4
- He, X. Y., Han, M. M., Zhao, Y. C., Tang, L., Wang, Y., Xing, L., ... & Jiang, H. L. (2024). Surface-engineered mesenchymal stem cell for refractory asthma therapy: Reversing airway remodeling. *Journal of Controlled Release*, 376, 972-984. doi:10.1016/j.jconrel.2024.10.056
- Hur, J., Kang, J. Y., Kim, Y. K., Lee, S. Y., Jeon, S., Kim, Y., ... & Rhee, C. K. (2020). Evaluation of human MSCs treatment frequency on airway inflammation in a mouse model of acute asthma. *Journal of Korean Medical Science*, 35(23). doi:10.3346/jkms.2020.35.e188
- Kang, S. Y., Park, D. E., Song, W. J., Bae, B. R., Lee, J. W., Sohn, K. H., ... & Cho, S. H. (2017). Immunologic regulatory effects of human umbilical cord blood-derived mesenchymal stem cells in a murine ovalbumin asthma model. *Clinical & Experimental Allergy*, 47(7), 937-945. doi:10.1111/cea.12920
- Kapoor, S., Patel, S. A., Kartan, S., Axelrod, D., Capitle, E., & Rameshwar, P. (2012). Tolerance-like mediated suppression by mesenchymal stem cells in patients with dust mite allergy-induced asthma. *Journal of Allergy and Clinical Immunology*, 129(4), 1094-1101. doi:10.1016/j.jaci.2011.10.048
- Ke, X., Do, D. C., Li, C., Zhao, Y., Kollarik, M., Fu, Q., ... & Gao, P. (2019). Ras homolog family member A/Rho-associated protein kinase 1 signaling modulates lineage commitment of mesenchymal stem cells in asthmatic patients through lymphoid enhancer-binding factor 1. *Journal of Allergy and Clinical Immunology*, 143(4), 1560-1574. doi:10.1016/j.jaci.2018.08.023
- Keyhanmanesh, R., Rahbarghazi, R., Aslani, M. R., Hassanpour, M., & Ahmadi, M. (2018). Systemic delivery of mesenchymal stem cells condition media in repeated doses acts as magic bullets in restoring IFN- $\gamma$ /IL-4 balance in asthmatic rats. *Life Sciences*, 212, 30-36. doi:10.1016/j.lfs.2018.09.049
- Lambrecht, B. N., Persson, E. K., & Hammad, H. (2017). Myeloid Cells in Asthma. *Myeloid Cells in Health and Disease* (pp. 739-757).
- Leite-Santos, F., Tamashiro, E., Murashima, A. D. A. B., Anselmo-Lima, W. T., & Valera, F. C. (2023). Which are the best murine models to study Eosinophilic Chronic Rhinosinusitis? A contemporary review. *Brazilian Journal of Otorhinolaryngology*, 89(6), 101328. doi:10.1016/j.bjorl.2023.101328
- Luo, X., Wang, Y., Mao, Y., Xu, X., Gu, W., Li, W., ... & Dong, L. (2024). Nebulization of Hypoxic hUCMSC-EVs Attenuates Airway Epithelial Barrier Defects in Chronic Asthma Mice by Transferring CAV-1. *International Journal of Nanomedicine*, 10941-10959. doi:10.2147/ijn.s476151
- Marchi, S., Guilbaud, E., Tait, S. W., Yamazaki, T., & Galluzzi, L. (2023). Mitochondrial control of inflammation. *Nature Reviews Immunology*, 23(3), 159-173. doi:10.1038/s41577-022-00760-x.

- Marinas-Pardo, L., Mirones, I., Amor-Carro, O., Fraga-Iriso, R., Lema-Costa, B., Cubillo, I., . . . Ramos-Barbon, D. (2014). Mesenchymal stem cells regulate airway contractile tissue remodeling in murine experimental asthma. *Allergy*, *69*(6), 730-740. doi:10.1111/all.12392
- Milián, E., & Díaz, A. M. (2004). Allergy to house dust mites and asthma. *Puerto Rico Health Sciences Journal*, *23*(1).
- Mo, Y., Kang, S. Y., Bang, J. Y., Kim, Y., Jeong, J., Jeong, E. M., . . . Kang, H. R. (2022). Intravenous Mesenchymal Stem Cell Administration Modulates Monocytes/Macrophages and Ameliorates Asthmatic Airway Inflammation in a Murine Asthma Model. *Mol Cells*, *45*(11), 833-845. doi:10.14348/molcells.2022.0038
- Pomés, A., & Arruda, L. K. (2023). Cockroach allergy: understanding complex immune responses to develop novel therapies. *Molecular Immunology*, *156*, 157-169. doi:10.1016/j.molimm.2023.03.001
- Rahbarghazi, R., Keyhanmanesh, R., Aslani, M. R., Hassanpour, M., & Ahmadi, M. (2019). Bone marrow mesenchymal stem cells and condition media diminish inflammatory adhesion molecules of pulmonary endothelial cells in an ovalbumin-induced asthmatic rat model. *Microvascular Research*, *121*, 63-70. doi:10.1016/j.mvr.2018.10.005
- Ren, J., Liu, Y., Yao, Y., Feng, L., Zhao, X., Li, Z., & Yang, L. (2021). Intranasal delivery of MSC-derived exosomes attenuates allergic asthma via expanding IL-10 producing lung interstitial macrophages in mice. *International Immunopharmacology*, *91*, 107288. doi:10.1016/j.intimp.2020.107288
- Rostamabadi, H., Chaudhary, V., Chhikara, N., Sharma, N., Nowacka, M., Demirkesen, I., . . . Falsafi, S. R. (2023). Ovalbumin, an outstanding food hydrocolloid: Applications, technofunctional attributes, and nutritional facts, A systematic review. *Food Hydrocolloids*, *139*, 108514. doi:https://doi.org/10.1016/j.foodhyd.2023.108514.
- Royce, S. G., Shen, M., Patel, K. P., Huuskes, B. M., Ricardo, S. D., & Samuel, C. S. (2015). Mesenchymal stem cells and serelaxin synergistically abrogate established airway fibrosis in an experimental model of chronic allergic airways disease. *Stem Cell Research*, *15*(3), 495-505. doi:10.1016/j.scr.2015.09.007
- Shin, J. W., Ryu, S., Ham, J., Jung, K., Lee, S., Chung, D. H., . . . & Kim, H. Y. (2021). Mesenchymal stem cells suppress severe asthma by directly regulating Th2 cells and type 2 innate lymphoid cells. *Molecules and Cells*, *44*(8), 580-590. doi:10.14348/molcells.2021.0101
- Tang, G. N., Li, C. L., Yao, Y., Xu, Z. B., Deng, M. X., Wang, S. Y., . . . & Fu, Q. L. (2016). MicroRNAs involved in asthma after mesenchymal stem cells treatment. *Stem Cells and Development*, *25*(12), 883-896. doi:10.1089/scd.2015.0339
- Tang, H., Han, X., Li, T., Feng, Y., & Sun, J. (2021). Protective effect of miR-138-5p inhibition modified human mesenchymal stem cell on ovalbumin-induced allergic rhinitis and asthma syndrome. *Journal of Cellular and Molecular Medicine*, *25*(11), 5038-5049. doi:10.1111/jcmm.16473
- Tortosa-Martínez, J., Beltrán-Carrillo, V. J., Romero-Elías, M., Ruiz-Casado, A., Jiménez-Loaiza, A., & González-Cutre, D. (2023). "To be myself again": Perceived benefits of group-based exercise for colorectal cancer patients. *European Journal of Oncology Nursing*, *66*, 102405. doi:10.1016/j.ejon.2023.102405
- Wang, J., Zhao, X., Tian, G., Liu, X., Gui, C., & Xu, L. (2022). Down-regulation of miR-138 alleviates inflammatory response and promotes wound healing in diabetic foot ulcer rats via activating PI3K/AKT pathway and hTERT. *Diabetes, Metabolic Syndrome and Obesity: Targets and Therapy*, 1153-1163. doi:10.2147/dmso.s359759
- Wright, D. B., Triana, T., Siddiqui, S., Pascoe, C. D., Ojo, O. O., Johnson, J. R., . . . Kanabar, V. (2013). Functional phenotype of airway myocytes from asthmatic airways. *Pulm Pharmacol Ther*, *26*(1), 95-104. doi:10.1016/j.pupt.2012.08.003
- Xie, H., Wu, L., Deng, Z., Huo, Y., & Cheng, Y. (2018). Emerging roles of YAP/TAZ in lung physiology and diseases. *Life Sciences*, *214*, 176-183. doi:https://doi.org/10.1016/j.lfs.2018.10.062.
- Xu, T., Xian, L.-L., Zhou, Y., Plunkett, B., Cao, X., Wan, M., & Gao, P. (2014). TGF-beta1 Mobilizes Mesenchymal Stem Cells In Allergic Asthma. *Journal of Allergy and Clinical Immunology*, *133*(2, Supplement), AB53. doi:https://doi.org/10.1016/j.jaci.2013.12.212.
- Yao, Y., Fan, X. L., Jiang, D., Zhang, Y., Li, X., Xu, Z. B., . . . Fu, Q. L. (2018). Connexin 43-Mediated Mitochondrial Transfer of iPSC-MSCs Alleviates Asthma Inflammation. *Stem Cell Reports*, *11*(5), 1120-1135. doi:10.1016/j.stemcr.2018.09.012
- Yu, H., Zhu, G., Qin, Q., Wang, X., Guo, X., & Gu, W. (2024). Mesenchymal Stromal Cell Therapy Alleviates Ovalbumin-Induced Chronic Airway Remodeling by Suppressing M2 Macrophage Polarization. *Inflammation*, *47*(4), 1298-1312. doi:10.1007/s10753-024-01977-9
- Zhao, R., Wang, L., Wang, T., Xian, P., Wang, H., & Long, Q. (2022). Inhalation of MSC-EVs is a noninvasive strategy for ameliorating acute lung injury. *Journal of Controlled Release*, *345*, 214-230. doi:https://doi.org/10.1016/j.jconrel.2022.03.025.
- Zhong, H., Fan, X. L., Fang, S. B., Lin, Y. D., Wen, W., & Fu, Q. L. (2019). Human pluripotent stem cell-derived mesenchymal stem cells prevent chronic allergic airway inflammation via TGF-beta1-Smad2/Smad3 signaling pathway in mice. *Molecular immunology*, *109*, 51-57. doi:10.1016/j.molimm.2019.02.017
- Zhuansun, Y., Du, Y., Huang, F., Lin, L., Chen, R., Jiang, S., & Li, J. (2019). MSCs exosomal miR-1470 promotes the differentiation of CD4+ CD25+ FOXP3+ Tregs in asthmatic patients by inducing the expression of P27KIP1. *International Immunopharmacology*, *77*, 105981. doi:10.1016/j.intimp.2019.105981

**Cite as:** Yuce, K. (2025). The effects of mesenchymal stem cells on asthma. *Front Life Sci RT*, *6*(1), 65-71.